THE GEOLOGY AND GEOCHEMISTRY OF AKAROA VOLCANO, BANKS PENINSULA, NEW ZEALAND

A Thesis
submitted in partial fulfillment
of the requirements for the degree
of
Doctor of Philosophy in Geology
in the
University of Canterbury
by
C. J. Dorsey

University of Canterbury
1988

FRONTISPIECE

These 512 × 512 pixel point-perspective views of Banks Peninsula were generated from a 500 m grid Digital Terrain Model of New Zealand and Landsat data, using the EPIC Image Processing Software developed by the Image Processing Group of the Division of Information Technology, Department of Scientific and Industrial Research. Bands 1, 2 and 4 of 500 × 500 subscenes of 100 m resolution Landsat data were draped over the DTM and colour-coded as blue, red and green respectively. Thus red areas indicate areas of active vegetation.

The two images are a stereo pair, and may be viewed with a pocket stereoscope

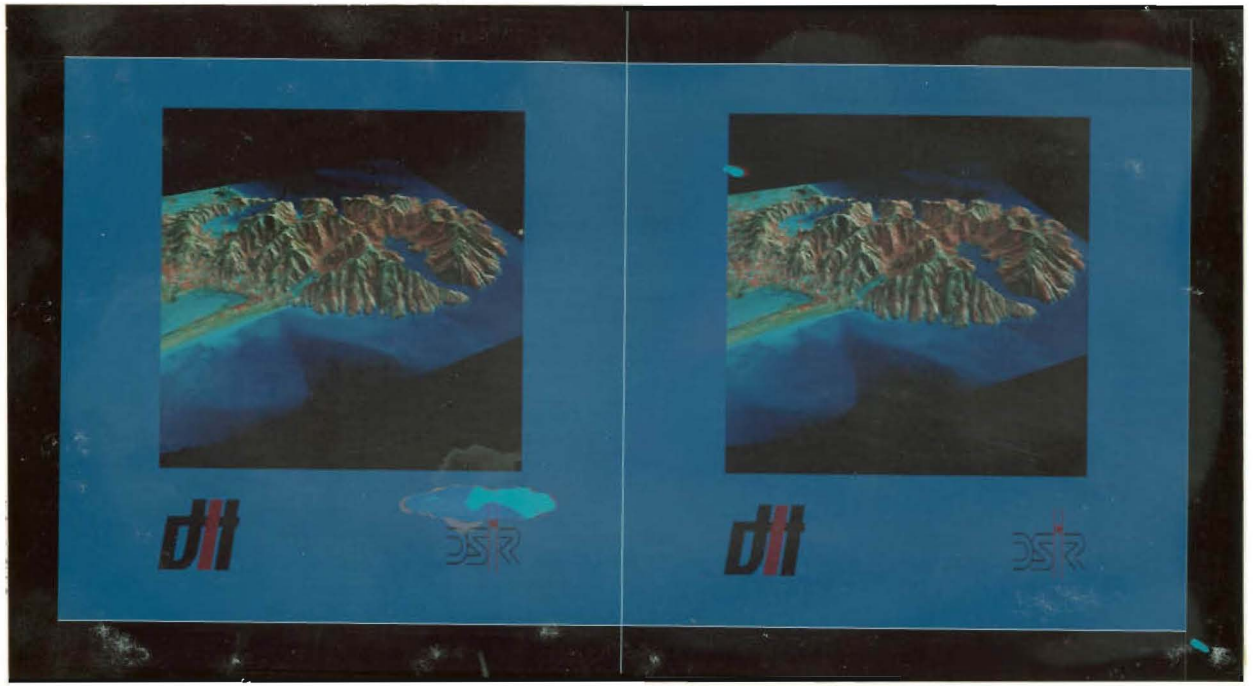

Dedicated in Love and Admiration
To The Memory Of
James Allen Dorsey
25 March 1928 – 1 December 1985

VOLUME I

Contents

List of Figures

List of Tables

ABSTRACT

This thesis presents a detailed geological, petrological and geochemical study of Akaroa Volcano, Banks Peninsula, New Zealand.

The Akaroa Volcanic Group is defined as comprising all the volcanic products of central, flank and parasitic vent eruptions in the south-eastern two-thirds of Banks Peninsula, which collectively form Akaroa Volcano. Field mapping has shown that the lavas and pyroclastics of which Akaroa Volcano is constructed can be grouped into an Early Phase and a Main Phase.

Early Phase rocks (?11–9 Ma) are restricted in outcrop to the inner shoreline of Akaroa Harbour. The oldest exposed basaltic lava flows of Akaroa Volcano are assigned to Early Phase I. Early Phase II comprises extensive trachyte tuffs, breccias, agglomerates, flows, sills, and a large dome, with minor basaltic tuffs, and appears to represent a major episode of eruption of trachytic lava marking the end of the construction of a proto-Akaroa Volcano. Weathered basaltic flows, tuffs, lahars, scoria cones and pyroclastic breccia of Early Phase III unconformably overlie rocks of Early Phase II. The contact between Early Phases II and III shows considerable relief indicating a period of erosion prior to eruption of Early Phase III flows and pyroclastics. A diverse stratigraphy and a significant portion of the early history of Akaroa Volcano remains buried beneath sea level. A period of prolonged weathering and erosion occurred prior to the eruption of Main Phase lava flows and pyroclastics.

The main cone of Akaroa Volcano is constructed predominantly of hawaiite lava flows and pyroclastics and rare mugearite, benmoreite and trachyte lava flows of the Main Phase, erupted 9–8 Ma. Activity was hawaiian to mildly strombolian in character. Throughout its eruptive history, Akaroa Volcano was intruded by predominantly trachytic dikes of the Akaroa radial dike swarm, and five large trachyte domes. Dikes radiate from a broadly defined central zone south to south-east of Onawe Peninsula which coincides with the inferred location of the main conduit, and with the maxima of local bouguer and isostatic gravity anomalies. Analysis of the gravity anomaly surfaces indicates a substantial sub-surface intrusive complex containing > 615 km^3 of intrusive material. Panama Rock trachyte dome can be

seen to have been fed by a large dike of the radial dike swarm and a similar origin is inferred for the other intrusive trachyte domes.

Akaroa Volcanic Group lavas have a mineralogy typical of alkaline volcanic associations, dominated by olivine, Ti-rich calcic clinopyroxene, titanomagnetite, plagioclase and apatite. Rare kaersutite megacrysts occur in evolved lavas, and peralkaline differentiates contain arfvedsonite and aenigmatite. Minor biotite and amphibole occur in coarse-grain basic lavas.

Akaroa Volcanic Group lavas comprise a mildly to moderately (sodic) alkaline association, with a trend of moderate iron enrichment. Two end-member lineages are recognised: a dominant basalt–hawaiite–mugearite–benmoreite–trachyte lineage with *ne*-, *hy*- and *qz*-normative variants, and a basanite–nepheline hawaiite–nepheline mugearite–nepheline benmoreite–phonolite lineage. Peralkaline differentiates are also recognised. The dominant lava type is hawaiite, rather than basalt, and most lavas have Mg numbers ($100 \times Mg^{2+}/Mg^{2+}+Fe^{2+}$) in the range 35–48, indicating that Akaroa Volcanic Group lavas do not represent primary magmas but have undergone significant high pressure fractionation.

Geochemically, Akaroa Volcanic Group lavas form a comagmatic suite characterised by (i) A logarithmic decrease in MgO, TiO_2, Cr, Ni and V; (ii) A linear decrease in CaO and FeO; (iii) A linear increase in Na_2O, K_2O, Y, Nb, Rb, La, Ce, Nd, Ga, Pb, Th, and Ba; (iv) A complex variation in Al_2O_3; (v) A rapid increase in P_2O_5 and Sr followed by a rapid decrease; and (vi) An increase in REE abundances with increasing differentiation. These variations are consistent with evolution by fractional crystallization of olivine, clinopyroxene, titanomagnetite, plagioclase, apatite and possibly kaersutite. Lavas have linear, parallel, LREE-enriched REE patterns ($Ce_N/Yb_N \approx 7$–9.5) indicative of magma generation by small degrees of partial melting of a garnet peridotite mantle source.

Covariance of $^{87}Sr/^{86}Sr$ and $^{143}Nd/^{144}Nd$ isotope ratios is consistent with derivation of Akaroa Volcanic Group magmas from a time-integrated, LREE-depleted mantle source, whereas Sm/Nd and Rb/Sr trace element ratios indicate a LREE-enriched source. Mantle enrichment processes prior to, or associated with, the melting event and/or very small degrees of partial melting ($< 1\%$) are postulated to account for this dichotomy. *Qz*-normative felsic lavas have high $^{87}Sr/^{86}Sr$ isotope ratios, and high-level crustal contamination appears to be an important process in the evolution of these lavas.

Chapter 1

INTRODUCTION

Banks Peninsula, with its remarkably symmetrical domal form rising from the flat expanse of the surrounding Canterbury Plains, has fascinated geologists for more than 120 years. Many papers have been published on aspects of Banks Peninsula geology since Sir Julius Von Haast presented his first report to the Canterbury Provincial Council, on the geology of Mt Pleasant, in 1860. However, most of these publications dealt with restricted topics or areas, and failed to produce any coherent model or synthesis for the evolution of the Banks Peninsula volcanoes.

An ultimate aim of studies of volcanic terrains such as Banks Peninsula is the development of integrated petrological models for their evolution. Such models are the synthesis of large volumes of data, derived from systematic mapping and sampling, detailed studies of particular areas and features, and the application of modern analytical methods, within the framework of current understanding of volcanic processes.

Significant advances have been made, especially in the last two decades, in the development of sophisticated equipment and techniques for geochemical analysis of, for example, radiometric ages, isotopic abundances and rare earth element distributions. In addition, improvements in equipment and techniques already available have increased the precision and accuracy of analyses. As a result, researchers today can extract considerably more information, of a greater precision and accuracy, from rock samples than was possible forty or fifty years ago when many of the papers about Banks Peninsula geology were published. Furthermore, advances in the understanding of volcanic processes and in the significance of new data allow the interpretation of available data within a new framework.

1.1 Purpose and Scope of Study

It is only in recent years that systematic mapping and detailed studies of large areas of the peninsula [Gebbies Pass, Thiele (1983); Central Banks Peninsula, Sewell (1985)] have been undertaken, involving the application of modern analytical techniques, with the aim of developing an integrated petrological model for the evolution of Banks Peninsula. Akaroa Volcano has not been the subject of such a study, and as such, represents a major gap in our knowledge of Banks Peninsula.

The aim of this study is to conduct a detailed geological, petrological and geochemical investigation of Akaroa Volcano. The data resulting from this study will supplement that already available from the study of other areas of Banks Peninsula and provide a sound base for future modelling of the evolution of Banks Peninsula and its significance in the regional tectonic environment.

The study area is defined as the area encompassed by the exposed products of the Akaroa Volcano, and is essentially that part of Banks Peninsula east of a line from Big Bay in the north to Kaituna Lagoon in the south (Fig. 1.1). Akaroa Volcano and its products represent some 65% of the 1200 km^2 of elevated area of Banks Peninsula. Road access is via State Highway 75 to Akaroa township, with other sealed roads to the main north-eastern bays, to Wainui, and from Little River to Bossu Road. Other areas, especially the south-western bays, are serviced by gravel roads. Significant lengths of roads are winding and steep.

1.2 Organisation of Thesis

Chapter 1 introduces the thesis research, describes the geological setting and discusses previous work. Chapter 2 describes the stratigraphy and volcanology of extrusive and pyroclastic rocks. Intrusive rocks are described in chapter 3. These chapters, accompanied by a series of maps and measured stratigraphic sections (Map Pocket), provide a general description of the geology of Akaroa Volcano and act as the basis for a discussion of the petrology and geochemistry of Akaroa Volcanic Group lavas. Chapter 4 describes the petrography and mineralogy of the various rock types, and Chapters 5 and 6 describe the major element, trace element and isotope geochemistry of Akaroa lavas. From the information presented in these chapters, a petrogenetic model for the evolution of Akaroa Volcano is presented in Chapter 7. Chapter 8 concludes with a geological history of Akaroa Volcano and Banks Peninsula. Descriptions of analytical methods, and all data used in this study are presented in a separately bound volume of appendices (Volume II).

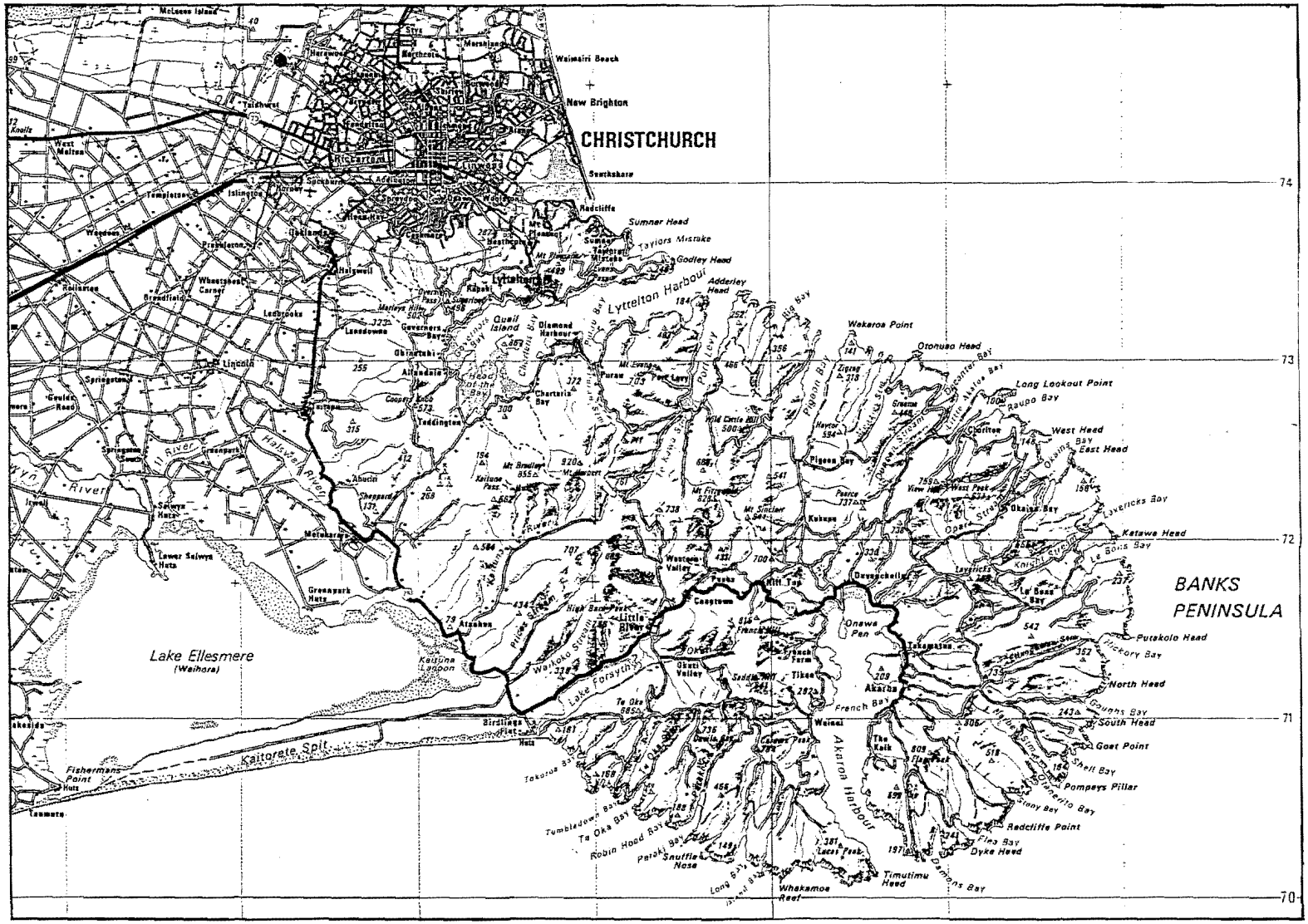

Figure 1.1: Location map of study area, taken from NZMS 270 metric series 1:250 000 topographic maps, sheet 21.

1.3 Physiographic Setting

1.3.1 Geomorphology

The most commanding feature of the Akaroa landscape is Akaroa Harbour itself (Figs. 1.1, 1.2). Running approximately north-south, with a dog-leg shape, waters of the harbour extend to the heart of the peninsula. Near-vertical cliffs at the Heads give way at first to stony beaches and then to tidal mudflats. Loess-clad lower slopes rise from the harbour, steepening up to the crater walls.

Outward radiating, gently sloping ridges terminate abruptly in sea cliffs of varying heights. The cliffs are lowest in the north-east (Pigeon Bay) and south-west (Lake Forsyth), but over much of the coastline, heights of over 90 m are common, reaching 180 m near Akaroa Heads. Valleys lead into bays of varying sizes, shapes, aspects and shoreline characteristics. Valleys themselves show a range of development, from sub-mature forms such as Prices Valley through forms illustrated by Pigeon Bay, Okains Bay and Little River, to Akaroa Harbour itself. A distinctive feature of this evolutionary sequence is the progressive development of an enlarged, amphitheatre-like catchment basin, by excessive headward erosion and tributary capture. Ridge-end cliffs reduce in height as they run into bays, but hillsides are often steep-sided and contain bluffs. Two larger bays (Okains Bay, Le Bons Bay) have extensive bay-head infilling, resulting in sandy beaches and small river estuaries. Tidal mudflats occur at the head of Akaroa Harbour in Barrys Bay and Duvauchelle Bay, and to a lesser extent in Pigeon Bay and Little Akaloa Bay.

The shingle fans of the Canterbury Plains lap against the west and south-west flanks of the peninsula, and Kaitorete Spit, a product of long-shore drift, has dammed the outlet of Okuti and Okana Rivers to form the coastal brackish Lake Forsyth. Sea cliffs, stacks and wave-cut platforms along the Kaituna Valley – Motukarara section of Highway 75 attest to the effects of marine erosion in this area, when the peninsula was still an island.

Thick deposits of loess, locally in excess of 10 m, mantle the lower slopes of the Akaroa Harbour basin and the outer flanks of the volcanic cone. Extensive exposures of rock are confined to steep valley walls where erosion is active, around the inner harbour shoreline, and along road cuttings.

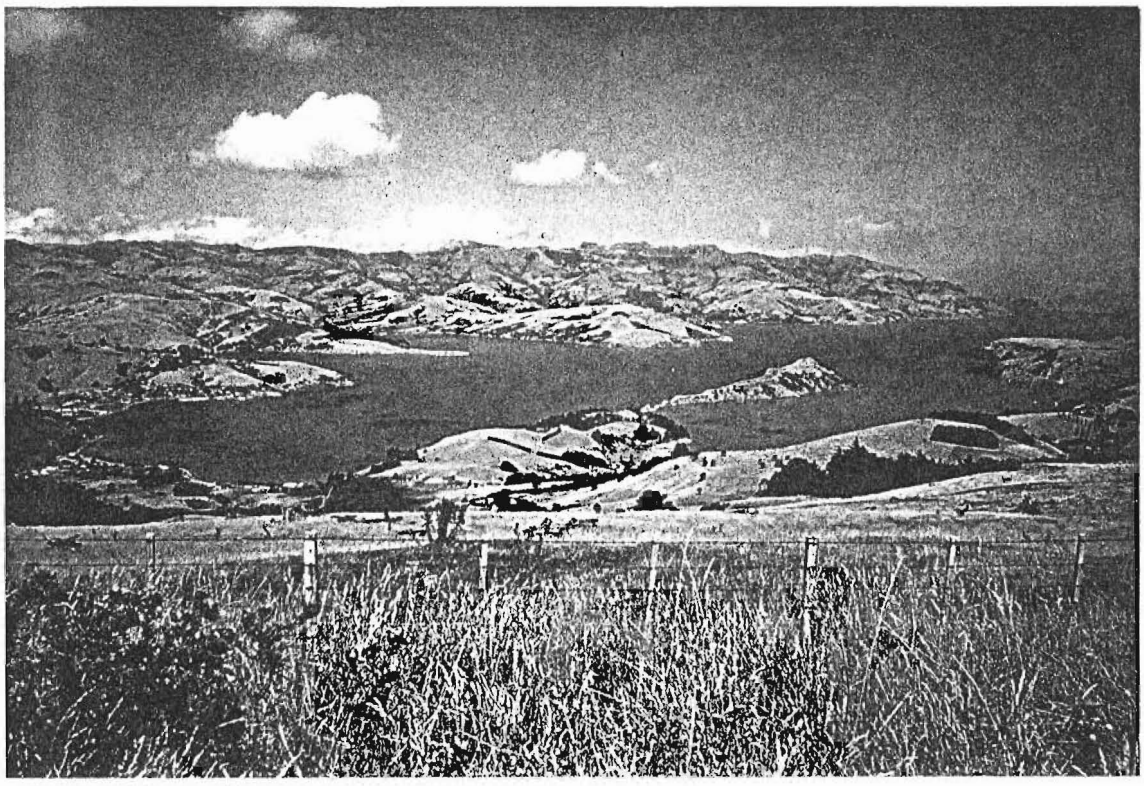

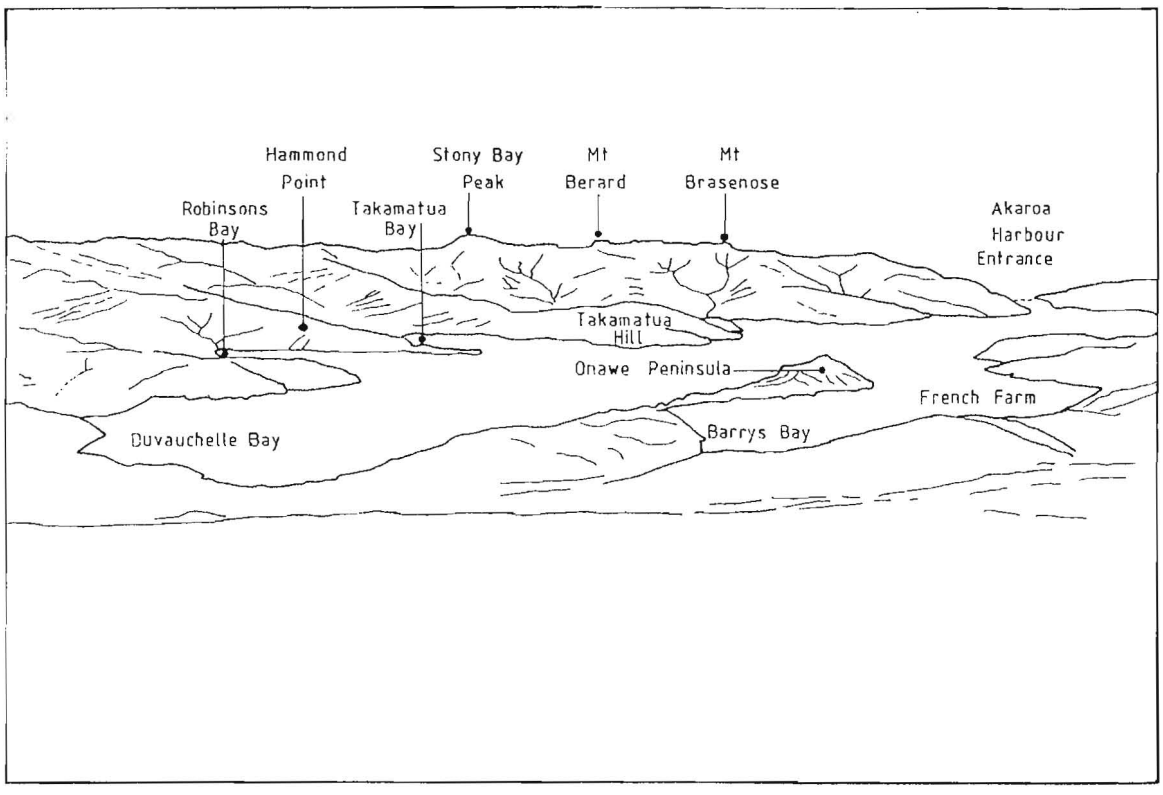

Figure 1.2: Akaroa Harbour, looking south from the Summit Road. (Below) Sketch taken from the photo, showing the main features of Akaroa Harbour.

1.3.2 Climate

The climate is moist and mild, becoming cooler towards the south. Mean annual precipitation is typically > 1000 mm, compared with < 800 mm for the Canterbury Plains. A distinctive feature is the high variability in precipitation and mean annual temperature ranges from one valley to the next, reflecting the interaction of dominantly easterly climatic influences with a wide range of aspects and topography.

1.3.3 Vegetation

Varying topography, aspect, soils and microclimate are reflected in indigenous flora types as rich and diverse as Nikau Palm groves, podocarp/cedar forests, beech forests, tussock and scrub and salt-tolerant plant communities. In addition there are the Polynesian introduced Karaka groves and the European introduced grasses, gorse and trees. Banks Peninsula is noteworthy in that it is the southern-most limit for a number of plant species.

Almost all of Banks Peninsula was once forest-clad, but the effects of man and nature have restricted indigenous species to small remnant forests and bushes in isolated valley headwaters and scenic reserves, and the dominant vegetation is now modified tussock grassland.

1.3.4 Wildlife

The rugged, cliffed coastline of eastern Banks Peninsula is home to many uncommon species of wildlife, including New Zealand Fur seals (*Arctocephalus fosteri*), the white-flippered penguin (*Eudyptula albasignata*) and the yellow-eyed penguin (*Megadyptes antipodus*), regarded as one of the world's rarest species of penguin. Tidal mudflats, such as those at the head of Akaroa Harbour, are an important feeding area, and have a high population of waterfowl, red-billed gulls, South Island pied oyster-catchers, white-faced herons and black swans.

Most indigenous terrestrial birdlife is found in small remnant bush and scrub areas. Many species have now disappeared as a result of habitat destruction and introduced predators.

2000 different species of arthropods are found on Banks Peninsula, including rare and endemic species like the Banks Peninsula weta, *Hemideina ricta*.

The information presented in this section was abstracted from "Banks Peninsula. A coastal recreation planning study. Vols I and II" (Ministry of Works and Development Study Team. Christchurch, 1978), and "Natural resources of the Canterbury region" (Ministry of Works and Development Environmental Design Section. Christchurch, 1983).

1.4 History

The earliest recorded human inhabitants of Banks Peninsula were the Waitaha tribe, whose occupation of the peninsula spanned the end of the moa-hunter period (1350–1500). As moas were gradually exterminated from the Canterbury Plains, the bays of the peninsula, rich in natural resources, became more and more attractive as a home to migrating tribes from the north.

The first of these tribes to make their presence felt on the peninsula were the Ngati-Mamoe tribe, who built strongholds on Mt Pleasant, Long Bay and at Lake Forsyth, and within four generations conquered and subdued all the Waitaha communities of the South Island. Members of the Ngati-Tahu tribe, heading south from Wellington by canoe, claimed Banks Peninsula in a campaign that culminated in the destruction of Pararakariki Pa at Long Bay about 1675. The Ngati-Tahu lived a peaceful existence for 140 years. The peace was eventually broken by the chief Tamaiharanui, who initiated the "Kai huanga" or "eat relation" feud. The feud was finally brought to an end, not by any peace agreement, or even from the rapid decline in the population, but by the need to unite against a common foe — Te Rauparaha.

Te Rauparaha, angered by the boasts of Kaikoura chiefs, sent several raiding parties south to Kaikoura and Banks Peninsula. Notable among these excursions was the 1830 raid, in which Te Rauparaha and his warriors entered Akaroa Harbour hidden aboard the brig Elizabeth, captained by John Stewart. The raids culminated in 1832 in Te Rauparaha's short-lived and successful siege of Onawe Pa on Onawe Peninsula. The fall of Onawe Pa effectively spelt the end of Maori occupation of Banks Peninsula. The Ngati-Tahu population, once numbering in the thousands, was so decimated that by 1880 they numbered less than 250.

The first Europeans to see Banks Peninsula were Captain Cook and his crew on the barque Endeavour, on February 16, 1770. Captain Cook named the area Banks Island, after the ships botanist, Joseph Banks. The error was not discovered until 1809, when a sealer, Captain Chase, attempted to pass through the supposed channel.

Flax traders and whalers became regular visitors from 1815 to 1840. In 1838, French

whaling captain Jean Langlois negotiated with local Maoris for the purchase of the whole of Banks Peninsula, for a down-payment of one woollen overcoat, six pairs of linen trousers, a dozen waterproof hats, two pairs of shoes, a pistol, two woollen shirts and a waterproof coat. Langlois returned to France to set up the Nanto-Bordelaise Company, to arrange the colonisation of Banks Peninsula by French emigrants. 63 emigrants arrived at Akaroa Harbour aboard the whaler Compte de Paris, to find the Union Jack flying and British magistrates administering justice under British sovereignty.

A French community did manage to survive however, under British rule, and many signs of French occupation still remain today — the traditional styled cottages, the names on the narrow streets (eg. Rue Lavaud), place names like Duvauchelle and family names like Brocherie and Le Lieve.

The information presented in this section was abstracted from "The natural and human history of Akaroa and Wairewa Counties: Selected essays" (Queen Elizabeth II National Trust, Wellington, 1987) and "Akaroa" (a set of broadsheets produced by the Langlois-Eteveneaux House and Museum, Akaroa).

1.5 Geological Setting

The Miocene volcanics of Banks Peninsula rest unconformably on a basement of Torlesse Terrane (Triassic), McQueens Volcanics (Cretaceous) and Charteris Bay Sandstone (Paleocene), which are exposed in Gebbies Pass at the head of Lyttelton Harbour (Fig. 1.3). Outcrops of Torlesse sediments occur as high as 300 m above sea level in this area, yet they occur more than 1000 m below sea level in the Leeston-1 borehole, just 30 km away (Weaver, 1980). This may reflect large scale regional faulting of the Mesozoic basement, or a substantial topographic high as suggested by Thiele (1983). The McQueens Volcanics are Cretaceous in age, a Rb/Sr age of 81 $\pm$ 2 Ma having been obtained from rhyolites (Weaver *et al*, 1986). The McQueens Volcanics are correlated with the calc-alkaline Mt Somers volcanics of inland Canterbury which are also of Cretaceous age.

The oldest Miocene volcanics are the Governors Bay Volcanics — basaltic to andesitic and rhyolitic lavas probably erupted 12–11 Ma (Weaver and Sewell, 1986). The Lyttelton Volcanics represent a mildly alkaline to transitional association (basalt to trachyte) of lava flows, pyroclastics and high-level intrusives (Fig. 1.4) erupted 11–10 Ma. Activity was of hawaiian to mildly strombolian style. Following the cessation of activity at Lyttelton Volcano, large breaches were formed in the north-east (now the Lyttelton Harbour), south-west (Gebbies Pass) and south-east (beneath the site of Mt Herbert and Mt Bradley) sectors of the crater wall. The south-east

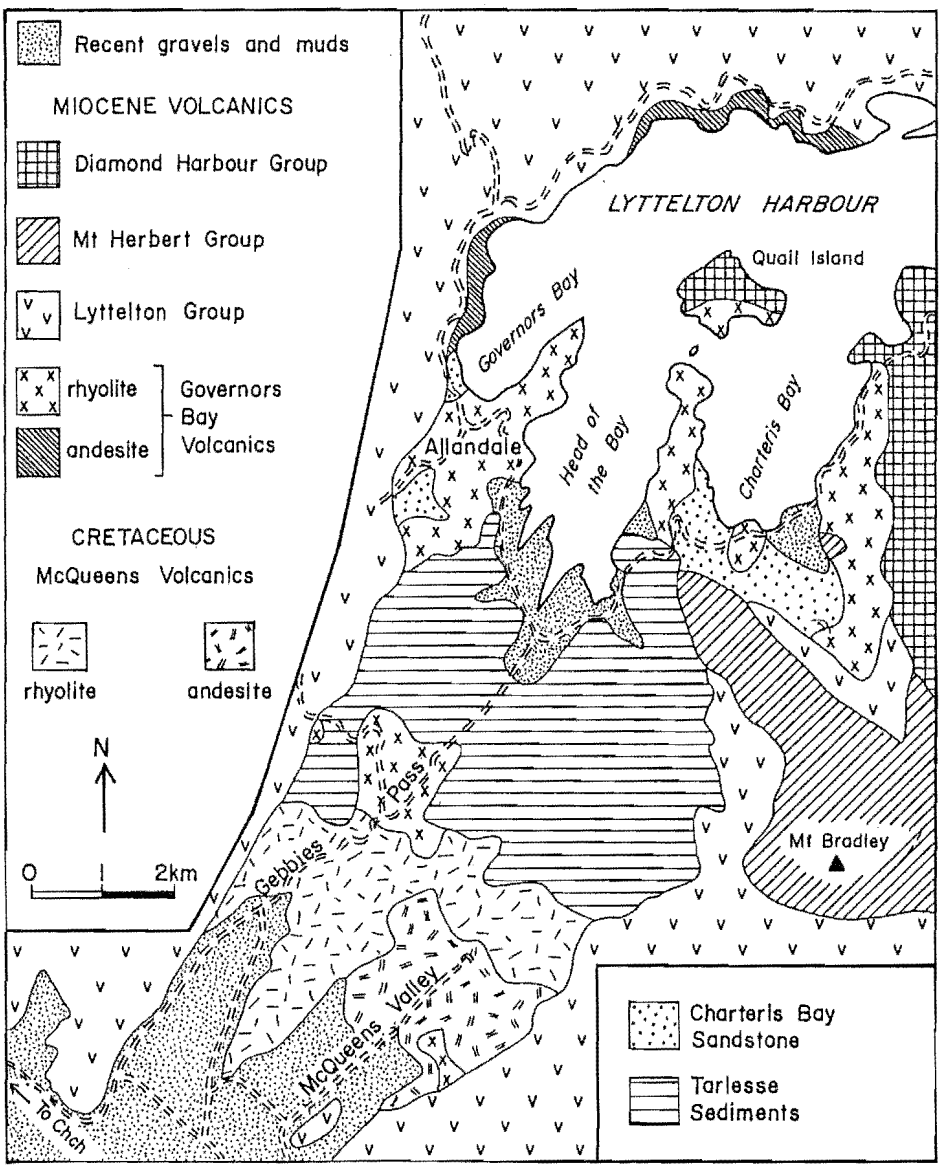

Figure 1.3: Geological map of Gebbies Pass, at the head of Lyttelton Harbour. After Weaver *et al* (1985).

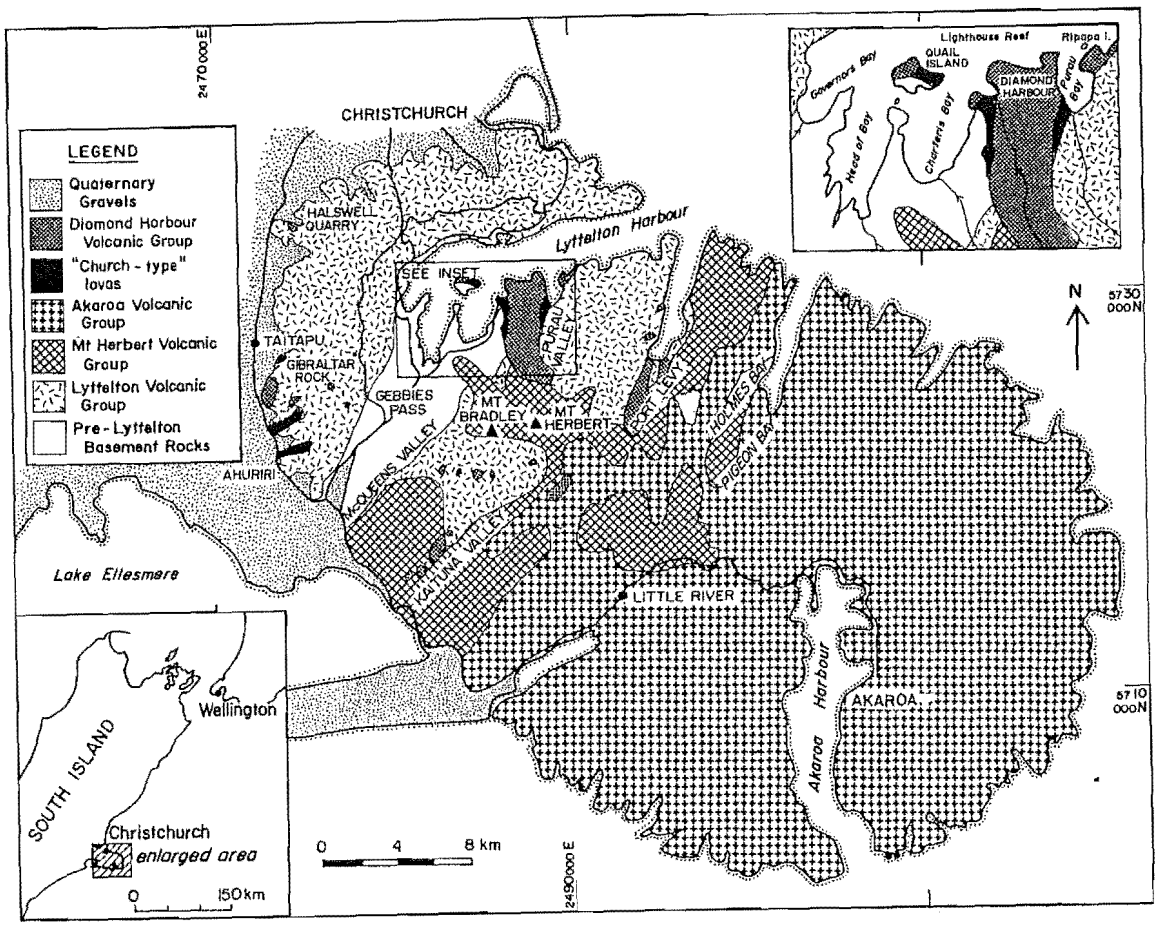

Figure 1.4: Simplified geological map of Miocene volcanic rocks of Banks Peninsula, from Sewell (1988).

breach has since been filled in by products associated with the Mt Herbert Volcanics.

The Mt Herbert Volcanics (9.7–8.0 Ma) comprise a volcanic complex of mildly alkaline basalt lavas, plugs, epiclastic and pyroclastic rocks that were erupted or deposited within the crater of, and on the outer south-eastern and eastern flanks of, Lyttelton Volcano. The Mt Herbert Volcanics have been subdivided into five formations, and a wide variety of volcanic products have been recognised, including lacustrine sediments, strombolian and surtseyan tuff cones (Sewell, 1985). These volcanics reflect the migration of volcanic activity from the Lyttelton centre towards Akaroa.

Activity associated with the Akaroa Volcano commenced about 9.0 Ma, and over a period of about 1.0 Ma a large composite cone of mildly alkaline basaltic to trachytic lava flows, pyroclastics and high-level intrusives was constructed.

As volcanic activity at Akaroa waned, new eruptions of basanitoid to basaltic lava flows, dikes and plugs of the Church Volcanics (8.1–7.3 Ma) began from vents in the crater and on the flanks of the dissected Lyttelton Volcano.

The youngest phase of volcanic activity on Banks Peninsula is represented by olivine-basalt to olivine-hawaiite lava flows, dikes and plugs, minor basanites and conglomerate units of the Stoddart Volcanics (7.0–5.8 Ma), which were erupted from vents around the old Lyttelton Volcano.

Radial drainage patterns developed on Lyttelton and Akaroa Volcanoes during their construction, and as activity waned, stream erosion became the dominant landscaping process. The origin of Lyttelton and Akaroa Harbours has been ascribed to the preferential development of two major radial channels, aided by rapid headward erosion of soft, near-vent, pyroclastic-rich lithologies. The influx of the sea would have further accelerated the process. There is no evidence of either Lyttelton or Akaroa Harbours having been the product of cataclysmic eruptions.

Banks Peninsula appears to have been unaffected by the Kaikoura Orogeny.

At this time (c. 5.0 Ma) Banks Peninsula was still an island lying tens of kilometres off the coast of the mainland. In the last 2.0 Ma, extensive glaciation of the Southern Alps produced enormous volumes of rock debris which were transported by major braided river systems down to the prograding east coast. The shallow seaway between Banks Peninsula and the mainland probably disappeared about 20 000 years ago as sea levels fell.

Loess deposits, locally in excess of 10 m thick, cover much of Banks Peninsula. Raeside (1964) points out that loess deposits are anomalously thick on the seaward

flanks of Banks Peninsula, and that the loess on these slopes and along much of the Canterbury coastline contains sponge spicules, suggesting that during low Pleistocene sea levels an abundant supply of loess was derived from the continental shelf east of Canterbury.

About 6000 years ago, with the retreating of the glaciers, sea level rose to a few metres above the present level. Many of the distinctive coastal features found around Banks Peninsula, such as sea cliffs, stacks and wave-cut platforms, were probably formed at this time.

Banks Peninsula has been a major influence on the form of the eastern coastline of the South Island. Not only has the peninsula protected the soft Quaternary gravels from the full ravages of the sea, but changes in the position of Kaitorete Spit reported by Armon (1973) are correlated with the adjustment of the coastline between Timaru and Banks Peninsula to form a curving shoreline facing the dominant direction of wave approach.

There is no evidence on Banks Peninsula of the raised beach terraces often found along the coasts to the north and south, and the many inlets, bay-head infilling and mudflats imply a history of subsidence rather than emergence.

1.6 Previous Work

Previous work on Banks Peninsula, and Akaroa Volcano in particular, can be characterised, with a few exceptions, by three groupings:

1. Attempts to explain the anomalous thickness of volcanic products in the central Banks Peninsula region, and resolving the number of phases of volcanic activity and the sources of eruptions.
2. Publications which concentrate on specific areas or features of Banks Peninsula geology.
3. Geochemistry and radiometric dating.

Early work by Haast (1860) recognised that Banks Peninsula was essentially volcanic in origin, and that several phases of activity were involved. Haast (1864) recognised five distinct periods of eruption on the peninsula:

1. Construction of Lyttelton and Akaroa Volcanoes

2. Eruptions from three vents near the summit of Mt Herbert
3. Eruption of trachyte from a fissure at Governors Bay
4. Lyttelton trachyte dike swarm
5. Eruption of basalts on Quail Island

but later revised his ideas (Haast, 1879) to recognise three major phases of activity: Lyttelton, Little River (although he was unsure of this) and Akaroa; two centres, at Mt Herbert and Mt Sinclair; and Quail Island.

Hutton (1885) concurred with Haast, and Marshall(1894) stated he was in favour of three eruptive centres associated with Lyttelton.

Speight (1908) doubted Haast's idea of a centre in Little River, preferring to attribute the valley's formation to stream erosion, and proposed three main periods of volcanic activity: Gebbies Pass rhyolites; Lyttelton and Akaroa Volcanoes; and Mt Herbert and Mt Sinclair. Quail Island was considered a candidate for a possible fourth period of activity.

Expanding on his earlier work, Speight (1917) recognised four phases of activity: Rhyolites at Gebbies Pass; Lyttelton and Akaroa Volcanoes; Mt Herbert, with a source in Kaituna Valley, and Mts Fitzgerald and Sinclair, associated with Akaroa Volcano; and Quail Island. Speight correlated the Gebbies Pass rhyolites with rhyolites at Malvern Hills, Rakaia Gorge and Mt Somers, and considered them to be Cretaceous in age. Pebbles of rhyolite were recognised in a trachyte tuff on Onawe Peninsula, indicating that the actual extent of rhyolites on Banks Peninsula may be much greater than the exposures in Gebbies Pass, and that Akaroa may also have been built on a basement of rhyolite. Mention was made of the syenite at Onawe Peninsula, as well as the similarity in composition and formation of the dike swarms on Lyttelton and Akaroa Volcanoes, centred just south of Quail Island and near Onawe Peninsula, respectively. Speight ascribed the formation of Lyttelton and Akaroa Harbours to stream erosion, although a moderate explosion or breach of the cone by lava flows may have been a catalyst.

Speight (1923) described the geology, and presented chemical analyses, of intrusive rocks of Banks Peninsula, including the Akaroa dike swarm and the syenite and gabbro exposed on Onawe Peninsula. Speight noted that the syenite and gabbro on Onawe Peninsula were the only plutonic rocks recognised on Banks Peninsula, and suggested that they represented either a basement complex or a deep-lying portion of the magma reservoir exposed by erosion. No chemical or petrographic gradation could be recognised between the syenite and the gabbro, and the contacts were not exposed. A basalt flow to the north of the gabbro showed evidence of

recrystallisation, which appeared to increase towards the gabbro. With respect to the dike swarm, Speight noted that the generally radial symmetry gave way to more chaotic criss-crossing close to the proposed source on Onawe Peninsula. Compositions ranged from basalt to trachyte but were dominated by trachyte.

Speight (1924) presented chemical analyses and petrographic descriptions of basic volcanic rocks from Banks Peninsula, including some from Akaroa Volcano.

Speight (1933), returning to the question of the anomalous thickness of volcanic products in central Banks Peninsula, attempted to determine the origin of the lavas forming Mts Herbert and Bradley, and the dip-slope from Mt Herbert down to Diamond Harbour, and was forced into the almost untenable position of proposing Akaroa Volcano as the source.

In a paper completely unrelated to discussions of the volcanic activities on Banks Peninsula, Willett(1943) describes briefly a diatomite deposit above Wainui, previously noted by Inglis (1882).

Speight (1940) described the basal rocks of Akaroa Volcano in terms of a basement, on which the main dome was constructed, similar to the Torlesse/rhyolite basement to Lyttelton Volcano. Features cited by Speight as evidence of a basement included

- The presence of the syenite and gabbro on Onawe Peninsula. Three possibilities for the relative ages were considered: that the syenite intruded the gabbro; that the gabbro was intruded at the edge of the syenite; and that the contact was faulted. The law of decreasing basicity was invoked to suggest that the syenite intruded the gabbro.
- Evidence of recrystallisation of a basalt flow adjacent to the gabbro.
- The large volume of trachytic products — tuffs, breccias and lavas — around the harbour shoreline, and the presence of rhyolite and greywacke clasts in the tuffs and breccias.
- The apparent abundance of very weathered volcanics around the shore line.
- The remnants of an old shore platform around Wainui and Tikao.

Speight (1943), in Part 1 of a major review of the geology of Banks Peninsula, discussed the physiography of the peninsula with particular attention to the formation of the harbours principally as a result of stream erosion.

In Part 2, Speight (1944) reviewed the geology of Akaroa Volcano. Speight considered Akaroa Volcano to be a composite cone constructed on a basement of plutonics, trachytoid rocks and very weathered basaltic material. A physiographic break

marked the approximate position of the pre-existing surface. Akaroa Volcano was constructed to an estimated height of 5000 ft, or 6000 ft allowing for submergence that was considered to have occurred. Flows on Mt Herbert were considered to be derived from a vent somewhere in Kaituna Valley, not from Akaroa, as previously held (Speight, 1933). Akaroa was therefore considered to be much younger than Lyttelton Volcano. Places and features of particular geological interest were noted, including Scenery Nook, Dam Rodgers cliff, Little River, the dike swarm, and four trachytoid intrusions.

Oborn and Suggate (1959) distinguished between lavas of the Akaroa Group and lavas forming Mt Herbert and Mt Bradley, which were assigned to the Mt Herbert Volcanics.

Liggett and Gregg (1965), in a paper mainly concerned with the Diamond Harbour Group, erected a new stratigraphy for Banks Peninsula, and produced a map of western Banks Peninsula showing the distribution of units of the new stratigraphy. In this new stratigraphy, the lavas of Mt Herbert and Mt Bradley were again assigned to the Akaroa Group.

Stipp and McDougall (1968) performed whole-rock, K-Ar age dating of samples from Banks Peninsula, with the aim of determining the actual ages of stratigraphic units as established by Liggett and Gregg(1965). A summary of the geochronology of Banks Peninsula is presented in Table 1.1 and K-Ar ages for Akaroa samples measured by Stipp and McDougall are presented in Table 1.2. Note that nine analyses from the original table in Stipp and McDougall (1968) are not included because the samples have since been shown to belong to volcanic groups other than Akaroa.

Evans (1970) presented paleomagnetic measurements and K-Ar age determinations for a sequence of lavas from Lighthouse Road, Akaroa, that spans a major portion of the Akaroa lava pile (Table 1.3). The sequence records seven reversals of the earth's magnetic field, and spans nearly 1.0 Ma.

Smith (1970) described the geology of the inner harbour area.

Price and Taylor (1980) described the geochemistry of the Banks Peninsula volcanoes, with respect to major and trace element analyses and rare earth patterns. Lavas were related by crystal fractionation, based on computer modelling. Price and Taylor (1980) adopted the stratigraphy of Liggett and Gregg (1965), and did not undertake any detailed geological investigations. This is reflected in their conclusions:

Table 1.1: Geochronological Summary of Banks Peninsula Volcanic Events (Ages in m.y.), after Stipp and McDougall (1968, Table 7, p1254).

Major Grouping	Beginning	Termination	Phase
Diamond	6.7	5.8†	Stoddart Formation
Harbour	6.9	6.8	Kaioruru Formation
Group	8.0	7.5	Church Formation and Pre-Kaioruru
Mt Herbert	8.5	8.0	2nd Phase Akaroa
region	9.0	9.0	1st Phase Activity
Akaroa	9.0‡	8.0†	Main Dome
Lyttelton	11.9‡	9.7†	Main Dome

† Youngest measured but probably ended somewhat later.
‡ Oldest measured but probably began somewhat earlier.

Table 1.2: Potassium-Argon Ages from the Akaroa Volcano, after Stipp and McDougall (1968, Table 3, p1246–1247).

Map Ref No.	Material	%K	$^{40}Ar^*/^{40}K$ x 10^{-4}	$\%^{40}Ar$ Atm	Calculated Age (x 10^6 yr)	General Location
32	Andesite	2.065	4.84	8.6	8.20 ± 0.19	Te Oka Road
28	Basalt	0.780	4.74	85.2	8.04 ± 0.20¶	Le Bons Bay
			4.68	87.4		
25	Basalt	1.239	4.79	33.5	8.18 ± 0.24	East Rim
17	Basalt	1.202	4.82	58.6	8.23 ± 0.26	Little River Sth
21	Andesite§	1.662	4.91	11.8	8.38 ± 0.25	Okains Bay
20	Basalt	1.184	4.93	16.3	8.41 ± 0.25	Wainui Quarry
16	Gabbro†	6.872	5.23	43.8	8.92 ± 0.13	Onawe Peninsula
14	Andesite§	1.694	5.29	55.5	9.02 ± 0.27	Pigeon Bay
13	Basalt	0.763	5.16	81.9	9.01 ± 0.26¶	Wainui Headland
			5.33	83.4		
12	Syenite‡	4.032	6.94	32.6	11.80	Onawe Peninsula

$\lambda_\beta = 4.72 \times 10^{-10}$ yr^{-1} $\lambda_\epsilon = 0.585 \times 10^{-10}$ yr^{-1}
$^{40}K = 1.19 \times 10^{-2}$ atom % $^{40}Ar^*$ = Radiogenic Argon
Atm = Atmospheric. All analyses are whole rock.
† biotite ‡ alkali feldspar § basaltic andesite ¶ averaged age

Table 1.3: Potassium-argon ages of samples from the Akaroa sequence, after Evans (1970, Table 1, p168–169, p182–183).

Sample	%K		Ar*	%^{40}Ar Atm.	Calculated Age (My)	Mean Age (My)
69-261	1.163	1.164	1.669	22.7	8.05 ± 0.14	8.28 ± 0.08
	1.165		1.722	30.3	8.30 ± 0.06	
69-262	1.768	1.759	2.668	4.8	8.52 ± 0.06	8.49 ± 0.02
	1.750		2.654	5.9	8.47 ± 0.06	
69-274	1.013	1.015	1.349	21.0	7.47 ± 0.13	
	1.016		1.319	12.6	7.30 ± 0.05	
			1.331	19.8	7.37 ± 0.05	
69-276	1.347	1.344	1.994	22.8	8.33 ± 0.14	8.42 ± 0.04
	1.341		2.019	11.8	8.43 ± 0.06	
69-278	1.288	1.286	1.961	10.6	8.56 ± 0.15	8.64 ± 0.03
	2.284		1.982	8.2	8.65 ± 0.06	
69-279	1.289	1.292	1.841	18.8	8.00 ± 0.14	8.53 ± 0.22
	1.294		2.039	22.7	8.86 ± 0.06	
			1.908	17.6	8.29 ± 0.06	
69-280	1.239	1.237	1.827	23.7	8.29 ± 0.14	8.25 ± 0.01
	1.235		1.818	5.4	8.25 ± 0.06	
69-281	1.036	1.037	1.573	21.1	8.52 ± 0.06	
	1.037					
69-282	1.350	1.350	2.045	24.9	8.51 ± 0.15	8.33 ± 0.07
	1.249		1.996	19.4	8.30 ± 0.06	
69-283	1.234	1.229	1.782	23.4	8.14 ± 0.14	8.27 ± 0.05
	1.224		1.815	26.9	8.29 ± 0.06	
69-284	1.112	1.111	1.707	24.1	8.63 ± 0.07	
	1.109					
69-285	1.223	1.222	1.870	23.2	8.59 ± 0.15	
	1.221					
69-287	1.533	1.539	2.350	19.3	8.57 ± 0.07	
	1.545					
69-288	1.763	1.761	2.708	18.9	8.63 ± 0.15	
	1.759					
69-294	2.071	2.078	3.238	14.4	8.75 ± 0.15	
	2.084					
69-296	0.946	0.950	1.578	81.1	9.33 ± 0.18	8.63 ± 0.21
	0.953		1.428	58.8	8.44 ± 0.07	
			1.504	60.4	8.89 ± 0.12	
69-298	1.184	1.184	1.817	64.1	8.61 ± 0.08	8.62 ± 0.01
	1.184		1.821	64.1	8.63 ± 0.10	
69-299	1.214	1.219	1.878	63.0	8.65 ± 0.07	8.73 ± 0.12
	1.224		1.935	69.5	8.91 ± 0.11	
69-301	1.502	1.498	2.406	11.7	9.01 ± 0.06	9.09 ± 0.08
	1.494		2.452	19.0	9.19 ± 0.07	
69-303	1.466	1.470	2.354	9.4	8.99 ± 0.16	8.90 ± 0.04
	1.474		2.325	10.2	8.88 ± 0.07	
69-304	1.256	1.251	2.045	37.0	9.18 ± 0.16	9.19 ± 0.01
	1.245		2.048	27.4	9.19 ± 0.07	
69-306	0.868	0.870	1.401	65.0	9.04 ± 0.16	
	0.871					

$\lambda_\beta = 4.72 \times 10^{-10}$ yr^{-1} $\lambda_\epsilon = 0.585 \times 10^{-10}$ yr^{-1} ^{40}K = 1.19×10^{-2} atom %
^{40}Ar* = Radiogenic Argon ($\times 10^{-11}$ mole g^{-1}) Atm = Atmospheric All analyses are whole rock.

> "Between 12 and 9.7 m.y. a large volcanic dome, composed mainly of hawaiite, was built at Lyttelton. Dykes, which intrude the Lyttelton volcanic sequence, range in composition from basalt to trachyte. Late, mildly alkalic, basaltic flank flows (7.5–5.8 m.y.) occur in several areas and they, and the differentiated rocks of the dyke swarm can be related by a crystal fractionation model which has been quantitatively tested."

Here, they are relating by crystal fractionation lavas of the Lyttelton dike swarm and the Diamond Harbour Group — lavas that are geochemically distinct, and separated temporally by 2.0 Ma and a period of severe dissection of the Lyttelton cone.

Falloon (1982) described the geology and geochemistry of the Saddle Hill — French Hill area, and the geochemistry of selected samples from Onawe Peninsula. Major and trace element analyses were presented for a wide range of rock types.

Sewell (1985, 1988), in a major stratigraphic and geochemical study of central Banks Peninsula geology, has erected a new stratigraphy for the Miocene volcanics of Banks Peninsula (Fig. 1.5), redrawn the geological map (Fig. 1.4) and proposed an evolutionary model for the geology of the peninsula (Fig. 1.6).

1.7 Nomenclature

Akaroa Volcanic Group lavas are mildly alkaline in composition and have therefore been classified according to the alkali olivine-basalt association terminology of Coombs and Wilkinson (1969) and MacDonald and Katsura (1964). Rocks are assigned names according to the samples' position on a plot of Differentiation Index versus plagioclase Ratio (Fig. 1.7). Major rock names are prefixed by normative mineral abbreviations (*ne-*, *hy-*, *qz-*) according to the degree of silica saturation. In the case of strongly undersaturated rocks, alkali olivine-basalts with $\geq 5.0\%$ normative *ne* are classified under the general term of basanitoids, and if modal nepheline is $> 5\%$ are termed basanites.

Fragmental deposits are classified according to grain-size and mechanism of fragmentation (pyroclastic, epiclastic) following the terminology of Schmid (1981) and Fisher and Schmincke (1984) (Table 1.4, 1.5). Fragmental deposits that are a direct result of volcanic activity are termed pyroclastic, while those deposits derived from weathering and erosion of older material are termed epiclastic. The term tuffaceous is applied to deposits containing significant proportions of both pyroclastic and epiclastic material. Grain size is determined by visual estimation. No attempt was

GROUP	ESTIMATED VOLUME	FORMATION	K/Ar AGE RANGE (Ma)	LITHOLOGY	MAIN LOCALITIES
DIAMOND HARBOUR VOLCANIC GROUP	20 km³	STODDART BASALT	7·0 - 5·8	Fresh, columnar-jointed, olivine ± clinopyroxene phyric basanites, olivine-basalts and olivine-hawaiites – rare olivine-basalt dikes	Taitapu - Ahuriri, Kaituna Valley Port Levy, Diamond Harbour, Quail Island
		KAIORURU HAWAIITE	6·9 - 6·8	Commonly weathered, vesicular, pale pink, olivine ± clinopyroxene-phyric and aphyric olivine-hawaiites	Diamond Harbour, Quail Island
"CHURCH TYPE" LAVAS	5 km³	CHURCH BASALT	8·0 - 7·3	Fresh, columnar-jointed, olivine ± clinopyroxene ± plagioclase-phyric olivine-basalts	Diamond Harbour, Quail Island, Taitapu - Ahuriri
		CHATEAU INTRUSIVES	8·0	Grey, columnar to knobbly-jointed aphyric hawaiites	Charteris Bay - Bradley Park
		DARRA BASANITOID	8·1 - 7·7	Fresh, columnar-jointed olivine ± clinopyroxene-phyric basanitoids -rare basanitoid dikes	Diamond Harbour, Quail Island, Ahuriri - Taitapu
AKAROA VOLCANIC GROUP	1200 km³		9·0 - 8·0	Fresh, medium to fine-grained, olivine-clinopyroxene-plagioclase-phyric and grey, aphyric hawaiites - rare trachyte domes and dikes	South side of Kaituna Valley - Port Levy
MT HERBERT VOLCANIC GROUP	100 km³	HERBERT PEAK HAWAIITE	8·5 - 8·0	Grey, columnar-jointed, aphyric and rarely olivine-phyric olivine-hawaiites	Mt Herbert - Mt Bradley
		PORT LEVY FORMATION	8·9 - 8·5	Grey-black, columnar-jointed, aphyric hawaiites-rare porphyritic basalts and mugearites	Port Levy - Western Valley
		ORTON BRADLEY FORMATION	9·5 - 8·6	Black, fresh aphyric, olivine-hawaiites & olivine ± clinopyroxene ± plagioclase-phyric olivine-basalts	Mt Herbert - Mt Bradley
		KAITUNA VALLEY HAWAIITE	9·7 - 9·5	Columnar-jointed, dark grey-black, fresh, olivine ± clinopyroxene-phyric olivine-hawaiites	Kaituna - McQueens Valleys
LYTTELTON VOLCANIC GROUP	350 km³		11 - 9·7	Moderately weathered, plagioclase ± olivine ± clinopyroxene-phyric hawaiites - trachyte lava flows and domes - numerous trachytic and basaltic dikes	North side of Kaituna Valley - Mt Herbert

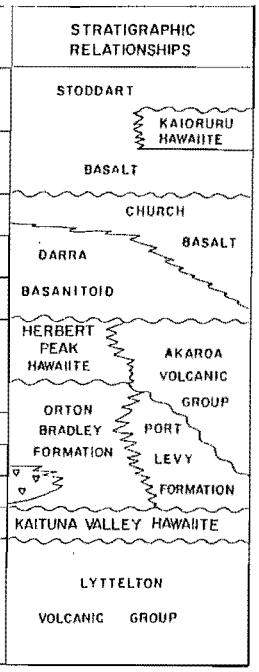

Figure 1.5: Stratigraphy for the Miocene volcanics of Banks Peninsula, as proposed by Sewell (1988).

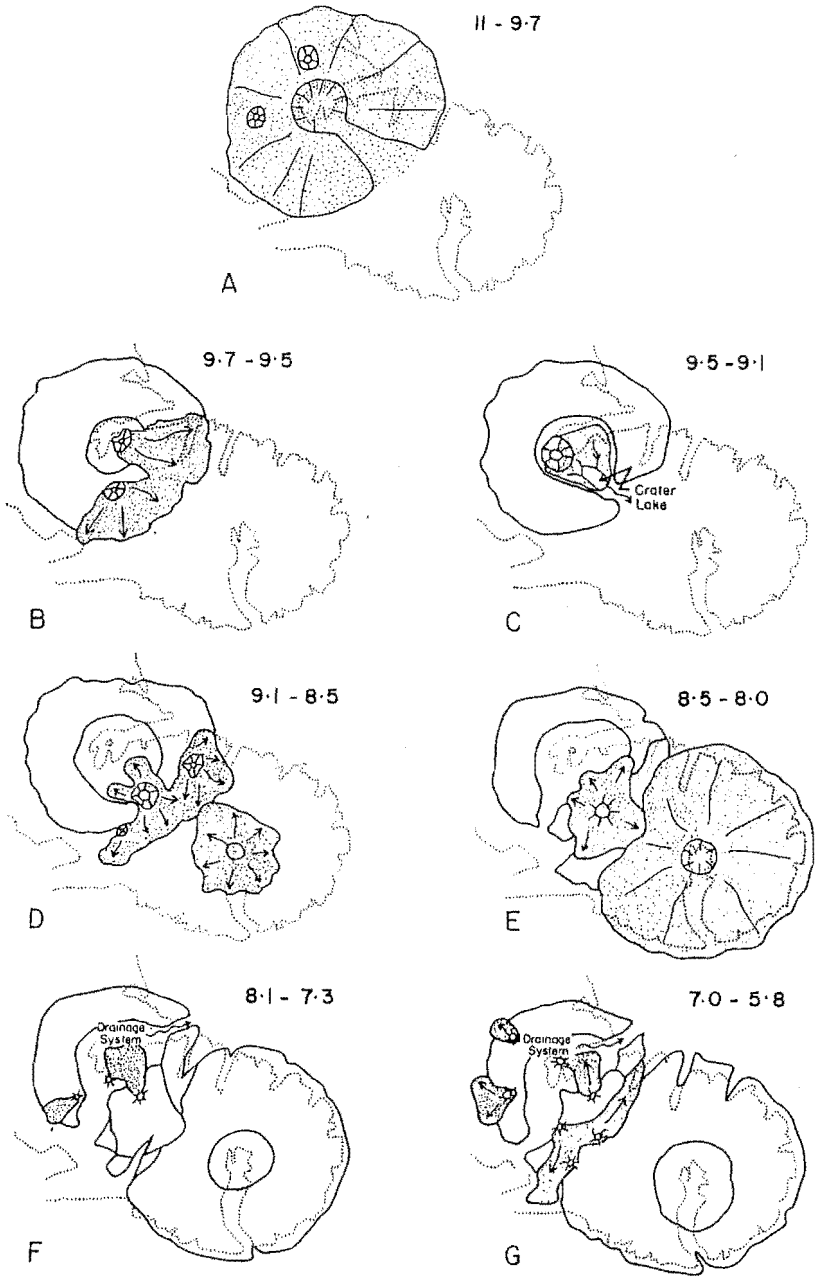

The geological evolution of Banks Peninsula volcanoes. A *11–9.7 Ma*: Construction of the main cone of Lyttelton Volcano. Breached in the southeast during final stages of eruption. B *9.7–9.5 Ma*: Initial eruptions of the Mt Herbert volcanics (Kaituna Valley Hawaiite) onto the southeastern flanks of the eroded Lyttelton cone. C *9.5–9.1 Ma*: Deep excavation of Lyttelton crater by erosion. Eruption of basalt lavas (Orton Bradley Formation) and formation of a lake on the crater floor (Mt Bradley Volcaniclastic Member). D *9.1–8.5 Ma*: Further eruptions of Mt Herbert volcanics from vents close to the crater wall breach (Orton Bradley Formation) and from near Port Levy (Port Levy Formation). Akaroa Volcano becomes active. E *8.5–8.0 Ma*: Construction of the main cone of Akaroa Volcano. Final eruptions of Mt Herbert volcanics (Herbert Peak Hawaiite). A new breach in the Lyttelton crater opens along Gebbies Pass. F *8.1-7.3 Ma*: Eruption of the "Church-type" lavas (Darra Basanitoid, Chateau Intrusives, Church Basalt) on the flanks and floor of the eroded Lyttelton crater. Breach in crater wall to form main channel along which Lyttelton Harbour developed. Excavation of Akaroa Volcano. G *7.0–5.8 Ma*: Eruption of the Diamond Harbour lavas (Stoddart Basalt, Kaioruru Hawaiite) from numerous vents on the flanks and floor of the eroded Lyttelton crater.

Figure 1.6: The geological evolution of Banks Peninsula volcanoes, after Sewell (1988).

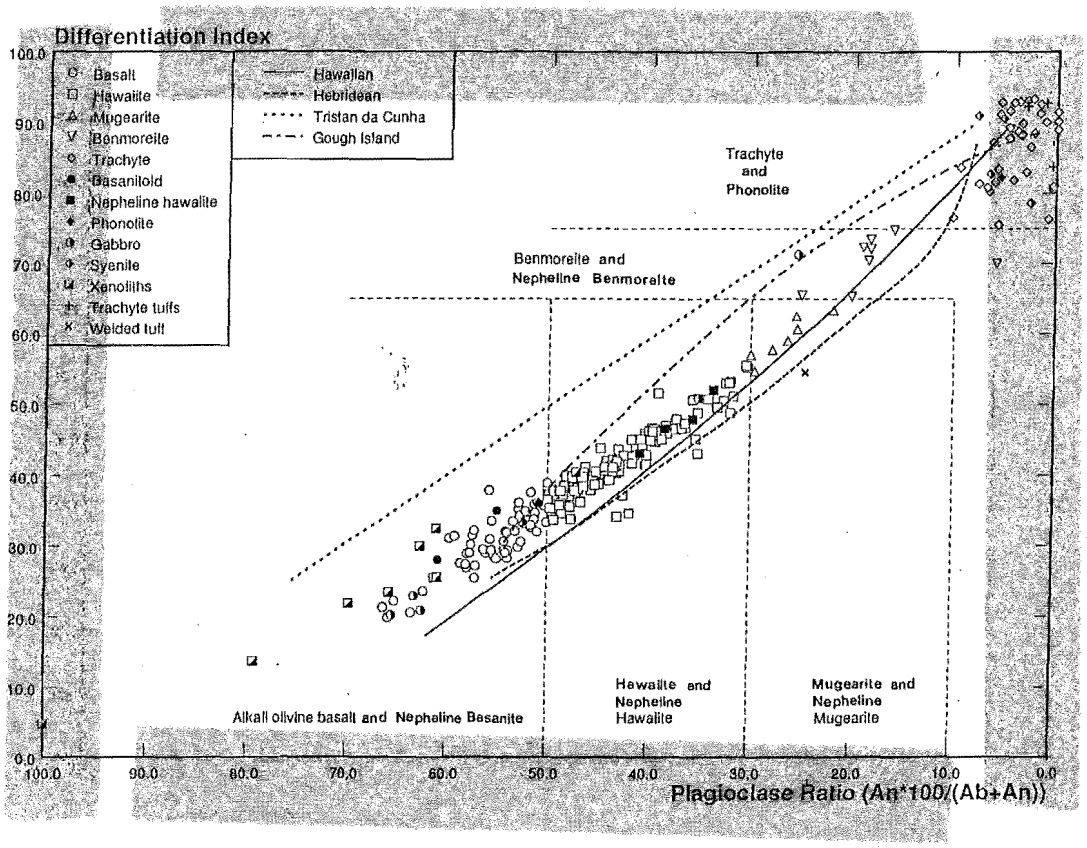

Figure 1.7: Plot of differentiation index versus plagioclase ratio, showing the fields used to assign compositional names to volcanic rocks.

made to perform quantitative grain-size analysis as most of the fragmental deposits described are moderately to well indurated.

Eruption types and their associated deposits are classified in general terms according to the inferred explosive nature of the eruption and the degree of fragmentation of ejecta, ranging from hawaiian (quietly effusive), through strombolian and Vulcanian to Plinian (explosive, exceptionally violent). The term "Surtseyan" is used to refer to the, often violent, eruption of basaltic magma through water and the associated deposits characterised by highly comminuted pumice fragments.

Table 1.4: Granulometric classification of pyroclasts and of unimodal, well-sorted pyroclastic deposits (after Schmid, 1981, Table 1).

Clast size (mm)	Pyroclast	Pyroclastic deposit	
		Mainly unconsolidated: tephra	Mainly consolidated: pyroclastic rock
	Bomb, block	Agglomerate, bed of blocks or bomb, block tephra	Agglomerate, pyroclastic breccia
64 mm			
	Lapillus	Layer, bed of lapilli or lapilli tephra	Lapilli tuff
2 mm			
	Coarse ash grain	Coarse ash	Coarse (ash) tuff
1/16 mm			
	Fine ash grain (dust grain)	Fine ash (dust)	Fine (ash) tuff (dust tuff)

Table 1.5: Terms for mixed pyroclastic–epiclastic rocks (after Schmid, 1981, Table 2).

Pyroclastic		Tuffites (mixed pyroclastic-epiclastic)	Epiclastic (volcanic and/or nonvolcanic)	Avg clast size (mm)
Agglomerate, agglutinate pyroclastic breccia		Tuffaceous conglomerate, tuffaceous breccia	Conglomerate, breccia	64
Lapilli tuff				2
(Ash) tuff	coarse	Tuffaceous sandstone	Sandstone	1/16
	fine	Tuffaceous siltstone	Siltstone	
		Tuffaceous mudstone, shale	Mudstone, shale	1/256
100	75		25	0% by volume
← Pyroclasts				
→ Volcanic + nonvolcanic epiclasts (+ minor amounts of biogenic, chemical sedimentary and authigenic constituents)				

Chapter 2

STRATIGRAPHY AND VOLCANOLOGY

2.1 Introduction

Products of the stratovolcanic centre of Akaroa Volcano form volumetrically and in area the most significant stratigraphic grouping on Banks Peninsula. Akaroa Volcano forms that part of Banks Peninsula east of a line from Big Bay in the north, to Kaituna Lagoon in the south (Fig. 1.1), some 780 km^2 of the total 1200 km^2 area of Banks Peninsula, with an estimated volume of 1200 km^3. In comparison, Sewell (1988) estimated volumes of the other major stratigraphic groups comprising Banks Peninsula at 350 km^3 (Lyttelton Volcanic Group), 100 km^3 (Mt Herbert Volcanic Group), 5 km^3 ("Church-type" lavas), and 20 km^3 (Diamond Harbour Volcanic Group). Since much of Lyttelton and Akaroa Volcanoes are below sea level, these estimates must be considered minima.

Thick loess deposits mask much of the Akaroa Harbour basin and the outer flanks of the volcano, restricting good exposures of lava sequences to steep valley walls, ridges, road cuttings and the inner harbour coastline.

Because of the large area over which Akaroa Volcano extends, and the relatively small areas of continuous exposure, no attempt has been made to map the entire volcano or to establish a formal stratigraphy. Rather, the approach adopted in this thesis is to illustrate in general terms the stratigraphy and volcanology of Akaroa Volcano through descriptions, maps and measured sections of specific geographic areas and volcanic features. These data, presented in this and the next chapter, provide the basis for a more detailed discussion of the petrology, geochemistry and

petrogenetic evolution of Akaroa Volcano, which is the main emphasis of this thesis. Appendix A contains locations and descriptions of samples referred to in this and successive chapters.

2.2 Definition of Akaroa Volcanic Group

The **Akaroa Volcanic Group** is defined as comprising all the volcanic products of central, flank and parasitic vent eruptions in the south-eastern two-thirds of Banks Peninsula, within the age range 9.0[1] to 8.0 Ma, which collectively form Akaroa Volcano. The term "Group" is used here, as in other stratigraphic studies of composite volcanoes (Romano, 1982), to collectively refer to a polymorphic set of units forming a single, discrete volcano. Formation status is reserved for the products of individual cone-forming episodes within the history of a volcano, and in the case of Akaroa, no formations are distinguished.

The term "Akaroa Volcanic Group" used here is synonymous with the same term proposed by Sewell (1988), and previously the Akaroa Volcanics (Oborn and Suggate, 1959) and the Akaroa Group (Liggett and Gregg, 1965).

The Akaroa Volcanic Group consists dominantly of lava flows with intercalated pyroclastic and epiclastic deposits, intruded by a radial dike swarm and numerous domes and sills. Minor plutonics (syenite and gabbro) are also present. Compositions of extrusives and shallow intrusives range from basanitoid to trachyte and phonolite, with extrusives dominated by hawaiite compositions and shallow intrusives dominated by benmoreite and trachyte compositions.

At its western boundary (Fig. 1.4), Akaroa Volcanic Group lavas unconformably overlie older formations of the Mt Herbert Volcanics. However, in the vicinity of Mt Herbert, Akaroa lavas interfinger with lavas from younger formations of the Mt Herbert Volcanics (Sewell, 1985). The contact between Akaroa Volcanic Group and the Mt Herbert Volcanics shows considerable relief, rising from sea level near Kaituna Lagoon to over 600 m at the head of Kaituna Valley. Over much of central Banks Peninsula the contact is over 300 m above sea level. The contact is not exposed for much of its length, but is marked by a broad break in slope with associated springs and swampy vegetation, or a thin brick-red pyroclastic horizon.

Mapping has shown that the lavas and pyroclastics of which Akaroa Volcano is constructed can be grouped into an Early Phase and a Main Phase. These phases correspond to distinct time periods within the evolution of the volcano. Intrusive

[1]This is a minimum age — rocks from the Early Phase (see discussion later in this chapter) and rocks buried beneath sea level may be considerably older.

rocks (see Chapter 3) occur throughout the stratigraphic succession, and appear to have been intruded at intervals throughout the history of the volcano. For this reason, they have not been assigned to a particular "phase".

2.3 The Early Phase

All rocks exposed around the inner shoreline of Akaroa Harbour, with the exception of the plutonics on Onawe Peninsula, belong to and comprise all the exposed extent of the Early Phase of Akaroa Volcano. The Early Phase includes all the volcanics which Speight (1940) suggested might form a substratum to Akaroa Volcano. Although Early Phase rocks are compositionally similar to younger volcanics of the Main Phase, they are separated from volcanics of the Main Phase by an erosional unconformity which is thought to represent a significant time break. The geology of these rocks is illustrated in Map 1 (Map Pocket).

The Early Phase is characterised by:

- A significantly higher proportion of trachytic material, compared with the Main Phase. This large volume of trachytic material occurs as a large trachyte dome, thick deposits of trachyte breccia and tuff, rare sills and flows.
- A higher proportion of pyroclastic and epiclastic material, and greater variations in compositional, lithological and volcanological attributes. Compositions range from basalt to trachyte. Volcanological forms include lahars, tuffs, breccias, strombolian scoria cones and lava flows.
- Very weathered basaltic flows intercalated with pyroclastic and epiclastic deposits, exposed around the shoreline.
- A significant proportion of the exposed dikes of the Akaroa dike swarm, which pervade the Early Phase.

The Early Phase can be subdivided into three sub-phases (Early Phase I, II and III) based on lithological content and stratigraphic position:

Early Phase I: The oldest basaltic lava flows exposed within Akaroa Volcano, occurring only on Onawe Peninsula.

Early Phase II: Trachyte lavas and pyroclastics (with minor basaltic tuffs) forming a major compositional marker horizon overlying Early Phase I.

Early Phase III: Weathered basaltic flows and pyroclastics overlying Early Phase II.

Syenite and Gabbro are exposed at the southern end of Onawe Peninsula. Although the plutonics appear to intrude rocks of the Early Phase, it is not clear whether they may also have intruded rocks of the Main Phase. Since their volcanological and stratigraphic relationship to both Early Phase and Main Phase rocks is uncertain, the syenite and gabbro are not included in either phase, even though they only occur within the outcrop area of the Early Phase. The syenite and gabbro are discussed in detail in Chapter 3.

2.3.1 Early Phase I

The oldest extrusive rocks exposed on Akaroa Volcano are very weathered, grey, fine-grained, aphyric basaltic lava flows, which crop out on the east and west sides of Onawe Peninsula, 5–10 m north of the gabbro. The contacts between Early Phase I lava flows and the gabbro are not exposed, but are considered to be intrusive.

2.3.2 Early Phase II

Welded Tuff

On the west side of Onawe Peninsula, the Early Phase I lava flow is conformably overlain by a dark grey-black, welded polylithic lapilli tuff. Clasts range in size from < 1 mm to 15 mm, are angular (occasionally sub-rounded) and welded by a dark grey-black, fresh, glassy basaltic lava. Clast lithologies include a wide range of basaltic to trachytic lavas, mudstones and sandstones. Two facies can be recognised — a fine-grained (clasts < 5 mm in diameter) facies and a coarse-grained (clasts 5–15 mm diameter) facies rich in mudstone and sandstone lithics. The relationship between the facies is gradational but spatially irregular.

Both upper and lower contacts appear to be conformable. The attitude of bedding within the tuff can not be measured, but as a whole the unit dips north at 5–10°.

Trachyte Tuff, Agglomerate, Sill and Flow

Trachyte lapilli tuff conformably overlies the welded tuff on the west side of Onawe Peninsula and the Early Phase I basaltic lava flow on the east side of Onawe Peninsula. Trachyte lapilli tuffs and agglomerates exposed on Takamatua Peninsula and the southern shore of French Farm Bay are considered to be coarse facies equivalents.

On the west side of Onawe Peninsula the trachyte tuff appears to conformably overlie the welded tuff, and is a cream-brown, poorly sorted, clast-supported, weakly indurated, massive to poorly bedded lapilli tuff. Clasts range from < 0.5 cm to 5 cm and are almost all trachytic. Bedding, where measured, gives conflicting and irregular attitudes, and is highly disrupted. The tuff appears to have suffered extensive hydrothermal alteration, and is intensely intruded by trachyte dikes.

On the east side of Onawe Peninsula the contact between the trachyte tuff and the underlying Early Phase I basalt flow is marked by a pale yellow-brown, weathered, very fine-grained, aphyric trachyte, which appears to have been intruded as a sill.

The trachyte tuff, which is exposed for $\approx$ 250 m along the shore platform and in the cliff at the back of the shore platform, is $>$ 5m thick and dips north to north-east at angles of 10–12°. To the south, the base of the unit is a massive to coarsely (decimetre scale) bedded, poorly sorted, clast-supported, subangular to subrounded, polylithic to monolithic, lapilli tuff. Clasts range in size from < 0.5 cm to > 4 cm, but are typically 1–2 cm in diameter. Clasts are entirely trachytic in composition, but there is considerable variation in lithological characteristics, with very fine grained, aphyric to weakly orthoclase-phyric, flow banded and pumiceous lithologies being common. To the north (up sequence), the unit grades into a yellow-brown to purple, very well laminated (millimetre scale), moderately sorted, coarse to fine tuff. Coarse tuff horizons alternate repetitively with fine tuff horizons — the contacts between horizons are always gradational and conformable (Fig. 2.1). Accretionary lapilli, 1–5 mm in diameter, occur in very thin, sparse horizons throughout the fine tuff. Speight (1940) reported that the tuff contained fragments of rhyolite and greywacke, but no such fragments were found during this study, despite repeated searches. However, sedimentary fragments (including ?Torlesse) do occur in the welded tuff immediately below the trachyte tuff on the west side of Onawe Peninsula.

Other small exposures of trachyte tuff, considered to be equivalents of the coarse basal portion of the trachyte lapilli tuff, occur to the north on the western and eastern shore platforms of Onawe Peninsula (N36C/04091542, N36C/04201539), and on the south coast of French Farm Bay (N36C/03451384).

Massive to coarsely bedded (decimetre scale), poorly to moderately sorted, clast supported, angular to subrounded, polylithic, coarse trachyte lapilli tuff-agglomerate exposed along the north-western coast of Takamatua Peninsula (N36C/05551361, N36C/05371327, N36C/05471270) is considered to be a coarse facies equivalent of the trachyte lapilli tuff exposed on Onawe Peninsula. At its best exposure (N36C/05371327), the trachyte agglomerate forms the shore platform and the cliff behind, some 20 m+ in thickness, and dips almost due east at 10°. Within the agglomerate, three distinct facies variants can be recognised. The dominant facies variant is a massive bedded, poorly sorted, clast supported, subangular to subrounded, polylithic, coarse lapilli tuff-agglomerate. Clasts range in size from < 1 cm to 30 cm, but are typically 2–5 cm in diameter. The clasts are entirely trachytic in composition and are often flow-banded or pumiceous (Fig. 2.2). The second facies variant is a massive bedded, moderately sorted, clast supported, subangular to subrounded, polylithic, fine lapilli tuff. Clasts are all fine grained, aphyric or pumiceous trachytes, ranging in size from 2–5 mm in diameter. Matrix material is absent. The third facies variant is a massive bedded, moderately sorted, clast supported, angular, polylithic, welded fine lapilli tuff. Clasts are all fine grained trachytes, range in size from 2–5 mm in diameter, are angular, with interdigitating boundaries, and appear to have been slightly flattened and welded in the plane of bedding. Matrix material is absent. These three facies variants interfinger to varying degrees, and all contacts appear gradational and conformable.

On the headland to the north of Lushingtons Bay (N36C/05371327), a 1 m thick, purple-brown to grey-green, fine grained, aphyric *qz*-trachyte lava flow occurs within the agglomerate.

Tikao Trachyte Dome

The peninsula between Petit Carenage Bay and Tikao Bay is composed entirely of trachyte. The contacts between the trachyte and adjacent rocks are not observed, but in Tikao Bay a lahar observed within a few metres of the trachyte appears to overlie the trachyte. The trachyte is at the same height topographically as the syenite of Onawe Peninsula and the trachyte agglomerate of Takamatua Peninsula. From a distance, the outcrop is distinctive in having a very planar upper surface.

In outcrop the trachyte is a massive, pale to dark green, fine grained, aphyric to weakly orthoclase-phyric trachyte. Along the north-east coast (N36C/03961288) the trachyte grades rapidly (over ≈ 5 m) from the north and south into a pale grey-white to purple-brown, open-textured, aphyric to glomerophyric, microsyenite. Coarse (up to 10 cm diameter) glomerophyric aggregates of coarse (> 1 cm diameter) orthoclase feldspar phenocrysts, and red-brown, coarse grained aphyric trachyte clasts occur throughout the coarse zone and the fine grained trachyte immediately to the north

Figure 2.1: Upper, very well laminated part of the trachyte lapilli tuff east side of Onawe Peninsula (N36C/04251468), showing alternation of coarse and fine tuff horizons.

Figure 2.2: Massive, poorly sorted, clast supported, polylithic coarse lapilli tuff-agglomerate variant of the trachyte agglomerate, exposed on the headland north of Lushingtons Bay (N36C/05371327). Note the abundance of flow-banded and pumiceous clasts, and the presence of both light and dark coloured clasts. Lens cap is for a 50 mm lens.

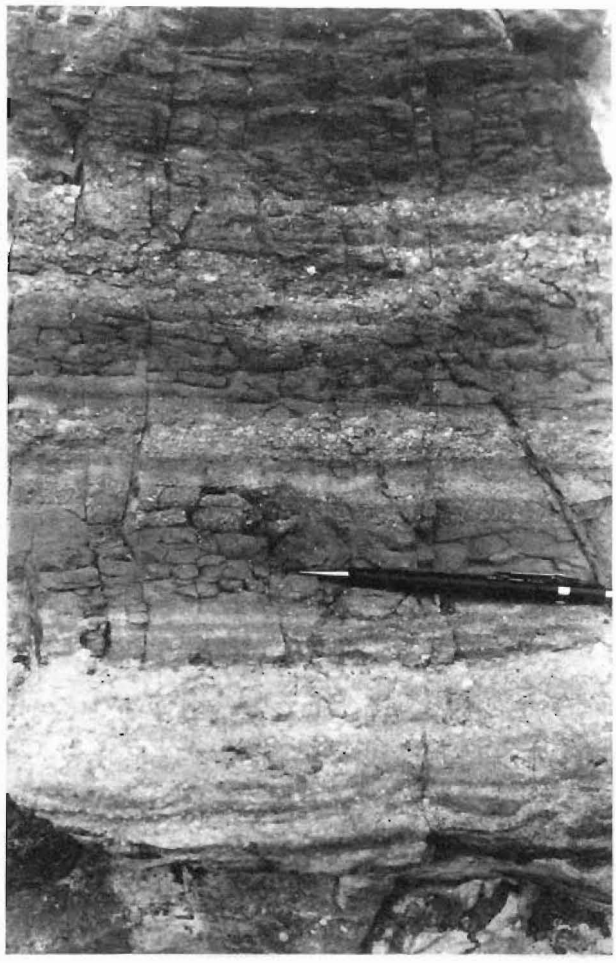

and south. This large trachyte body is thought to be an exogenous dome.

2.3.3 Early Phase III

The trachytic rocks of the basement complex are immediately overlain by basaltic flows, lahars, tuffs, scoria cones and breccias of the Early Phase III. The contact between Early Phase III rocks and older rocks shows considerable relief (20–100 m), indicating a period of erosion prior to eruption of Early Phase III flows and pyroclastics.

Flows, Tuffs and Lahars

The Early Phase III is dominated by very weathered basaltic flows. The lava flows are often lensoidal in outcrop and exhibit variable and irregular attitudes, although they often dip away from the centre of the harbour. The lavas are very weathered, dark grey-black, fine to coarse grained, aphyric or rarely weakly plagioclase-olivine-pyroxene phyric basanitoids to *ne*-hawaiites. Flows may be intercalated with thin (< 1 m thick), red to red-brown, massive to well laminated (centimetre scale), moderately sorted, occasionally reverse or normally graded, very fine to coarse basaltic tuffs. Where both top and bottom contacts are exposed, and outcrop permits, the basaltic tuffs can be seen to mantle underlying units. Rare lahars may also be present. Speight (1940) commented on the excessive decomposition of rocks, especially around Duvauchelle, and concluded that they were part of an earlier episode of activity.

Scoria Cone and Breccia Pipe

At the northern end of Onawe Peninsula, northward dipping Early Phase III flows overlap the southern flanks of a basaltic scoria cone (N36C/04161585). The cone is constructed of red-brown, well bedded, fine to medium basaltic ash containing abundant basaltic scoria and lava bombs. The bedding dips at angles of 20° to 25° away from the approximate centre of the circular outcrop (N36C/04151585). Bomb morphologies include ribbon, spindle and cow-dung bombs (Fig. 2.3). Smaller (100–150 mm diameter) spindle bombs are particularly well shaped. The scoria cone is intruded by a 20 m diameter, oval-shaped pipe of yellow-brown, massive, poorly sorted, subangular to subrounded, coarse lapilli tuff-agglomerate. The clasts appear to be entirely trachytic in composition, and are hydrothermally altered and weathered, sometimes to a clayey consistency.

Coarse Pyroclastic Breccia

A massive, unsorted, angular, welded, polylithic very coarse pyroclastic breccia is exposed in a cliff, beneath overhanging Early Phase III flows (Fig. 2.4), on the east side of Onawe Peninsula (N36C/04201529). Clasts range in size from 1 cm to > 1 m, and are typically angular in shape. Some ribbon or dike-shaped clasts have been preserved. Clast lithologies include a variety of fine grained, aphyric and orthoclase-phyric trachytes, dark grey-black, fine grained, aphyric vesicular and non-vesicular basalts and dolerites. Clasts are welded together by a pale green, weathered, aphyric trachyte lava.

2.4 The Contact Between the Early Phase and the Main Phase

Very fresh, very fine to fine grained, dark grey-black, aphyric or occasionally plagioclase-olivine-pyroxene-phyric basanitoids to *qz*-hawaiites and rare intercalated very red, very fine grained, friable basaltic tuffs can be seen resting unconformably on Early Phase III rocks, particularly between Tikao Bay and Wainui on the west side of the harbour, and on the eastern and upper slopes of Hammond and Takamatua Peninsulas on the east side of the harbour.

The contact generally dips at 5° to 10° away from the centre of the harbour, and shows considerable relief. The strong relief and the very fresh lavas immediately overlying very weathered lavas suggests that this contact represents a substantial period of quiescence in the construction of the volcano, during which time erosion was active.

The very fresh lavas are more like lavas of the Main Phase than lavas of the Early Phase, and may be more appropriately assigned to the Main Phase. However, there is an unexposed stratigraphic interval of > 100 m, between the fresh lavas exposed around the harbour and the base of measured stratigraphic sections through the Main Phase (see section 2.5). This stratigraphic gap is marked, in the inner harbour basin, by a distinct break in slope between 100 m and 300 m above sea level, and very thick loess deposits. The break in slope may represent a major stratigraphic boundary.

Figure 2.3: A large spindle bomb in a basaltic scoria cone at the northern end of Onawe Peninsula (N36C/04101598).

Figure 2.4: Unsorted, welded, polylithic, very coarse pyroclastic breccia exposed on the east side of Onawe Peninsula (N36C/04201529).

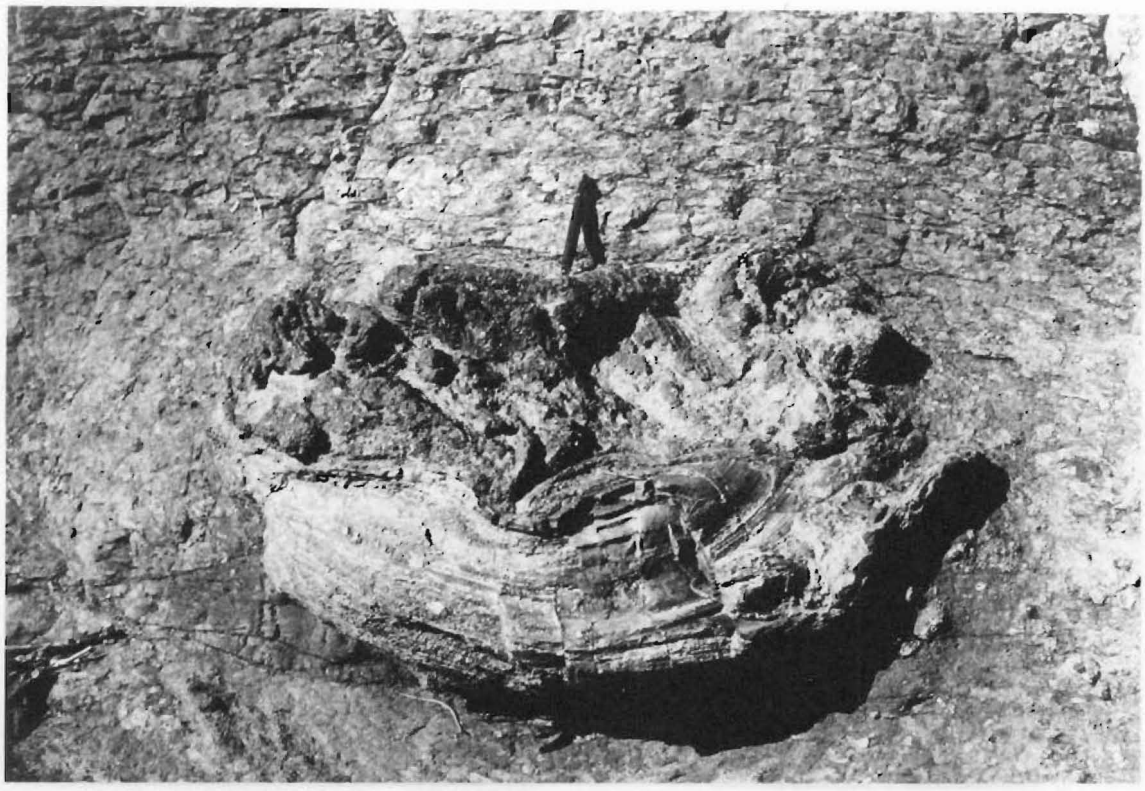

2.5 The Main Phase

The Main Phase is characterised by fresh, grey, fine grained, aphyric to strongly porphyritic basalt and hawaiite lava flows. More evolved lava compositions (mugearite, benmoreite, trachyte) are rare. All flows are observed to dip away from the centre of Akaroa Harbour at angles of 5° to 7°. Flows can rarely be traced more than a few hundred metres, and where visible, cross-sections of flow units tend to have lensoid shapes which pinch-out towards the sides of the flow, suggesting that most flows have followed valleys then existing on the developing volcano. Flow thicknesses vary from 0.2 m to 40 m. Autobreccias are often not observed, but thin (< 1 m) autobreccias are inferred to be present between most flows, marked by the presence of thin, grassed soil horizons between flow units. Minor pyroclastic deposits — typically red, fine grained basaltic tuffs — may be intercalated with the lava flows. Rare trachyte and basalt dikes of the Akaroa dike swarm can be observed intruding flows and pyroclastics.

Four measured stratigraphic sections from different sectors of the volcano (Fig. 2.5) illustrate the geology of the Main Phase.

2.5.1 Saddle Hill

The geology of the Saddle Hill measured section is presented in Map 2 and Sheet 1 of the Measured Stratigraphic Sections (see Map Pocket).

The Saddle Hill section is located on the inside of the eroded crater on the western side of Akaroa Harbour, and extends along a spur from Trig G (N36C/02581143, at 282 m asl), via Rocky Peak (N36C/01461255, at 426 m asl) and the crater rim, to Saddle Hill (N36C/98591151, at 833m asl). The total height of the measured section is 551 m.

The Saddle Hill section represents a section through approximately the lower 75% of the Main Phase. The base of the section extends down to within 160 m of rocks of the Early Phase.

The Pulpit Rock trachytoid intrusion (N36C/99651330), which intrudes flows of the Saddle Hill section, is described more fully in section 3.4.4.

Overall, the section comprises dark grey to light grey, fine to coarse grained, aphyric, plagioclase-phyric, plagioclase-olivine-phyric or olivine-pyroxene-phyric basalts and hawaiites, and rare mugearites. The lower 210 m of the section is characterised by dark grey, medium to coarse grained, very olivine-pyroxene-phyric to weakly plagio-

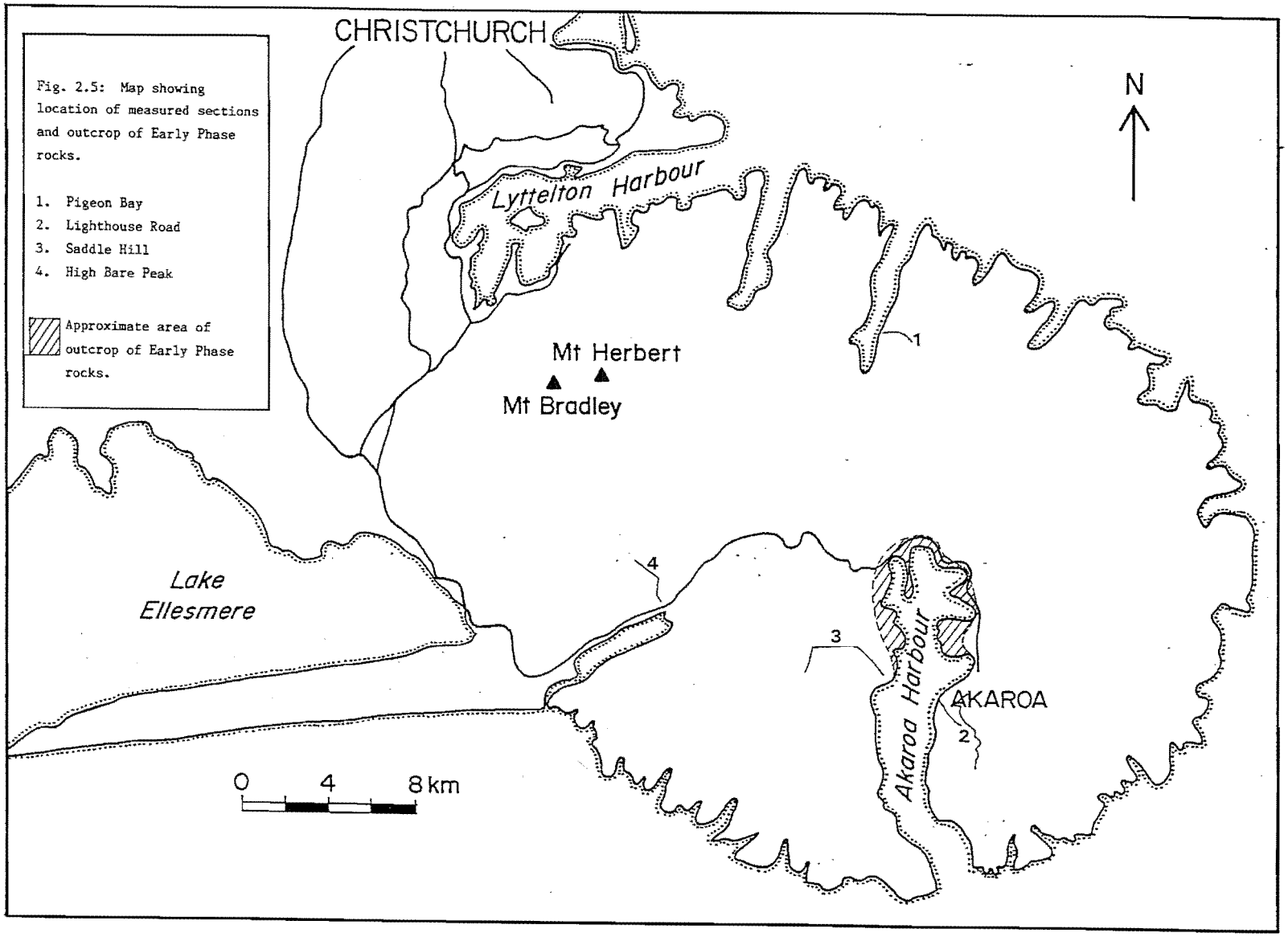

Fig. 2.5: Map showing location of measured sections and outcrop of Early Phase rocks.

1. Pigeon Bay
2. Lighthouse Road
3. Saddle Hill
4. High Bare Peak

Approximate area of outcrop of Early Phase rocks.

clase-olivine-phyric *ne*-basalts, and dark grey, fine to very fine grained, aphyric to weakly plagioclase-olivine-phyric *ne*-hawaiites. The next 70 m of the section is characterised by dark grey, very fine grained aphyric *ne*-mugearites and aphyric or weakly plagioclase-olivine-phyric *ne*- and *hy*-hawaiites. Towards the top of the section there is a trend to lighter grey, fine grained, very vesicular, very plagioclase-phyric *hy*-basalts and *ne*- and *hy*-hawaiites. Vesicles are irregularly shaped, up to 1 cm maximum dimension and may represent 30–50% of the volume of the rock. Plagioclase phenocrysts may be up to 1 cm in length, are euhedral, and may account for 5–50% of the rock. There appears to be a tight coupling between vesicular and plagioclase-porphyritic textures.

2.5.2 High Bare Peak

The geology of the High Bare Peak measured section is presented in Map 3 and Sheet 1 of the Measured Stratigraphic Sections (see Map Pocket).

The High Bare Peak section is located on the western flanks of Akaroa Volcano, some 14 km from the centre of Akaroa Harbour. The section is the most westerly of the measured sections, and is located within 800m of the contact between Akaroa Volcanic Group and the Mt Herbert Volcanics. The section extends along a spur from the north end of Lake Forsyth (N36C/91401370 at 210 m asl) north past Trig I to N36C/91231497 at 520 m asl, then north-west to High Bare Peak (N36C/90201570 at 756 m asl). The total height of the measured section is 546 m.

The High Bare Peak section represents a section through approximately the upper 30% of the Main Phase, and "straddles" the boundary between the Mt Herbert Volcanics and the Akaroa Volcanic Group which occurs between 300 m and 400 m asl in the area of the section. At the contact, lavas of the Akaroa Volcanic Group unconformably overlie lavas of the Mt Herbert Volcanics.

Overall, the section shows less variation in lithology than other sections. The section is dominated by dark grey to light grey, fine grained, aphyric or weakly plagioclase-phyric, plagioclase-olivine-phyric or olivine-phyric *ne*-hawaiites and occasional dark grey to light grey, fine grained, aphyric *hy*-hawaiites. There is a general, but weakly developed trend up-sequence from dark grey, plagioclase-, olivine- or plagioclase-olivine-phyric lavas to grey aphyric lavas.

2.5.3 Pigeon Bay

The geology of the Pigeon Bay measured section is presented in Map 4 and Sheet 1 of the Measured Stratigraphic Sections (see Map Pocket).

The Pigeon Bay section is located on the eastern wall of the valley occupied by Pigeon Bay, on the northern flanks of Akaroa Volcano. The valley runs approximately north-south, providing a cross-section through the north side of the Akaroa cone, and an excellent section in which to observe variations in flow morphology with distance from the central vent. This section differs from the other sections in which the view is essentially a constant distance from the central vent and variations in stratigraphy and flow morphology are in the plane normal to flow direction. The section extends up the face of the valley wall, from $\approx$ 80 m asl (N36A/02702610) to Haytor Peak (N36A/03952595, at 594 m asl) on the valley rim. The total height of the measured section is 514 m.

The Pigeon Bay section represents a section through approximately the upper 75% of the Main Phase.

Some flows can be traced for more than a kilometre along the valley, but most flows can only be traced for a few hundred metres. Flows are often observed to pinch-out both up-slope and down-slope. Autobreccias are observed between most flow units, and range in thickness from 0.25–5.0 m. There is a moderate correlation between flow thickness and thickness of adjacent autobreccias.

The section is dominated by dark grey to grey, fine to medium grained, aphyric, plagioclase-phyric, or plagioclase-olivine-phyric, *ne*- and *hy*-hawaiites. These lavas are interspersed with occasional dark grey, very fine to fine grained, aphyric, plagioclase-phyric or plagioclase-olivine-phyric *ne*- and *hy*-basalts, and aphyric *hy*-mugearites and *ne*-benmoreites.

There is a moderate trend up-sequence from dark grey, aphyric lavas to grey, aphyric or weakly plagioclase-olivine-phyric lavas.

2.5.4 Lighthouse Road

The geology of the Lighthouse Road measured section is presented in Map 5 and Sheet 2 of the Measured Stratigraphic Sections (see Map Pocket).

The Lighthouse Road section is located on the inside of the eroded crater wall on the south-eastern side of Akaroa Harbour, and consists of two parts. The main part

follows Lighthouse Road from where it leaves Akaroa Township (N37A/06700992, at ≈ 160 m asl) to the intersection of Lighthouse Road and Flea Bay Road, on the crater rim (N37A/07700642, at ≈ 620 m asl), and has a total height of some 460 m. The other part of the Lighthouse Road section follows Green Point Stream from where it crosses Kaik Road (N37A/06160966, at ≈ 60 m asl) up Green Point Stream to its source, near Lighthouse Road (N37A/06650925, at 270 m asl), and has a total height of some 210 m. The upper 70% of the Green Point Stream part overlaps stratigraphically with the base of the main Lighthouse Road section.

The Lighthouse Road section represents a section through approximately the lower 75% of the Main Phase. The base of the section extends down to within 80 m vertically of rocks of the Early Phase.

Lighthouse Road section is significantly different from other sections, in terms of the type of exposure, and the lithologies present. Since the section follows the road, continuous sequences of stratigraphy are observed in road cuttings along most of the length of the section. As a result, autobreccias and pyroclastics, which in other sections may be obscured by loess and pasture, are clearly exposed along the Lighthouse Road section. There is a much greater variation in chemistry and lithology in the Lighthouse Road section, compared with other sections.

Pyroclastics are common throughout the section, and include (in order of abundance):

- Thin, 5–25 cm (rarely up to 2.5 m), fine to very fine grained, red to yellow-brown , well bedded, occasionally normally graded, friable basaltic tuffs which mantle underlying units.
- Grey to red, coarse to medium grained, massive bedded, scoriaceous basaltic lapilli tuff-agglomerates. The clasts of scoriaceous basalt range up to 30 cm in diameter, are angular to subrounded, and include occasional lava bombs.
- Rare laharic deposits occur within the sequence, and are typically a massive, unbedded, very weathered, subrounded, matrix to clast supported, polymict, lapilli tuff-agglomerate. The matrix is usually a red-brown to grey, medium to coarse tuff.
- A single soil horizon, 25 cm thick, has been recognised within the succession (N37A/07760798), between two red, very fine grained basaltic tuffs.

The Lighthouse Road section shows the greatest range of lava compositions of any of the sections, and includes most rock types from *ne*-basalt to *qz*-trachyte. Overall, the section is dominated by dark grey, fine grained aphyric or plagioclase-olivine-phyric to grey, fine grained, olivine- or plagioclase-phyric *ne*- and *hy*-hawaiites.

There is an up-sequence trend towards grey, vesicular, aphyric, plagioclase-olivine-phyric to very plagioclase-phyric *hy-* and *qz*-hawaiites. This increase in vesicularity and plagioclase phenocryst content, and lighter colourings is similar to trends observed in the Saddle Hill section.

2.6 Scenery Nook

Throughout Akaroa Volcano there are a number of examples of pyroclastic activity associated with small flank or parasitic vents (eg. Purple Peak, N36C/10701020). None, however, are as visually spectacular or as geologically complex as Scenery Nook. Scenery Nook is a small cove on the south coast of Akaroa Volcano, west of Akaroa Heads (N37A/03900100). This portion of the coastline is characterised by gently sloping lava flows forming the flanks of Akaroa Volcano, truncated by near-vertical cliffs rising to 100m+ above sea level. Scenery Nook consists of two horseshoe-shaped bays. The western bay is confined by near-vertical cliffs which make direct access impossible, except by boat. It is possible, however, to observe much of the geology of the western bay from the surrounding cliffs. Access can be gained to the eastern bay at its eastern end, and the geology observed along the shoreline. Fig. 2.6 is a sequence of panoramic photos of Scenery Nook, and Fig. 2.7 is a sketch map of the geology of the area.

2.6.1 General geology

Exposed within Scenery Nook are basaltic lava flows, volcanic breccias, boulder conglomerates, tuffs and fluvially reworked pyroclastic and epiclastic deposits. These deposits represent a complex of environments associated with a large parasitic vent. The pyroclastics and associated lavas have been subdivided into 7 lithotypes. All lithotypes are exposed in the eastern bay, and a measured stratigraphic section taken on the eastern side of the bay includes all but two of the lithotypes (Fig. 2.8).

2.6.2 Lithotypes 0A, 0B, 1

The pyroclastics rest unconformably on a basaltic lava flow (lithotype 0B), and are overlain by basaltic lavas (lithotype 0A).

Figure 2.6: Panoramas of Scenery Nook illustrating features of the geology.

A: View looking east towards the eastern cliffs of the western bay (N37A/03370100). Note the *ne*-mugearite dike (D) intruding strombolian ash cone (7B) deposits which dip away and to the right (arrows). 0A = lava flows of lithotype 0A.

B: (Over, Top) View looking west towards western cliffs of eastern bay. Western cliffs of the western bay can be seen in the background at left. Arrows mark the direction of dip of strombolian ash deposits.

C: (Over, Bottom) View looking NNE towards NE cliffs of the eastern bay. 0A = flow of lithotype 0A.

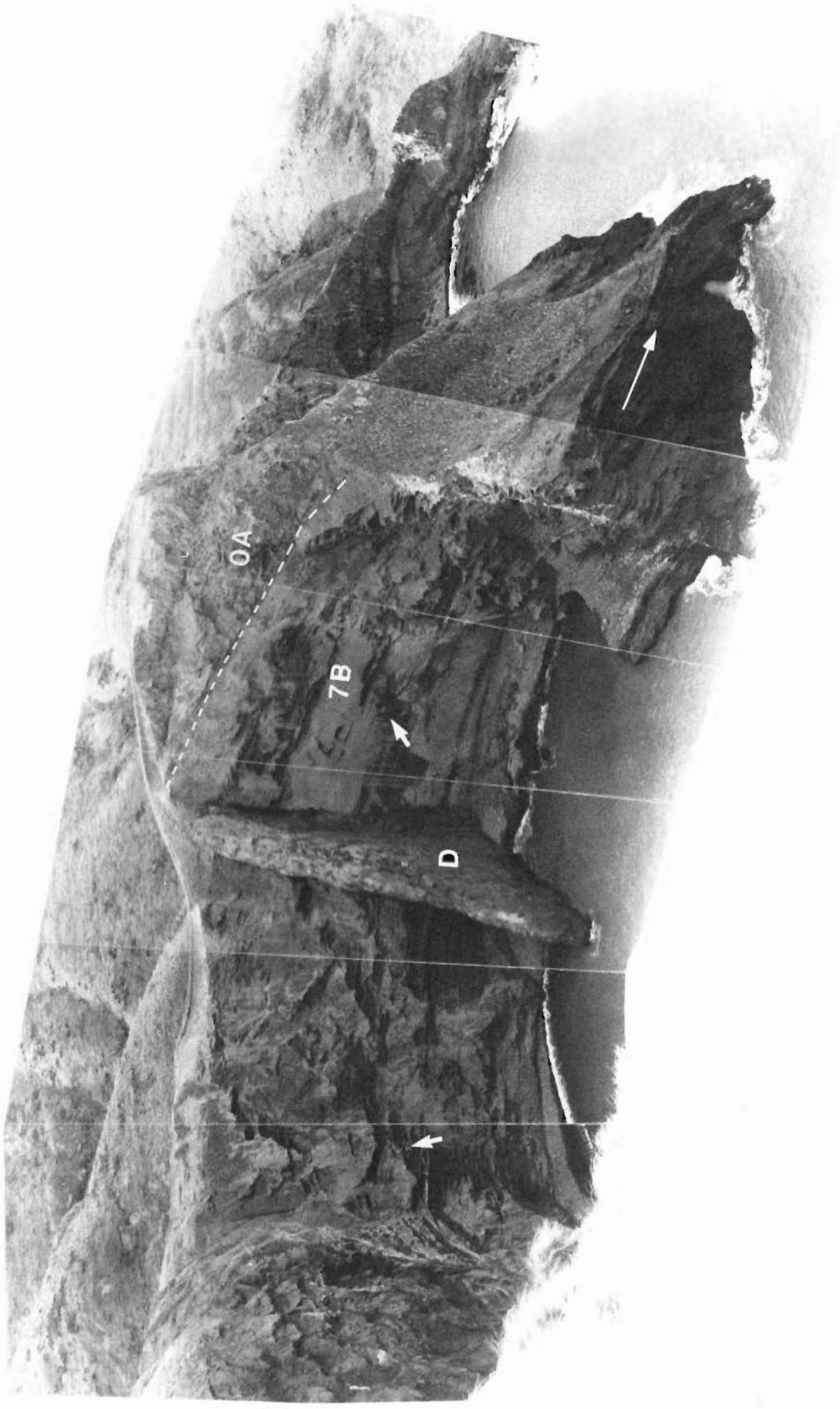
0A
7B
D


0A
7B
7B
0A

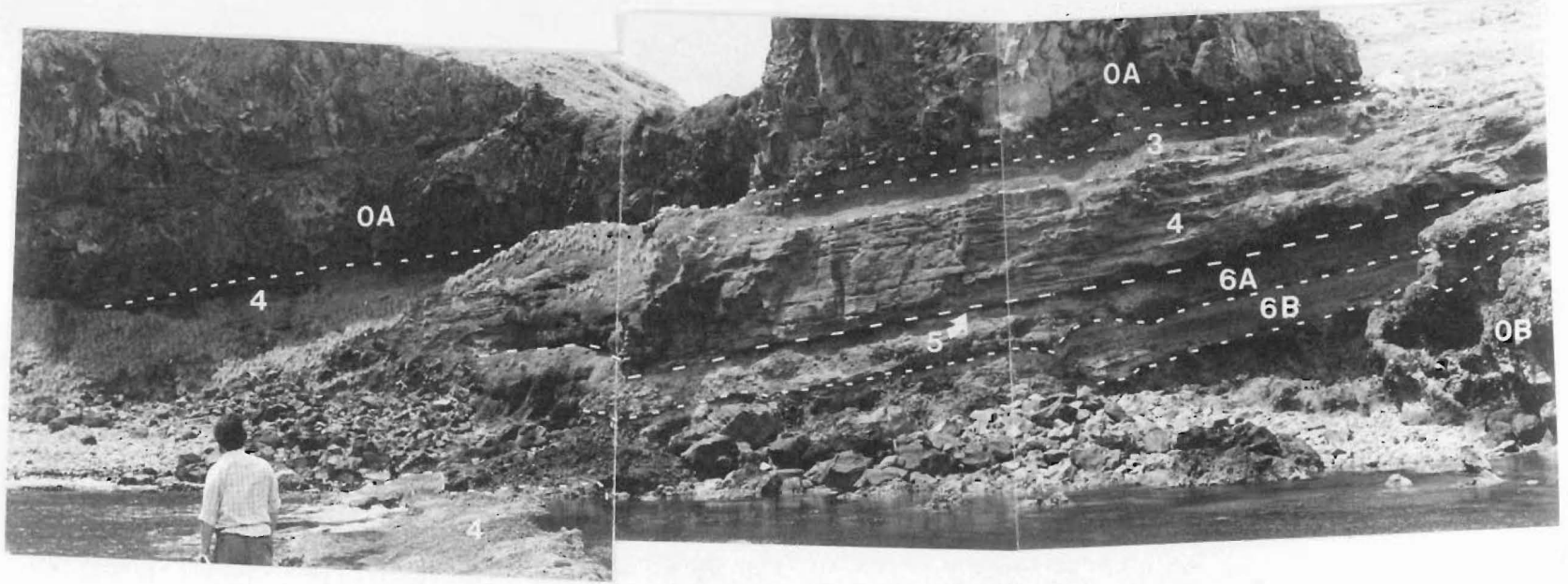
0A
4
4
0A
3
4
6A
6B
5
0B

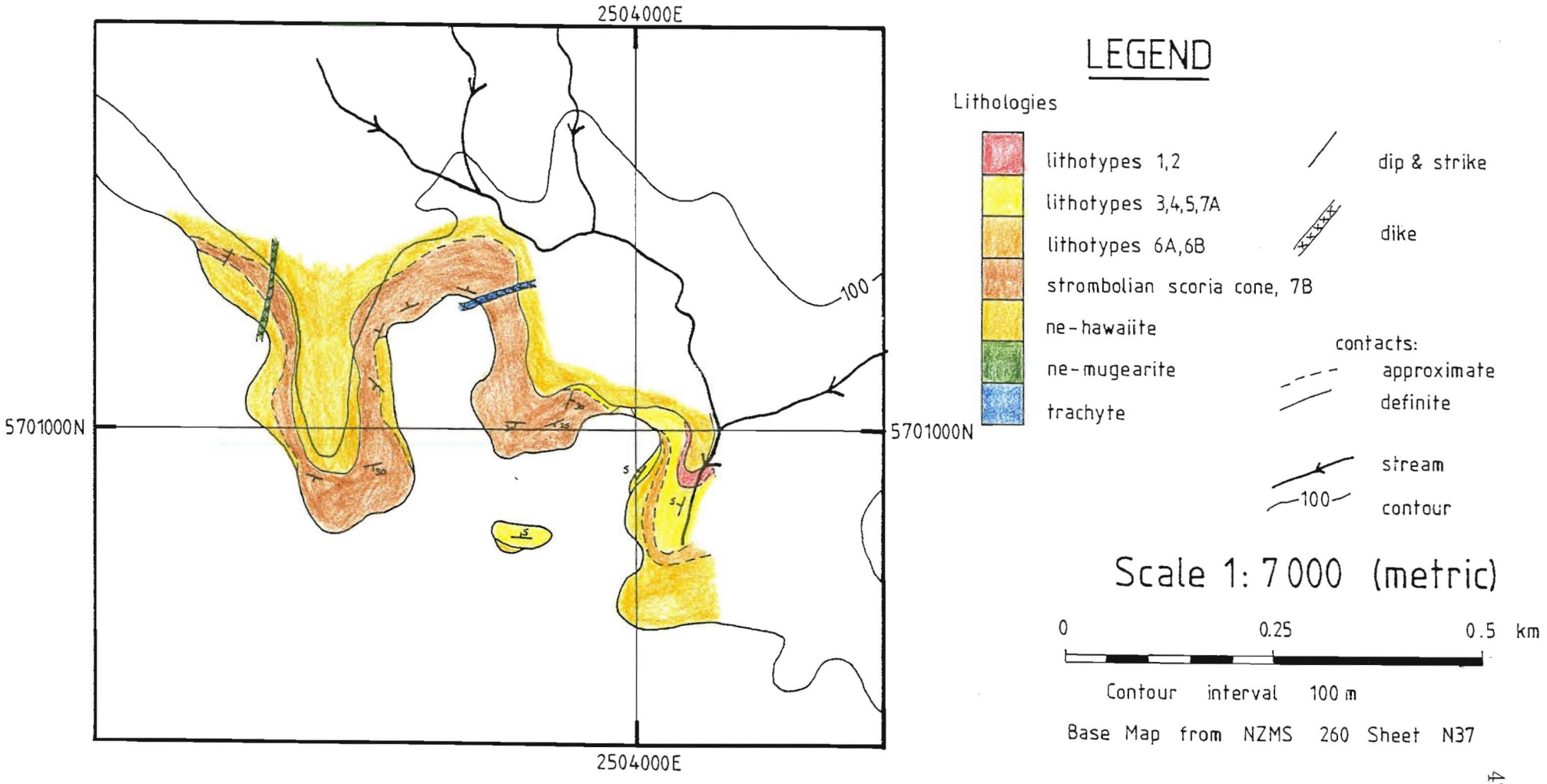

Figure 2.7: Sketch map of the geology of Scenery Nook.

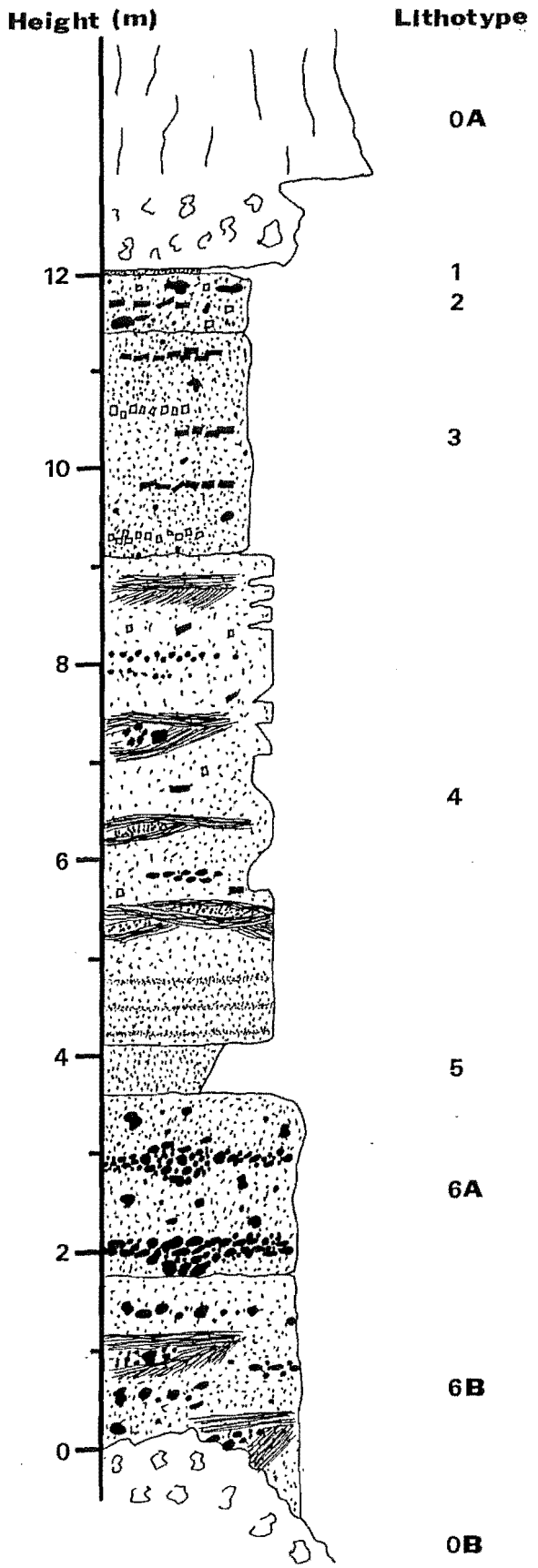

Figure 2.8: Measured stratigraphic section from the eastern side of the eastern bay of Scenery Nook (N37A/04060096 — N37A/04030100). Numbers refer to lithotypes described in the text.

Lithotype 0A is a sequence of 2–20 m+ thick, light grey, fine grained, crudely columnar jointed plagioclase-pyroxene phyric basaltic flows with brecciated upper and lower surfaces (Fig. 2.6c). Flows rest on and are intercalated with lithotype 1. Lithotype 0A is seen everywhere to overlie the pyroclastics of lithotypes 2–7. At the western end of eastern bay (N37A/03950105, Fig. 2.6b) flows are seen to abut against a strombolian scoria cone, suggesting that the lavas flowed around rather than over the cone.

Lithotype 0B is exposed on the eastern shore of the eastern bay (Fig. 2.6c, 2.8), on the seaward side of the small island in the centre of Scenery Nook and to the west of the western bay. At its eastern exposure, lithotype 0B is a *ne*-hawaiite. Flow morphology is of the aa type, with the upper surface of the flow very brecciated and having strong relief (> 2 m).

Lithotype 1 is a brick-red, indurated, sparsely plagioclase-pyroxene phyric, fine basaltic tuff. Units similar to lithotype 1 are seen in many locations around Akaroa Volcano, as thin, often persistent horizons between basaltic lava flows, and commonly mantle underlying units.

2.6.3 Lithotypes 2–6

Lithotypes 2–6 are exposed only on the eastern side of the bay (Fig. 2.6c, 2.8), where they dip NW at 5–10°. All contacts are conformable except between lithotypes 6A and 6B, where lithotype 6A can be seen to erode into lithotype 6B in places.

Lithotype 2 is a red, indurated, plagioclase-pyroxene crystal-rich, matrix supported, unsorted, polylithic coarse tuff. Plagioclase and pyroxene crystals make up ≈ 30% of the unit and are concentrated in finely bedded (cm scale) horizons. Crystals range in size up to 10 mm, but are typically 1–2 mm. Plagioclase crystals lie flat in the plane of bedding. Clasts range in size from matrix up to 150 mm (typically 30–40 mm), and show a range of basaltic lithologies including vesicular, non-vesicular, oxidised, and non-oxidised. Many clasts are well rounded and lie flat in the plane of bedding.

Lithotype 3 is an orange, finely bedded (cm scale), plagioclase-pyroxene crystal-rich coarse tuff. Crystals are concentrated into thin (<1 cm thick) lenses that are either plagioclase- or pyroxene-rich. Rare, rounded basaltic lithics up to 50 mm, appear to be water-sorted.

Lithotype 4 crops out in the eastern cliffs around the eastern bay, in the shore platform and on the inland side of the small island in the centre of Scenery Nook. Everywhere it is seen to dip gently (5–10°) towards the strombolian scoria cone.

Lithotype 4 is an orange-brown, finely bedded (cm scale) coarse tuff to lapilli, plagioclase-pyroxene crystal tuff. Alternating coarse and fine beds occasionally show ?normal and/or ?reverse grading. Plagioclase (5–10 mm) and pyroxene crystals (< 5 mm) make up $\approx$ 30% of the unit. Single or groups of black, matrix-supported, moderately indurated, moderately well rounded, dense, non-vesicular, up to 20 mm, basaltic lithics occur throughout the unit. Occasional persistent horizons of highly vesicular, angular, 10–40 mm, red oxidised, juvenile basaltic clasts appear to follow topography. Horizons of well-sorted, lapilli ash with fine, well developed, low angle cross bedding grading into planar bedding are common (Fig. 2.9), and consist of highly comminuted, vesicular, juvenile lithics. The boundaries between lithologies are often gradational or indistinct. The presence of at least two populations of basaltic lithics suggests some fluvial reworking of primary pyroclastic material.

Lithotype 5 is a chocolate brown, indurated, reversely graded, fine to medium tuff containing occasional $\approx$ 1 mm plagioclase crystals.

Lithotypes 6A is an orange-brown, poorly sorted, coarsely irregular to poorly bedded, medium tuff to matrix- or clast-supported, monolithic boulder conglomerate (Fig. 2.10). Abundant black, angular, vesicular, highly plagioclase-phyric basalt clasts may be concentrated in clast supported, poorly to well defined lenses and channel fills. Clast sizes range from matrix to 250 mm but are typically < 100 mm.

Lithotype 6B is similar to 6A, but has a much lower proportion of clasts, and clast lithologies are much more variable, showing variations in degree of rounding, oxidation and vesiculation, as well as composition. Clasts tend to be concentrated in thin (decimetre scale) lenses interspersed with matrix-rich horizons. Matrix-rich horizons often show cross-stratification, channels infilled with coarser ash and clasts, and well developed laminations on a fine (cm) scale. Occasional volcanic bombs may be present (Fig. 2.11).

2.6.4 Lithotypes 7A and 7B

The most commanding feature of Scenery Nook is a large strombolian scoria cone (Fig. 2.6), more than 100 m thick at its centre in the western bay of Scenery Nook (N37A/03750110), and with a diameter of more than 1.2 km. The scoria cone overlies lithotype 0B on the western peninsula (N37A/03630105), and is everywhere overlain by lava flows of lithotype 0A. The relationship between the scoria cone and lithotypes 2–6 is obscure — nowhere are they seen in contact, and at their closest proximity (in the eastern bay, N37A/03990102) the critical area is covered by grass.

The strombolian deposits consistently dip at angles of 25–30° away from the centre of the cone, and a 2 m thick *ne*-mugearite dike intruding the cone (Fig. 2.6a)

is also orientated towards the cone's centre, in the western bay of Scenery Nook (N37A/03750110). A trachytic dike intrudes the western flanks of the cone, west of Scenery Nook (N37A/03560117).

The scoria cone is constructed almost entirely of **lithotype 7B** — a yellow brown, coarsely bedded (dm scale), poorly sorted, matrix-supported, pebble to boulder breccia (Fig. 2.12). The matrix is composed of welded cinders and pumice fragments up to 20 mm, which are flattened parallel to bedding. Clasts are essentially monolithic, with dark, vesicular, basaltic spindle and pancake bombs, and cinders and lava splatters up to 800 mm, flattened in the plane of bedding. Most clasts have chilled margins and vesicular cores. Impact structures and reddened zones of matrix may be associated with larger clasts.

Lithotype 7A is only exposed at the western end of the eastern bay of Scenery Nook (N37A/03960102), where it is seen to rest conformably on lithotype 7B on the flanks of the scoria cone (Fig. 2.6b). Lithotype 7A is a yellow, fine to coarse tuff with sparse, dark fine grained vesicular basalt clasts, similar to parts of lithotype 4.

2.7 K-Ar Dating

Stipp and McDougall (1968) determined ages between 9.02 ± 0.27 Ma for flows near sea level in Pigeon Bay (sample GA2010) and at Wainui (sample GA2009), and 8.04 ± 0.20 Ma for a flow (sample GA2024) from ≈ 1500 ft in Le Bons Bay. In general, the ages determined are consistent with both stratigraphy and geographic location — samples at higher stratigraphic positions and altitudes or further away from the centre of Akaroa Harbour giving younger ages.

Stipp and McDougall (1968) obtained an age of 8.92 ± 0.13 Ma from biotite in the gabbro from Onawe Peninsula (sample GA2019), indicating contemporaneity with the earliest lavas of the Main Phase which are topographically not much higher than the gabbro. An age of 11.8 Ma was obtained from alkali feldspar in the syenite (GA2174). This is significantly older than any other age obtained for Akaroa Volcano, being contemporaneous with the oldest Lyttelton Group lavas. Stipp and McDougall (1968) themselves acknowledge that the age must be regarded with suspicion. The syenite contains irregularly shaped cavities and many are infilled with secondary quartz, indicating that considerable gas-phase activity may have occurred during and for some time after crystallisation of the syenite. Under such conditions, the older age may reflect the presence of excess argon (Livingston *et al*, 1967). On these grounds, the 11.8 Ma age for the syenite is considered to be incorrect.

Ages determined by Evans (1970) for samples from 73 Main Phase flows from Light-

Figure 2.9: Lithotype 4, exposed on the eastern side of the eastern bay of Scenery Nook (N37A/04040097).

Figure 2.10: Lithotypes 6A and 6B exposed on the eastern side of the eastern bay of Scenery Nook (N37A/04040098), resting unconformably on a very brecciated aa lava flow (lithotype 0B). Note the strongly developed channelling (above figure), infilled with angular, fresh basalt clasts. The overhanging cliff is constructed from lithotype 4. Lithotype 5 can be seen immediately underlying lithotype 4 at the top left of the photograph.

Figure 2.11: Volcanic bomb incorporated in a cross-stratified horizon of lithotype 6B on the eastern side of the eastern bay of Scenery Nook (N37A/04040098).

Figure 2.12: Lithotype 7B — a strombolian scoria cone deposit — exposed at the western end of the eastern bay of Scenery Nook (N37A/03960102). Note the coasely defined bedding, spindle bombs and flattened cinders distinctive of strombolian deposits.

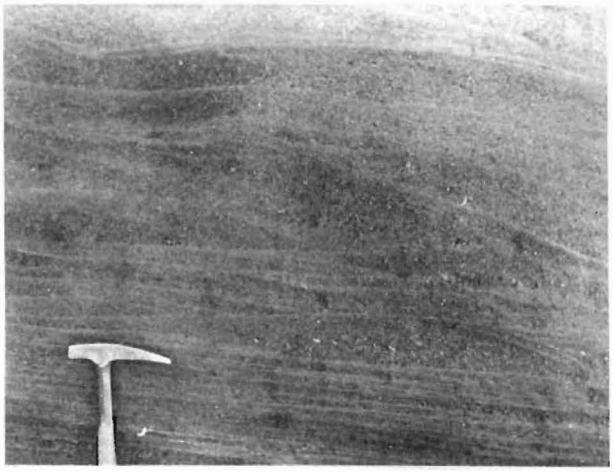

house Road and Green Point Stream, over a height of 685 m, range from 9.13 ± 0.13 to 8.38 ± 0.13 Ma, and are in broad agreement, both with stratigraphy and topographic position, and with ages determined by Stipp and McDougall (1968). Evans (1970) calculated a rate of eruption, based on a 0.75 Ma duration of activity and a volume of erupted material of 350 km^3, of 5×10^5 m^3 yr^{-1}, compared with recent rates of Kilauea (10^8 m^3 yr^{-1}) and Mauna Loa (2×10^7 m^3 yr^{-1}) (Stearns, 1966). However, 1200 km^3 is considered a better estimate of the volume of erupted material, which represents a rate of 1.6×10^6 m^3 yr^{-1} for construction of the Main Phase. These figures should be treated with caution, since the rate of eruption from such a large composite volcano is unlikely to be constant over any period of time, nor is it likely to be constant throughout the spatial extent of the volcano.

Sewell (1985, 1988) established a new stratigraphy for Banks Peninsula and obtained K-Ar ages determinations for some stratigraphic units, which constrain the possible age range of lavas of the Main Phase of Akaroa Volcano to 9.5–8.1 Ma.

K-Ar dating was carried out by the author at the Institute of Nuclear Sciences, Lower Hutt, New Zealand, on 10 samples from Akaroa Volcano. Descriptions of the analytical methods are presented in Appendix E and the results are presented in Appendix B.

A sample from the Tikao trachyte dome (N36C3256) returned an age of 11.63 ± 0.46 Ma, which is not unreasonable, in view of the fact that the dome forms part of the Early Phase, which may be considerably older than flows at the base of the Main Phase. Sample N36C3305, from the south coast of Takamatua Peninsula, returned an age of 10.18 ± 0.33 Ma. Stipp and McDougall (1968) obtained an minimum age of 9.01 ± 0.26 Ma from a flow at Wainui which is stratigraphically just above N36C3305. An age of 8.76 ± 0.81 for sample N36C3037 from the base of the Saddle Hill section (see Map 2, Map Pocket) is consistent with stratigraphy and other age determinations. Other dates obtained have been rejected as being inconsistent with stratigraphy or accepted dates.

Chapter 3

INTRUSIVE ROCKS

3.1 Introduction

Intrusive rocks are widespread and were emplaced throughout the extent and history of Akaroa Volcano. They can be grouped into three categories:

1. Plutonics
2. Dikes of the Akaroa dike swarm
3. Trachyte domes

With the exception of the gabbro on Onawe Peninsula and numerically minor basaltic dikes of the dike swarm, intrusive rocks are trachytic in composition. Descriptions and locations of all samples referred to in this chapter are presented in Appendix A.

3.2 Plutonics

Syenite and gabbro are exposed at the southern end of Onawe Peninsula, close to the centre of Akaroa Harbour and the inferred site of the main eruptive vent. These rocks are the only plutonic rocks exposed anywhere on Banks Peninsula.

A massive outcrop of *qz*-syenite forms the southern one-third of Onawe Peninsula and the highest point of the peninsula (N36C/04061475). The syenite body is

roughly oval in shape with a maximum diameter of 450 m and an estimated volume (above sea level) of 7 million m^3. In outcrop the syenite is coarse-grained, massive and displays spheroidal weathering (Fig. 3.1). Lithologically, the syenite comprises orthoclase feldspar with minor amounts of clinopyroxene, red-brown amphibole and magnetite. Secondary drusy quartz (often amethyst) infills irregular shaped cavities.

Immediately to the north of the syenite, small outcrops of *ne*-gabbro occur on both the east and west sides of Onawe Peninsula (N36C/03921494, N36C/04251475). The contacts between the syenite and the gabbro are not exposed on either side of the peninsula, so that stratigraphic relationships cannot be observed. On the east side of Onawe Peninsula, gabbro exposed 5–10 m above the shore platform, near the inferred contact with the syenite, is very weathered and friable, and appears to have been baked and sheared. The gabbro is volumetrically minor in comparison to the syenite. On the west side of Onawe Peninsula, the gabbro is exposed for 15–20 m along the shore. The gabbro forms a massive outcrop, and is composed of plagioclase feldspar, biotite, amphibole, magnetite and minor amounts of pyroxene and olivine.

On the east side of Onawe Peninsula, the southern 1–2 m of gabbro near the contact with the syenite contains segregations of material more felsic in composition than the gabbro. These "schlieren" are generally irregular or lensoid in form and up to 10 cm in diameter. The boundary between the schlieren and the host gabbro appears gradational but rapid. The schlieren range from a monzodiorite to a monzonite.

Both the syenite and the gabbro are intruded by trachyte dikes of the Akaroa dike swarm.

Geological relationships between the gabbro and syenite, and between the plutonics and adjacent volcanics, are obscured. Volcanics immediately to the north dip north at angles of 10–20° and do not appear to have buried the plutonics. Furthermore, the syenite crops out at 108 m asl within 100 m of lava flows and ashes which are observed on the shore platform. This evidence points to the contacts being either intrusive or faulted. As there is no other evidence of faulting either on Onawe Peninsula or elsewhere on Akaroa Volcano, the contacts between the gabbro and the syenite, and between the plutonics and adjacent volcanics are considered to be intrusive. There is little field evidence to indicate whether the syenite or the gabbro is the older of the two, other than that the gabbro appears to be sheared and baked near the contact with the syenite, and felsic schlieren in the gabbro might be interpreted as intrusions of syenitic magma.

Speight (1923) noted that the contacts between the syenite and gabbro on both sides of Onawe Peninsula were masked by soil and slip material. Speight described

Figure 3.1: Massive outcrop of syenite forming the southern tip of Onawe Peninsula (N36C/04251468).

a leucocratic variety of the gabbro, but stated that there was no chemical or microscopic evidence for a progressive change from gabbro to syenite, and concluded that one rock was injected into the other. As to the relative ages of the syenite and gabbro, Speight suggested that the syenite was related to the trachyte dikes of the dike swarm, which belonged to a late volcanic phase, and therefore the syenite might be younger. It is unclear whether the leucocratic gabbro described by Speight (1923) is the schlieren observed in this study. While there is good petrographic and geochemical evidence (see chapters 4 and 5) that the schlieren have compositions intermediate between syenite and gabbro, and the schlieren are concentrated in the gabbro near the contact with the syenite, there is no evidence of a gradational contact between the syenite and gabbro. Speight (1940) again noted that contacts between the syenite and gabbro, and between the plutonics and other volcanic rocks, were not exposed. Three possibilities were considered:

1. The gabbro was intruded by the syenite
2. The syenite was intruded by the gabbro
3. The contact was faulted

Speight could not distinguish between any of these possibilities on the basis of field evidence, but thought that the syenite was probably younger, assuming that the law of decreasing basicity holds for plutonic rocks.

3.3 The Dike Swarm

3.3.1 Introduction

The dike swarms of Lyttelton and Akaroa volcanoes are distinctive features of the geology of both volcanic edifices, and have attracted the attention of a number of workers. Most workers considered both dike swarms to be radially distributed about the central vents and to have been emplaced late in the evolution of the volcanoes. Greater attention has been paid to the Lyttelton dike swarm as it is considered to be better exposed than that of Akaroa.

Marshall (1894) and Speight (1908) described specific examples of dikes from Lyttelton.

Speight (1917) presented a map of Lyttelton showing the location and orientation of dikes, and described the dikes of the Lyttelton swarm in general terms. Speight

noted that the dikes range in composition from basalt to trachyte (although trachyte dikes predominate), and range in thickness up to 18 m. The dikes were described as having a "radial orientation", but a centre was not pinpointed.

Speight (1923) described in some detail the composition of Lyttelton and Akaroa dikes. As to their orientation, Speight noted that the swarms were similar in nature, with dikes on the margins of the volcanoes being clearly radial in orientation, but dikes around the harbours being much more irregular in orientation. No dikes were found around the crater rim of Akaroa.

Speight (1938) suggested that the centre of the Lyttelton dike swarm, south-west of Quail Island, differed from the main conduit from which the cone was constructed, which was inferred to lie to the north of Quail Island. The dikes were considered to be later than the main cone.

Speight (1944) described the Akaroa dike swarm, particularly in relation to the trachyte intrusions at Panama Rock, View Hill, Devils Gap and Pulpit Rock.

Frost (1965) attempted a computer analysis of the Lyttelton dike swarm, and concluded that the centre of the dike swarm was located on Potts Peninsula, south of the point proposed by Speight (1938). It should be noted that Frost's data was derived from the map published by Speight (1938), not from actual measurements, and that there is no geological evidence on Potts Peninsula for a centre.

Shelley (1987), in a study of the Lyttelton dike swarm, proposed the existence of two principal centres of Lyttelton activity — Lyttelton 1 and Lyttelton 2. Dike trends were recorded systematically around Lyttelton Volcano and rose diagrams of dike orientations were constructed for each 10° segment around the volcano (Fig. 3.2). Contours of the numbers of trend lines (traced from rose diagram maxima) per 1% area revealed the presence of two loci which were interpreted as two principal sites for vents of the Lyttelton Volcano. The two centres fall just to the east and west of the centre proposed by Frost (1965). A number of points should be noted:

1. No mathematical analysis of the data was attempted; instead, a graphical analysis of the data was performed.

2. As a consequence of point #1 the data were treated essentially as grouped data, which introduces additional statistical errors and may mask important variations (Snedecor and Cochran, 1980).

3. Frequency distributions may be represented graphically as a histogram, in which each class is represented by a rectangle with area proportional to the class frequency. In general, all classes in a frequency distribution have equal width, and therefore class frequency is effectively represented by the height of

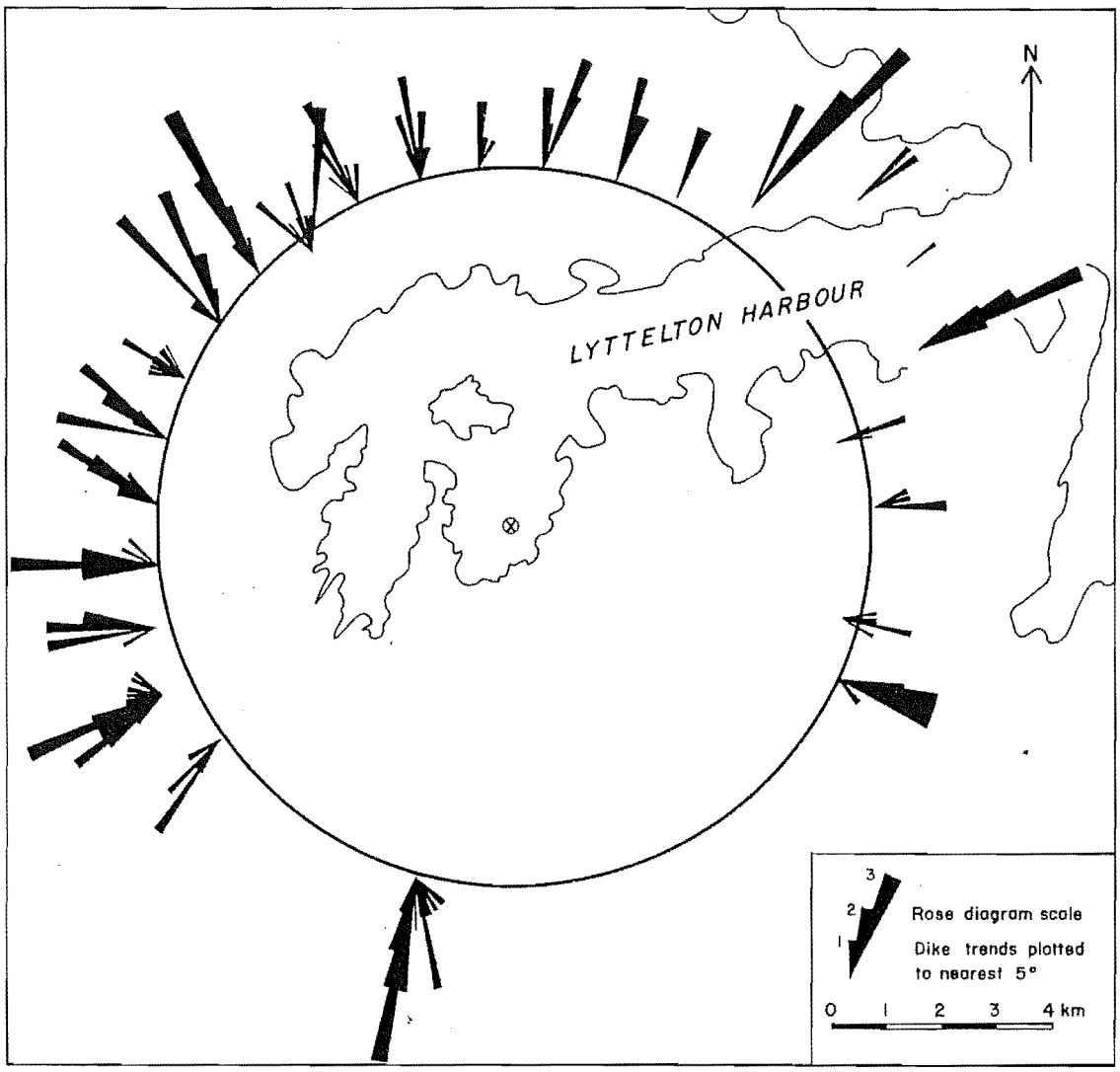

Figure 3.2: Rose diagrams to show dike trends around the Lyttelton crater rim (shown as a circle). The centres of the rose diagrams are spaced at exactly 10° intervals and placed within those 10° segments at the locality most central to the readings made. After Shelley (1987).

the rectangle. However, there are important cases where the use of variable class widths is advisable, and in such cases the height of the rectangle is adjusted accordingly (Spiegel, 1972; Snedecor and Cochran, 1980). Since rose diagrams are just histograms with classes arranged as segments of a circle, the class frequency should be represented by the area of the segment. The radius of each segment is thus not a linear scale, but increases by a factor of $\sqrt{2}$ as the class frequency doubles. The use of a linear scale for segment radii (cf. Shelley, 1987) will therefore over-emphasize larger class frequencies, resulting in a loss of graphical integrity and an increase in perceptual problems (Tufte, 1983).

4. As a consequence of points #1–#3, the trend lines used to locate the two eruptive centres actually represent approximations of the modes of sets of grouped data, rather than the means of a set of sample populations.

3.3.2 General Characteristics of the Akaroa Dike Swarm

Dikes occur throughout the geographical extent of Akaroa Volcano, but the population density varies both systematically and significantly. In the inner harbour area, dikes are ubiquitous along the shoreline, and on Onawe Peninsula the country rock is so intensely intruded by dikes that significant portions of the shore platform are constructed almost entirely of dike material. The density of dikes falls off rapidly away from the inner harbour shoreline, and dikes are rare along the Akaroa Summit Road and further afield. While exposures are generally poor away from the inner harbour shoreline, some parts of the Summit Road around the crater rim and particularly Bossu Road on the western rim of the crater, have stretches of good road-side exposure in which dikes are notable by their absence. In part, the variation in density of dikes is a function of distance from the centre of the radial distribution.

Dike compositions range from basalt to trachyte, but trachytic compositions dominate; an estimated 85–90% of all dikes observed are of benmoreite-trachyte composition. Trachytic dikes around the inner harbour, and particularly on Onawe Peninsula, show extensive hydrothermal alteration, and are soft, bleached creamy-white, and exhibit leisegange banding.

Dike thicknesses range from < 0.1 m to > 20 m, but thicknesses of 1–2 m are typical. Thicknesses are generally consistent along the exposed length of dikes, although offshoots may develop which are much thinner than the parent dike. Observed dike thicknesses are comparable with thicknesses of dikes recorded from major dike swarms elsewhere (Table 3.1).

Table 3.1: Thicknesses of dikes from major dike swarms

Description, Location	Dike Thickness (m)		Reference
	Average	Maximum	
Dikes in rift zones, Hawaii	0.5–1.0	few > 3.0	MacDonald and Abbott (1970)
Tertiary dike swarm, E. Iceland	3.5	–	Walker (1958)
Tertiary dikes, Mull, Scotland	1.5	some > 50	Bailey *et al*, (1924)
Basic Tertiary dikes, Scotland	2.0	–	Richey (1939)
Independence dike swarm, E. California	1.0	–	Chen and Moore (1979)
Basic dikes, Colorado Plateau	0.5–4.0	–	Gregory (1917), Gilluly (1929), Williams (1936)
Lyttelton dike swarm	1.0	20	Shelley (1987)

Dikes are generally consistent in orientation along their exposed length, although there are two distinct exceptions to this rule, exemplified by dikes exposed around the inner harbour shoreline. Smaller dikes ($\leq$ 1 m thick), especially those seen on the shore platforms of Onawe Peninsula, often show considerable variation in orientation along their length, resulting in curved and sometimes quite contorted paths, but there is no consistent sense of curving, within an outcrop or around the volcano. Dikes may display lateral displacements or "jumps" in position along their trace. Displacements may be greater than the thickness of the dike, with no visible connection between the segments of the dike. As with the more curved and contorted dikes, there is no consistent sense of displacement, such as en echelon sequences.

Although measurements of inclination were not taken, most dikes appear to be near vertical in inclination. Where dikes depart from this general rule there is no apparent association with spatial distribution or the composition of the dike or the country rock.

The exposed vertical extent of a dike is rarely more than a few metres; one of the few significant exceptions to this is a trachytic dike exposed to the north of Purple Peak (N36D/10701024) with a visible vertical extent of $\approx$ 50 m.

When exposed, the termination of a dike is typically abrupt for dikes $\geq$ 1.0 m thick, and tapering for dikes $\leq$ 1.0 m thick.

Dikes may exhibit cross-cutting relationships with one another. This is particularly evident on Onawe Peninsula. There is however no consistent trend of dikes of one orientation cutting dikes of another orientation, or of one composition cutting another. On Onawe Peninsula and around the inner harbour shoreline it is common to observe dikes that appear to have been intruded into the centre of an older dike,

parallel to its strike. In every case observed, the composition of the younger dike is similar to that of the older dike; examples of a basaltic dike intruding the centre of a trachytic dike (or vice versa) were not observed. Such a relationship may reflect pulses of magma flowing through the dike (Delaney and Pollard, 1982).

Trachyte dikes often show fissility parallel to trend, and vesicles may be concentrated near the margins. Both basaltic and trachytic dikes may display columnar jointing normal to the wall of the dike.

One dike can be seen to have fed an endogenous trachyte dome (Panama Rock, N36D/13131790). No dikes have been seen feeding lava flows, although this possibility cannot be ruled out.

3.3.3 Mapping of the Akaroa Dike Swarm

The location, orientation, thickness and composition of 643 dikes encountered while mapping were recorded, and these data are presented in Appendix C and Map 6 (see Map Pocket). Dikes occurring outside the inner harbour area covered by Map 6 were extrapolated along strike to the edge of the map, and are shown in different colours to distinguish them from dikes actually exposed in the map area. Only two dikes from outside the map area do not extrapolate into the map area. Dike compositions shown in Appendix B and Map 6 are a field identification only; dikes were classified as either basalt or trachyte based on field characteristics, and in reality this is probably a distinction between basalt-mugearite and benmoreite-trachyte compositions.

A visual examination of Map 6 reveals the following features:

1. Dikes extrapolated from outside the map area (these are seen only at the margins of the map) and dikes occurring away from the shoreline are clearly orientated radially, with respect to a centre in Akaroa Harbour. From Wainui clockwise around to Akaroa township there is a clear and consistent change in the trends of dikes.

2. Dikes around the harbour shoreline from Wainui to Akaroa show the same radial trend, being orientated towards the centre of the harbour. Between different geographic regions dikes show a logical and progressive swing in orientation. However, there is more variation apparent in dike orientations within each region. In part this reflects the greater abundance of dikes producing more irregularities or "noise", but it also reflects the appearance of a second population of dikes concentric to the centre in the harbour. This is particularly evident along the shoreline between Barrys Bay and French Farm, French

Farm and Petit Carenage, and on the south-west coast of Petit Carenage. In these areas dikes of the concentric population can be seen orientated at high angles ($> 45°$) to dikes of the radial population.

3. On Onawe Peninsula (see inset, Map 6) the two populations can still be discerned, but there is much more "noise" from dikes which can not easily be assigned to one or other population. Almost all of the dikes on Onawe Peninsula are exposed on the shore platform, are generally ≤ 1.5 m thick, and as noted above, many dikes show considerable variation in orientation along strike. These dikes are assigned to a third, "random" population.

4. Basalt dikes are a minority in comparison with trachyte dikes. There is no discernible difference in orientation between basalt and trachyte dikes of the same region, and there is no significant variation in the proportion of basalt dikes between the radial, concentric and random populations.

In order to characterise more accurately the nature of the radial, concentric and random populations, and to locate the center(s) of the radial and concentric populations, a statistical analysis of the dike orientation data is required.

3.3.4 Statistical Analysis of Dike Orientations

Dike orientation measurements are orientations (eg. 37–217°), not directions (eg. 37°), since there is no way to tell from the outcrop which way the dike was intruded, although Shelley (1985) describes a laboratory technique based on U-stage measurements of feldspar (010) orientations. In the case of the radial population, it is logical to assume that the dikes originated from the center of the volcano and were intruded outwards, and therefore one can measure the direction away from the center. However this assumption can not be applied to dikes of the concentric and random populations. The first step in the statistical analysis, therefore, is to normalise the data. All dike orientations were recalculated to 0–179° as follows:

$$\text{if } \theta = 360° \text{ then } \theta = \theta - 360°$$
$$\text{if } \theta \geq 180° \text{ then } \theta = \theta - 180°$$

and the frequency distribution calculated for 1° sectors from 0–179°. The data were then transformed so that diametrically opposed sectors have the same frequency count. All analyses are performed on this normalised frequency distribution.

Rose diagrams have been constructed for 13 geographic regions, and for the total dike population (Fig. 3.3). In each diagram, the area of each 5° sector represents

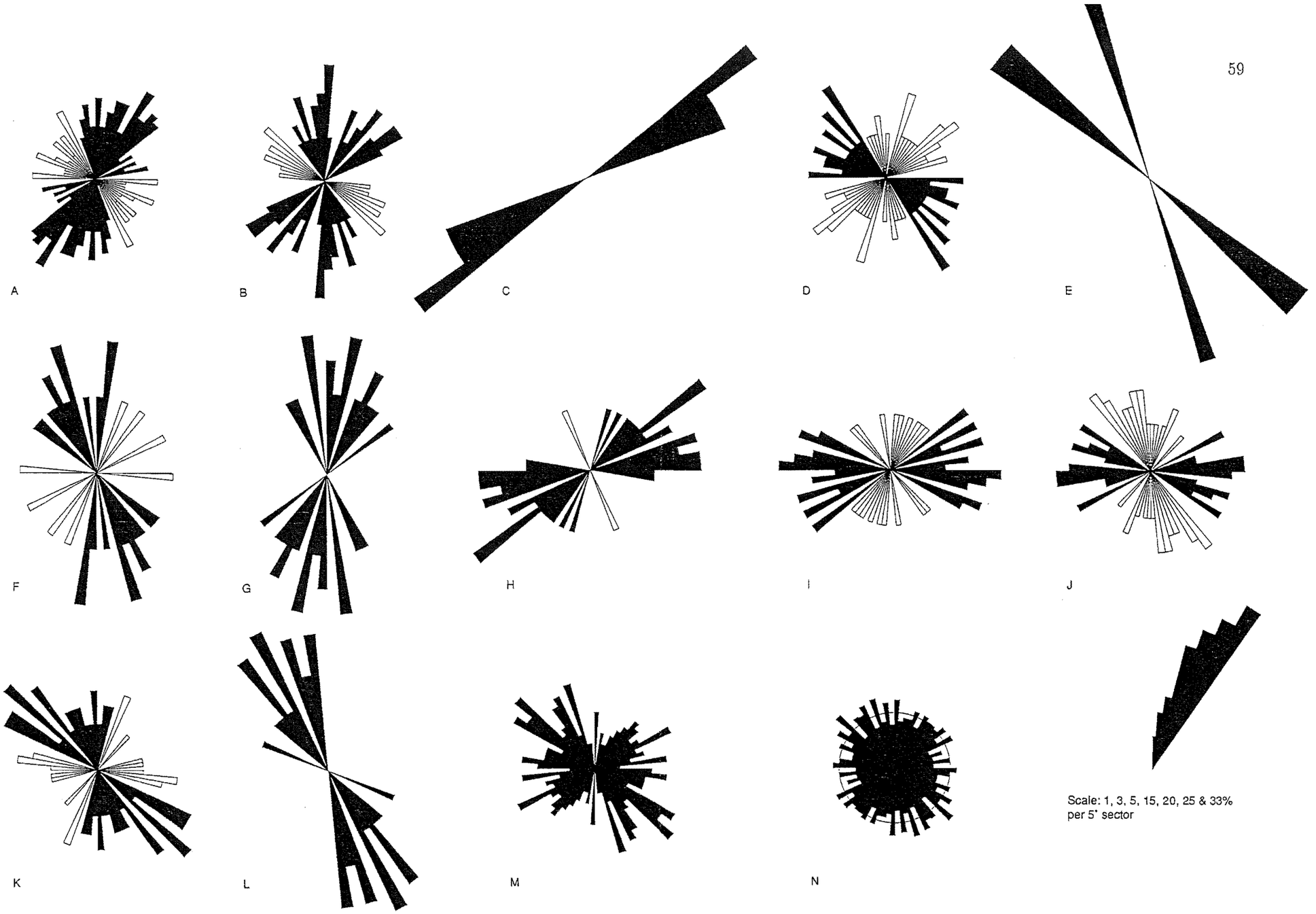

Figure 3.3: Rose diagrams of dike orientations for localities around Akaroa Harbour. Solid sectors are for dikes of the radial population. Hollow sectors are for dikes of the concentric population. A = Tikao; B = French Farm; C = French Farm West; D = Barrys Bay; E = NW Summit Rd; F = Nth Onawe Peninsula; G = NNE Summit Rd; H = NE Summit Rd & Robinsons Bay; I = ENE Summit Rd & Hammonds Pt; J = E Summit Rd & Nth Takamatua Peninsula; K = ESE Summit Rd & Sth Takamatua Peninsula; L = Lighthouse Rd & Green Pt; M = Onawe Peninsula; N = All dikes (circle is perfect radial distribution).

the percentage of dikes in that geographic region with orientations in that 5° range. Note that since frequency is represented by area, the radius does not increase linearly with frequency, but by a factor of $\sqrt{2}$ as the frequency doubles.

The rose diagram of all dikes (Fig. 3.3n) shows a very homogeneous distribution of orientations, and the outline of a perfect homogeneous distribution is included for comparison. Such a distribution can be expected from a radial and/or concentric and/or random population, but not from a strongly modal population. Rose diagrams for individual regions support the concept of a radial (Fig. 3.3 c, e, g, l) and a concentric (Fig. 3.3 a, b, d, f, h, i, j, k) population, although in some cases (Fig. 3.3 a, f, i, k) the distinction is less marked.

In order to use these data to determine the center of the dike swarm it is necessary to determine the "mean" direction for each area. However, vectorial and orientational data distributed circularly about a compass present special statistical problems. For example, the arithmetic mean of 340° and 160° is 250°, when intuitively one would expect an answer of 340° or 160°. The inadequacy of conventional statistical methods for analysing directional data has been recognised for some time (Jizba, 1953; Chayes, 1954) and a number of authors have tried to develop suitable methods. Rao and Sengupta (1972) proposed a method based on the calculation of a resultant vector from the direction cosines of the dike orientations, and their method is adopted here.

One assumption is made here, in addition to those implicit in the method proposed by Rao and Sengupta (1972); each dike orientation is treated as a vector, even though the "direction" is not known, with the realisation that the resultant vector will actually represent an orientation defined by the vector and its complement.

Taking the data in Appendix C as a sample of size n of the total dike population, with orientations $\alpha_1, \ldots \alpha_n$, and treating each observation as a unit vector with components $\cos\alpha_i$ and $\sin\alpha_i$ the direction cosines are calculated:

$$V = \sum_{1}^{n} \cos\alpha_i$$

$$W = \sum_{1}^{n} \sin\alpha_i$$

and from these the mean sample direction (resultant vector) is calculated:

$$\gamma = \tan^{-1}(W/V)$$

Variability or scatter of azimuths is represented by the magnitude of the resultant vector, R, where

$$R = \sqrt{(W^2 + V^2)}$$

and the consistency or concentration of azimuths is measured by the consistency ratio (Reiche, 1938) expressed as a percent

$$L = (R/n) \times 100$$

No attempt has been made to apply any form of weighting to this statistical analysis, based for example on dike thicknesses or length of exposed trace. A weighting system is only as valid as the assumptions on which it is based, and it is not clear which factors, such as dike thickness, reflect the "strength" of any intrusion, and are therefore useful as weighting factors.

Results are tabulated in Table 3.2.

The results for the total population of an area are in general agreement with visual estimates of the mean direction from the rose diagrams where the radial population is the dominant or only population present. Where both populations are well represented, the calculated resultant vector appears to reflect some average of the two population means.

An attempt has been made, therefore, to separate the radial and concentric populations based on a visual examination of the rose diagrams (Fig. 3.3), and the resultant vector calculated for each population in each area (Table 3.2). Note that in some areas (Fig. 3.3 c, e, g, l) there is no concentric population represented, and on Onawe Peninsula the presence of a third random population makes the distinction between populations impossible, so that no resultant vector can be calculated for the concentric population in these areas. The results are in much better agreement with visual estimates, and the resultant vectors for the radial and concentric populations are shown on Map 6. The "centre of gravity" of the dike swarm, defined by the area of mutual overlap of the span of the radial population in each area, is also shown on Map 6.

The radial and concentric populations of the Akaroa dike swarm have as their centre a broadly defined oval-shaped zone including the southern half of Onawe Peninsula and the area to the south and south-east of Onawe Peninsula extending as far south as the southern limit of Petit Carenage.

Table 3.2: Results of statistical analysis of dike orientation data for the total population, the radial population and the concentric population.

	Total Population				Radial Population				Concentric Population			
Location	n	γ°	R	L	n	γ°	R	L	n	γ°	R	L
Tikao	114	62	65.84	57.76	88	41	58.74	66.75	26	125	24.24	93.22
French Farm	55	82	27.27	49.57	46	67	20.93	45.49	9	119	8.82	97.94
French Farm W	5	57	4.98	99.58	5	57	4.98	99.58	–	–	–	–
Barrys Bay	56	95	38.02	67.90	25	120	23.72	94.88	31	64	19.40	62.58
NW Summit Rd	3	141	2.90	96.65	3	141	2.90	96.65	–	–	–	–
N Onawe Pen.	19	112	8.95	47.10	15	135	7.69	51.26	4	53	3.58	89.58
NNE Summit Rd	17	42	8.15	47.94	17	42	8.15	47.94	–	–	–	–
NE Summit Rd	27	67	24.32	90.06	26	65	24.34	93.61	1	157	1.00	100.00
ENE Summit Rd	36	81	29.55	82.08	27	86	25.33	93.81	9	55	4.82	53.55
E Summit Rd	50	110	35.25	70.50	26	93	24.69	94.97	24	142	13.74	57.27
ESE Summit Rd	52	119	35.98	69.19	40	133	30.00	75.00	12	72	10.07	83.94
Lighthouse Rd	23	153	22.26	96.77	23	153	22.26	96.77	–	–	–	–
Onawe Pen.	172	103	125.15	72.76	172	103	125.15	72.76	–	–	–	–

3.3.5 Interpretation of Results and the Origin of the Akaroa Dike Swarm

It has been a matter of some debate as to whether dikes form by the injection of fluid magma into pre-existing joints and fractures, or whether dikes propagate because the magma pressure within the dike fractures the host rock ahead of the advancing dike tip.

A number of studies have suggested that dikes form when magma is injected into pre-existing joints and fractures (eg. Curry and Ferguson, 1970; MacDonald and Abbott, 1970). Johnson (1961), in a study of the radial dike swarms associated with West Spanish Peak and Dike Mountain in south-central Colorado, suggested that the radial distributions resulted from selective intrusion into a pre-existing joint complex associated with intermittent orogenic stresses of varying direction and magnitude during folding of the syncline into which the magmas were intruded. Chen and Moore (1979) suggested that the Late Jurassic Independence dike swarm, a swarm of sub-parallel dikes up to 40 km wide and 250 km long, was intruded along a regional fracture system associated with crustal extension.

Other studies have suggested that dike propagation may occur when the magma pressure, or driving pressure, exceeds the minimum horizontal compression of the regional stress. Anderson (1938, 1951) noted that magma pressure in excess of the compressive stress acting across the dike plane generates tension in the host rocks beyond the dike tip, resulting in the propagation of a fracture which the magma invades. Odé (1957) suggested that the radial dike pattern of the Spanish Peaks area, Colorado, could be explained by the superposition of a local stress field (caused by hydrostatic pressure exerted by the intrusive mass) on a regional stress field. The local stress field was primarily responsible for the radial distribution of dikes, and deviations from radiality were a consequence of the influence of the regional stress field. Odé was able to model the stress fields mathematically in terms of principal stress trajectories. Delaney and Pollard (1981) report a detailed study of a large segmented dike of the radial dike swarm associated with Ship Rock, New Mexico. A prominent joint set parallel to segments of the dike was shown to be localised around the dike and unrelated to regional joint patterns. Delaney and Pollard were able to show that magma had not intruded the regional joint set, since the mean orientation of the regional joint set is 70–90° compared with 52–66° for segments of the dike and associated localised joints. Delaney and Pollard postulated that the localised joint set sub-parallel to dike segments was the result of crack propagation and reorientation associated with the forceful injection of magma into the host rock. Furthermore, segmentation of the dike was attributed to local rotation of the direction of least principal compressive stress. Similar results were obtained in a study of dike swarms in Monument Valley (Ziony, 1966).

Delaney *et al* (1986) pointed out that dikes may either be intruded along pre-existing regional joint sets, or may propagate by forceful intrusion and autogeneration of cracks ahead of the advancing dike tip, and that the particular mode of formation depends on the tectonic environment at the time of magma injection. It is, therefore, important to treat each dike or dike swarm as an independent case. Delaney *et al* proposed the following criteria for evaluating models of dike formation:

- If dikes in a swarm have dissimilar strikes but the same age, then they are insensitive to the direction of least compressive regional stress at the time of emplacement, or the stress state was not homogeneous.
- In the absence of adjacent joints and dike-parallel regional joints, the dike must have created its own single fracture perpendicular to the direction of least compressive regional stress acting at the time of emplacement.
- Where dike-parallel adjacent joints are absent but dike-parallel regional joints are present, the dike may have been injected along older joints. In this case it is necessary to verify that the joints are older than the dike.
- Where there are only dike-parallel adjacent joints, it is critical to determine the relative ages of the dike and joints.

Spence and Turcotte (1985) suggest that the direction of injection of a dike is a preferred orientation associated with either a pre-existing set of joints, in which case the dike trend would be parallel to the regional joint set, or the current stress state, in which case the injection would occur perpendicular to the least principal compressive stress.

Nakamura (1977) suggested that volcanoes could be used as indicators of regional tectonic stress. Dikes will develop in a direction perpendicular to the minimal horizontal compression of the regional stress, and dike orientations in a radial dike swarm are a function of the stress field generated by magmatic forces superimposed on the existing regional stress field at the time of injection. Fracturing and dike formation will occur when magmatic pressure in the conduit exceeds the tensile stress of rocks and the minimum compressive stress of the regional stress field. An ideal radial dike swarm indicates either that magmatic pressure within the conduit is much greater than other stresses, or that other stresses are homogeneous in horizontal directions. At some distance from the central vent, dikes may deviate from the radial pattern, reflecting the underlying regional stress field and the decreasing influence of magmatic stresses.

In a study of Etna Volcano, Frazzetta and Villari (1981) noted a similar spatial variation in structural elements (fractures, eruptive fissures, faults, lineaments, dikes).

Near the main vent, these structural elements approximate a radial distribution, but overall there is a strongly developed sigmoidal pattern. This was attributed by Frazzetta and Villari to the superposition of a regional stress field with a sinistral transcurrent east-west system and the maximum stress axes oriented north-east and north-west.

In the light of the studies discussed above, the following points are important in interpreting the origin of the radial pattern of the Akaroa dike swarm:

1. Dikes are orientated radially about a broadly defined centre which is coincident with the centre of the volcano's conical form, the maxima for conical-shaped magnetic and gravity anomaly surfaces, and the presence of plutonic rocks. A similar distribution occurs within the Lyttelton dike swarm (Shelley, 1987).

2. Dike frequencies decrease away from the centre of the radial pattern. Considering the strong evidence that dikes tend to be injected laterally from a conduit, rather than vertically (Shelley, 1985; Rubin and Pollard, 1987), it seems logical to conclude that the dikes originated from the centre of the radial pattern — the main eruptive vent and associated magmatic plumbing system — and were injected outwards from this centre.

3. The radial pattern does not appear to degrade with distance from the centre. Furthermore, the Akaroa dike swarm is strikingly similar in form to the Lyttelton dike swarm with its centres just 25 km to the north-west, yet the two dike swarms appear to have formed independently of one another. The implication is that the radial pattern reflects a local magmatic stress field, and that the regional stress field is either insignificant or homogeneous in the horizontal plane.

The radial distribution of the Akaroa dike swarm is interpreted as resulting from the superposition of a magmatic stress field concentric about the main eruptive conduit on a regional stress field in which stresses in the horizontal plane were homogeneous.

Koide and Bhattacharji (1975) provide a theoretical analysis of such stress distributions around magma reservoirs of various aspect ratios, suggesting the conditions and regions of formation of various types of fractures. Their model is based on the assumption of an isolated prolate magma reservoir in an isotropic, homogeneous, elastic rock body (Fig. 3.4) under isotropic lithostatic stress.

Stress distributions around prolate magma reservoirs of aspect ratios (D:H) 1:4, 1:10 and 1:100 were calculated, assuming a magma pressure of -2 kb[1] at the apex,

[1]Tensile stress is considered as positive, and effective pressure as negative.

a lithostatic stress of -1 kb (corresponding to pressure at a depth of 4 km), and an average interstitial hydrothermal pressure of -0.9 kb around the magma reservoir. Patterns of stress distribution near the apex of elongated magma reservoirs (aspect ratios of 1:10 – 1:100) were shown to be similar to that of a near-spherical magma body (aspect ratio 1:1.4), but the stress concentration is much higher.

These stress distribution patterns indicate a zonal distribution of fractures around such magma reservoirs (Fig. 3.5 a, b). For a near-spherical magma reservoir (aspect ratio 1:1.4), radial tensile fractures predominate, with arcuate, segmented concentric fractures occurring in a restricted region close to the vertical rotation axis of the magma reservoir (Fig. 3.6). The distributions of fractures round a more elongate magma reservoir are more complex. If interstitial fluid and magma pressures are small compared with the lithostatic stress, radial fractures dominate, accompanied by a few segmented concentric fractures (Fig. 3.7a), similar to a near-spherical magma reservoir. If, however, interstitial fluid and magma pressures become large compared to lithostatic stress, concentric fractures then predominate, forming en echelon patterns (Fig. 3.7b).

Moving from the outer limits of Akaroa Volcano towards the proposed centre of the dike swarm, there are three distinct zones of dikes:

1. A broad zone extending from the periphery of the volcano almost to the inner harbour, in which only radial dikes occur.

2. A zone encompassing all of the inner harbour shoreline, in which both radial and concentric dikes occur, with concentric dikes forming a significant, if not dominant in some areas, proportion of the population.

3. A zone, exposed only on Onawe Peninsula, in which radial, concentric and randomly orientated dikes occur.

This distribution is very similar to that presented by Koide and Bhattacharji (1975). The radial and concentric dikes are interpreted as a reflection of the influence of a stress field in which interstitial fluid and magma pressures were not significantly larger than the lithostatic stress, acting on a weakly prolate (aspect ratio 1:1.4 – 1:10) magma body during construction of the volcano. The randomly orientated dikes on Onawe Peninsula are considered to be members of one of the other two populations (probably the radial population) that have been influenced by the significantly less homogeneous country rock near the central vent, where a much higher proportion of pyroclastic material is intercalated with lava flows.

It is simplistic to think of just one or two major, stationary vents; rather, the location of the central vent and associated plumbing probably moved often, following

Figure 3.4: (Left) Diagrammatic representation of a prolate magma body and its coordinate system. After Koide and Bhattacharji (1975).

Figure 3.5: (Right) Diagrammatic sketch for zonal distribution of modes of fractures around a prolate magma reservoir (magma pressure -2 kb, lithostatic stress -1 kb, hydrothermal fluid pressure -0.9 kb). EO,EO' = extent of concentric and radial continuous tension fractures; B,B' = extent of concentric and radial brittle faults; RT,CT = zones of radial and concentric continuous tension fractures; RS,CS = zones of radial and concentric brittle faults. The initial symbol (eg RT.CS) denotes the dominant mode of fractures. (Scale is arbitrary). After Koide and Bhattacharji (1975). **A:** Near-spherical magma reservoir of aspect ratio 1:1.4. **B:** Vertically elongate prolate magma reservoir of aspect ratio 1:100.

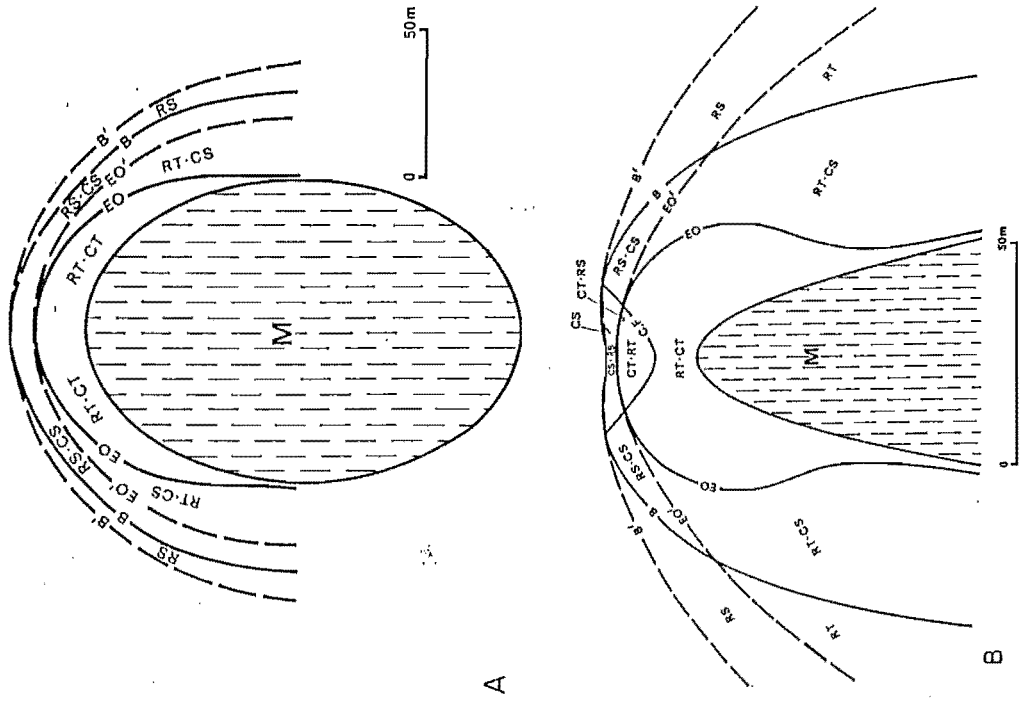
50m
0
B'
RS
B
RT·CS
EO'
EO
RT·CT
M
RS·CS
RT·CS
RT
CS
CT·RS
CT·RT
RT·CT
A
B

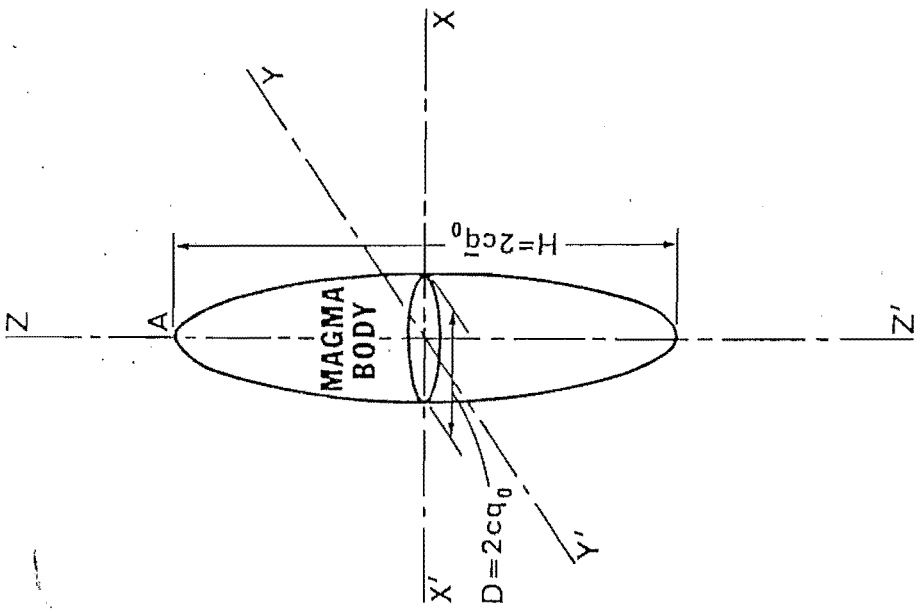
X
Y
H=2cq0
Z
A
MAGMA BODY
Z'
X'
D=2cq0
Y'

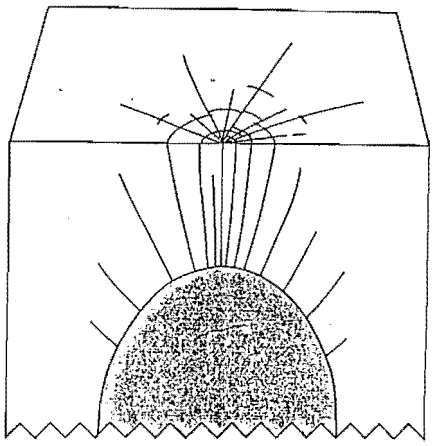

Figure 3.6: Possible fracture pattern around a near-spherical prolate magma reservoir due to magma pressure higher than lithostatic stress. After Koide and Bhattacharji (1975).

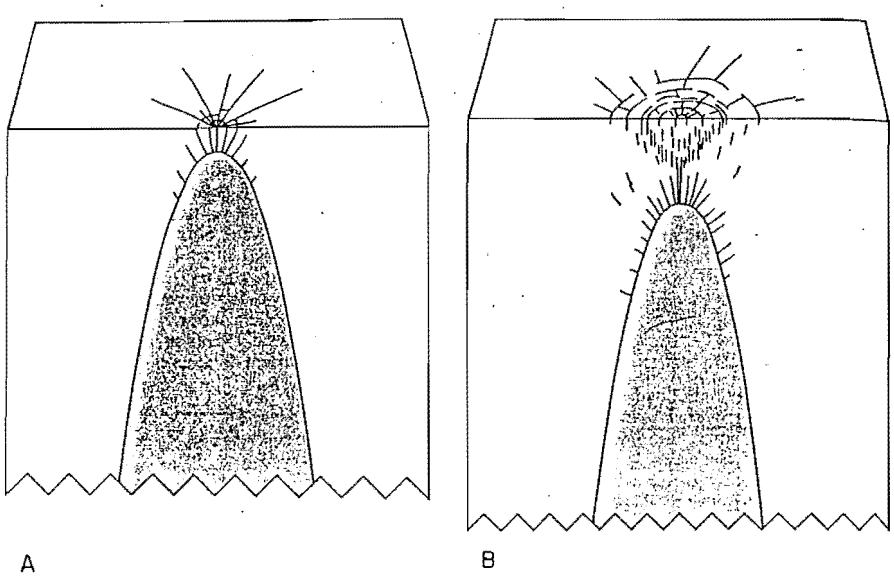

Figure 3.7: Possible development of fracture patterns around a vertically elongate prolate magma reservoir due to progressive increase of magma and hydrothermal fluid pressures shown in sequence of A and B. After Koide and Bhattacharji (1975). **A:** Formation of predominant radial fractures at an initial phase of intrusion when magma and hydrothermal fluid pressures are low (but higher than lithostatic stress). **B:** Predominant concentric and peripheral radial fracture patterns due to the increase of magma and hydrothermal fluid pressures.

a random path close to the summit of the volcano. The result would be a broad central zone exhibiting near-vent volcanological characteristics, and this is reflected in the broad zone of dike intersections shown on Map 6.

3.3.6 Gravity and Magnetic Anomalies

The volume of intrusive material in the sub-surface plumbing system of the volcano can be estimated from the gravity anomalies associated with the volcano. Pronounced positive bouguer gravity anomalies are associated with Lyttelton (> 58 mGal) and Akaroa (> 64 mGal) Volcanoes, and these persist in isostatic gravity anomalies (> 56 mGal for Lyttelton and > 54 mGal for Akaroa), indicating that the anomalies are the reflection of dense sub-surface intrusive material (Fig. 3.8).

The mass of sub-surface intrusives can be estimated from the isostatic anomaly (Reilly, 1972) by applying Gauss' theorem of mass deficiency:

$$\Delta M = (1/2\pi G) \int_{-\infty}^{+\infty} \int_{-\infty}^{+\infty} \Delta g\,(x, y)\, dx\, dy$$

where $\int_{-\infty}^{+\infty} \int_{-\infty}^{+\infty} \Delta g\,(x, y)\, dx\, dy$ is the surface integral of the anomaly. The volume of intrusives can then be calculated, assuming a density contrast between the intrusives and the country rock.

For the Dunedin Volcanic Complex, Reilly (1972) calculated an integrated anomaly of 890 mGal km, equivalent to 2.1×10^{13} kg or 105 km^3 of intrusives, assuming a density contrast of 0.2 Mg/m^3. Similar calculations have been performed for Lyttelton and Akaroa, and the results are presented in Table 3.3.

The isostatic gravity anomalies for Lyttelton and Akaroa are conic in form and the surface integral was approximated by a cone. Calculations were performed for the Dunedin Volcanic Complex using this approximation to provide a comparison with Reilly (1972). Reilly (1972) went further to develop a computer model of the intrusive plumbing system, which suggested a volume of intrusives $\approx$ 5 times the original estimate. In this light, the value of 615 km^3 for the volume of intrusives beneath Akaroa Volcano should be considered a minimum value.

Figure 3.8: Bouguer and Isostatic gravity anomalies for Banks Peninsula. After Reilly (1966, 1969).

A: Bouguer gravity anomalies; anomaly values are in mGal; contour interval is 2 mGal.

B: Isostatic gravity anomalies; anomaly values are in mGal; contour interval is 2 mGal.

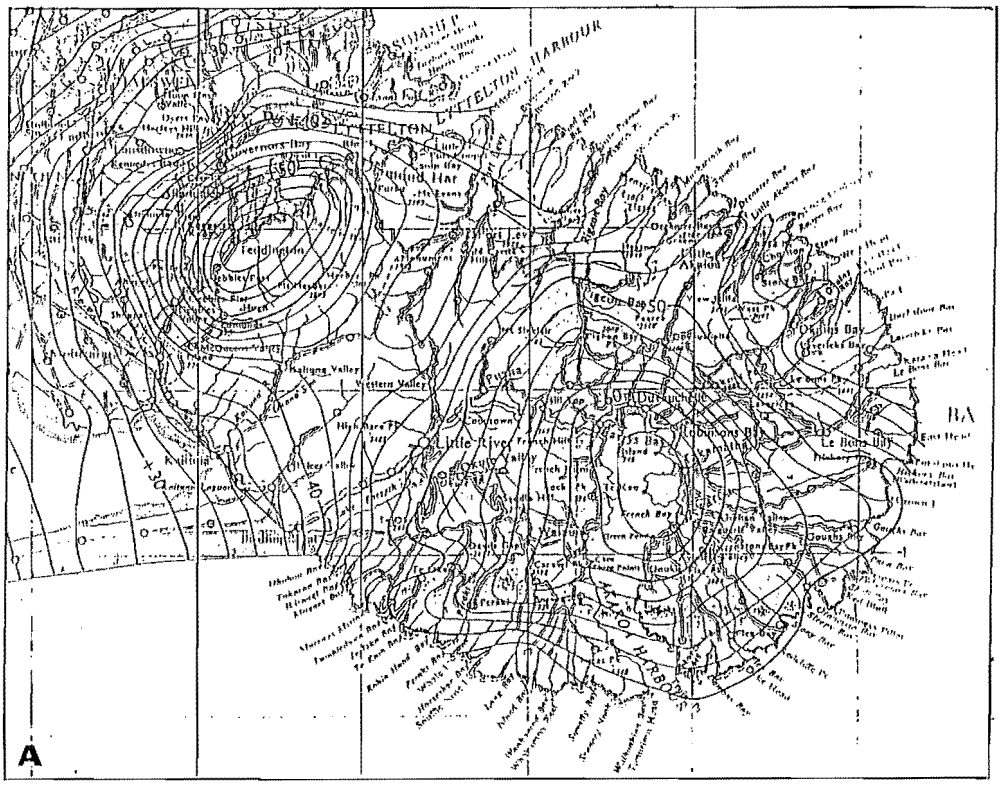
A

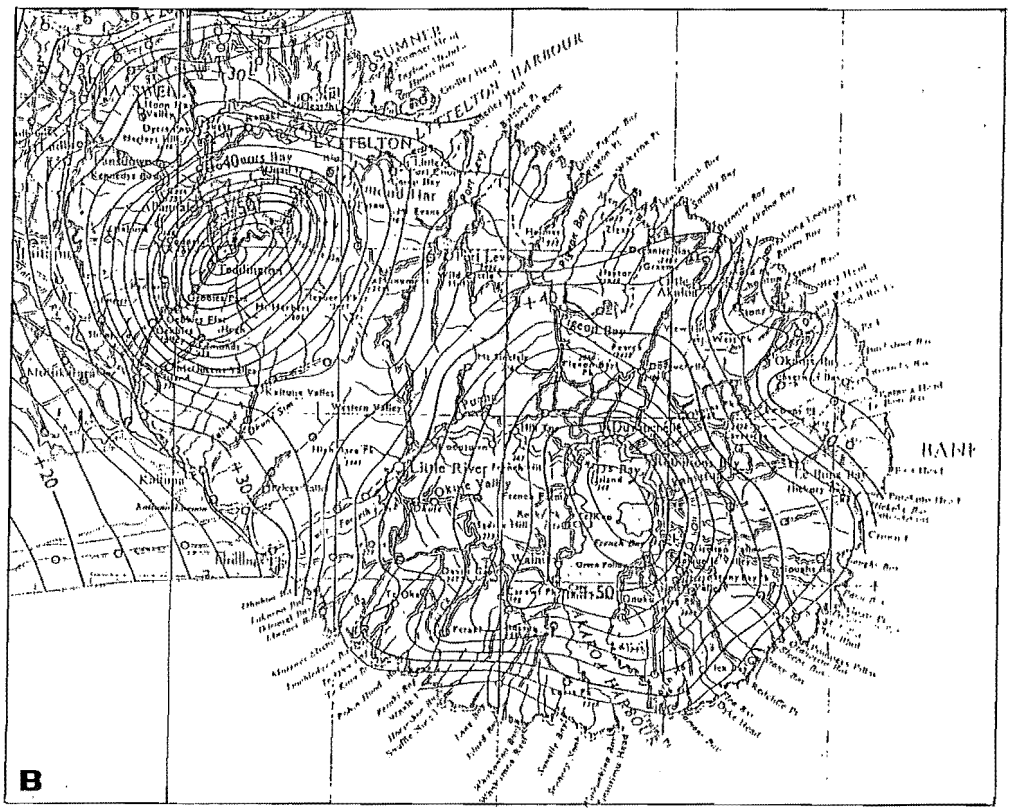
B

Table 3.3: Calculation of volume of sub-surface intrusives from isostatic gravity anomalies for Dunedin Volcanic Complex, Lyttelton and Akaroa Volcanoes.

Data/Calculation [units]	Dunedin Volcanic Complex	Lyttelton Volcano	Akaroa Volcano
Maximum anomaly [mGal]	+43.5	+57.0	+55.0
base anomaly [mGal]	+35.0	+35.0	+35.0
h (Max - base) [mGal]	8.5	22.0	20.0
r (average radius) [km]	9.6	8.0	15.7
density of intrusives [Mg/m^3]	2.87	2.87	2.87
density of country rock [Mg/m^3]	2.67	2.67	2.67
density contrast [Mg/m^3]	0.20	0.20	0.20
$\Delta g = 1/3(\pi r^2 h)$ [mGal km^2]	820	1475	5162
$\Delta M = 1/(2\pi G)\,\Delta g$ [$\times 10^{13}$ kg]	2.1	3.5	12.3
Volume of intrusives [km^3]	100	175	615

Units: mGal $10^{-5} m/s^2$; G = 6.67×10^{-11} Nm^2/kg^2

3.3.7 Dikes as Feeders of Lava Flows

It is a commonly held belief that in shield and composite volcanoes, such as those of Banks Peninsula, most dikes are the feeders of lava flows, and that many of the flows forming the more distal flanks of these volcanoes were fed by dikes. This is not supported by field evidence on Akaroa Volcano. Of the more than 600 dikes observed on Akaroa Volcano, none was observed feeding a lava flow. Gudmundsson (1984) points out that of the 21,000 dikes observed in four dike swarms near the margins of the Columbia Plateau, only a few have been seen to pass into lava flows, and none of the dikes mapped in Scotland and the Faeroe Islands have been seen to pass into a lava flow.

There are two possible explanations why dikes are not observed feeding lava flows:

1. Very few, if any, flows were fed by dikes. The corollary to this is that Akaroa lavas had sufficiently low viscosity that individual flows travelled up to 18 km from the vent during construction of what is a remarkably symmetrical cone. Rubin and Pollard (1987), in a mathematical analysis of dike propagation, show that the tendency of a dike to erupt rather than propagate is enhanced by the proximity of a surface (eg. the surface of the earth) and the blade-like geometry of the dike. However, this tendency to erupt is counteracted by the driving pressure at the dike centre. Thin near-vertical dikes which may propagate for tens of kilometres at shallow depths without erupting have been reported from the rift zones of Hawaiian volcanoes.
2. Many flows were fed by dikes, but the probability of actually observing the connection between a dike and a flow is very small because:
   - The probability of seeing the terminus or upper edge of a dike is very low
   - Only a small part of the terminus or upper edge of a dike may be connected to the lava flow
   - Not all dikes in a swarm may be feeder dikes

It is not possible, within the nature and scope of this study to distinguish between these options.

3.4 Trachyte Domes

Five large trachyte intrusive domes are exposed within Akaroa Volcano. Speight (1944) described four of them — Panama Rock, View Hill, Devils Gap and Pulpit

Rock. A fifth intrusion — Ellangowan — was discovered by aerial photographic reconnaissance during this study. In the following sections, the geology of each trachyte dome is summarised, and in section 3.4.6 the origin of these domes, including evidence of their intrusive nature, is discussed.

3.4.1 Devils Gap

Devils Gap trachyte dome is exposed on the south-eastern flanks of Akaroa Volcano, and is named after Devils Gap, a col between the intrusion itself and an adjacent prominent south-west dipping basaltic lava flow (Fig. 3.9, 3.10).

There are actually two intrusive bodies exposed at Devils Gap. The larger intrusion, here referred to as Devils Gap Senior, is a striking feature, appearing to rise up the flanks of the spur along which Gap Road runs, near Trig X (N37A/95850900), at 500–700 m asl. A smaller, less well exposed intrusion, here referred to as Devils Gap Junior, occurs 2.25 km further east, at 300–400 m asl (N37A/96800900).

Both intrusions appear to be elongate along the local dike trend (the theoretical local trend for dikes is marked on the map). Both intrusions are trachytic in composition, and intrude basalt and hawaiite lava flows of the Main Phase of Akaroa Volcano.

The contact between Devils Gap Senior and the country rock is exposed along most of the perimeter of the intrusion. Along the western edge of the intrusion, the contact dips steeply east at angles of 80–90°, but along the south-eastern edge, the contact dips at more moderate angles (40–50°) to the west. The contact is sharp, and weak baking of the country rock below the contact occurs within a narrow < 0.5 m zone. Fissility, and columnar and tabular jointing are developed within Devils Gap Senior. Fissility is generally parallel to the contact with the country rock or parallel to the local dike swarm trend. Dips are generally towards the east at angles of 62–90°, with the steepest dips being along the western and northern edges of the intrusion. Columnar jointing is generally orientated at a high angle to fissility, typically trending 130–160° and plunging 0–50°. Tabular jointing is generally orientated at a high angle to fissility, striking north-west—south-east (90–140°) and dipping north-east at angles of 38–90°.

Devils Gap Junior is exposed in a cliff face at the end of a spur to the east of Devils Gap Senior. Accessible exposure is limited, with contacts not visible. Fissility, and columnar and tabular jointing are developed within Devils Gap Junior. Fissility is developed at small angles to the cliff face (160–175°) dipping west at 40–50°, or parallel to the local dike swarm trend. Columnar jointing trends approximately east (80°) out of the cliff face, plunging at 45°.

LEGEND

for Figs 3.9, 3.12, 3.13, 3.16 & 3.17

TOPOGRAPHY

100 — CONTOUR (M)

STREAM

ROAD

TRACK

TRIG

•735 SPOT HEIGHT (M)

CONTACTS

DEFINITE

APPROXIMATE

INFERRED

STRUCTURE

FISSILITY

TABULAR JOINTING

CONTACTS

COLUMNAR JOINTING

REGIONAL DIKE TREND

COMPOSITION

TRACHYTE

BENMOREITE

UNDIFFERENTIATED COUNTRY ROCK

SCALE 1: 7 000 (metric)

0 0.25 0.5 km

CONTOUR INTERVAL 100m

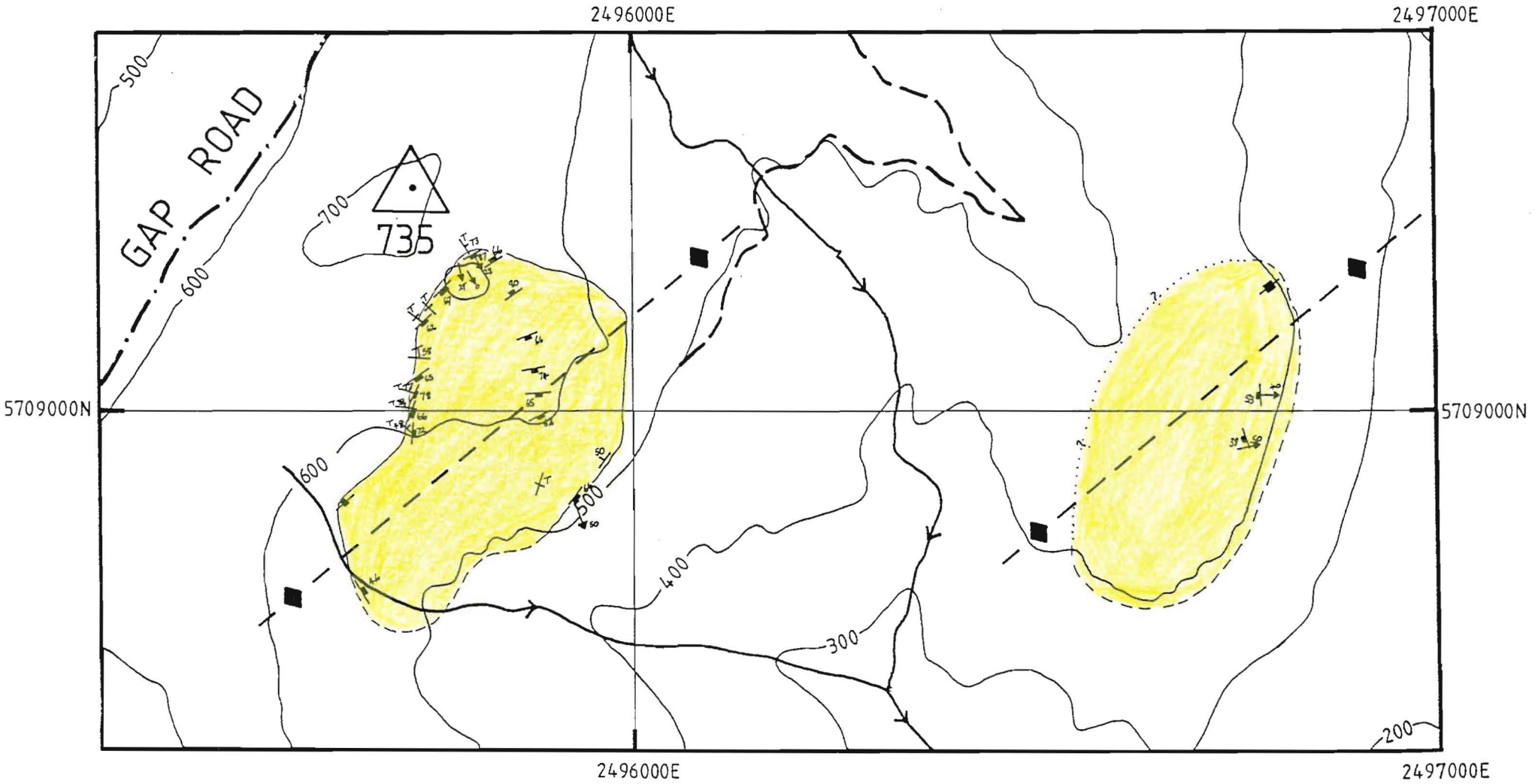

Figure 3.9: Sketch map of the geology of Devils Gap trachyte intrusion.

3.4.2 Panama Rock

Panama Rock trachyte dome (Fig. 3.11) is exposed on the eastern flanks of Akaroa Volcano, at the intersection of Panama Road (after which the intrusion is named) and Camerons Track (N36D/13421803), 400–600 m asl. Panama Rock is the only one of the five large trachytoid intrusions for which a feeder dike can be observed (Fig. 3.12).

The main body of the intrusion forms an oval-shaped dome with precipitous slopes on the crest of a ridge running east-west away from the centre of the volcano. The contact between Panama Rock and the country rock was not observed anywhere along the perimeter of the main intrusion, although country rock and intrusive material can be observed within 1–2 m of each other around much of the perimeter of the intrusion. The intrusion was fed by a large (> 5 m thick) dike which trends west-south-west—east-north-east ($\approx 60°$) and can be seen to connect with the main body of the intrusion at it's south-western edge. The feeder dike can be traced west-south-west across Panama Road, and on the west side of Panama Road a second large (3–4 m thick) trachyte dike can be seen within 40 m of the main feeder dike. This second dike can be traced west-south-west across the hillside, where it can be seen to widen considerably, and is considered to be an offshoot connected at depth to the main feeder dike. Panama Rock is elongate to, and the feeder dike strikes parallel to, the local dike trend.

Panama Rock is trachytic in composition, and intrudes *ne*-basalts (N36D3016 at N36D/12821785, N36D3021 at N36D/13061811), intercalated with occasional red basaltic ashes of the Main Phase of Akaroa Volcano.

The dominant structural element within Panama Rock is the fissility of the trachyte. In the main body of the intrusion, fissility is orientated parallel to the intrusive contact. The dip of the fissility increases from 38° near the centre of the intrusion, to 90° at the intrusive contact. Along the feeder dike, fissility trends parallel to the dike trend ($\approx 50°$) and is vertical. Fissility within the offshoot dike on the west side of Panama Road is orientated at an acute angle to the walls of the dike. Within the feeder dike, tabular jointing is very well developed, with joint planes very planar and evenly spaced at 3–5 cm intervals. Joint orientation is normal to the trend of the dike and fissility, at 172°/85°W.

3.4.3 Ellangowan

Ellangowan trachyte dome (Fig. 3.13, 3.14) is exposed on the eastern flanks of Akaroa Volcano, 400–500 m asl on the south-facing northern slopes of the valley

Figure 3.10: Devils Gap trachyte intrusion, taken from Bossu Road, looking west. Devils Gap Junior is at bottom centre, Devils Gap Senior at centre, and at top centre is a masssive 20+ m thick basaltic lava flow dipping south-west.

Figure 3.11: Panama Rock and the feeder dike, taken from on top of the feeder dike at its south-western end, looking north-east.

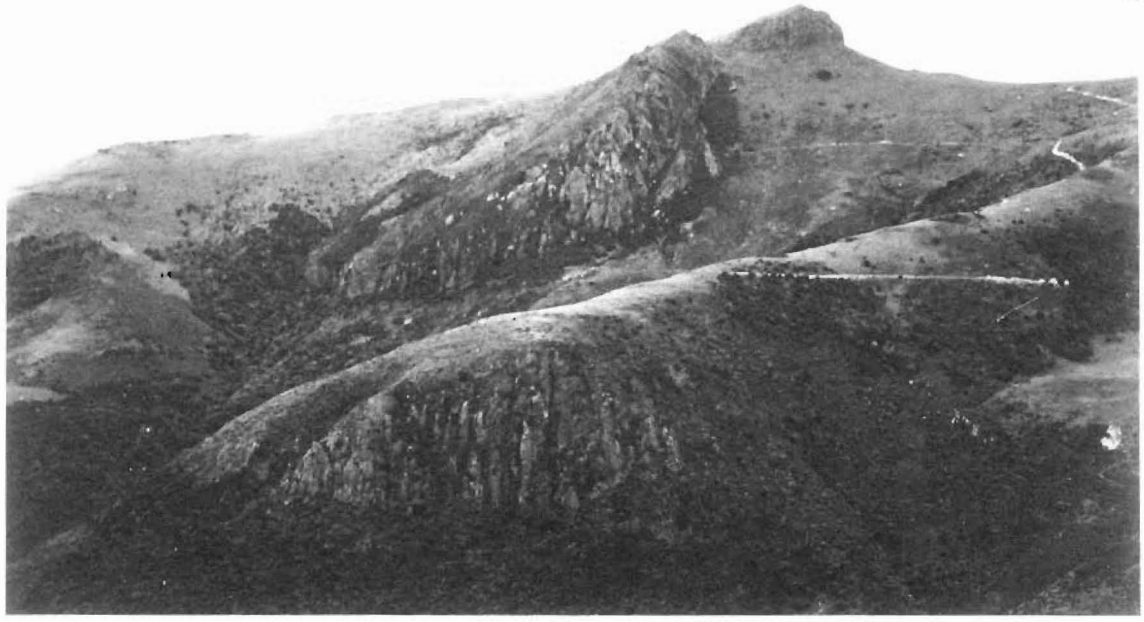

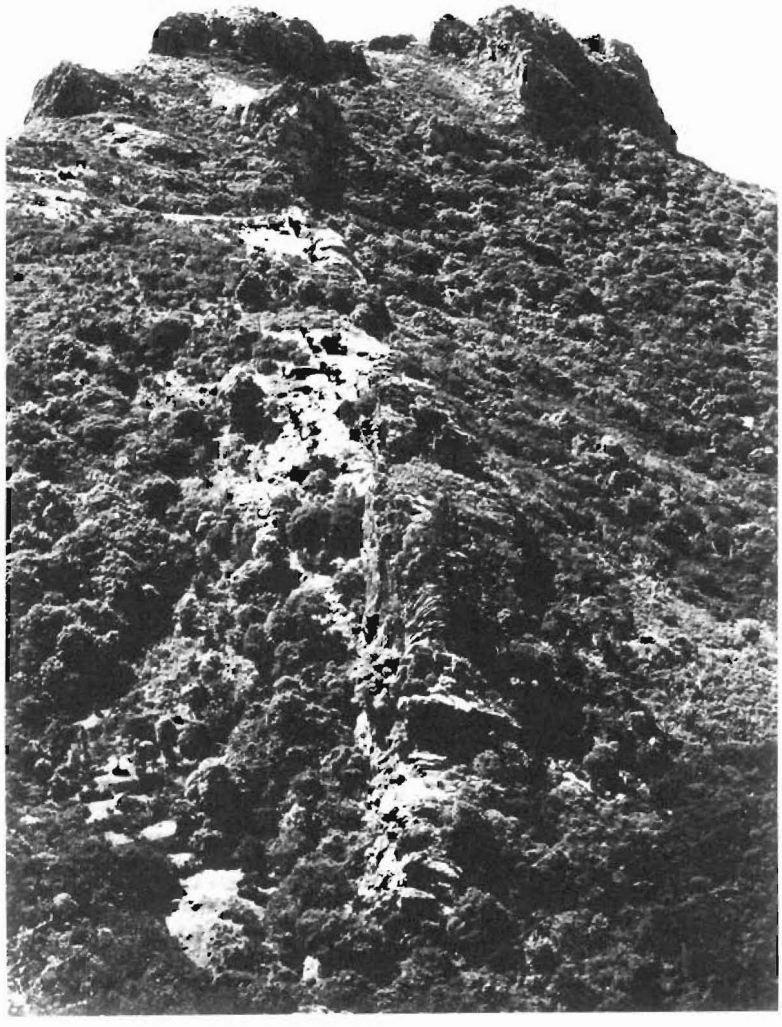

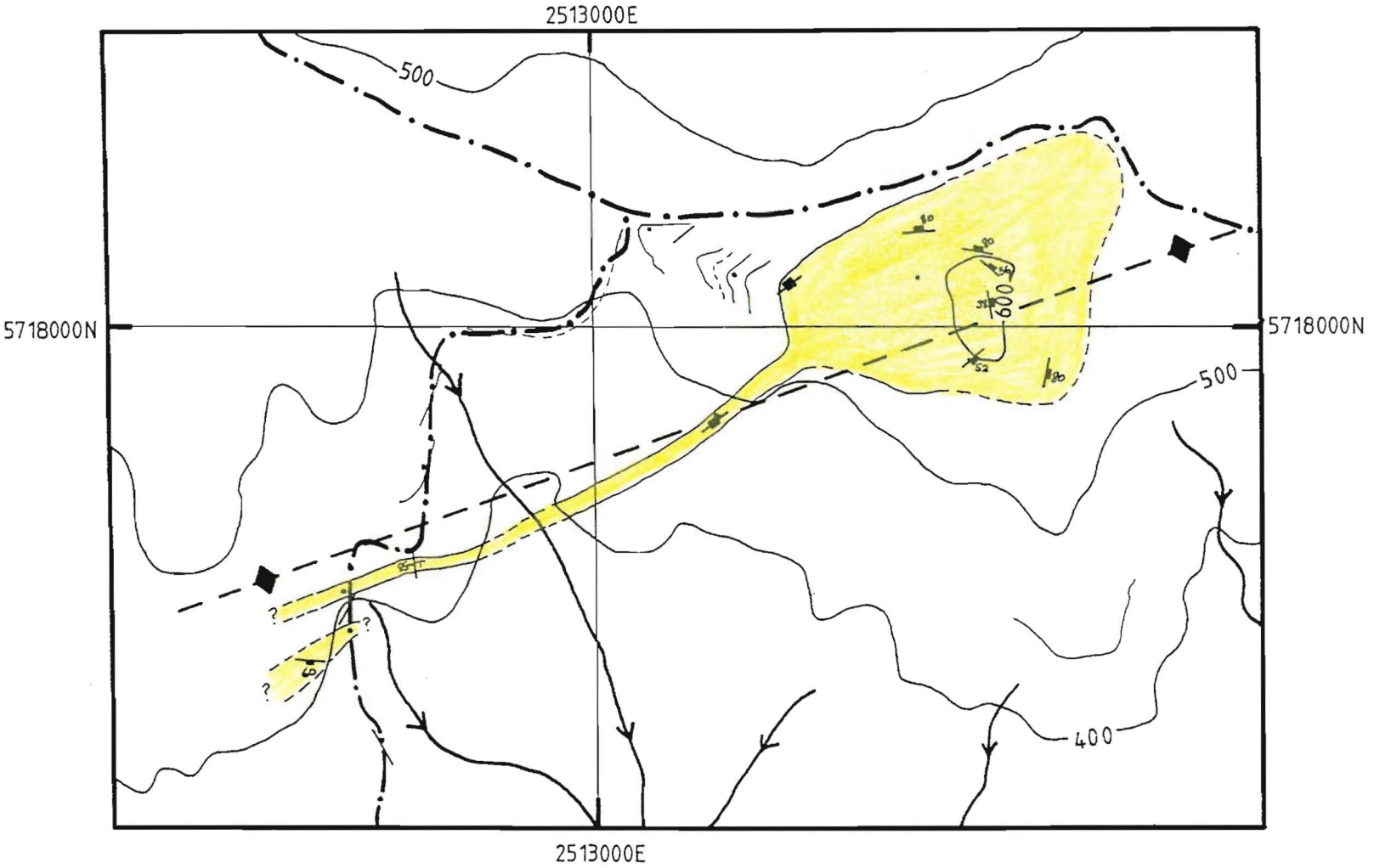

Figure 3.12: Sketch map of the geology of Panama Rock trachyte intrusion. Legend as for Fig. 3.9.

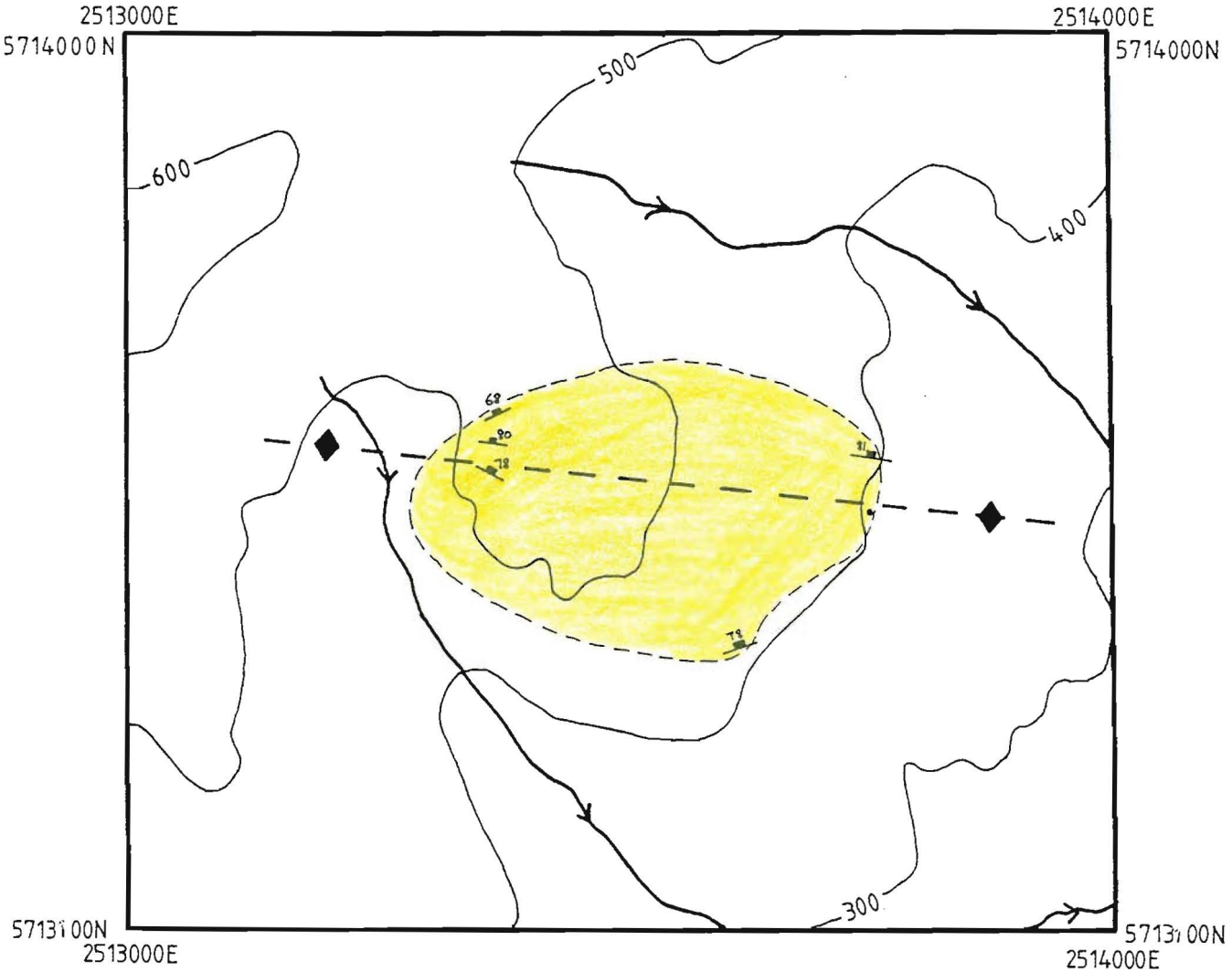

Figure 3.13: Sketch map of the geology of Ellangowan trachyte intrusion. Legend as for Fig. 3.9.

occupied by Ellangowan Stream (after which the intrusion is named) and 4.5 km due south of Panama Rock (N36D/13551345).

Ellangowan trachyte intrusion forms an oval-shaped dome elongated parallel to the local dike trend. The contact between Ellangowan and the country rock was not observed anywhere along the perimeter of the intrusion, although country rock and intrusive material can be observed within 1–2 m of each other around much of the perimeter of the intrusion.

Ellangowan is composed of *qz*-trachyte (N36D3000 at N36D/13621339, N36D3600 at N36D/13761353) and intrudes basalt and hawaiite lava flows of the Main Phase of Akaroa Volcano.

Structural elements are poorly developed on Ellangowan, compared with the other large trachytoid intrusions, and the only element measured was fissility. Fissility is generally orientated parallel to the intrusive contact or the local dike trend, and dips north at high angles (68–81°).

3.4.4 Pulpit Rock

Pulpit Rock trachyte dome (Fig. 3.15) is exposed on the eastern wall of the erosional crater of Akaroa Volcano, at the head of French Farm Valley (N36C/99651329), 310–510 m asl. Pulpit Rock is the only one of the five large trachytoid intrusions which occurs within the eroded crater.

The intrusion forms an oval-shaped dome on the north facing slopes of an east-west trending ridge (Fig. 3.16). Unlike the other trachytoid intrusions, the long axis of Pulpit Rock does not appear to be orientated parallel to the local dike trend. It should be noted, however, that the position of the intrusion with respect to the surrounding topography is such that a significant portion of the intrusion may be hidden beneath flows forming the ridge to the south, and the true shape of the intrusion may differ from the observed outcrop pattern. The headwaters of the stream occupying French Farm Valley have nearly dissected the intrusion into inequal portions. The north-east face of Pulpit Rock forms a striking, near-vertical rock face rising more than 75 m above the valley floor. The contact between Pulpit Rock and the country rock was not observed anywhere along the perimeter of the intrusion, although country rock and intrusive material can be observed within 1–2 m of each other around much of the perimeter of the intrusion. A second, smaller heart-shaped trachyte intrusion crops out on the ridge to the south-east of Pulpit Rock (N36C/98961269), and may be related at depth to the main trachyte intrusion.

Pulpit Rock is composed of a weathered *ne*-trachyte (N36C3111 at N36C/99721317)

Figure 3.14: Ellangowan trachyte intrusion, taken from Hickory Bay Road, looking north.

Figure 3.15: Pulpit Rock trachyte intrusion, looking west from the eastern shore of Akaroa Harbour.

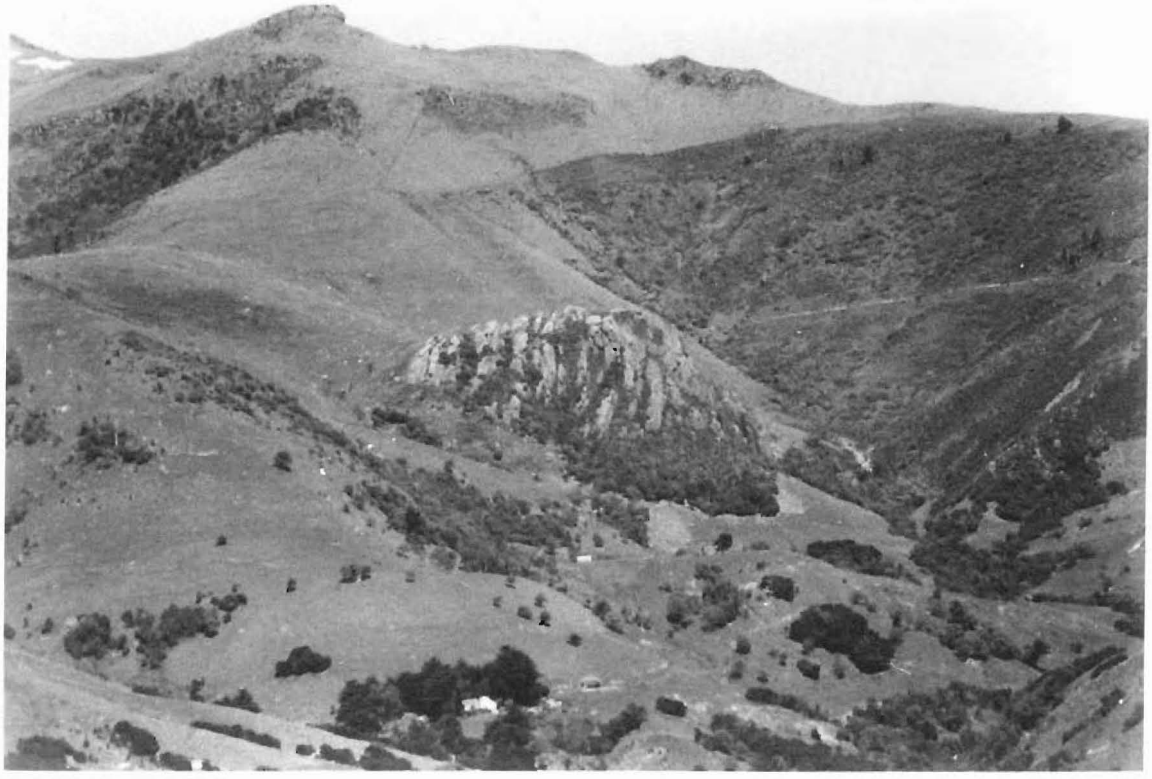

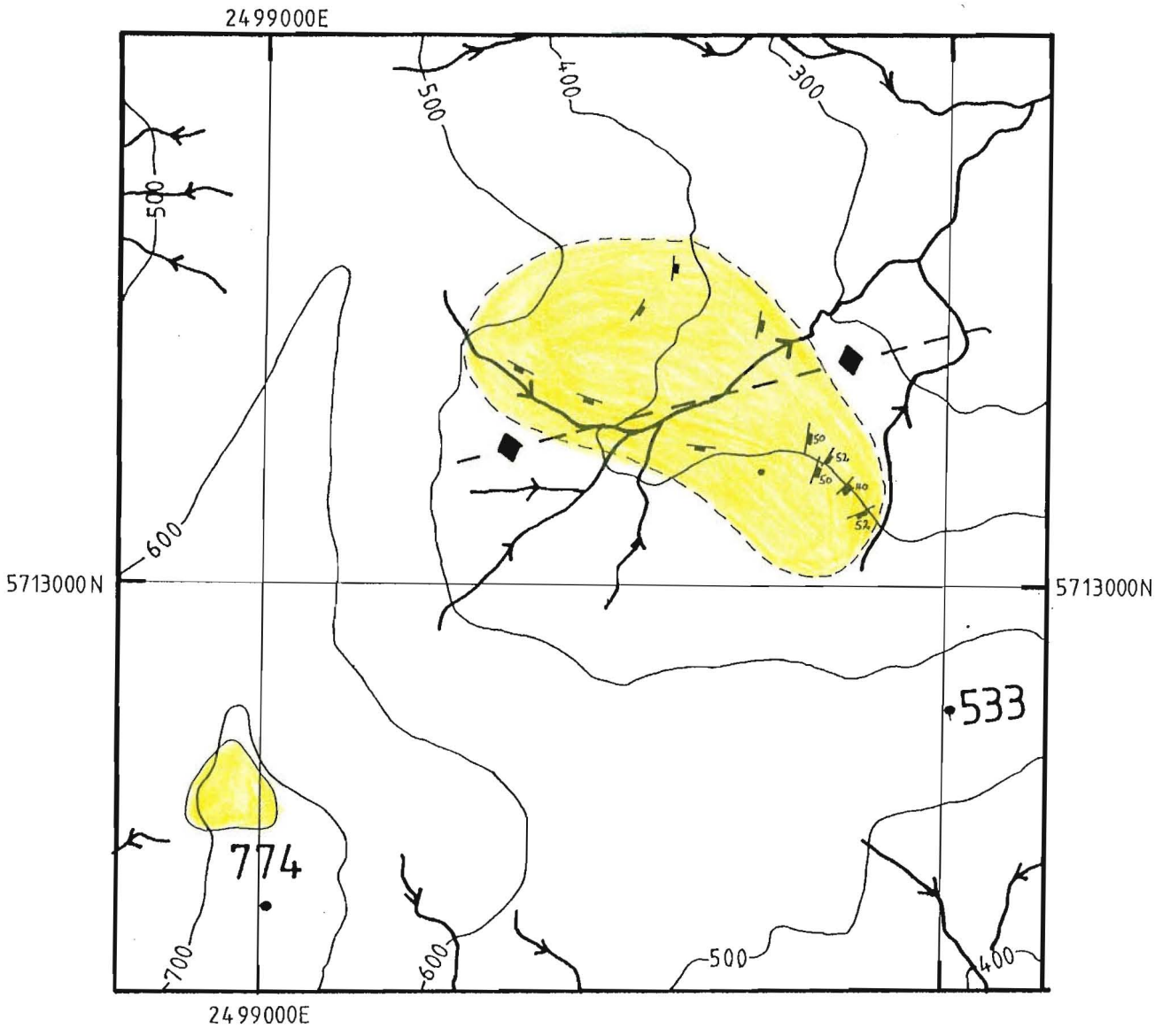

Figure 3.16: Sketch map of the geology of Pulpit Rock trachyte intrusion. Legend as for Fig. 3.9. Note scale is 1:10 000.

and intrudes *hy*-basalt to *ne*-mugearite lava flows (see Map 2, Map Pocket) of the Main Phase of Akaroa Volcano.

The dominant structural element within Pulpit Rock is the fissility of the trachyte. Fissility is generally orientated sub-parallel to the intrusive contact, and dips from the centre of the intrusion towards the contact at angles of 40° to 52°.

3.4.5 View Hill

View Hill dome (Fig. 3.17) is exposed on the north-eastern flanks of Akaroa Volcano, 350 m south-west of View Hill (after which the intrusion is named), at 700–750 m asl (N36C/09052265).

The intrusion forms an oval-shaped dome, elongate sub-parallel to the local dike trend, on the crest of a ridge running north-east—south-west away from the centre of the volcano. The contact between View Hill and the country rock can be observed along the north-eastern and eastern edges of the intrusion. Elsewhere along the perimeter of the intrusion, country rock and intrusive material can be observed within 1–2 m of each other. Where visible, the contact is sharp and dips towards the centre of the intrusion at angles of 30–48°. The country rock is weakly baked with 20–30 cm of the contact.

View Hill is the only one of the five large intrusions which is not trachytic in composition, but composed of benmoreite. The country rock consists of basalts and hawaiites intercalated with red-brown basaltic ashes and scoriaceous ashes of the Main Phase of Akaroa Volcano.

The dominant structural element within View Hill is the fissility of the benmoreite. Fissility is generally orientated parallel to the intrusive contact, although this variation is not as well developed as, for example, in Panama Rock. The dip of the fissility is generally to the north or east, and ranges from 18° to 90°, but this variation does not appear to be consistently related to position within the intrusion.

3.4.6 Origin of the Trachyte Domes

Several lines of evidence support the contention that the five large trachyte domes are intrusive in nature:

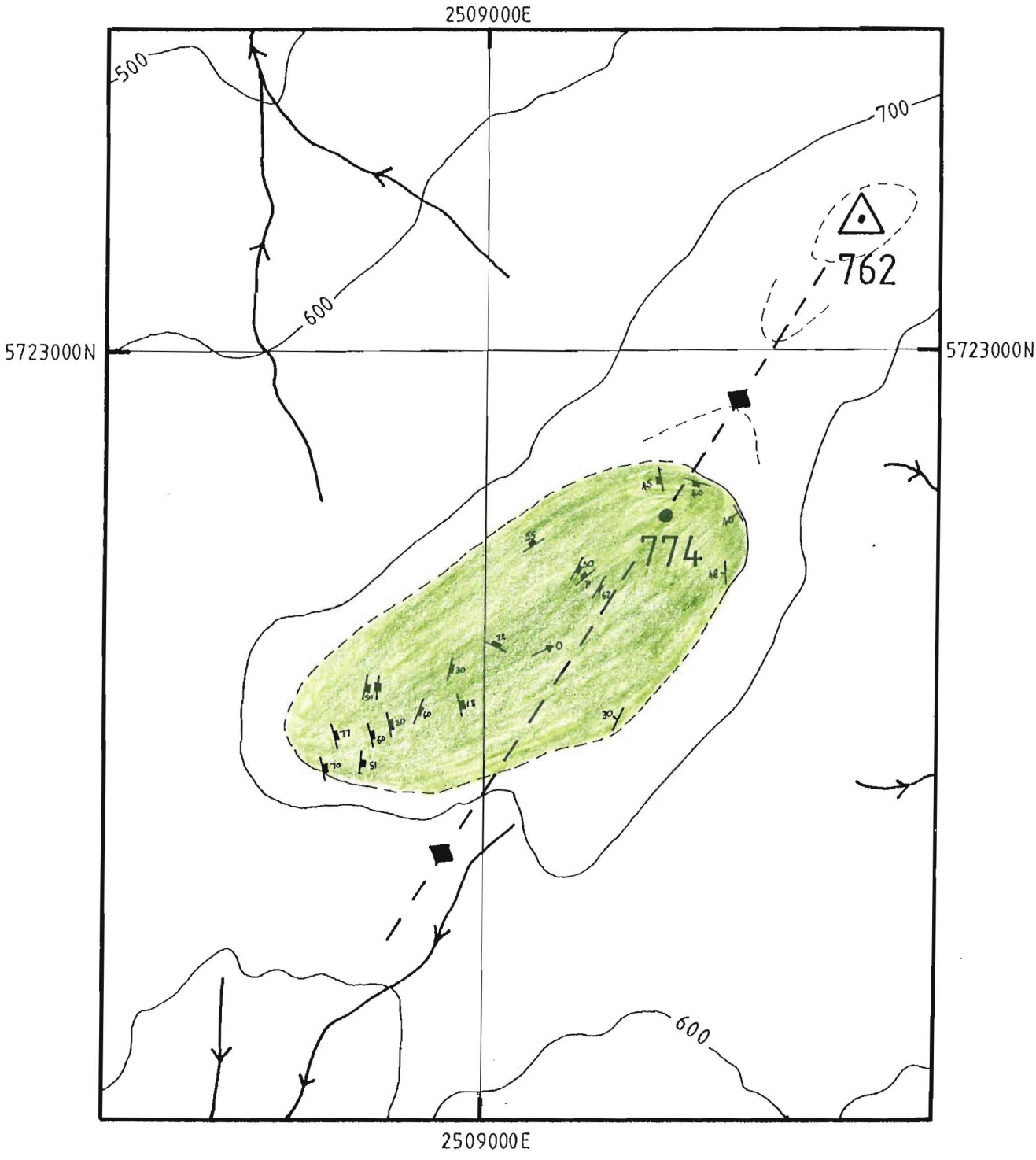

Figure 3.17: Sketch map of the geology of View Hill intrusion. Legend as for Fig. 3.9.

- The contact between the domes and the country rock (flows and minor intercalated pyroclastics) is discordant with the local geological trend.
- The contact with the country rock, when visible, is sharp and there is weak baking of the country rock. The contact generally dips at high angles away from the centre, or at moderate angles towards the centre of the intrusion.
- Autobreccias and debris fans normally associated with flows, coulées and extrusive domes are absent (cf. many of the lava domes of Dunedin Volcano; Price and Coombs, 1975).

The trachyte domes have a number of other features in common:

- With the exception of Pulpit Rock, they are all exposed on the outer flanks of the volcano. Furthermore, all outcrops occur between 350 m and 760 m asl — approximately $\frac{1}{4} - \frac{1}{2}$ way up the flanks of the volcano, based on a projected height of $\approx$ 1500 m.
- They are all composed of trachyte, except View Hill, which is composed of benmoreite, and they intrude basalt and hawaiite lava flows and minor pyroclastics of the Main Phase of Akaroa Volcano.
- They are all oval-shaped domes in form (with the possible exception of Devils Gap) and the long axis of the dome is parallel to the local dike trend, with the exception of Pulpit Rock. In the case of Panama Rock, the intrusion can be seen to be fed by a dike which also strikes parallel to the local dike trend.
- They all exhibit fissility in the trachyte (or benmoreite) which is orientated parallel to the contact with the country rock, and dips at moderate to steep angles away from the center of the intrusion towards the contact. Dips tend to increase towards the contact. Where columnar and tabular jointing are present, they tend to be orientated at a high angle to both the contact and the fissility.

These lines of evidence suggest that the trachyte domes are all intrusive bodies fed by trachyte dikes of the radial dike swarm. As noted in section 3.3.7, recent models of dike propagation (Rubin and Pollard, 1987) portray dikes as having a blade-like geometry and propagating laterally from the magma source. The trachyte domes are considered to have formed near the surface of the volcano, when magma driving pressure was insufficient to fracture rock ahead of the advancing dike tip but sufficient to cause updoming of overlying flows and lateral expansion of the dike towards the dike top. The fact that all the domes occur at about the same elevation may indicate that all the domes were intruded during a single major phase of intrusive activity.

Chapter 4

PETROGRAPHY AND MINERALOGY

4.1 Introduction

In this chapter, the petrography and mineralogy of Akaroa Volcano lavas are discussed in two parts.

Petrographic descriptions of thin sections from 87 samples are presented in Appendix D. Proportions of mineral phases present in each thin section were estimated using the visual estimation charts of Terry and Chilingar (1955). Plagioclase anorthite contents quoted in Appendix D and in petrographic descriptions in this chapter were determined using the Michel-Levy method (Shelley, 1975) and are minimum estimates. In the petrographic descriptions, the general term "clinopyroxene" is used as the compositions of crystals are generally unknown. All pyroxene crystals for which probe data are available, are high-Ca clinopyroxenes (diopside — hedenbergite, high-Ca augite). The term "titaniferous clinopyroxene" is used for Ti-rich pyroxenes. Orthopyroxenes are not found in the rocks of Akaroa Volcano. A description of microprobe analytical techniques is presented in Appendix E. Microprobe analyses of minerals from 14 rock samples are presented in Appendix F, and the data are summarised here for the minerals analysed — olivine, pyroxene, feldspar, magnetite, amphibole and biotite. As the number of samples on which microprobe data were obtained was limited, the compositional range determined for an individual mineral in a particular rock type must be treated as an estimate only. The overall variation in chemistry for a particular mineral across a range of rock types is of greater significance.

4.2 Petrography

4.2.1 Basanitoids

Basanitoids are holocrystalline, aphanitic and porphyritic with intergranular groundmasses.

Phenocrysts are dominantly olivine and magnetite, with subordinate plagioclase and titaniferous clinopyroxene. Olivine phenocrysts (0.1–2.5 mm) are commonly subhedral, and may have rims altered to red-brown iddingsite or green bowlingite. Magnetite phenocrysts (0.05–1.0 mm) are anhedral. Plagioclase phenocrysts (0.1–3.2 mm) are subhedral to euhedral bytownites (An_{70}–An_{75}), and display normal and/or oscillatory zoning. Most have a well developed sieve texture and/or resorbed and embayed margins. Pink to purple-brown, anhedral to euhedral titaniferous clinopyroxene phenocrysts (0.4–3.0 mm) have sieve textured cores, corroded rims and are occasionally strongly zoned at the margins.

The groundmasses consist of subequal proportions of labradorite (An_{65}–An_{68}), colourless to pale purple-brown clinopyroxene–titaniferous clinopyroxene, and magnetite, and minor amounts of iddingsitised olivine and colourless apatite.

4.2.2 Basalts

Basalts are typically holocrystalline, porphyritic and aphanitic with intergranular and occasionally pilotaxitic groundmasses. Rarely seriate/hiatal or pseudo-ophitic textures are present.

In terms of phenocryst assemblages, basalts can be divided into four groups (in decreasing order of abundance):

1. Plagioclase > olivine > magnetite phyric lavas
2. Plagioclase > olivine > clinopyroxene > magnetite phyric lavas
3. Aphyric lavas
4. Olivine > clinopyroxene phyric lavas

Olivine-clinopyroxene-phyric lavas contain up to 30% phenocrysts, whereas other porphyritic lavas typically have < 10% phenocrysts. Plagioclase phenocrysts (0.4–3.5 mm) are subhedral to euhedral calcic labradorites (An_{63}–An_{67}). Sieve texture

and strong normal and/or oscillatory zoning are common. Some phenocrysts have resorbed cores or margins with secondary overgrowths, usually of more sodic plagioclase. Olivine phenocrysts (0.2–2.5 mm) are anhedral to euhedral, and have red-brown iddingsite or green bowlingite rims. Occasionally, smaller crystals are completely iddingsitised. Pink to purple-brown coloured clinopyroxene and titaniferous clinopyroxene phenocrysts (0.4–1.0 mm) are typically anhedral to subhedral, and occasionally show hourglass or patchy zoning, or resorbed cores with inclusions of olivine, plagioclase and magnetite. Magnetite inclusions may be concentrated in Ti-rich zones. Magnetite phenocrysts (0.2–0.5 mm) are anhedral, and typically represent about 1% of the rocks.

The groundmasses consist of labradorite (An_{50}–An_{70}), colourless to pale green or pink coloured clinopyroxene or weakly titaniferous clinopyroxene, magnetite, and minor amounts of iddingsitised olivine and colourless apatite.

4.2.3 Hawaiites

Hawaiites are holocrystalline, aphanitic, and porphyritic or aphyric, with intergranular and often pilotaxitic groundmasses. Rarely, some lavas may exhibit hypocrystalline, intersertal, glomerophyric or felty textures. The porphyritic lavas can be subdivided into four groups based on phenocryst assemblages.

Plagioclase-olivine-clinopyroxene-magnetite phyric hawaiites: Phenocryst phases have the relative abundances plagioclase > olivine > magnetite > clinopyroxene. Plagioclase phenocrysts (0.4–5.0 mm) are subhedral to anhedral labradorites (An_{61}–An_{65}) with resorbed and embayed cores, normal/oscillatory zoning and sieve texture. Anhedral olivine phenocrysts (0.2–3.5 mm) are often partly to completely replaced by iddingsite, bowlingite and/or calcite. Clinopyroxenes (0.3–4.5 mm) are anhedral, pink coloured, and often zoned from green cores to purple-brown titaniferous rims. Some are resorbed and embayed, or exhibit hourglass or patchy zoning (Fig. 4.1). Magnetite phenocrysts (0.1–0.8 mm) are anhedral, embayed and resorbed, and rarely sieve textured.

Plagioclase-olivine-magnetite phyric hawaiites: Phenocryst phases have relative abundances plagioclase > olivine > magnetite. Plagioclase phenocrysts (0.2–6.0 mm) are anhedral to euhedral sodic labradorites (An_{43}–An_{63}, typically An_{55}) with strong normal/oscillatory zoning. Resorbed, embayed and sieve textured crystals are common. Olivine phenocrysts (0.1–3.2 mm) are subhedral to anhedral, and are often iddingsitised, bowlingitised or pseudomorphed by a calcite/bowlingite mixture. Magnetite phenocrysts (0.05–1.5 mm) are subhedral to anhedral, resorbed and embayed. Sample N36C3670 contains traces of red-brown apatite as a phenocryst phase.

Plagioclase phyric hawaiites: The plagioclase phenocrysts (0.4–4.5 mm) are calcic labradorite (An_{53}), subhedral to euhedral, and display some sieve texture and normal/oscillatory zoning.

Olivine-magnetite phyric hawaiites: Olivine phenocrysts (0.06–1.5 mm) are anhedral to euhedral, and may be iddingsitised. Magnetite phenocrysts (0.08–0.8 mm) are anhedral.

The groundmasses of hawaiite lavas consist of euhedral calcic andesine (An_{33}–An_{61}, typically An_{45}) laths, colourless to pale green, or rarely pink to purple-brown titaniferous clinopyroxene, magnetite and apatite. Anhedral, iddingsitised olivine, green chlorite, calcite or dark brown devitrified glass may also be present.

4.2.4 Mugearites

Mugearites are holocrystalline, aphanitic and aphyric with intergranular groundmasses. Occasionally, trace amounts of anhedral magnetite phenocrysts and red-brown apatite microphenocrysts may be present (Fig. 4.2). Red-brown apatite is distinctive in all lavas except basalts and basanitoids. "Common" apatite forms colourless, euhedral acicular prisms, and is ubiquitous as a groundmass phase in lavas, and occasionally in coarse grained rocks. Red-brown apatite is easily distinguished from "common" apatite. Red-brown apatite occurs only as single phenocrysts, or in glomerophyric aggregates of, or as inclusions in, magnetite, plagioclase, clinopyroxene and olivine. It forms euhedral hexagonal or prismatic crystals with a pale red-brown tint which darkens rapidly at the margins of the crystal. Prismatic sections contain very closely spaced lamellae highlighted by inclusions of Fe/Mg? oxides. In hexagonal sections these lamellae form three sets at 60°. Although apatite does not have a good cleavage, it is hexagonal, and therefore could theoretically develop three cleavages at 60°. Falloon (1982) reports U-stage measurements of three cleavages at 60° in crystals similar to the one shown in Fig. 4.2a, and reported microprobe analyses that confirmed the identification as apatite. Knutson and Green (1975) describe similar apatites from a high pressure megacryst assemblage in a near-saturated hawaiite, and suggest that the apatite crystallised at pressures greater than 6 kb.

The groundmasses of mugearites consist of euhedral sodic andesine/calcic oligoclase (An_{30}), colourless to pale green clinopyroxene, magnetite and apatite. In sample N36C3318, the groundmass clinopyroxene is completely and specifically pseudomorphed by a carbonate, probably an Fe-rich variety.

4.2.5 Benmoreites

Benmoreites are holocrystalline, aphanitic, and porphyritic or aphyric, with intergranular or rarely pilotaxitic groundmasses. Porphyritic lavas contain minor amounts of plagioclase, clinopyroxene, magnetite and olivine as phenocryst phases. Kaersutite megacrysts may also be common. Plagioclase phenocrysts (0.0–5.6 mm) are calcic oligoclase to andesine in composition (An_{20}–An_{50}), and may be sieve textured, with overgrowths and strong normal/oscillatory zoning (Fig. 4.3). Subhedral to euhedral, pale green or pink to purple-brown clinopyroxene and titaniferous clinopyroxene (0.15–0.60 mm) phenocrysts may be zoned from purple-brown titaniferous cores to green rims. Sector or hourglass zoning is also common in titaniferous clinopyroxenes. Magnetite phenocrysts (0.1–0.8 mm) are subhedral to euhedral. Olivine phenocrysts (0.4 mm) are subhedral to euhedral. Red-brown, pleochroic, subhedral amphibole megacrysts are surrounded by opacite margins of magnetite and clinopyroxene. Distinguishing individual species within the red-brown amphiboles is often difficult without chemical data, but the presence of Ti-rich minerals, apparently as the products of the breakdown of the amphibole, suggests the amphibole is kaersutite. The groundmass of both phyric and aphyric benmoreites consists of anhedral to euhedral oligoclase (An_{15}–An_{24}), colourless to green or rarely pink coloured clinopyroxene, magnetite and apatite. Subhedral to anhedral, iddingsitised, yellow-brown Fe-rich olivine is often present, and often has a corona of green pleochroic clinopyroxene. Rarely, red-brown apatite may be present.

4.2.6 Trachytes and Microsyenites

Trachytes are holocrystalline, aphanitic, and porphyritic or aphyric with trachytic groundmasses. Rarely, they may exhibit a seriate texture. Porphyritic lavas may be divided into 3 groups based on phenocryst assemblages.

Plagioclase-clinopyroxene-magnetite phyric trachytes: Oligoclase phenocrysts (0.4–5.6 mm) are subhedral to anhedral, weakly normal/oscillatory zoned, sieve textured and resorbed. Some show weakly developed perthitic textures. The clinopyroxene is subhedral to anhedral, (0.2–1.0 mm), pale green to green pleochroic, often with pink coloured cores. Magnetite (0.1–0.6 mm) is anhedral, resorbed and embayed.

Plagioclase-magnetite phyric trachytes: Oligoclase (0.8–4.0 mm) is subhedral, sieve textured, sometimes weakly glomerophyric, and exhibits exsolution lamellae. Magnetite (0.1–0.4 mm) is anhedral to euhedral.

Figure 4.1: Resorbed and embayed titaniferous clinopyroxene phenocryst in a *ne*-hawaiite (N36C3690). Field of view is 3.16 mm. cpl.

Figure 4.2: Red-brown apatite microphenocrysts in a *hy*-mugearite (N36A3581). (Top) Euhedral hexagonal section with three sets of lamellae at 60°. Field of view is 0.50 mm. ppl. (Bottom) Prismatic section with very fine closely spaced lamallae. Field of view is 1.12 mm. ppl.

Figure 4.3: Very sieve textured plagioclase phenocryst in a *ne*-benmoreite (N36A3585). Although this is an extreme example, sieve texture is a common feature of plagioclase phenocrysts from all lava types from basanitoid to trachyte. Field of view is 4.2 mm. cpl.

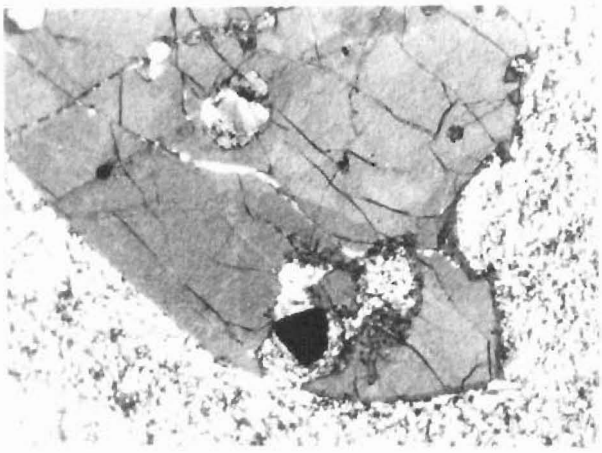

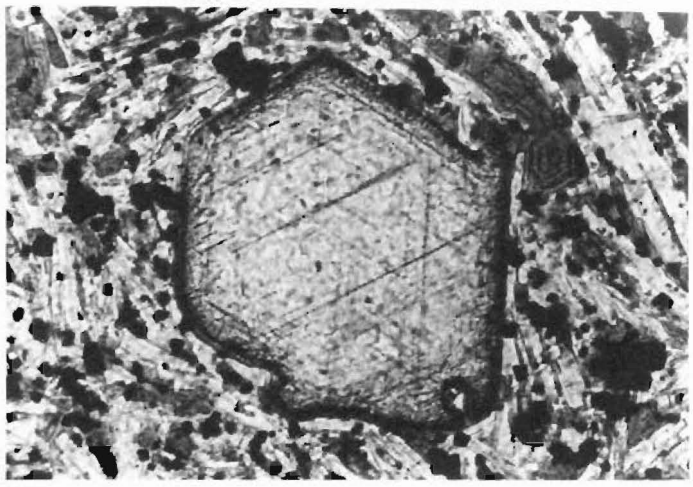

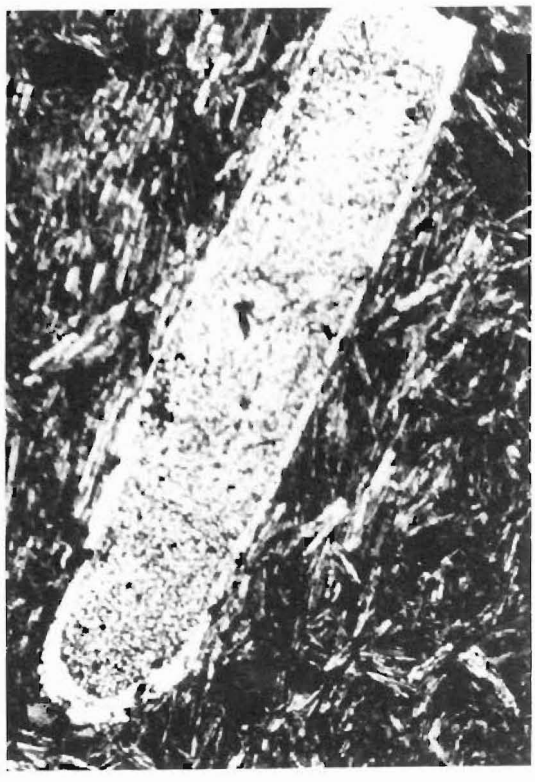

Kaersutite-plagioclase phyric trachytes: Oligoclase (1.0–2.5 mm) is subhedral to anhedral. Red-brown pleochroic, anhedral kaersutite megacrysts have opacite margins of magnetite and clinopyroxene produced from the breakdown of the amphibole (Fig. 4.4).

The groundmasses consist of euhedral albite laths, green pleochroic clinopyroxene, magnetite and red-brown anhedral Fe oxide (possibly pseudomorphing olivine and clinopyroxene). Other minerals that may be present include pleochroic, yellow-brown to blue-green arfvedsonite, pleochroic red-brown aenigmatite (Fig. 4.5), intersertal quartz, apatite, anhedral iddingsitised olivine and brown glass devitrifying to ?alkali feldspar and quartz.

The microsyenite from the coarse zone of the Tikao Trachyte has a holocrystalline, phaneritic, granular and weakly consertal texture. A sharp contact between the microsyenite and fine grained trachyte lava typical of the Tikao Trachyte can be observed in a thin section from sample N36C3639 (Fig. 4.6). The microsyenite is dominated by subhedral to anhedral albite/Na-oligoclase, often with anorthite coronas. The angular interstices between feldspar crystals are lined with a thin layer of red-brown Fe oxide and filled with calcite. In sample N36C3639, the mineral lining the cavities is colourless, uniaxial negative and fast along, and has low birefringence, straight extinction, and refractive index intermediate between plagioclase and calcite. Prismatic crystals, orientated at high angles to the plagioclase crystal face, form radiating fans which coalesce to produce a thin, persistent layer. The mineral is thought to be scapolite (Fig. 4.7). Scapolite crystallisation is controlled by high CO_2 pressures or abundant brine:

$$\underbrace{3NaAlSi_3O_8 + 3CaAl_2Si_2O_8}_{plagioclase} + NaCl + CaCO_3 \rightleftharpoons$$

$$\underbrace{3NaAlSi_3O_8.NaCl + 3NaAlSi_3O_8.CaCO_3}_{scapolite}$$

The microsyenite outcrops at sea level on the shore of the inner Akaroa Harbour, which is a substantial source of brine. The abundance of calcite infilling cavities in the microsyenite suggests that CO_2 was also available in some volume.

4.2.7 Syenite and Gabbro

The syenite from Onawe Peninsula has a holocrystalline, phaneritic and intergranular texture, and is composed almost entirely of subhedral to euhedral orthoclase and albite/Na-oligoclase (0.4–3.0 mm), with minor subhedral clinopyroxene, red-brown

Figure 4.4: (Left) Kaersutite megacryst in a *ne*-trachyte (N37A3506), breaking down at the margins to magnetite and clinopyroxene. Field of view is 1.04 mm. ppl.

Figure 4.5: (Right) Pleochroic blue-green arfvedsonite (A) and red-brown aenigmatite (E) in the groundmass of a *qz*-trachyte (N36D3600). Field of view is 1.4 mm. ppl.

Figure 4.6: Contact between phaneritic, ?consertal textured microsyenite (right) and aphyric, aphanitic and intergranular trachyte (left), from the Tikao trachyte dome (N36C3639). Field of view is 3.9 mm. cpl.

Figure 4.7: Scapolite (arrowed), lining the cavities in the microsyenite of the Tikao Trachyte (N36C3639), and forming a reaction rim between subhedral albite/oligoclase (A) and secondary calcite (C). Field of view is 2.25 mm. ppl.

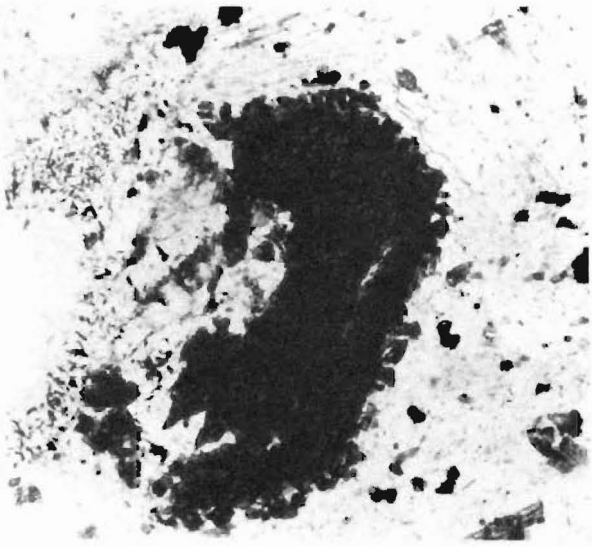

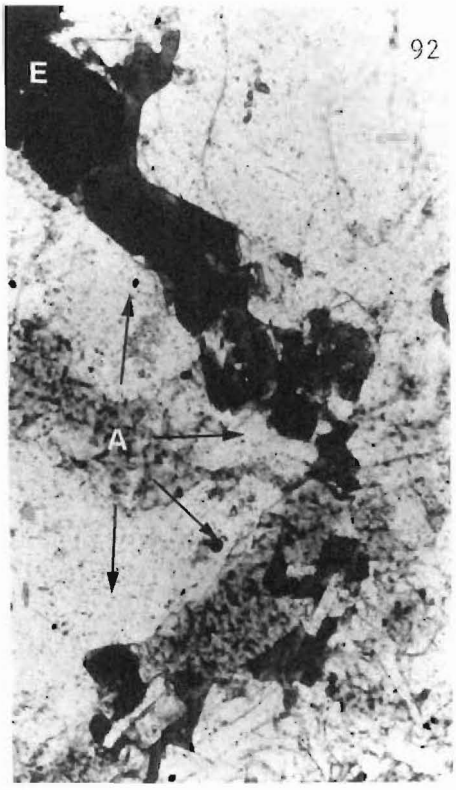
E
A

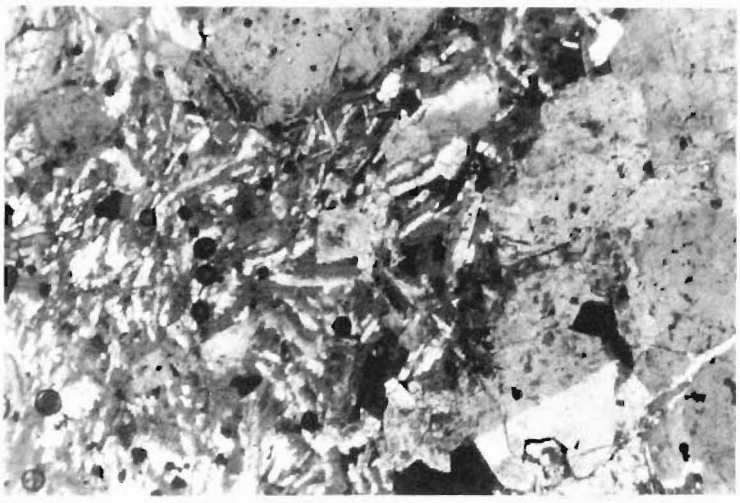

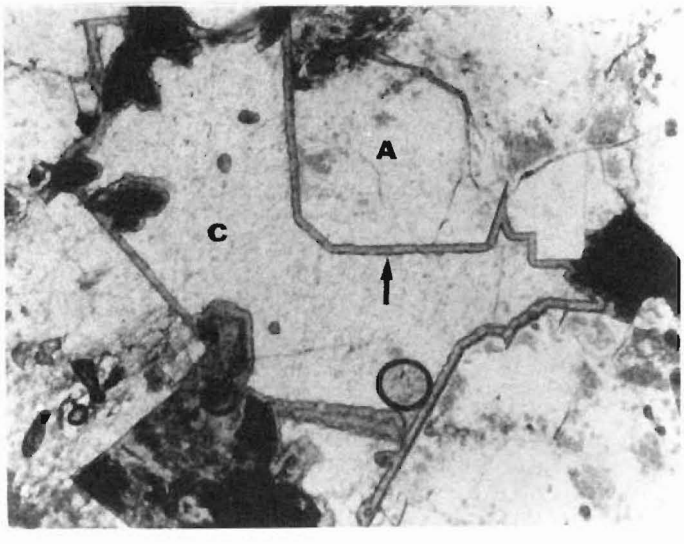
A
C

amphibole and magnetite. Interstitial secondary quartz with undulose extinction is also present (Fig. 4.8). The feldspar crystals commonly have overgrowths of weathered, brown, turbid anorthoclase. This turbid, brownish appearance is often ascribed to the presence of incipient sericite or a kaolin-like mineral. However, Deer *et al* (1966) note that in many cases this appearance is due to the presence of liquid-filled vacuoles trapped during magmatic crystallisation or by related hydrothermal activity. The presence of secondary quartz infilling cavities between feldspar crystals is further evidence for the syenite having experienced significant hydrothermal activity.

The gabbro has a holocrystalline, phaneritic, intergranular, and occasionally subophitic texture. Euhedral calcic labradorite to sodic bytownite (An_{68}–An_{73}) occasionally displays strong normal zoning. The dominant ferromagnesium minerals are pink coloured clinopyroxene, coarse (> 4.0 mm) olivine, and magnetite. Clinopyroxene and olivine may be partly or completely pseudomorphed by calcite. Minor amounts of biotite, red-brown amphibole and colourless apatite are also present (Fig. 4.9).

Samples from the schlieren in the gabbro have compositions intermediate between the gabbro and the syenite. A monzodiorite (N36C3154) has a holocrystalline, phaneritic and intergranular texture, and is dominated by subhedral to euhedral calcic andesine (An_{48}), with anhedral pink coloured clinopyroxene, magnetite and olivine occupying the interstices. Olivine is extensively replaced by calcite and Fe oxide. Minor amounts of biotite, red-brown amphibole, apatite and chlorite are also present. A monzonite (N36C3154) is similar in texture and composition to the syenite. It has a holocrystalline, very coarse (10.0–30.0 mm), intergranular texture, and is composed almost entirely of euhedral oligoclase (An_{17}) and orthoclase feldspar, with traces of red-brown apatite, biotite and magnetite.

4.2.8 Xenoliths

Lava flows exposed near sea level in Haylocks Bay were discovered to contain gabbroic to monzodioritic xenoliths. Whereas coarse grained xenoliths have been reported previously from other parts of Banks Peninsula (Sewell, 1985), this is the only site within Akaroa Volcano known to contain such xenoliths.

The xenoliths occur in two adjacent dark grey-black, fine to medium grained, aphyric basaltic lava flows exposed on the west side of Haylocks Bay, for some 200+ m along the shore line (N37A/08450230). The boundary between xenolithic material and the host lava is distinct and abrupt. The xenoliths vary in size from 1–30 cm diameter, and are subangular to subrounded in shape.

The xenoliths are completely crystalline, granular to intergranular textured and composed of coarse, 1–5 mm, subhedral crystals of feldspar, olivine, clinopyroxene, magnetite, iron oxide, apatite and amphibole. Xenolith mineralogy shows considerable variation and is summarised in Table 4.1.

Table 4.1: Summary of xenolith mineralogy from Lighthouse Reserve. Minerals enclosed in single parentheses "()" comprise 1–10% of the xenolith. Minerals enclosed in double parentheses comprise < 1% of the xenolith.

- plagioclase-clinopyroxene-(magnetite-Fe oxide)
- plagioclase-clinopyroxene-(Fe oxide-magnetite)-((apatite))
- plagioclase-clinopyroxene-(olivine-magnetite-apatite)
- plagioclase-clinopyroxene-(magnetite)-((apatite-amphibole))
- plagioclase-clinopyroxene-(magnetite-olivine)-((apatite-Fe oxide))
- plagioclase-((clinopyroxene-olivine-Fe oxide-magnetite))
- olivine-clinopyroxene-Fe oxide-magnetite-((plagioclase))
- clinopyroxene-magnetite-((olivine-Fe oxide-plagioclase))

Some xenoliths exhibit varying forms of primary igneous layering. Sample N37A3637 comprises thin (3–10 mm), discontinuous, monomineralic layers (Fig. 4.10). Sample N37A3638 displays well developed, persistent layering on a centimetre scale, defined by feldspar-rich (± minor olivine + clinopyroxene + magnetite + iron oxide) and olivine–clinopyroxene–magnetite–iron oxide-rich (± minor feldspar) layers (Fig. 4.11). The boundary between the two layers is abrupt.

Petrographically, the xenoliths are holocrystalline, phaneritic and granular to intergranular (Fig. 4.12). The dominant mineral phase is calcic labradorite (An_{60}–An_{70}) in the gabbroic xenoliths, and calcic andesine/sodic labradorite (An_{45}–An_{58}) in monzodiorite compositions. Clinopyroxene is the dominant mafic phase. Crystals may show reverse zoning with Fe-rich cores (Z^c increases towards cores). Anhedral magnetite, iddingsitised olivine and red-brown Fe oxide are also common. The red-brown Fe oxide occasionally appears to replace olivine. Colourless or red-brown apatite and red-brown amphibole may be present in trace amounts.

Figure 4.8: Secondary quartz (Q) infilling cavities between albite/oligoclase and orthoclase crystals in the syenite from Onawe Peninsula (N36C3146). Note the presence of brown turbid overgrowths of anorthoclase (A). Field of view is 3.4 mm. cpl.

Figure 4.9: Typical view of the gabbro from Onawe Peninsula (N36C3156). B = Biotite; C = Clinopyroxene; M = Magnetite; O = Olivine; P = Plagioclase; Field of view is 4.2 mm. cpl.

Figure 4.10: (Left) Plagioclase–olivine–clinopyroxene–magnetite–Fe Oxide xenolith (N37A3637) from Lighthouse Reserve, showing a well developed igneous layering defined by thin, sub-parallel, discontinuous, monomineralic layers. Lens cap is $\approx$ 95 mm.

Figure 4.11: (Right) Xenolith from Lighthouse Reserve exhibiting very well developed igneous layering, defined by coarse clinopyroxene–olivine–Fe oxide–magnetite-rich and plagioclase-rich layers. (N37A3638).

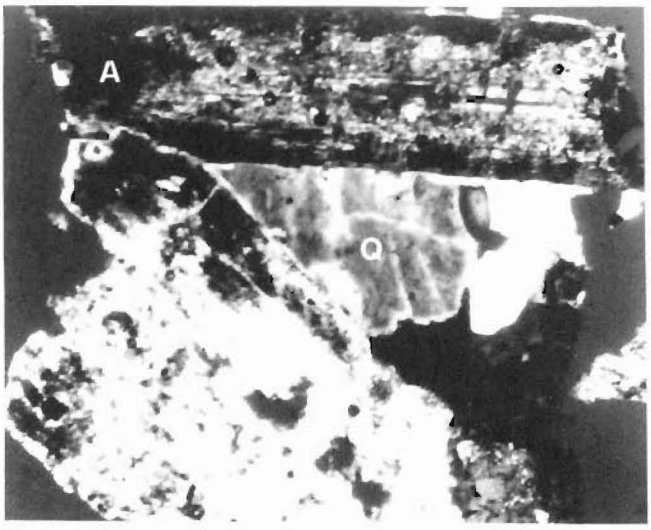
A
Q

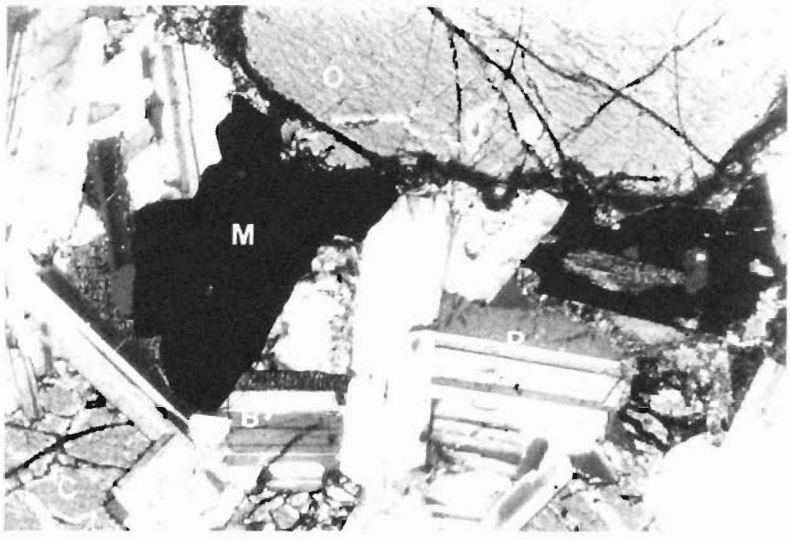
Q
M

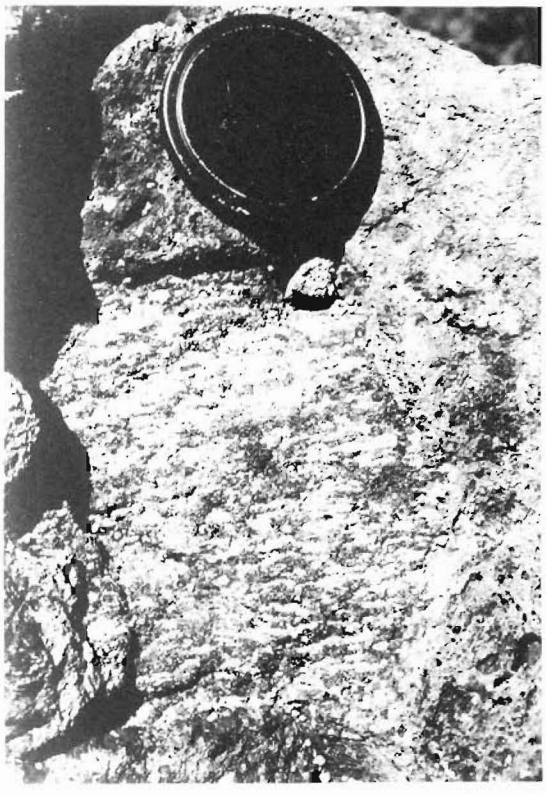


3cm

4.2.9 Pyroclastics

Most pyroclastic deposits are too friable, weathered or hydrothermally altered, or too fine grained for much to be gained from a petrographic study. Notable exceptions are the welded lapilli tuff from Onawe Peninsula and clasts from the trachyte tuff-agglomerate on Takamatua Peninsula.

Welded lapilli tuff

The black welded polylithic lapilli tuff from Onawe Peninsula consists of 0.4–2.0 mm, angular to rounded clasts welded together by minor amounts of dark basaltic glass. There is considerable variation between samples in terms of grain size, sorting, clast lithology, accessory minerals and the abundance of basaltic glass.

Clasts can be assigned to one of the following lithological groups:

1. Isolated, anhedral to euhedral plagioclase crystals.
2. Lava, dominantly basaltic, with a range of textures including aphyric, phyric and pilotaxitic.
3. Well sorted, fine ($\approx$ 0.04 mm) quartz-arenite, similar to Paleocene quartz-arenites known to occur beneath Lyttelton Volcano (B. Field, *pers. comm.*). (Fig. 4.13). Some fragments show bedding defined by alternating layers of fine (0.01 mm), medium (0.05 mm) and coarse (0.15 mm) grains. Rarely, fragments appear to be partly recrystallised to a very fine, almost cryptocrystalline texture.
4. Poorly sorted, fine to coarse litharenite (Torlesse sediments?).
5. Coarse (0.2 mm), moderate to well sorted quartz-arenite, in which the individual grains have indistinct and irregular grain boundaries, and varying extinction. Grains may contain abundant trails of inclusions or colourless to pale green chlorite needles (Fig. 4.13). Occasionally, within fragments there is a gradation to well sorted fine quartz-arenite (group #3). The texture of these fragments is suggestive of a quartz-arenite in which the quartz has been transformed to tridymite under thermal metamorphic conditions, and on cooling, reverted back to quartz, retaining the metamorphic texture (D. Shelley, *pers. comm.*).

The dark basaltic glass which welds the clasts together is often rich in inclusions of magnetite, or less commonly, may contain spherulites formed from the devitrification of the glass. In some samples, the glass contains incipient cordierite crystals with well developed cyclic and (130) twinning (Fig. 4.14).

Cordierite is most commonly developed in thermally metamorphosed rocks derived from argillaceous sediments, at an early stage in metamorphism. Tridymite occurs most often in acid volcanic rocks. There is some debate, however, whether tridymite occurs magmatically or as the result of pneumatolytic action (Deer *et al*, 1966). Furthermore, Deer *et al* (1966) state that the presence of tridymite does not necessarily imply that the temperature exceeded the inversion-point of tridymite (870°C). It seems likely that these minerals formed as a result of the metamorphism and assimilation of sedimentary material by basaltic lava prior to and during the eruption of the tuff.

Trachyte tuff-agglomerate clasts

Trachyte clasts from the trachyte tuff-agglomerate on Takamatua Peninsula have a hypocrystalline, porphyritic, flow-banded and spherulitic texture. Oligoclase phenocrysts (0.4–1.6 mm) may be present in trace amounts. The groundmass consists of alternating spherulite-rich/plagioclase lath-poor and plagioclase lath-rich/spherulite-poor layers. Glass may be present throughout. The groundmass plagioclase is albite/oligoclase. The spherulites appear to result from the devitrification of the groundmass glass to alkali feldspar and ?quartz.

4.3 Chemical Mineralogy

4.3.1 Olivine

Olivine compositions are shown in Fig. 4.15. Olivine phenocrysts from lavas and shallow intrusions are typically normally zoned, with Mg-rich cores and Fe-rich rims. Some phenocrysts do exhibit reverse zoning. Groundmass olivine compositions are similar to, or more Fe-rich, than phenocryst rim compositions.

In basalts, phenocrysts generally have cores of Fo_{68}–Fo_{84} (average Fo_{76}), and rims of Fo_{61}–Fo_{73}, averaging Fo_{68}. Groundmass olivine compositions range from Fo_{61} to Fo_{73}, averaging Fo_{65}. Olivine phenocrysts in hawaiites have cores and rims of Fo_{68}–Fo_{73} and Fo_{58}–Fo_{63} respectively, while groundmass compositions are Fo_{60}–Fo_{61}.

Figure 4.12: Granular to intergranular texture of plagioclase, clinopyroxene and magnetite in a xenolith from Lighthouse Reserve (N37A3632). Field of view is 4.2 mm. ppl.

Figure 4.13: Fragments of well sorted fine quartz-arenite (Q) of group #1 and ?recrystallised medium quartz-arenite (R) of group #5 amongst clasts of basaltic lava, in the welded lapilli tuff from Onawe Peninsula (N36C3696). Field of view is 3.7 mm. cpl.

Figure 4.14: Welded lapilli tuff from Onawe Peninsula (N36C3140). (Left) Dark basaltic glass in the welded lapilli tuff of Onawe Peninsula (N36C3140), containing incipient cordierite (C). Field of view is 3.0 mm. cpl. (Bottom right) Close-up of incipient cordierite crystal. Note the well developed cyclic and (130) twinning. Field of view is 0.9 mm. cpl.

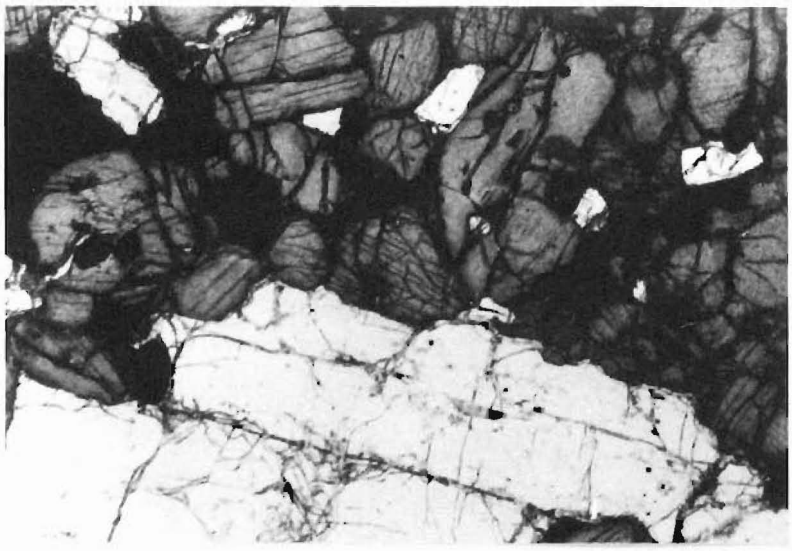

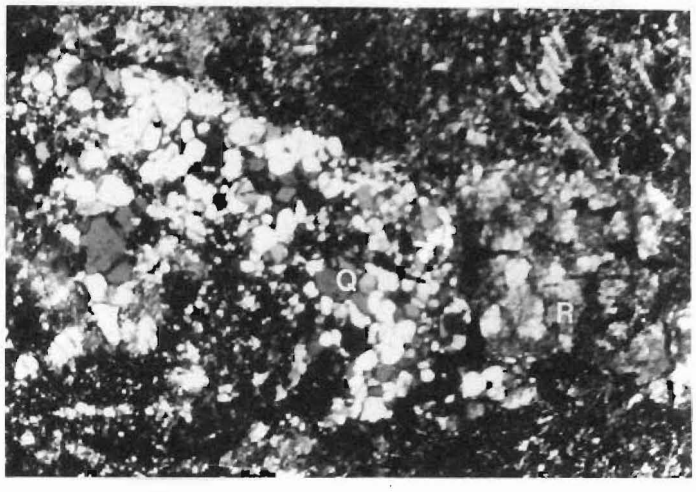
Q
R

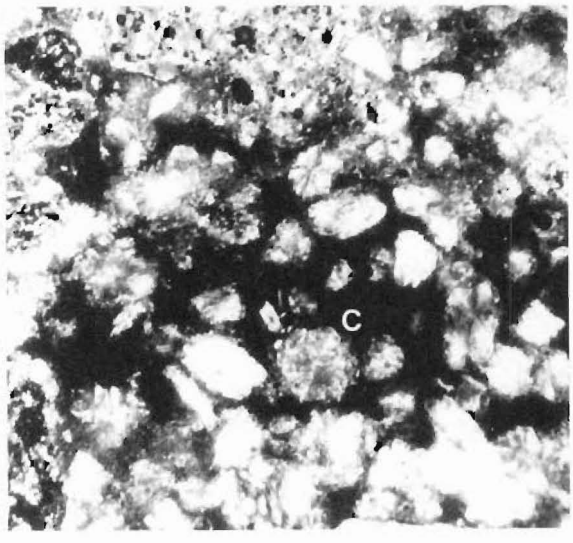
C

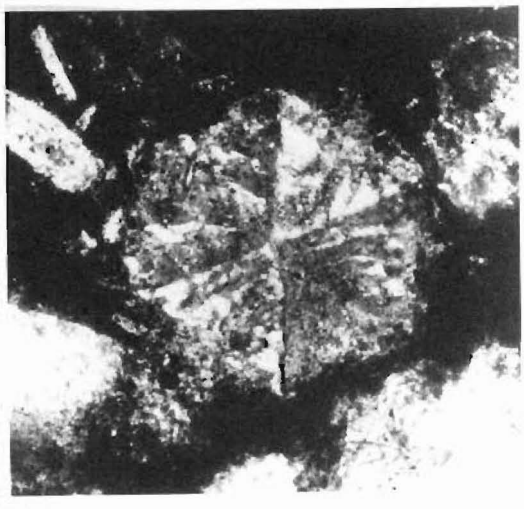

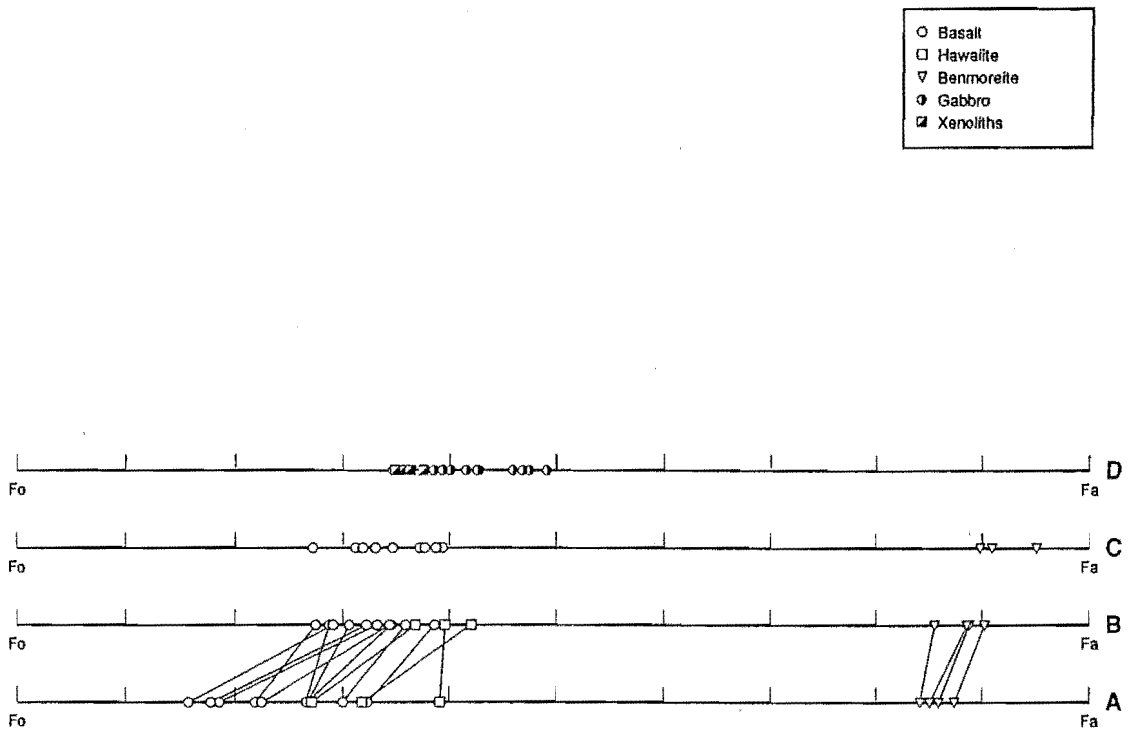

Figure 4.15: Olivine compositions from microprobe analyses, plotted on a linear Fo–Fa scale.

A: Olivine phenocryst cores

B: Olivine phenocryst rims (tie lines connect core-rim analyses from the same phenocryst)

C: Groundmass olivines

D: Olivines from the *ne*-gabbro and monzodiorite schlieren (Onawe Peninsula), and xenoliths from Lighthouse Reserve.

Olivines in more evolved rocks (*ne*-benmoreites) are considerably more Fe-rich than in the more basic lavas, with phenocryst cores of Fo_{13}–Fo_{16} and rims of Fo_{10}–Fo_{14}. Groundmass compositions range from Fo_5 to Fo_{10}.

Olivines from the coarse-grained xenoliths at Lighthouse Reserve range from Fo_{62} to Fo_{65}. There is a weak chemical variation within the olivine crystals with rims being slightly more Fe-rich and showing a wider range of compositions. Olivines from the gabbro on Onawe Peninsula range from Fo_{57} to Fo_{65} (average Fo_{61}), and are not zoned.

In comparison, olivines in the schlieren in the gabbro are significantly more Fe-rich (Fo_{51}–Fo_{57}, average Fo_{55}) than their counterparts in the host rock, and similar in composition to olivines in hawaiite lava flows. As in the gabbro, the crystals are not zoned.

Olivines in coarse grained rocks show similar trends in Fo content versus rock type to lavas (ie. the Fo content of olivines decreases from gabbro to monzodiorite), but Fig. 4.15 shows that olivines in the coarse grained rocks have lower Fo contents than olivines in the equivalent extrusive lavas. However, the compositions of plagioclase crystals in coarse grained rocks are similar to plagioclase compositions in extrusive lavas. The implication is that the coarse grained rocks are not simply coarse grained equivalents of extrusive lavas, but have crystallised from more evolved magma compositions.

Olivines in the coarse-grained rocks (gabbro, schlieren and xenoliths) contain small quantities of NiO (0.22–0.47 wt% NiO) and CaO concentrations decrease towards the rims of phenocrysts. In comparison, olivines from lavas contain no measurable Ni, and the CaO content is higher in the phenocryst rims and groundmass (0.15–0.40 wt% and 0.16–0.47 wt%) than in the phenocryst (0.13–0.32 wt%). The CaO content of olivine from benmoreites is significantly higher (0.86–2.20 wt%) than in olivine from basalts and hawaiites (0.13–0.47 wt%). The high CaO contents suggest that the olivine crystallised at low pressure at or near the surface (Simkin and Smith, 1970).

Roedder and Emslie (1970) studied the equilibria between olivine and basaltic liquids ($SiO_2 < 50\%$) over a range of temperatures (1150–1300°C) and f_{O_2} ($10^{-0.68}$–10^{-12}), to understand the conditions under which olivine will crystallise from a melt. They obtained a value of 0.3 for the temperature-independent distribution coefficient

$$K_D = \frac{(X^{Ol}_{FeO})(X^{liq}_{MgO})}{(X^{liq}_{FeO})(X^{Ol}_{MgO})}$$

where X_A^B is the mole fraction of chemical species A in phase B. Roedder and Emslie (1970) produced a graph showing the dependence of olivine composition on the composition of the liquid, expressed in terms of the mole fractions of FeO and MgO (Fig. 4.16). This graph can be used to estimate the Fo content and the temperature of crystallisation of olivine, from the mole fractions of FeO and MgO in the liquid.

Fo content and temperature estimates for Akaroa Volcanic Group lavas, presented in Table 4.2, were calculated using FeO and MgO wt% values from whole-rock analyses (recalculated to mole fractions) as approximations for the mole fractions of FeO and MgO in the liquid.

The results are generally in good agreement with the actual Fo contents determined from microprobe analyses. The calculated Fo content of olivines in sample N36A3589 is significantly different from the measured Fo content, however the sample is a *ne*-benmoreite and therefore way outside the range of lava compositions used by Roedder and Emslie to calibrate figure 4.16. Any estimates will therefore be subject to large errors.

The calculated Fo contents of olivines from lavas fall within the high end of the range of measured Fo contents for phenocryst cores, and are consistently higher than the measured ranges of Fo contents for phenocryst rims and groundmass crystals. Calculated Fo contents for olivines in coarse grained rocks are consistently higher than measured values.

A number of points should be considered when evaluating these results:

- The method developed by Roedder and Emslie (1970) assumes that olivine is the first phase to crystallise from a basaltic liquid, and that the liquid behaves as an ideal solution. However, multicomponent silicate liquids do not behave as ideal solutions, and little of the thermodynamic data required to take account of the non-ideality of such geological systems (such as activity coefficients) are available. Pyroxene crystallising before olivine might result in the Fo content of olivines being lower than predicted.
- Fo contents of phenocryst cores, determined by microprobe, underestimate the true Fo content of the phenocryst core. Assume a rock contains euhedral olivine crystals that are normally zoned (Mg-rich cores and Fe-rich rims) and have not suffered any corrosion or reaction with the melt. A thin section cut through such a rock will contain a set of random cross-sections through these crystals. All sections will cross two crystal faces and therefore the true composition of the rims of the olivine phenocrysts can be determined by analysing the rims of olivine sections. However, the probability of a random section passing through the true core of a phenocryst is very small. A microprobe

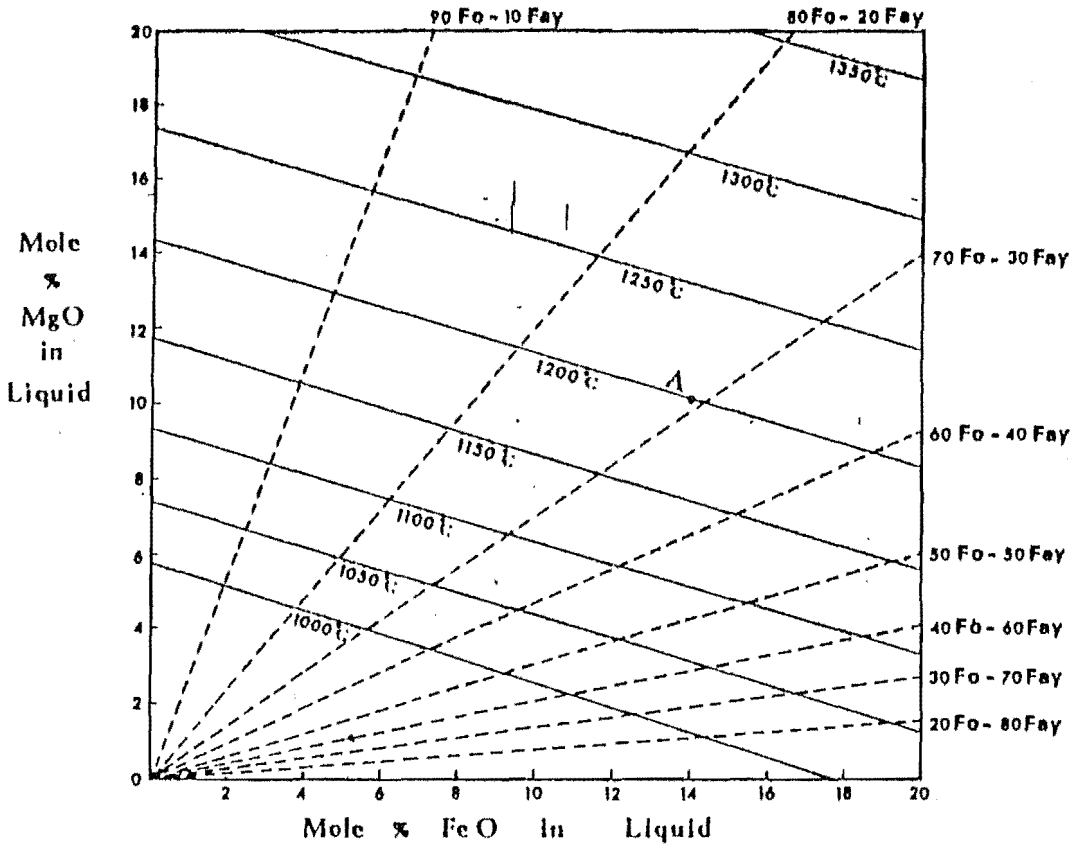

Figure 4.16: Olivine saturation surface as determined by the mole % MgO and FeO in the liquid, after Roedder and Emslie (1970).

Table 4.2: Estimates of Fo content and temperature of crystallisation of olivines from Akaroa Volcanic Group lavas, after the method of Roedder and Emslie (1970).

Sample	N36C3066	N36C3071	N36C3126	N36C3154	N36C3155	N37A3373	N36A3589	N37A3635
Rock type	*ne*-basalt	*ne*-basalt	*hy*-basalt	monzodiorite	*ne*-gabbro	*ne*-hawaiite	*ne*-benmoreite	*ne*-gabbro
Mole % FeO	10.26	10.04	7.55	8.75	11.62	9.38	4.90	9.89
Mole % MgO	12.30	16.74	7.05	4.97	10.47	7.02	1.05	7.70
Fo (calc.)	80	85	75	65	75	71	38	72
Temp. °C	1219	1282	1100	1063	1197	1111	<1000	1129
Fo (meas.):								
Core	70–82	68–84	73–78	52–57	58–65	61–73	13–16	64
Rim	64–67	61–71	69–72	51–57	57–65	58–63	10–14	62–65
Groundmass	63–68	61–62	–	–	–	–	5–10	–

analysis of the centre of the olivine section is therefore an analysis of some point in the olivine crystal between the true core and the rim. Pearce (1984), in a study of magmatic zoning, with particular reference to olivine, estimated that the probability of a random plane intersecting within 10% of the centre of an olivine crystal is P = 0.1. Thus a thin section of a porphyritic rock may have only a few crystals suitable for measuring the composition of the core of the phenocryst, and in a plutonic rock several thin sections may be required to obtain suitable sections. In this study 7–12 olivine phenocrysts from each sample were analysed, and the results therefore underestimate the true upper range of Fo contents.

- In this study, whole-rock analyses determined by XRF included only tFe_2O_3 — the values of Fe_2O_3 and FeO were calculated using the method of Thompson *et al* (1972). The mole % FeO used to estimate Fo content from figure 4.16 is, therefore, itself an estimate, and subject to error.

Temperature estimates show that in general olivines in more evolved rocks crystallised at lower temperatures, and olivines in coarse grained rocks crystallised at lower temperatures than their extrusive equivalents. This is consistent with variations in extrusion temperature estimates with lava type (Carmichael *et al*, 1974).

4.3.2 Pyroxene

Akaroa Volcanic Group lavas typically contain a single, often Ti-rich, calcic clinopyroxene, characteristic of the alkali rock series. Pyroxene compositions from microprobe analyses are shown on the pyroxene quadrilateral (Fig. 4.17). The pyroxene crystallisation trend is similar to crystallisation trends from other alkali volcanic provinces (Fig. 4.18), with an increase in the Fe:Mg ratio towards more evolved lavas and a moderate calcium depression in intermediate lavas.

Pyroxenes from lavas show a crystallisation trend from diopside to hedenbergite. Phenocrysts are typically normally zoned with the Fe:Mg ratio increasing from core to rim. Groundmass pyroxenes are generally more Fe-rich than phenocrysts. Pyroxenes in *ne*-basalts are typically salites with phenocryst cores and rims $Ca_{47}Mg_{43}Fe_{10}$–$Ca_{49}Mg_{37}Fe_{14}$ and $Ca_{49}Mg_{41}Fe_{10}$–$Ca_{49}Mg_{36}Fe_{15}$ respectively, and groundmass pyroxenes $Ca_{49}Mg_{39}Fe_{12}$–$Ca_{44}Mg_{36}Fe_{20}$. In *hy*-basalts, groundmass pyroxenes are noticeably less calcic ($Ca_{46}Mg_{40}Fe_{14}$–$Ca_{45}Mg_{36}Fe_{19}$). Pyroxenes in more fractionated rocks are significantly more Fe-rich, with ferrosalite microphenocrysts ($Ca_{47}Mg_{22}Fe_{31}$–$Ca_{48}Mg_{16}Fe_{36}$) and groundmasses ($Ca_{48}Mg_{13}Fe_{39}$–$Ca_{48}Mg_{12}Fe_{40}$) in *ne*-benmoreites, and hedenbergite ($Ca_{47}Mg_6Fe_{47}$) in the groundmasses of *qz*-trachytes.

Pyroxenes from coarse grained rocks are significantly less calcic than their extru-

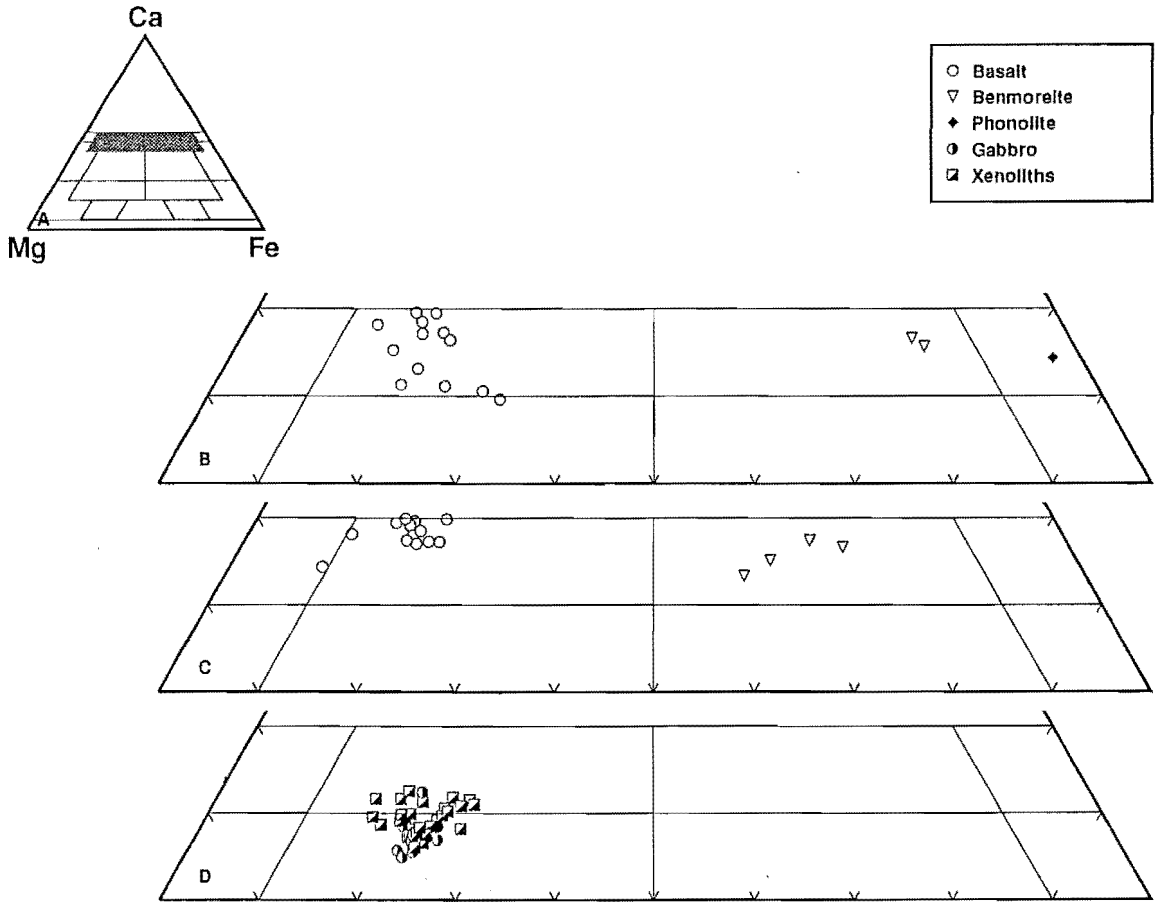

Figure 4.17: Pyroxene compositions from microprobe analyses, plotted on the pyroxene quadrilateral. Solid bars on the $MgSiO_3$–$FeSiO_3$ baseline are the ranges of olivine compositions from figure 4.15.

A: Location of figures B–D in the system $CaMgSi_2O_6$–$CaFeSi_2O_6$–$Mg_2Si_2O_6$–$Fe_2Si_2O_6$.

B: Pyroxene phenocryst cores and rims

C: Groundmass pyroxenes

D: Pyroxenes from the *ne*-gabbro (Onawe Peninsula), and the *ne*- gabbro and monzodiorite xenoliths from Lighthouse Reserve.

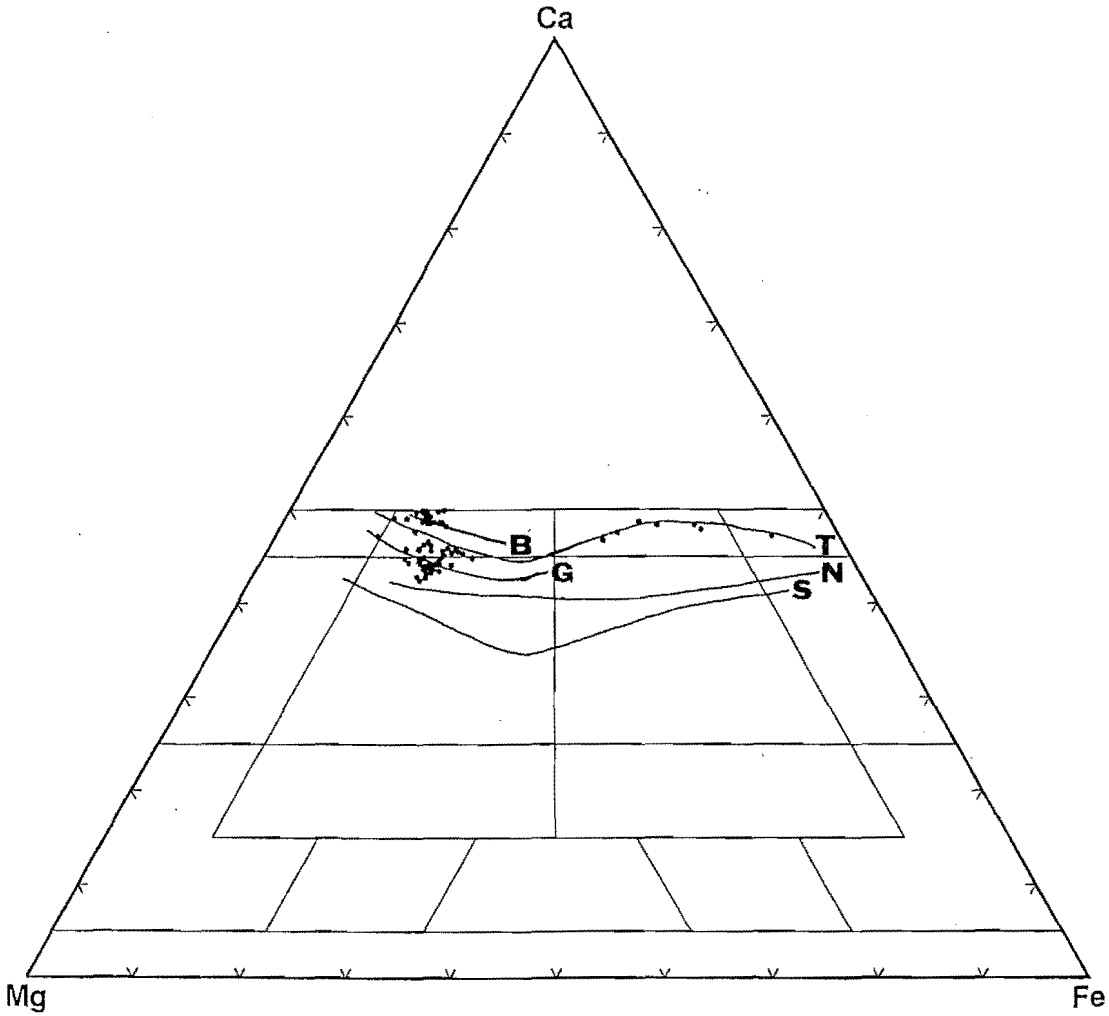

Figure 4.18: Comparison of pyroxene compositions from the Akaroa Volcanic Group with pyroxene fractionation trends from other volcanic provinces: S = Skaergaard Intrusion, G = Garbh Eilean Sill, B = Black Jack Sill (Deer *et al*, 1966, p127); N = Nandewar Volcano (Abbott, 1969, p122); T = This study.

sive equivalents, and straddle the boundary between salite and augite compositions. Pyroxenes from the *ne*-gabbro on Onawe Peninsula are typically augites ($Ca_{46}Mg_{39}Fe_{15}$–$Ca_{43}Mg_{39}Fe_{17}$), whereas pyroxenes in the *ne*-gabbro and monzodiorite xenoliths from Lighthouse Reserve range from augite ($Ca_{43}Mg_{40}Fe_{17}$) to salite ($Ca_{46}Mg_{36}Fe_{18}$). Pyroxenes in coarse grained rocks are weakly normally zoned, with rims slightly more Fe-rich.

Pyroxene crystallisation trends with respect to the Fe:Mg ratio are paralleled by trends in TiO_2 and Al_2O_3 wt% abundances. Pyroxenes in basalts have moderate to high TiO_2 (1.0–3.83 wt%) and Al_2O_3 (2.05–7.76 wt%) contents, compared with much lower levels (TiO_2 0.0–0.38 wt%, Al_2O_3 0.8–3.71 wt%) in benmoreites and trachytes. Pyroxenes in the *ne*-gabbro from Onawe Peninsula have significantly lower TiO_2 (0.65–1.93 wt%) and Al_2O_3 (1.38–3.58 wt%) than pyroxenes from *ne*-basalts. However, pyroxenes in *ne*-gabbro and monzodiorite xenoliths from Lighthouse Reserve have TiO_2 (1.0–2.35 wt%) and Al_2O_3 (3.44–6.3 wt%) contents similar to *ne*-basalt lavas.

High Ca contents in pyroxenes from lavas reflect the absence of plagioclase as a significant liquidus phase. The inferred depression in the calcium contents of pyroxenes from intermediate lavas may reflect the extensive plagioclase fractionation seen in some hawaiites. The lower calcium contents of pyroxenes from coarse grained rocks suggest that these rocks are not simply the coarse equivalents of basalt lava flows, and taken with the higher Fe:Mg ratios in olivines from coarse grained rocks, is evidence that the gabbros and monzodiorites crystallised from magmas more evolved than those erupted as basalt and hawaiite lava flows.

4.3.3 Feldspar

Feldspars are the most abundant minerals in lavas of the Akaroa Volcanic Group, occurring as phenocrysts and groundmass phases in all rock types. Feldspar compositions are plotted on the system $CaAl_2Si_2O_8$–$NaAlSi_3O_8$–$KAlSi_3O_8$ (Fig. 4.19). Feldspar compositions form a continuum from bytownite ($An_{81}Ab_{18}Or_1$) to sanidine ($An_0Ab_{50}Or_{50}$); the gap in the trend between $An_{38}Ab_{60}Or_2$ and $An_{26}Ab_{70}Or_4$ reflects a lack of microprobe data from mugearites, not a natural bimodality. The feldspar fractionation trend is comparable with trends from other alkalic provinces, particularly those exhibiting sodic lineages (Fig. 4.20).

Feldspars are typically normally zoned, but oscillatory zoning is also very common, and reverse zoning does occur.

In *ne*-basalts (Fig. 4.19 a, b), phenocrysts have cores of calcic labradorite ($An_{62}Ab_{36}Or_2$–$An_{70}Ab_{29}Or_1$) and rims of labradorite ($An_{55}Ab_{43}Or_2$–$An_{74}Ab_{25}Or_1$).

Figure 4.19: Feldspar compositions from microprobe data plotted on the $NaAlSi_3O_8$–$KAlSi_3O_8$–$CaAl_2Si_2O_8$ system. Arrows indicate the general trend of core–rim zoning.

A: Feldspar phenocryst cores and rims from *ne*-basalts

B: Groundmass feldspars from *ne*-basalts

C: Feldspar phenocryst cores and rims from *hy*-basalts

D: Groundmass feldspars from *hy*-basalts

E: Feldspar phenocryst cores and rims from *ne*-hawaiites

F: Groundmass feldspars from *ne*-hawaiites

G: Feldspar phenocryst cores and rims from *ne*-benmoreites

H: Groundmass feldspars from *ne*-benmoreites

I: Feldspar phenocryst cores and rims from *qz*-trachytes

J: Feldspar phenocryst cores and rims, and groundmass laths from the phonolite

K: Feldspar cores and rims from the *ne*-gabbro of Onawe Peninsula

L: Feldspar cores and rims from the monzodiorite schlieren in the *ne*-gabbro of Onawe Peninsula

M: Feldspar cores and rims from the *ne*-gabbro xenoliths of Lighthouse Reserve

N: Feldspar cores and rims from the monzodiorite xenoliths of Lighthouse Reserve

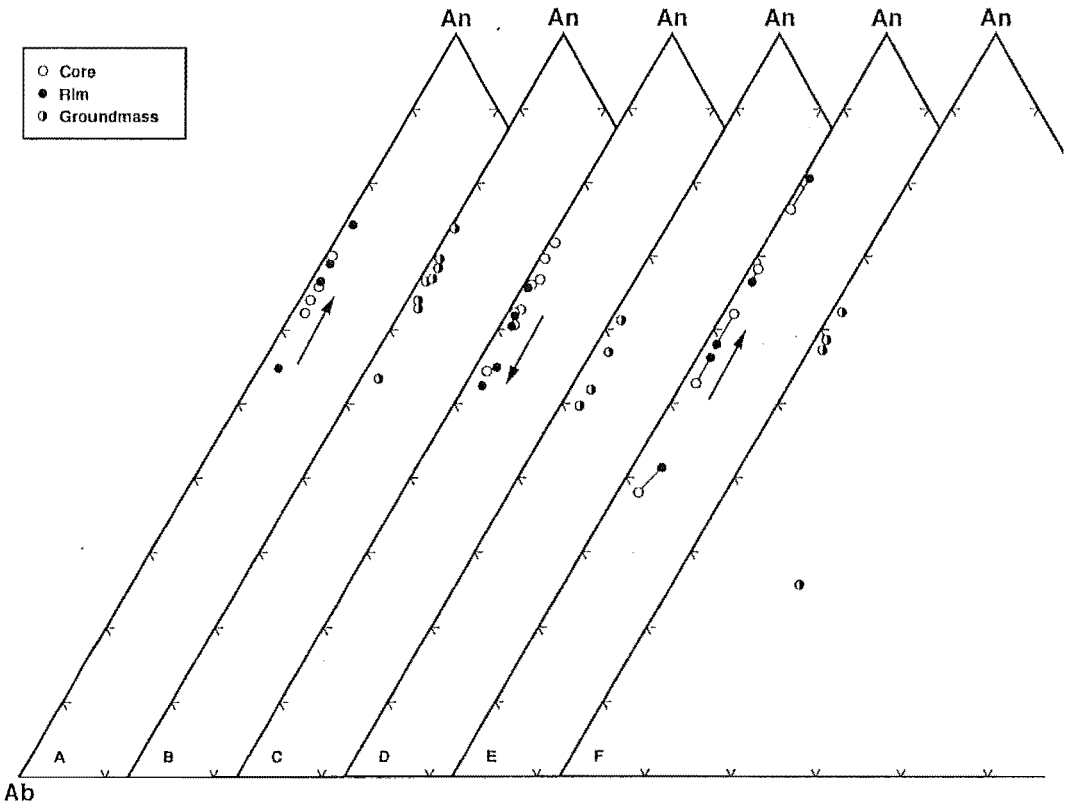
Core
Rim
Groundmass
An
An
An
An
An
An
A
B
C
D
E
F
Ab

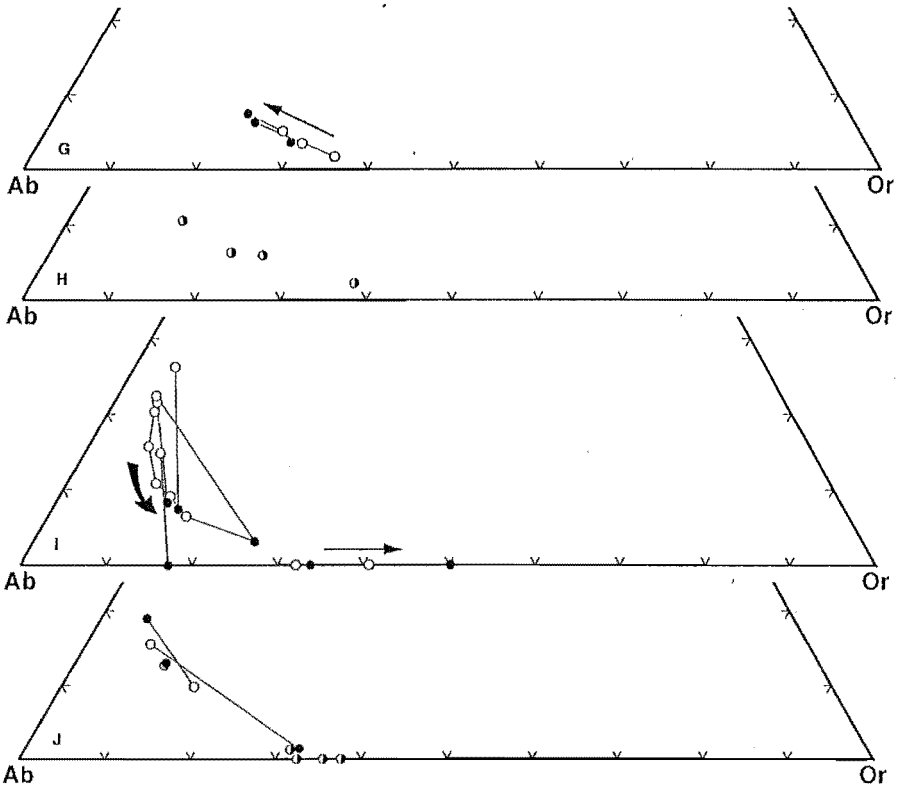
G
Ab
Or
H
Ab
Or
I
Ab
Or
J
Ab
Or

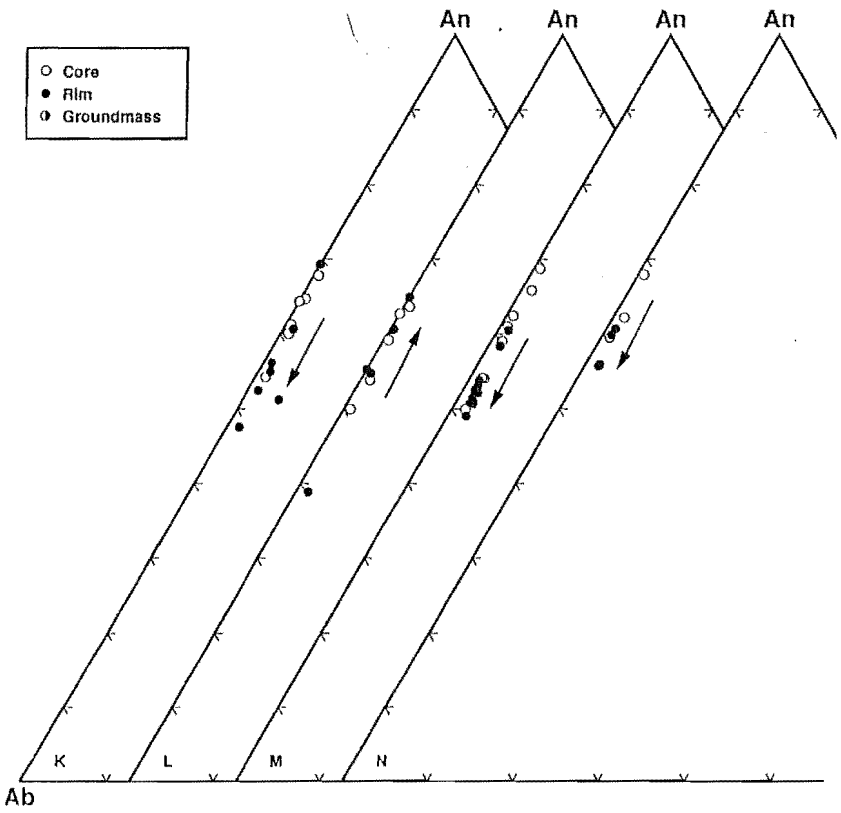
An
An
An
An
Core
Rim
Groundmass
K
L
M
N
Ab

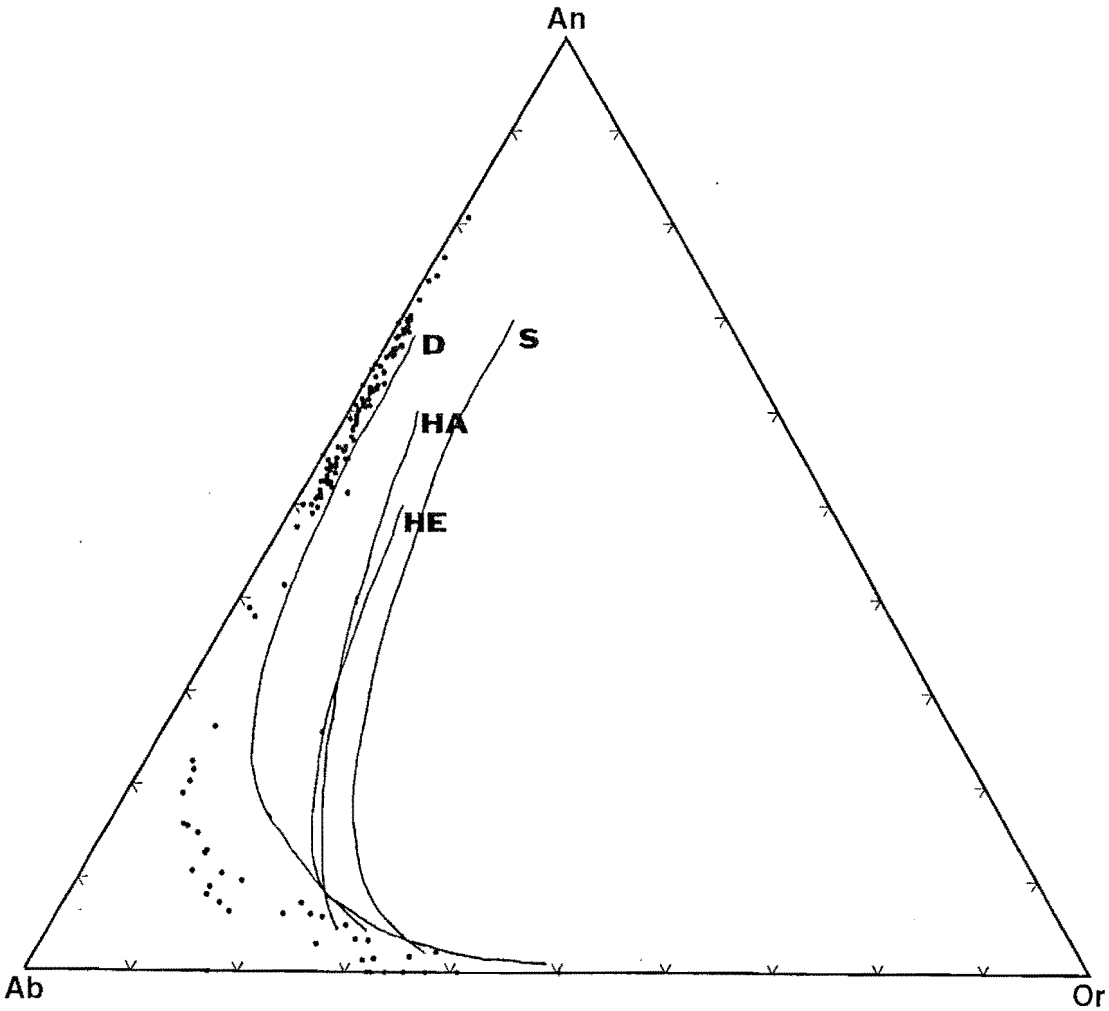

Figure 4.20: Comparison of feldspar compositions from the Akaroa Volcanic Group (filled circles) with feldspar fractionation trends from other volcanic provinces: HA = Hawaiian alkali series (MacDonald and Kutsura, 1964); HE = Hebridean province (Tilley and Muir, 1962); D = Dunedin Volcanic Province (Price and Chappell, 1975); S = Saint Helena (Baker, 1969). Hawaiian, Hebridean and Saint Helena trends are normative feldspar compositions

Groundmass feldspars are labradorites and Na-bytownites ($An_{53}Ab_{45}Or_2$–$An_{74}Ab_{25}Or_1$) and almost identical in composition to phenocryst rims. *Hy*-basalts (Fig. 4.19 c, d) have feldspar phenocrysts of labradorite ($An_{52}Ab_{46}Or_2$–$An_{67}Ab_{32}Or_1$) and groundmass laths of sodic labradorite ($An_{50}Ab_{48}Or_2$–$An_{61}Ab_{37}Or_2$). There is a general decrease in An content from phenocryst cores to rims, and from phenocrysts to groundmass laths. Feldspars in *ne*-hawaiites (Fig. 4.19 e, f) show a much greater compositional range than feldspars in basalts. Phenocrysts are often reversely zoned with cores of andesine to sodic bytownite ($An_{38}Ab_{60}Or_2$–$An_{76}Ab_{23}Or_1$) and rims of andesine to bytownite ($An_{41}Ab_{55}Or_4$–$An_{81}Ab_{18}Or_1$). Groundmass feldspars are generally more sodic, and range from calcic oligoclase to labradorite ($An_{26}Ab_{59}Or_{15}$–$An_{63}Ab_{36}Or_1$). *Ne*-benmoreites (Fig. 4.19 g, h) have feldspar phenocrysts of anorthoclase (cores $An_5Ab_{67}Or_{28}$–$An_2Ab_{63}Or_{35}$, rims $An_7Ab_{71}Or_{22}$–$An_4Ab_{67}Or_{29}$) and groundmass laths of anorthoclase to sanidine ($An_{11}Ab_{76}Or_{13}$–$An_2Ab_{60}Or_{38}$). Feldspar phenocrysts in *qz*-trachytes (Fig. 4.19i) have cores of oligoclase to sanidine ($An_{26}Ab_{69}Or_5$–$An_0Ab_{59}Or_{41}$) and rims of anorthoclase to sanidine ($An_8Ab_{79}Or_{13}$–$An_0Ab_{50}Or_{50}$). Rims have lower An and/or higher Or contents than cores. One crystal (points 1.1–1.9, sample N36D3600) exhibits a fine example of oscillatory normal zoning. All spot analyses fall on a smooth curve from $An_{22}Ab_{73}Or_5$ to $An_3Ab_{71}Or_{26}$ (Fig. 4.19i) that passes within 2.0 wt% of the albite field. Feldspar phenocrysts in *ne*-trachytes (Fig. 4.19j) are oligoclase to anorthoclase (cores $An_{16}Ab_{77}Or_7$–$An_{10}Ab_{75}Or_{15}$, rims $An_{19}Ab_{76}Or_5$–$An_1Ab_{67}Or_{32}$). Groundmass feldspars are potassic anorthoclase to sodic sanidine ($An_1Ab_{68}Or_{31}$–$An_0Ab_{62}Or_{38}$). All analyses fall on a smooth curve from $An_{19}Ab_{76}Or_5$ to $An_0Ab_{62}Or_{38}$, which has a distinctly lower Ab content than the curve for *qz*-trachytes. When comparing the sub-parallel trends for *ne*-benmoreites, *ne*- and *qz*-trachytes, there is a consistent increase in Ab content from *ne*-benmoreite to *qz*-trachyte.

Feldspars in coarse grained rocks are similar in composition to their fine grained equivalents. Feldspars from the *ne*-gabbro of Onawe Peninsula and the *ne*-gabbro xenoliths from Lighthouse Reserve (Fig. 4.19 k, m) have labradorite cores ($An_{50}Ab_{48}Or_2$–$An_{69}Ab_{30}Or_1$) and rims of andesine or labradorite ($An_{48}Ab_{51}Or_1$–$An_{69}Ab_{31}Or_0$). Monzodiorite schlieren from the *ne*-gabbro on Onawe Peninsula and monzodiorite xenoliths from Lighthouse Reserve (Fig. 4.19 l, n) have feldspar cores of labradorite ($An_{50}Ab_{49}Or_1$–$An_{65}Ab_{35}Or_0$). The compositional range is similar to, but more restricted than the compositional range of feldspars in *ne*-hawaiites.

Since feldspar compositions cover a wide spectrum from $> An_{80}$ to Or_{50}, and analyses are available from most members of the alkali rock series, this is a good opportunity to apply geothermometric calculations to the data to estimate the range of temperatures over which plagioclase crystallised from the melt.

Kudo and Weill (1970) developed an igneous plagioclase geothermometer based on the exchange reaction:

$$\underbrace{NaAlSi_3O_8}_{plagioclase} + \underbrace{CaAl_2Si_2O_8}_{liquid} \rightleftharpoons \underbrace{NaAlSi_3O_8}_{liquid} + \underbrace{CaAl_2Si_2O_8}_{plagioclase} \tag{4.1}$$

for which equilibrium conditions are defined by the equation:

$$\Delta\frac{\mu^0}{RT} = \ln\frac{\lambda}{\sigma} + \ln\frac{\gamma_{Na}\gamma_{Si}}{\gamma_{Ca}\gamma_{Al}} \tag{4.2}$$

where:

$$\mu^0 = \mu^0_{An} - \mu^0_{Ab} + \mu^0_{Na} + \mu^0_{Si} - \mu^0_{Ca} - \mu^0_{Al}$$

$$\lambda = \frac{X_{Na}X_{Si}}{X_{Ca}X_{Al}}$$

$$\sigma = \frac{X_{Ab}}{X_{An}}$$

Activity coefficients are not known for the species in equation 4.2, but assuming that the activity coefficients are similar in form to those found for regular solutions ($\ln\gamma$ = Cϕ/T, where C is a constant and ϕ is some function of composition) then equation 4.2 can be rewritten as a function of temperature:

$$y(T) = \ln\frac{\lambda}{\sigma} + \ln\frac{C'\phi'}{T} \tag{4.3}$$

Calibrating the geothermometer using data from experimental and natural systems allows the definition of a series of regression curves relating T to plagioclase and liquid composition at given water pressures (dry, 0.5 kb, 1.0 kb, 5.0 kb).

Mathez (1973) suggested improvements to the Kudo-Weill geothermometer to correct for the non-ideal behavior of plagioclase, using "activity coefficient corrections".

Temperatures of plagioclase/liquid equilibrium at a range of P_{H_2O} values have been calculated for all Akaroa Volcanic Group lavas for which plagioclase compositions from microprobe analysis are available, using the Kudo-Weill geothermometer and the Mathez activity corrections. Results are tabulated in Table 4.3.

Calculated temperatures are internally consistent, ranging from > 1200°C for basaltic lavas to < 900°C for benmoreites and trachytes. The Mathez activity correction

Table 4.3: Temperatures of plagioclase/liquid equilibrium for Akaroa Volcanic Group lavas, calculated at different P_{H_2O} values, using the Kudo-Weill geothermometer and the Mathez activity corrections. Calculation methods after Kudo and Weill (1970) and Mathez (1973). Note "Dry" should be read as "Dry" for Kudo-Weill temperatures and "Basalt" for Mathez activity corrected temperatures.

			Kudo-Weill (°C)			Mathez (°C)		
Sample	Rock Type	P_{H_2O}	$\bar{x}$	± sd	n	$\bar{x}$	± *sd*	*n*
N36C3066	*ne*-basalt	Dry	1275	± 41	4	1232	± 4	4
		0.5 kb	1225	± 38		1112	± 53	
		1.0 kb	1191	± 38		1226	± 101	
N36C3126	*hy*-basalt	Dry	1263	± 24	5	1254	± 7	5
		0.5 kb	1214	± 22		1184	± 29	
		1.0 kb	1181	± 22		1337	± 54	
N36C3154	monzodiorite	Dry	1216	± 49	5	1222	± 31	5
		0.5 kb	1167	± 46		1147	± 38	
		1.0 kb	1131	± 46		1324	± 48	
N36C3155	*ne*-gabbro	Dry	1237	± 25	2	1242	± 11	2
		0.5 kb	1190	± 24		1184	± 1	
		1.0 kb	1158	± 23		1347	± 11	
N36C3156	*ne*-gabbro	Dry	1243	± 36	5	1242	± 12	5
		0.5 kb	1198	± 33		1177	± 40	
		1.0 kb	1164	± 33		1332	± 76	
N37A3373	*ne*-hawaiite	Dry	1258	± 75	5	1236	± 29	5
		0.5 kb	1208	± 70		1141	± 40	
		1.0 kb	1173	± 70		1283	± 87	
N36A3589	*ne*-benmoreite	Dry	834	± 67	3	933	± 47	3
		0.5 kb	806	± 62		712	± 110	
		1.0 kb	755	± 68		998	± 62	
N36D3600	*qz*-trachyte	Dry	863	± 16	2	965	± 10	2
		0.5 kb	827	± 14		722	± 29	
		1.0 kb	766	± 16		1052	± 13	
N36D3619	*ne*-trachyte	Dry	1047	± 42	2	993	± 180	2
		0.5 kb	1003	± 39		981	± 48	
		1.0 kb	959	± 40		1075	± 237	
N37A3634	*ne*-gabbro	Dry	1282	± 16	3	1284	± 7	3
		0.5 kb	1234	± 15		1240	± 6	
		1.0 kb	1202	± 15		1401	± 14	
N37A3635	*ne*-gabbro	Dry	1255	± 4	4	1266	± 3	4
		0.5 kb	1209	± 4		1223	± 4	
		1.0 kb	1177	± 4		1391	± 4	
N37A3636	*ne*-gabbro	Dry	1230	± 22	4	1241	± 12	4
		0.5 kb	1185	± 21		1187	± 8	
		1.0 kb	1161	± 37		1354	± 8	
N37A3637	monzodiorite	Dry	1242	± 12	4	1247	± 3	4
		0.5 kb	1192	± 11		1186	± 10	
		1.0 kb	1157	± 11		1360	± 21	

produces lower T estimates for trachytic rocks compared with the Kudo-Weill estimates. It is difficult to determine the absolute accuracy of the temperature estimates, but comparisons with published data on temperature ranges (Carmichael *et al*, 1974; Kudo and Weill, 1970; Mathez, 1973) indicate that the results from this study are reasonable estimates of crystallisation temperatures. The Kudo-Weill estimates compare favourably with temperatures estimated from olivine compositions (section 4.3.1), although Kudo-Weill estimates tend to be slightly higher.

In evaluating these results, the following points should be kept in mind:

- Variations between temperature estimates using the Kudo and Weill (1970) and Mathez (1973) methods, and the Roedder and Emslie (1970) method may in part be explained by assumptions that have been made in each method.
- The Kudo-Weill geothermometer has a long response time compared with other geothermometers, and may therefore produce temperatures that antedate those determined from geothermometers with faster response times.
- The Kudo-Weill geothermometer assumes that:
    1. The liquid is an ideal solution, so that the activity of a species is equal to its mole fraction in the liquid.
    2. Plagioclase crystals are in equilibrium with the liquid.
    3. Plagioclase crystals are not strongly zoned.
    4. The effect of dry pressure is negligible.

  While the effect of dry pressure may be unknown, the liquid from which plagioclase may crystallise does not behave as an ideal solution, and corrections by Mathez (1973) and Orville (1972) attempt to correct activity coefficients for the non-ideality of the solution. However, until significantly more thermodynamic data, including the activities of species in multicomponent silicate liquids are available, such calculations will have to rely on estimates of activity coefficients.

  Plagioclase in basalts and hawaiites from the Akaroa Volcanic Group are often strongly zoned, and to counteract this effect, X_{An} and X_{Ab} were determined from analyses of phenocryst rims, as this is the last plagioclase composition in equilibrium with the liquid. Many feldspars in Akaroa Volcanic Group lavas also show varying degrees of corrosion and resorption — sieve textures are quite common and embayed margins and rounded crystals are also observed. These textures suggest that many plagioclase crystals were not in equilibrium with the surrounding liquid at some stage in their history.

Clearly, the results for Akaroa Volcano must be viewed from the perspective that the calculated temperatures are **estimates** only, and that all the results taken together give an idea of the temperature **range** and the **trend** of temperature variation with rock type, but that specific temperatures for a rock sample can **not** be treated as precise measurements of the temperature at which plagioclase crystallised from the liquid.

4.3.4 Iron-Titanium Oxides

Titaniferous magnetite is ubiquitous in Akaroa Volcanic Group rocks, both as a phenocryst phase and a groundmass phase.

In lavas, TiO_2 contents decrease from 25.45–29.61 wt% in basalts, to 19.14–25.3 wt% in *ne*-hawaiites and 14.06–17.69 wt% in *ne*-benmoreites. Magnetites from coarse grained rocks have a lower average but a greater range of TiO_2 contents, compared with their fine grained equivalents. Magnetites from the *ne*-gabbro and monzodiorite schlieren of Onawe Peninsula, and the *ne*-gabbro and monzodiorite xenoliths from Lighthouse Reserve have TiO_2 contents of 13.0–28.88 and 2.64–39.82 respectively.

MgO and Al_2O_3 are the major accessory constituents in titaniferous magnetites, and generally vary sympathetically. Mean MgO and Al_2O_3 wt% contents are low to moderate in basalts (MgO = 2.38, Al_2O_3 = 1.92), the *ne*-gabbro from Onawe Peninsula (MgO = 1.21, Al_2O_3 = 2.84), and *ne*-benmoreites (MgO = 0.0, Al_2O_3 = 1.18), but are slightly higher in *ne*-hawaiites (MgO = 4.08, Al_2O_3 = 5.49). Magnetites in xenoliths from Lighthouse Reserve have a higher average MgO and Al_2O_3, and show a much greater range of values (MgO 2.49–12.4 wt%, Al_2O_3 0.49–16.37 wt%).

Some analyses of grains from the coarse grained rocks, which petrographically appear to be magnetites, have very high TiO_2 contents (48.56–65.76 wt%) and may be ilmenite exsolution lamellae.

The high TiO_2 contents of magnetites from Akaroa Volcanic Group rocks indicates that significant amounts of the ulvöspinel end member of the magnetite-ulvöspinel$_{ss}$ are present. All analyses have been recalculated according to the method of Carmichael (1967), to estimate FeO and Fe_2O_3 (microprobe analyses determined total iron as tFeO) and the mole fractions of the ulvöspinel molecule in the spinel phase and the ilmenite molecule in the rhombohedral phase. The results are plotted on the system FeO–Fe_2O_3–TiO_2 (Fig. 4.21). Most analyses plot close to the ulvöspinel–magnetite$_{ss}$ join. There is a trend of increasing magnetite:ulvöspinel ratio from basalts ($Usp_{71}Mt_{29}$–$Usp_{87}Mt_{13}$) to benmoreites ($Usp_{37}Mt_{63}$–$Usp_{49}Mt_{51}$).

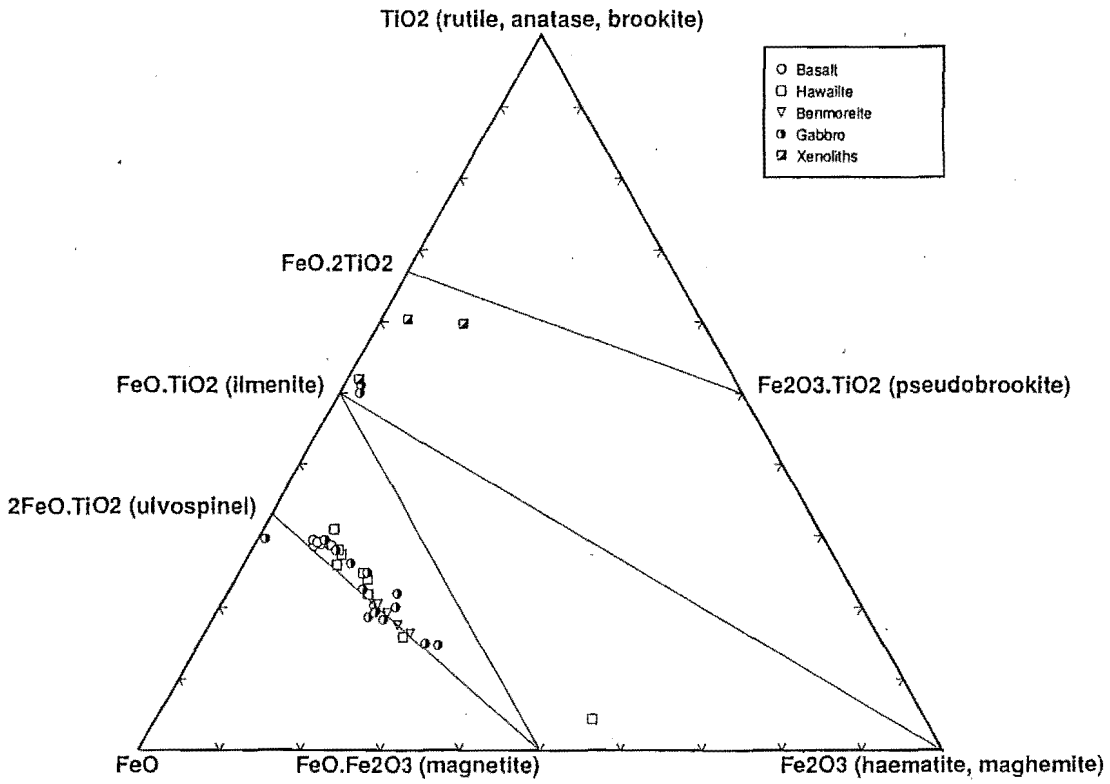

Figure 4.21: Magnetite compositions from microprobe data plotted on the system FeO–Fe_2O_3–TiO_2.

Magnetites in coarse grained rocks show a much greater range in ulvöspinel content, and particularly, analyses from the same microprobe section may exhibit a wide range of compositions. For example, magnetites from the monzodiorite xenolith range from Usp_8Mt_{92} to $Usp_{79}Mt_{21}$. Analyses with very high TiO_2 contents (> 48.0 wt%) were recalculated as if they were a rhombohedral phase, rather than a spinel phase (see Carmichael, 1967).

Buddington and Lindsley (1964) used experimental data to construct surfaces in f_{O_2}–T–X space for magnetite–ulvöspinel$_{ss}$ and coexisting hematite–ilmenite$_{ss}$. Portions of the surfaces were then projected onto the f_{O_2}–T plane (Fig. 4.22). This figure can be used to estimate the temperature and f_{O_2} at which titaniferous magnetite and the rhombohedral phase can coexist. Results for coarse grained rocks of the Akaroa Volcanic Group, in which both titaniferous magnetite and rhombohedral phases are present, are presented in Table 4.4.

Table 4.4: Estimates of temperature and f_{O_2} for coexisting titaniferous magnetite and rhombohedral phases in coarse grained rocks from Akaroa Volcano. Values for T°C and $-\log_{10} f_{O_2}$ were read directly from Fig. 4.22.

Sample	Rock Type	Mole Fraction		T°C	$-\log_{10} f_{O_2}$
		Usp	Ilm		
N36C3154	monzodiorite	53	96	820	14.8
		67	96	950	12.2
		37	96	760	16.0
N36C3156	ne-gabbro	56	95	875	13.6
		48	95	830	14.5
N37A3635	ne-gabbro	47	97	750	17.0
		32	97	680	18.6
		65	97	860	14.5
N37A3637	monzodiorite	79	94	1120	10.0
		8	84	600	18.0
		40	84	940	11.0
		40	94	770	15.6

Except for one result, most temperatures are in the range 750–950°C, some 200–300°C lower than temperature estimates from other methods. There are two possible explanations for this anomaly — either the mole fractions of ulvöspinel and ilmenite are in error, or the temperature estimates represent some other equilibrium event.

The assumption that analyses with very high TiO_2 values (> 48.0 wt%) are rhombohedral (ilmenite) phases may not be valid. Recalculation of some of these analyses

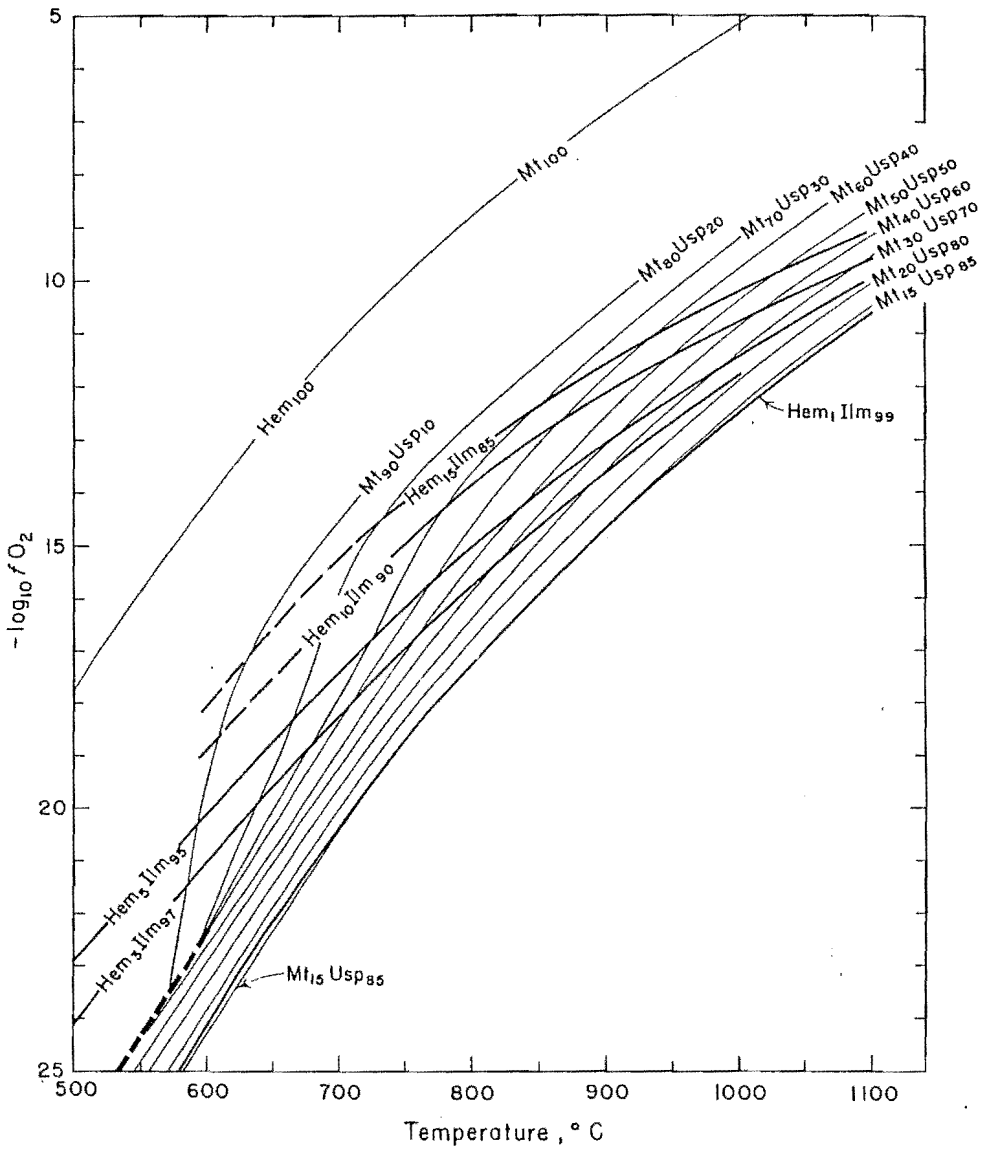

Figure 4.22: Projection on to f_{O_2}–T plane of conjugate f_{O_2}–T–X surfaces for magnetite–ulvöspinel$_{ss}$ and ilmenite–hematite$_{ss}$ (after Buddington and Lindsley, 1964).

as rhombohedral phases (according to the method of Carmichael, 1967) produced negative values for Fe_2O_3, and ilmenite mole fractions greater than 100%. Furthermore, on a plot of the system FeO–Fe_2O_3–TiO_2, these analyses plot above the ilmenite–hematite$_{SS}$ join, not on or below as expected. This might be explained if the ilmenite exsolution lamellae were significantly thinner than the diameter of the electron beam of the microprobe. These analyses would then represent "averages" of magnetite–ulvöspinel$_{SS}$ and ilmenite–hematite$_{SS}$, which would invalidate the recalculations.

The other possibility is that the temperature estimates relate to some equilibrium event other than the original crystallisation of the titaniferous magnetite. Buddington and Lindsley (1964) suggest that magnetite–ilmenite intergrowths are not the result of the unmixing of ilmenite from a magnetite–ilmenite$_{SS}$, but that all TiO_2 enters magnetite as ulvöspinel. The ulvöspinel is then oxidised to ilmenite, which "exsolves" from the magnetite host. Thus an original magnetite–ulvöspinel$_{SS}$ would be oxidised to a complex of magnetite–ulvöspinel$_{SS}$ and ilmenite–hematite$_{SS}$. This oxidation occurs in the presence of H_2O:

$$\underbrace{3Fe_2TiO_4}_{ulvöspinel} + H_2O_{(l)} \rightleftharpoons \underbrace{3FeTiO_3}_{ilmenite} + \underbrace{Fe_3O_4}_{magnetite} + H_{2(g)}$$

Only small quantities of H_2O are required — 18g of H_2O will produce sufficient O_2 to oxidise 671g of ulvöspinel (Buddington and Lindsley, 1964). Less H_2O is required if the H_2 can escape preferentially from the fluid, as this would drive the equilibrium dissociation reaction for H_2O to the right:

$$2H_2O \rightleftharpoons 2H_{2(g)} + O_2$$

The equilibrium dissociation constant for CO_2 in the reaction

$$CO_2 \rightleftharpoons CO + \frac{1}{2}O_2$$

is similar to the equilibrium constant for the dissociation of H_2O over the relevant temperature range, so the presence of abundant CO_2 in fluids interacting with titaniferous magnetite will not significantly affect the oxidation process. Other evidence has been cited for the presence of CO_2- and SiO_2-rich fluids circulating through the syenite and gabbro of Onawe Peninsula. It seems reasonable to assume, therefore, that sufficient fluid existed for the oxidation of the original magnetite–ulvöspinel$_{SS}$,

and the estimated temperatures may reflect the temperature of equilibration between coexisting magnetite–ulvöspinel$_{SS}$ and ilmenite–hematite$_{SS}$ oxidation products. This could reasonably be expected to be lower than the temperature at which the original magnetite–ulvöspinel$_{SS}$ crystallised.

4.3.5 Amphibole

Amphiboles occur in the *ne*-gabbro and associated monzodiorite schlieren of Onawe Peninsula, and in a *ne*-gabbro xenolith from Lighthouse Reserve. Red-brown amphiboles have been observed in *ne*-benmoreites and *ne*- and *qz*-trachytes, and alkali amphiboles have been observed in *qz*-trachytes, but microprobe analyses are not available for these occurrences. Biotite accompanies the amphibole in the gabbro and monzodiorite from Onawe Peninsula.

Since only total iron as FeO was measured by microprobe, all amphibole analyses have been recalculated using the method of Papike (1974) to estimate the relative abundances of Fe^{2+} and Fe^{3+}. Using these estimates, amphiboles have been named according to the amphibole classification scheme of Leake (1978).

All amphiboles from Akaroa Volcano are Ti-rich, pargasitic or kaersutitic members of the calcic amphibole group.

Amphiboles in the monzodiorite schlieren are typically titanian ferroan pargasitic hornblende, although titanian ferroan pargasite, titanian pargasite and kaersutite compositions are present. Amphiboles in the *ne*-gabbro of Onawe Peninsula show much more compositional variation. The dominant composition is titanian ferroan pargasite, but titanian ferroan pargasitic hornblende, kaersutite, titanian pargasitic hornblende, titanian pargasite and edenitic hornblende compositions also occur. Kaersutite occurs in a *ne*-gabbro xenolith from Lighthouse Reserve.

Amphibole rims tend to have lower TiO_2 and K_2O, and higher Na_2O (wt%) than the cores. Over all the amphiboles analysed the main chemical trend is one of varying MgO:FeO+Fe_2O_3 ratio.

4.3.6 Biotite

Biotite occurs in the *ne*-gabbro, and the monzodiorite schlieren within the gabbro, from Onawe Peninsula. Biotite is not found in the gabbro and monzodiorite xenoliths from Lighthouse Reserve, or any lava flows or fine grained intrusives.

A solid solution series exists between biotite and phlogopite, and an arbitrary distinction is made between the two minerals on the basis of the Mg:Fe ratio — phlogopite has Mg:Fe > 2:1; biotite has Mg:Fe < 2:1. On this basis, all analyses are biotites, except one (point 3.2, sample N36C3155) from the *ne*-gabbro, which is a phlogopite.

The Mg:Fe ratio ranges from 1.102–2.703, with an average of 1.512 ± 0.344 (1 s.d.). Compared to published analyses (Deer *et al*, 1966), biotites and phlogopites from Akaroa Volcanic Group rocks are high in TiO_2 (average 5.24 wt%), and low in Al_2O_3 (average 14.8 wt%).

4.4 Comparison of Akaroa Volcanic Group Mineralogy with other New Zealand Cenozoic Volcanics

Akaroa Volcanic Group lavas have a mineralogy typical of mildly alkaline volcanic associations. Cenozoic, intraplate, mildly alkaline volcanic rocks are known from numerous localities throughout New Zealand including the Campbell Plateau, Chatham Islands and Dunedin Volcano.

The petrology of Cenozoic volcanic rocks from the Campbell Plateau (Auckland Islands, Campbell Island, Antipodes Island) and the Chatham Islands has been summarised by Gamble *et al* (1986). On Auckland and Campbell Islands, the dominant lava types are mildly alkaline (< 5% normative *ne*) to transitional (*hy*-normative) basaltic lavas erupted from fissure vents. Evolved lavas ranging up to rhyolitic composition are also present, and gabbroic intrusions, thought to represent the unroofed upper parts of subvolcanic magma chambers, are exposed in the eroded cores of the volcanoes. On Antipodes Island and the Chatham Islands, pyroclastics ranging from basanite to phonolite are dominant.

Basic rocks are characterised by clinopyroxene and olivine and minor plagioclase and Fe-Ti oxide phenocryst phases, whereas in more evolved rocks plagioclase and Fe-Ti oxide phenocrysts dominate over olivine and clinopyroxene. In felsic rocks sodic plagioclase, rare alkali feldspar, quartz and Fe-Ti oxides are phenocryst phases. Pargasite–kaersutite megacrysts and phenocrysts are reported from lavas of the Chatham Islands and Antipodes Island. Amphibole megacrysts are frequently corroded, embayed and mantled by rhonite and Fe-Ti oxides. The groundmass of basic lavas contains clinopyroxene, plagioclase and minor olivine and Fe-Ti oxides. Felsic lavas generally have a cryptocrystalline groundmass dominated by feldspar with traces of quartz and aegirine. A diverse suite of amphibole and clinopyroxene

megacrysts, and gabbroic, spinel lherzolite and pyroxenite xenoliths are recorded from the Eocene and Pliocene volcanics of the Chatham Islands.

Olivine compositions range from Fo_{86} to Fo_{39}, and wide compositional ranges may occur within individual samples. Although Ca-poor pyroxenes do occur in the interstices of the gabbros of Auckland and Campbell Islands, Ca-rich clinopyroxenes are the dominant pyroxene. Salite and calcic augite compositions are the most common in basaltic and intermediate lavas, but diopside and endiopside compositions are also represented. Pyroxenes from felsic lavas are ferroaugite and aegirine. Plagioclase occurs as phenocryst or microphenocryst and groundmass phases in nearly all rocks. Phenocrysts typically exhibit normal and/or oscillatory zoning. Plagioclase compositions form a continuum from anorthite (in gabbroic inclusions) to oligoclase and anorthoclase in rhyolites, trachytes and phonolites. Alkali feldspars in rhyolites, trachytes and phonolites range from anorthoclase to sodic sanidine. Titanomagnetite is the ubiquitous Fe-Ti oxide phase in most rocks, but may be accompanied by ilmenite in basic rocks.

Coombs *et al* (1986) summarised the petrology of the Dunedin Volcanic Group. Mafic and intermediate members of the sodic alkali olivine basalt–trachyte lineage have a relatively simple mineralogy of olivine and titaniferous calcic augite, which both show a tendency towards iron-enrichment, titanomagnetite and plagioclase. Of note is the occasional occurrence of kaersutite and/or its rhonite-bearing decomposition products in the sodic series, and kaersutite partly or completely replaced by dense aggregates of it's low-pressure magmatic decomposition products in potassic lavas, which Price and Chappell (1975) suggested was indicative of crystallisation under high P_{H_2O} and P_{O_2} conditions.

Chapter 5

MAJOR, TRACE AND RARE EARTH ELEMENT GEOCHEMISTRY

5.1 Introduction

In this chapter data on the major, trace and rare earth element geochemistry of Akaroa Volcanic Group lavas are presented.

Major element analyses and CIPW norms for 278 samples are presented in Appendix G. It is a common practice to quote CIPW norm analyses when presenting major element analyses, yet the literature contains many examples of CIPW norms which are in error or inconsistent with the corresponding major element analysis. An analysis of the sources of these errors and procedures for improving CIPW norm calculations are presented in Appendix G.

Trace element analyses, trace element ratios, and coordinates for the Pearce and Cann (1973) tectonic discrimination diagrams are presented in Appendix H for the same set of 278 samples.

Rare earth element analyses for 12 samples are presented in Appendix I.

A comparison of published and measured analyses of international laboratory standards is presented at the beginning of each appendix (Tables G3, H1, I1 in Appendices G, H and I respectively), for estimating the accuracy of analyses.

5.2 Major Element Geochemistry

5.2.1 Overview

Akaroa Volcanic Group lavas are mildly to moderately alkaline in character, plotting above the alkaline–subalkaline dividing line of Irvine and Baragar (1971) on an alkali–silica diagram (Fig. 5.1), and have been classified according to the alkali-olivine basalt association terminology of Coombs and Wilkinson (1969) and MacDonald and Katsura (1964). Rocks are assigned names according to the projection of the rock on a plot of differentiation index versus plagioclase ratio (Fig. 5.2). Rock names are prefixed by normative mineral abbreviations (*ne*-, *hy*-, and *qz*-) according to the degree of silica saturation.

The majority of rocks analysed (53%) are mildly undersaturated, weakly *ne* normative ($ne < 5$ wt%) basalts, hawaiites, mugearites, benmoreites and trachytes. *Hy*- and *qz*-normative equivalents of this series form smaller but significant populations, at 28% and 16% respectively, of the rocks analysed. For all rock types, *ne*-, *hy*- and *qz*-normative variants exist.

Moderately undersaturated, strongly *ne*-normative ($ne > 5$ wt%) compositions account for approximately 3% of the rocks analysed.

Following the proposals of Coombs and Wilkinson (1969), Green and Ringwood (1967), and MacDonald and Katsura (1964), alkali-olivine basalts with more than 5 wt% *ne* in the norm are classified as basanitoids, or basanites if nepheline appears in the mode. Three *ne*-basalts from Akaroa Volcanic Group (N36C3036, N36C3273, N36C3316) have more than 5 wt% normative *ne* ($ne = 5.51$, 8.29, 6.04 wt%, respectively). Nepheline has not been positively identified in the mode, so these rocks are classified as basanitoids. A comparison of Akaroa Volcanic Group basanitoids with basanitoids and basanites from other volcanic provinces is presented in Table 5.1.

Four *ne*-hawaiites (N36C3276, N37A3449, N37A3457, N36C3659) have more than 5 wt% normative *ne* ($ne = 5.31$, 6.96, 5.77, 6.08 wt%, respectively) and are here classified as nepheline hawaiites, following the proposals of Coombs and Wilkinson (1969), to distinguish them from *ne*-hawaiites which have < 5 wt% normative *ne*.

A sample (N36D3619) from a dike on the eastern rim of the crater (N36D/10701024), which projects into the trachyte field on a plot of differentiation index versus plagioclase ratio, has 10.69 wt% normative *ne*. Coombs and Wilkinson (1969) suggest that 10% normative *ne* corresponds to > 10% modal nepheline, and that lavas with more than 10% normative or modal *ne* be classified as phonolites. This terminology

Figure 5.1: Alkali–silica diagram for Akaroa Volcanic Group. The line labelled I&B is the alkaline–subalkaline dividing line of Irvine and Baragar (1971).

Figure 5.2: Differentiation index versus plagioclase ratio for Akaroa Volcanic Group, with trends from other volcanic provinces after Coombs and Wilkinson (1969).

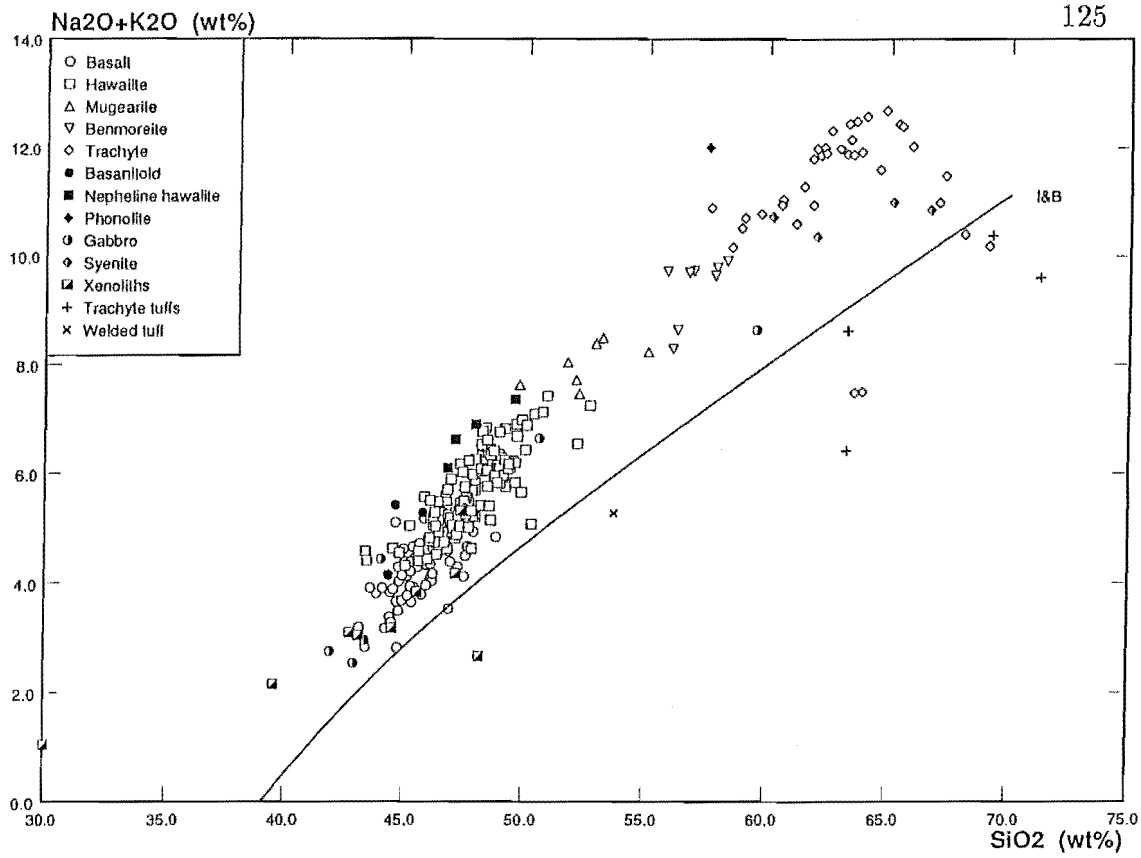
Na2O+K2O (wt%)
Basalt
Hawaiite
Mugearite
Benmoreite
Trachyte
Basanitoid
Nepheline hawaiite
Phonolite
Gabbro
Syenite
Xenoliths
Trachyte tuffs
Welded tuff
I&B
SiO2 (wt%)

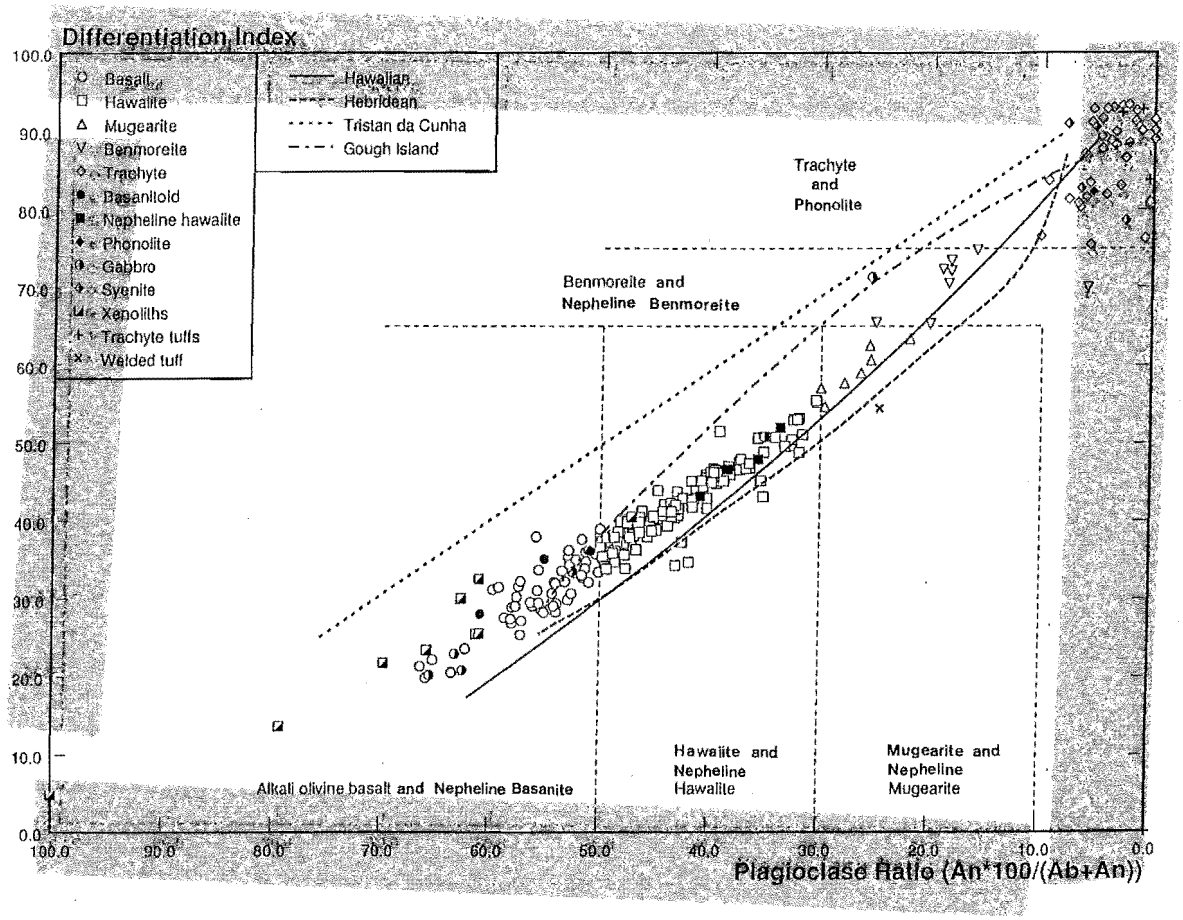
Differentiation Index
Basalt
Hawaiite
Mugearite
Benmoreite
Trachyte
Basanitoid
Nepheline hawaiite
Phonolite
Gabbro
Syenite
Xenoliths
Trachyte tuffs
Welded tuff
Hawaiian
Hebridean
Tristan da Cunha
Gough Island
Trachyte and Phonolite
Benmoreite and Nepheline Benmoreite
Hawaiite and Nepheline Hawaiite
Mugearite and Nepheline Mugearite
Alkali olivine basalt and Nepheline Basanite
Plagioclase Ratio (An*100/(Ab+An))

is adopted here, to be consistent with terminology for other rock types, and sample N36D3619 is classified as a phonolite. Nepheline has not been positively identified in the mode, but chemically the rock is similar to phonolites from other volcanic provinces (Table 5.2).

It should be noted that this classification is arbitrary — other authors have used or suggested other classifications for phonolitic lavas. For example, Chapman (1970) suggests the term phonolite for lavas with modal nepheline > 15 wt%, and trachyphonolite for lavas with 10–15% modal nepheline. S. D. Weaver (*pers. comm.*) suggests the terms phonolite for lavas with > 15% normative *ne*, trachyphonolite for lavas with 10–15% normative *ne*, and phonolitic trachyte for lavas with < 10% and > 5% normative *ne*. Alternatively, to maintain consistency with the basanitoid/basanite terminology, the terms phonolitoid for lavas with normative $ne > 5\%$, and phonolite for lavas with normative $ne > 5\%$ and nepheline positively identified in the mode, might be appropriate. This is the first recorded occurrence of phonolite on Banks Peninsula, although Sewell (1985) reports occurrences of more basic undersaturated rocks (basanitoids).

Three samples, from a trachyte dike (N36C3045), Devils Gap trachyte intrusion (N37A3506), and Ellangowan trachyte intrusion (N36D3600), are peralkaline trachytes. These trachytes have atomic Al/(Na + K) ratios in the range 0.9855–0.9957 and 0.32–1.15 wt% normative *ac*. The presence of acmite in the norm is indicative of peralkaline trachytes and reflects the presence of sodic pyroxenes and amphiboles in the mode. Sample N36D3600 from Ellangowan trachyte intrusion has arfvedsonite, a green pleochroic sodic pyroxene (Na-hedenbergite? aegirine-augite?), aenigmatite, albite, magnetite and minor interstitial quartz in the groundmass. Sample N37A3506 from Devils Gap trachyte intrusion has megacrysts of kaersutite, which is breaking down at the margins to pyroxene and magnetite, set in a groundmass that includes a green pleochroic sodic pyroxene (Na-hedenbergite? aegirine-augite?).

The welded tuff from the west side of Onawe Peninsula, which contains abundant sedimentary rock fragments and incipient cordierite, has 12.04 wt% *C* and 16.58 wt% *Q* in the norm. *C* and *Q* are also common in the norms or more evolved lavas, but the concentrations are considerably lower : 0.0–9.0 wt% *Q* and 0.0–5.0 wt% *C*.

Analyses of trachytic pyroclastics and clasts from trachytic pyroclastics contain traces of *hm* (0.04–0.72 wt%), *ru* (0.1–1.64 wt%), and abundant *C* (0.6–12.04 wt%) and *Q* (4.23–25.57 wt%). This may reflect the pyroclastic origin of the material, contamination by crustal material, or alteration by sea water.

Table 5.1: Comparison of Akaroa Volcanic Group basanitoids with basanitoids and basanites from other volcanic provinces.

Sample Id	1	2	3	4	5	6	7	8	9	10
SiO2	44.38	44.63	45.78	44.49	42.49	44.38	42.65	42.25	41.68	43.26
TiO2	3.58	3.36	3.52	3.00	2.98	2.54	4.23	4.18	4.06	3.31
Al2O3	16.04	16.27	16.34	13.21	13.57	14.90	11.53	10.29	12.92	13.36
tFe2O3	15.56	13.76	13.90	13.99	–	–	–	–	–	–
Fe2O3	2.00	2.00	2.00	2.00	4.17	2.82	2.74	2.23	3.06	3.67
FeO	12.20	10.58	10.71	10.79	9.04	8.85	13.70	11.15	8.48	8.44
MnO	0.19	0.22	0.17	0.18	0.18	0.19	0.19	0.19	0.18	0.20
MgO	5.77	5.87	5.11	9.32	9.79	8.32	9.65	11.27	12.13	10.62
CaO	10.66	9.30	9.28	10.18	11.47	10.69	11.66	12.69	11.32	11.01
SrO	–	–	–	–	–	–	–	–	–	0.11
BaO	–	–	–	–	–	–	–	–	–	0.04
Na2O	3.22	3.96	3.94	3.68	3.52	3.48	2.36	3.33	3.16	3.49
K2O	0.92	1.46	1.34	1.38	0.60	1.26	0.75	1.35	1.48	1.25
P2O5	0.46	0.75	0.57	0.66	0.59	0.60	0.53	1.06	0.84	0.70
CO2	–	–	–	–	0.20	0.44	–	–	–	0.10
H2O+	–	–	–	–	1.02	0.77	–	–	–	0.28
H2O-	–	–	–	–	0.94	0.70	–	–	–	0.15
LOI	-0.53	0.60	-0.13	0.40	–	–	0.27	–	–	–
Total	100.25	100.18	99.82	100.49	100.56	99.94	100.26	99.99	99.31	99.99
or	5.44	8.63	7.92	8.16	3.55	7.45	4.43	7.98	8.75	7.39
ab	17.08	18.21	22.19	11.81	11.44	15.28	10.20	0.73	2.42	9.04
an	26.60	22.31	22.94	15.45	19.45	21.31	18.65	9.14	16.70	17.12
ne	5.51	8.29	6.04	10.47	9.94	7.67	5.29	14.87	13.17	11.10
wo-di	9.72	7.90	8.09	12.84	13.50	10.45	14.92	19.58	14.19	13.69
en-di	4.66	4.12	4.00	7.68	9.20	6.59	8.51	12.74	10.49	9.73
fs-di	4.92	3.56	3.93	4.48	3.23	3.20	5.76	5.49	2.32	2.71
en-hy	–	–	–	–	–	–	–	–	–	–
fs-hy	–	–	–	–	–	–	–	–	–	–
fo	6.81	7.36	6.12	10.88	10.64	9.90	10.88	10.74	13.82	11.72
fa	7.93	7.01	6.63	7.00	4.12	5.31	8.11	5.09	3.36	3.60
mt	2.90	2.90	2.90	2.90	6.05	4.09	3.97	3.23	4.44	5.32
il	6.80	6.38	6.68	5.70	5.66	4.82	8.03	7.94	7.71	6.29
ap	1.07	1.74	1.32	1.53	1.37	1.39	1.23	2.46	1.95	1.62
cc	–	–	–	–	0.45	1.00	–	–	–	0.23
aq	–	–	–	–	1.96	1.47	–	–	–	0.43
Total	99.42	98.40	98.76	98.89	100.56	99.94	99.99	99.99	99.31	99.99

1. Basanitoid, Akaroa Volcano, this study, sample N36C3036.
2. Basanitoid, Akaroa Volcano, this study, sample N36C3273.
3. Basanitoid, Akaroa Volcano, this study, sample N36C3316.
4. Basanitoid, Central Banks Peninsula, Sewell (1985), sample M36B2446.
5. Nepheline basanite, Dunedin Volcano, Coombs and Wilkinson (1969), Table 7, sample 1.
6. Basanitoid, Dunedin Volcano, Coombs and Wilkinson (1969), Table 7, sample 2.
7. Basanite, Antipodes Island, Gamble *et al* (1986), sample 81/7.
8. Basanite, Chatham Islands, Gamble *et al* (1986), sample VUW 14465.
9. Basanite, Antarctica, Kyle (1981), Table 11, sample 2.
10. Basanitoid (average of 12 analyses), Antarctica, Goldich *et al* (1975), Table 10, sample 30.

Akaroa Volcanic Group basalts and basanitoids (DI > 50%) plot close to the 9 kb cotectic for olivine + plagioclase + clinopyroxene in equilibrium with basaltic liquid, on the normative nepheline–olivine–diopside–hypersthene–quartz system (Fig. 5.3), consistent with magma evolution in relatively deep mantle reservoirs. A high pressure relationship between basalt and basanitoid magmas is suggested, whereas members of the basalt–trachyte and basanitoid–phonolite lineages are probably related by low pressure crustal processes. The scatter in projections suggests that either Akaroa Volcanic Group basalts and basanitoids are not primary melts but have undergone some fractionation, or that initial magmas were in equilibrium with some mineral assemblage other than olivine + plagioclase + clinopyroxene, perhaps involving apatite or amphibole.

Akaroa Volcanic Group lavas have Mg numbers (atomic $Mg/(Mg + Fe^{2+}) \times 100$) in the range 2.34–77.79. The highest Mg number (77.79) is for a xenolith from Lighthouse Reserve (N36C3632) and reflects its cumulate origins. The most primitive non-cumulate Akaroa Volcanic Group lavas are *ne*-alkalic basalts with Mg numbers > 60, but most basalts and hawaiites have Mg numbers in the range 35–48. Green (1970, 1971) suggests that the composition of residual mantle olivine ranges from Fo_{88} to Fo_{92}, and that a primary basalt magma in equilibrium with mantle olivine should have Mg numbers in the range 68–77. These magmas would have high ($\gg$ 100 ppm) Cr, Ni and V contents. Sun and Hanson (1975) calculate that the separation of 5% olivine (Fo_{86}) and 5% clinopyroxene ($En_{58}Fs_{10}Wo_{32}$) from a primitive alkali basalt reduces the Mg number considerably (eg. from 73 to 69). Furthermore, the Ni content of an alkali basalt ($\approx$ 300–400 ppm) in equilibrium with mantle peridotite ($\approx$ 2000 ppm Ni) would be reduced by 50%. Mg numbers, and Cr, Ni and V contents for the three most primitive Akaroa Volcanic Group lavas are tabulated in Table 5.3.

On the criteria suggested by Green (1970, 1971) and Sun and Hanson (1975), the most primitive, non-cumulate Akaroa Volcanic Group basalts are not primary basaltic magmas, but have undergone significant (> 10%) high pressure fractionation of olivine and clinopyroxene. The mineralogy of Akaroa Volcanic Group basanitoids and basalts is consistent with this interpretation. Basanitoids typically have olivine + magnetite (± plagioclase ± clinopyroxene) phenocryst assemblages. Basalts with olivine + clinopyroxene phenocryst assemblages are less common than basalts with plagioclase + olivine + clinopyroxene + magnetite phenocrysts but have up to 30% phenocrysts, compared with < 10% phenocrysts in basalts with plagioclase as a phenocryst phase. Furthermore, most phenocrysts exhibit moderate to severe corrosion and sieve textures, indicating disequilibrium with the host basaltic liquid.

The contention that basic lavas from the Akaroa Volcanic Group may have undergone early high pressure fractionation of olivine and clinopyroxene is supported by frequency distributions of lavas by rock type and SiO_2 content (Fig. 5.4). Hawaiites

Table 5.2: Comparison of the Akaroa Volcanic Group phonolite with phonolites from other volcanic provinces.

Sample Id	1	2	3	4	5	6	7	8
SiO_2	57.52	54.82	53.60	59.92	54.17	56.13	56.19	52.97
TiO_2	0.20	1.16	0.55	0.06	1.88	1.07	0.62	0.58
Al_2O_3	18.51	20.41	24.25	19.86	19.14	16.13	19.04	18.79
tFe_2O_3	6.66	–	–	–	–	–	–	–
Fe_2O_3	2.50	1.99	0.64	1.69	2.87	4.00	2.79	3.46
FeO	3.74	2.52	1.36	1.70	2.22	4.57	2.03	3.36
MnO	0.25	0.18	0.04	0.18	0.17	0.35	0.17	0.20
MgO	0.34	1.24	0.61	0.05	2.18	1.59	1.07	1.57
CaO	2.05	3.46	2.29	1.07	4.48	2.43	2.72	2.96
Na_2O	8.00	8.50	9.21	8.94	7.21	7.24	7.79	8.95
K_2O	4.00	4.57	6.08	4.93	3.69	4.99	5.24	4.24
P_2O_5	0.12	0.26	0.08	0.17	0.44	0.20	0.18	0.22
CO_2	–	–	–	–	–	–	0.08	0.12
H_2O+	–	–	0.70	0.07	0.61	0.86	1.57	0.84
H_2O-	–	–	0.72	1.29	0.22	0.35	0.37	0.74
LOI	1.95	0.49	–	–	–	–	–	–
Total	99.60	99.60	100.13	99.93	99.28	99.91	99.86	99.00
or	23.64	27.01	35.93	29.13	21.81	29.49	30.97	25.06
ab	47.97	30.90	16.38	47.14	37.55	34.22	35.43	27.89
an	2.78	4.04	6.87	–	8.96	–	1.51	–
ne	10.69	22.23	33.34	14.93	12.71	11.36	16.52	24.46
ac	–	–	–	0.83	–	5.36	–	2.37
wo	–	–	–	–	–	–	0.59	–
wo-di	2.76	4.77	1.66	1.75	4.34	4.49	3.71	5.21
en-di	0.44	3.06	0.91	0.10	3.75	1.89	2.67	2.71
fs-di	2.55	1.39	0.68	1.85	–	2.62	0.71	2.36
en-hy	–	–	–	–	–	–	–	–
fs-hy	–	–	–	–	–	–	–	–
fo	0.29	0.02	0.42	0.01	1.18	1.45	–	0.84
fa	1.84	0.01	0.35	0.27	–	2.22	–	0.81
mt	3.62	2.88	0.93	2.03	2.26	3.11	4.04	3.83
il	0.38	2.20	1.04	0.11	3.57	2.03	1.18	1.10
hm	–	–	–	–	1.31	–	–	–
ap	0.28	0.60	0.19	0.39	1.02	0.46	0.42	0.51
cc	–	–	–	–	–	–	0.18	0.27
aq	–	–	1.42	1.36	0.83	1.21	1.94	1.58
Total	97.23	99.11	100.13	99.93	99.28	99.91	99.86	99.00

1. Phonolite, Akaroa Volcano, this study, sample N36D3619.
2. Phonolite, Tahiti, McBirney and Aoki (1968), Tables 1 and 3, sample 45.
3. Kaersutite phonolite, Antarctica, Kyle (1981), Table 10, sample 7.
4. Phonolite, St Helena, Baker (1969), Table 2, sample 11.
5. Phonolite, Tenerife, Ridley (1970), Table 4, sample 9.
6. Glassy phonolite, Mt. Suswa, East Africa, Nash *et al* (1969), sample W118.
7. Phonolite, average of 340 analyses, Le Maitre (1976, p602).
8. Phonolite, Dunedin Volcano, Price and Chappell (1975, p169), sample 14.

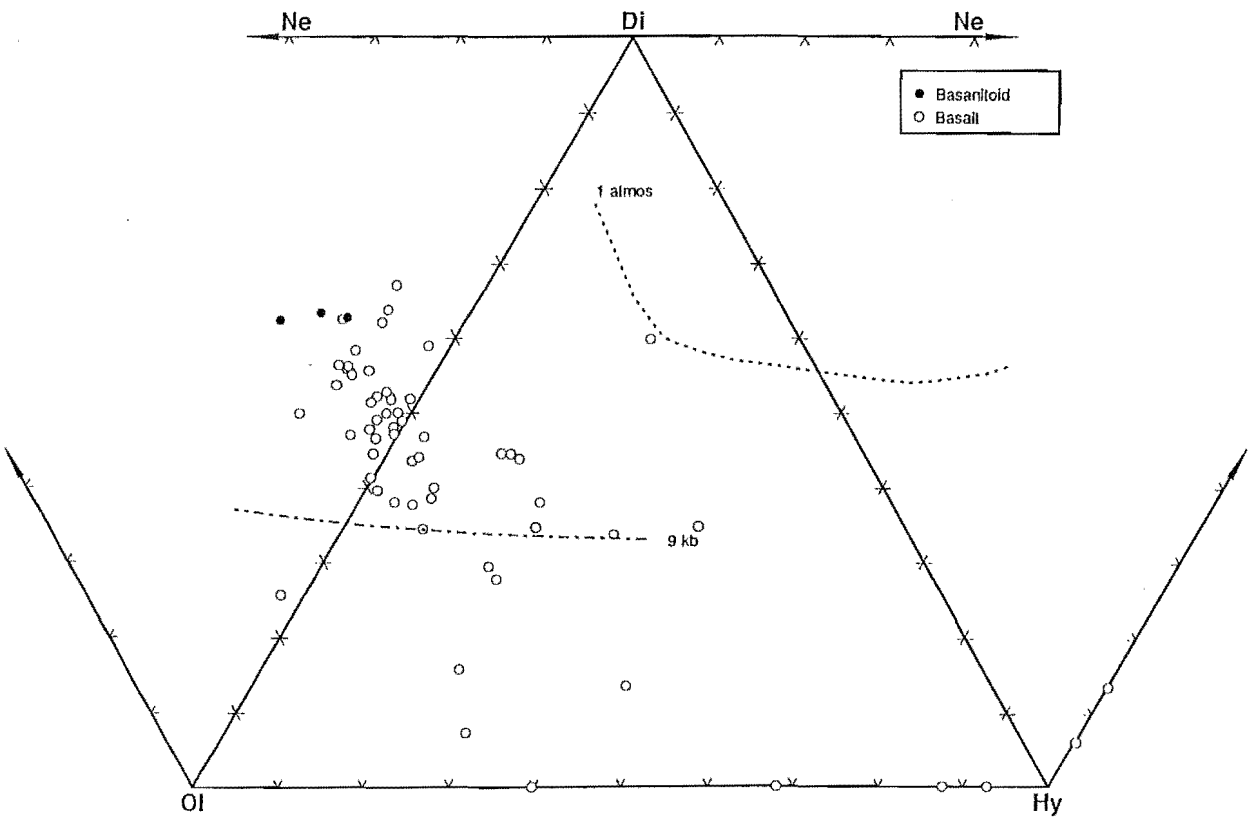

Figure 5.3: Normative *ne–ol–di–hy–qz* diagram for basic (DI > 50%) Akaroa Volcanic Group lavas. Lines labelled 9 kb and 1 atmos are the 9 kb and 1 atmosphere cotectic curves for basaltic liquids in equilibrium with olivine + clinopyroxene + plagioclase (after Thompson *et al*, 1983).

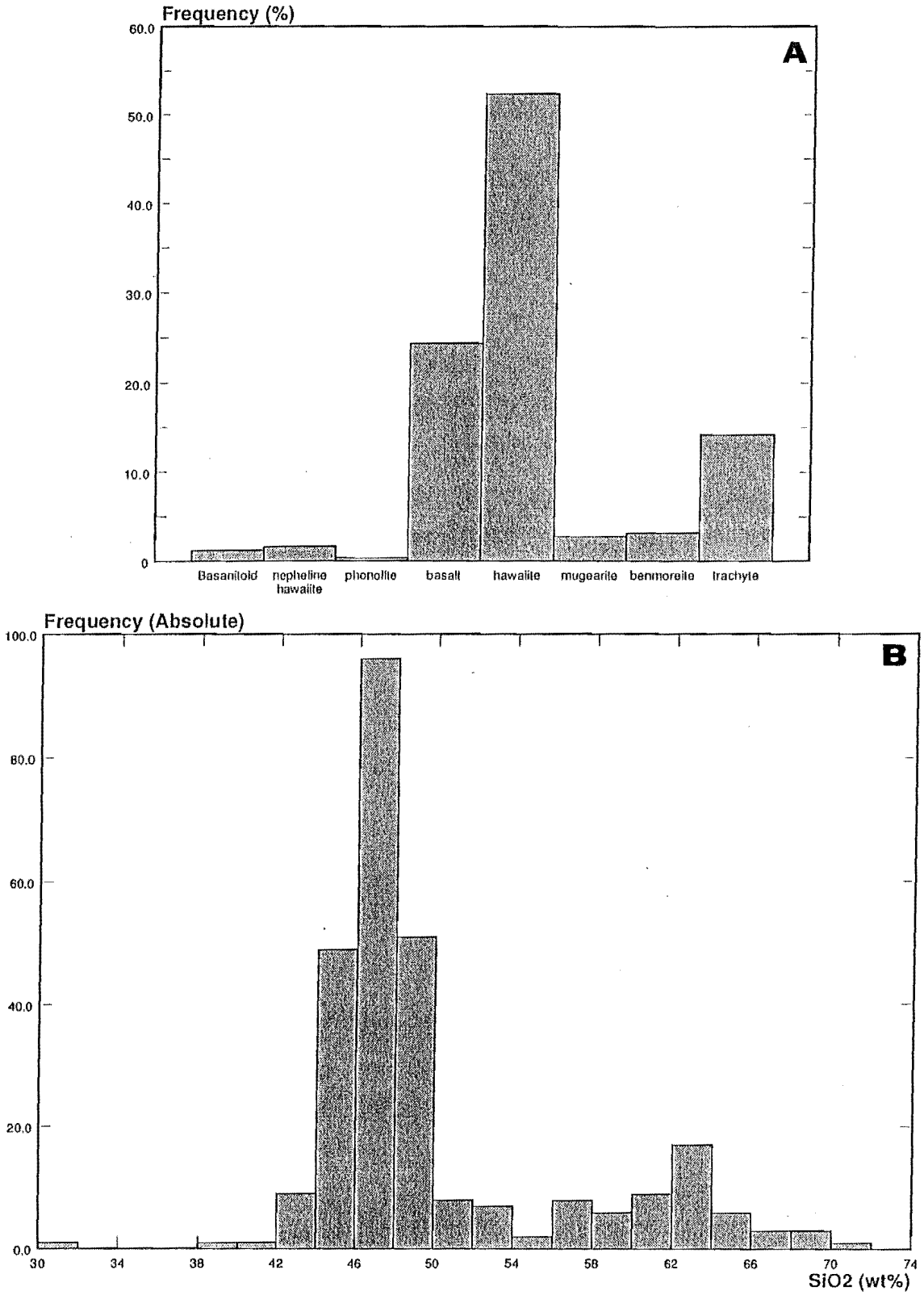

Figure 5.4: Frequency distributions of Akaroa Volcanic Group lavas. A: By rock type. B: By SiO_2 content.

Table 5.3: Tabulation of Mg Number, V, Cr and Ni for the three most primitive lavas from Akaroa Volcanic Group.

Sample	Rock type	Mg number	V	Cr	Ni
N36C3037	*ne*-basalt	61.55	309.0	376.8	200.5
N36C3071	*ne*-basalt	62.50	323.6	419.3	239.9
N36C3652	*ne*-basalt	62.34	102.9	20.1	15.6

with SiO_2 contents of 46–50 wt% are the most abundant rock type, rather than basalts. Similar distributions, in which hawaiites dominate over basalts, have been reported from Banks Peninsula (Price and Taylor, 1980; Falloon, 1982; Thiele, 1983; Sewell, 1985; Weaver and Sewell, 1986), Dunedin Volcanic Group (Coombs and Wilkinson, 1969; Price and Taylor, 1973; Price and Chappell, 1975; Coombs and Reay, 1986), Canterbury and North Otago (Coombs *et al*, 1986; Coote, 1987; Duggan and Reay, 1986) and Campbell Island (Morris, 1984). Although basalts, hawaiites and trachytes dominate over intermediate rock types, mugearites and benmoreites do occur, and no Daly Gap exists in the Akaroa Volcanic Group.

Akaroa Volcanic Group lavas show a trend of moderate iron enrichment on an AFM plot (Fig. 5.5) typical of alkali basalt–trachyte associations. The extreme differentiation of trachytic lavas is evident. The trend for Hawaiian alkalic lavas (MacDonald and Katsura, 1964; Coombs and Wilkinson, 1969) forms a lower bound on the level of iron enrichment, while the Hebridean trend (Tilley *et al*, 1967) most closely approximates the trend of Akaroa Volcanic Group lavas.

In terms of normative feldspar compositions (Fig. 5.6), Akaroa Volcanic Group basalts–benmoreites show a progressive decrease in *An* content, with nearly constant *Ab:Or* ratios. In contrast, trachyte normative feldspar compositions are dominated by variations in the *Ab:Or* ratio.

5.2.2 Variation of Major Element abundances with fractionation

Major element abundances have been plotted against SiO_2 as a fractionation index because:

1. SiO_2 shows a wide range of abundance in non-cumulate rocks (43 wt% to > 70 wt%)

Figure 5.5: Na_2O+K_2O–tFeO–MgO diagram for Akaroa Volcanic Group, with trends for other volcanic provinces (after Coombs and Wilkinson, 1969).

Figure 5.6: Normative *An–Ab–Or* diagram for Akaroa Volcanic Group, with trends for other volcanic provinces (after Coombs and Wilkinson, 1969).

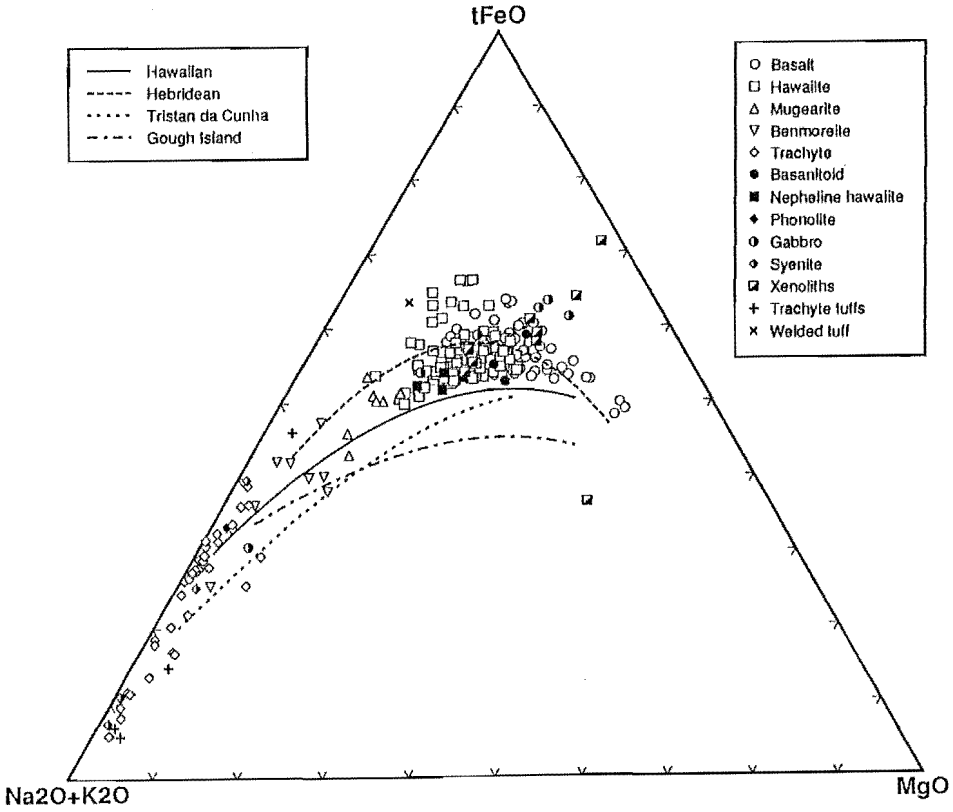
tFeO
Na2O+K2O
MgO
Hawaiian
Hebridean
Tristan da Cunha
Gough Island
Basalt
Hawaiite
Mugearite
Benmoreite
Trachyte
Basanitoid
Nepheline hawaiite
Phonolite
Gabbro
Syenite
Xenoliths
Trachyte tuffs
Welded tuff

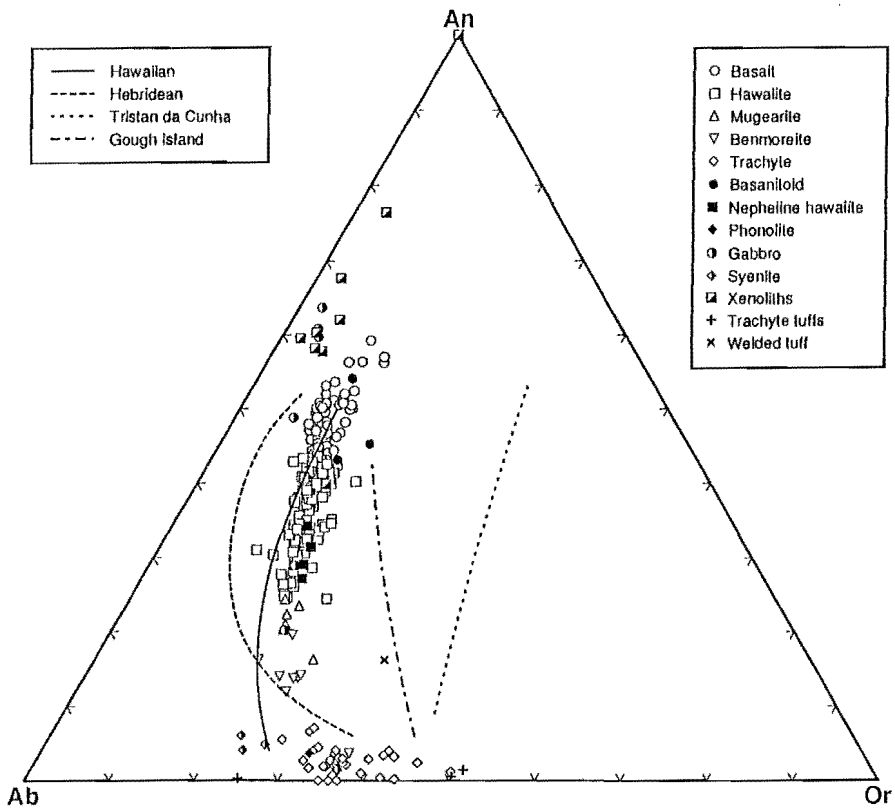
An
Ab
Or
Hawaiian
Hebridean
Tristan da Cunha
Gough Island
Basalt
Hawaiite
Mugearite
Benmoreite
Trachyte
Basanitoid
Nepheline hawaiite
Phonolite
Gabbro
Syenite
Xenoliths
Trachyte tuffs
Welded tuff

2. SiO_2 increases systematically from basalt to trachyte
3. The resulting graphs appear to be the most useful in interpreting element variations.

The variations in major element chemistry with SiO_2 wt% are presented graphically in figures 5.7 to 5.15. Overall, fractionation (and increased SiO_2 wt% content) is marked by

- An increase in $Na_2O + K_2O$
- A decrease in MgO, TiO_2, CaO, tFe_2O_3 and MnO
- An increase, followed by a decrease in P_2O_5
- A complex variation in Al_2O_3

In the following sections, these trends will be discussed in detail.

MgO, TiO_2, CaO and tFe_2O_3: MgO (Fig. 5.7) exhibits a well defined exponential decrease with increasing SiO_2. Basalts show the greatest variation in MgO content, from 10.72 wt% to < 3.0 wt%, over a small range of SiO_2 values (43–47 wt%). In comparison, MgO contents in hawaiites decrease much less rapidly, from 6.0 wt% to ≈ 2.0 wt%, over a similar range in SiO_2 values (45–50 wt%). MgO contents in trachytes are < 1 wt%.

Lavas of the basanitoid–phonolite series follow the same trend, as do the syenite and monzonite schlieren in the gabbro, from Onawe Peninsula. The variation in MgO reflects, initially, the fractionation of olivine + clinopyroxene, with crystallisation of Mg- rich olivine (Fo_{68}–Fo_{85}) being the major influence on MgO content. In hawaiites olivine becomes less important, compared with clinopyroxene, as a fractionating phase, and the appearance of plagioclase as a phenocryst phase in part negates the effect of olivine fractionation. In more evolved rocks, the decreasing rate of reduction of MgO reflects the lower absolute MgO content and the decrease in modal clinopyroxene.

Gabbroic and monzodioritic xenoliths from Lighthouse Reserve and the gabbro from Onawe Peninsula show a rapid, linear decrease in MgO content, from 12 to 3 wt% MgO, reflecting the relative abundance of olivine, clinopyroxene, plagioclase and magnetite as cumulus phases. In general, MgO contents are less than those of lavas with equivalent SiO_2 contents, rather than being higher as might be expected. Furthermore olivine phenocrysts have lower Fo contents compared with olivines in basalt lava flows.

This apparent dichotomy might be interpreted as follows. Near-primary Mg-rich magmas undergo polybaric fractionation of Mg-rich olivine as they rise through the crust. Some magma is erupted without undergoing any significant fractionation in a low-P high level crustal reservoir. Most magma, however, undergoes fractionation in a high level magma reservoir, and the xenoliths and gabbro may be cumulates formed during fractional crystallisation of magmas of hawaiitic composition.

TiO_2 (Fig. 5.8) decreases linearly from >4 to < 1 wt% from basalt through to benmoreite, and is approximately constant at 0.3–0.5 wt% in trachytes. Lavas of the basanitoid–phonolite series follow the same trend. Gabbroic and monzodioritic xenoliths from Lighthouse Reserve and the gabbro, syenite and monzodiorite/monzonite schlieren from Onawe Peninsula in general follow the trend of extrusive lavas. Some xenoliths and one sample from the gabbro are depleted/enriched in TiO_2 compared to lavas with equivalent SiO_2 contents, and this reflects the variations in the proportion of cumulus magnetite. The decrease in TiO_2 is due to the presence of magnetite as a ubiquitous phenocryst and groundmass phase in all lavas.

The linear decrease in CaO content (Fig. 5.9) from $\approx$ 12.0 wt% in basalts to < 1 wt% in trachyte reflects fractionation of clinopyroxene and plagioclase. Xenoliths in general fall close to the trend of lavas, and variations in SiO_2 with constant CaO (at $\approx$ 11 wt% CaO) reflect variations in the ratio of olivine:clinopyroxene:magnetite. One xenolith (N37A3638) falls well off the trend (at 30.04 wt% SiO_2, 6.96 wt% CaO). This xenolith is composed almost entirely of olivine, clinopyroxene, magnetite and Fe oxide.

tFe_2O_3 (Fig. 5.10) decreases linearly from $\approx$ 15 wt% in basalts to < 6 wt% in trachytes, reflecting fractionation of olivine, clinopyroxene and magnetite. Most xenoliths fall on a similar but steeper linear trend, and in general have lower tFe_2O_3 values than lavas of similar SiO_2 content. This behaviour is similar to that observed for MgO, and reflects the relative proportions of cumulus phases.

MnO (Fig. 5.11) behaves in a similar fashion to tFe_2O_3, although the trend is poorly defined due to the absence of a MnO-rich phenocryst phase.

Na_2O and K_2O: Na_2O and K_2O increase approximately linearly with increasing SiO_2 content (Fig. 5.12, 5.13), although the trend is less well defined and "feathered" in the trachytes. Of particular interest are lavas of the basanitoid/phonolite series which plot above the main basalt–trachyte trend on the Na_2O versus SiO_2 plot (Fig. 5.12), and are clearly more sodic. Basalts through to hawaiites have Na_2O:K_2O ratios of > 2.0, and mugearites through to trachytes have Na_2O:K_2O ratios between 1.0 and 2.0. In comparison, lavas of the basanite/phonolite series have Na_2O/K_2O ratios varying from 3.0 for basanites to 2.0 for a phonolite. The more sodic, alkaline nature of the basanite–phonolite series can also be observed in alkali–silica (Fig.

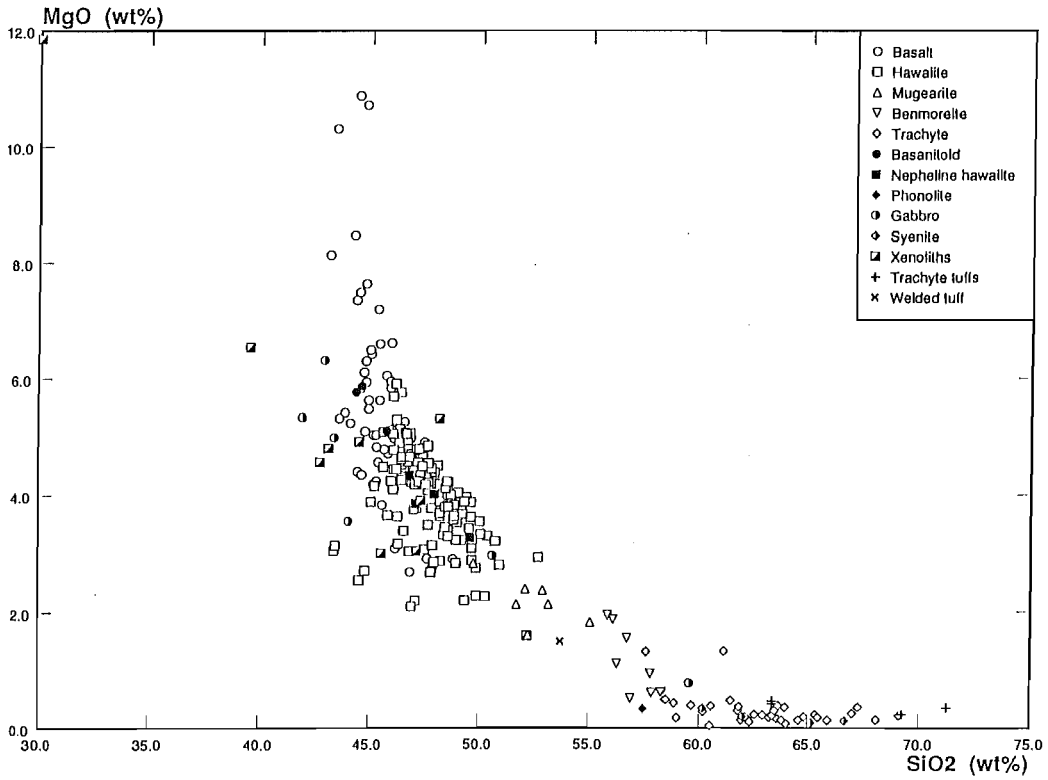

Figure 5.7: MgO (wt%) versus SiO_2 (wt%) for Akaroa Volcanic Group.

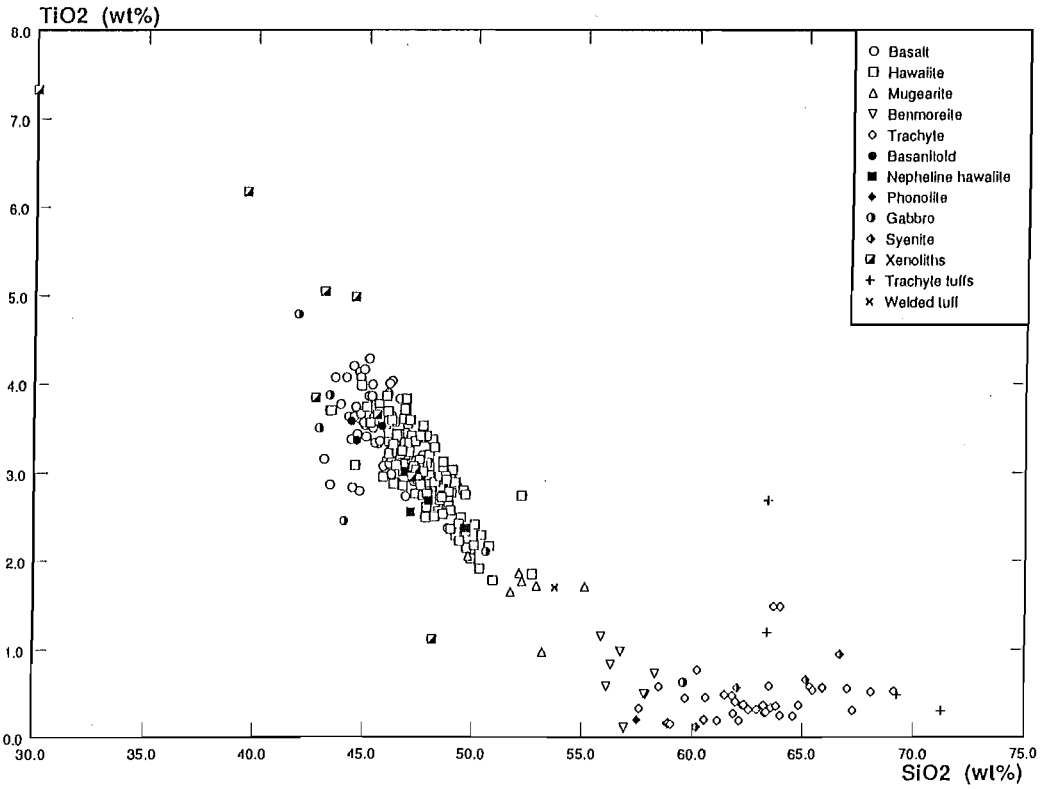

Figure 5.8: TiO_2 (wt%) versus SiO_2 (wt%) for Akaroa Volcanic Group.

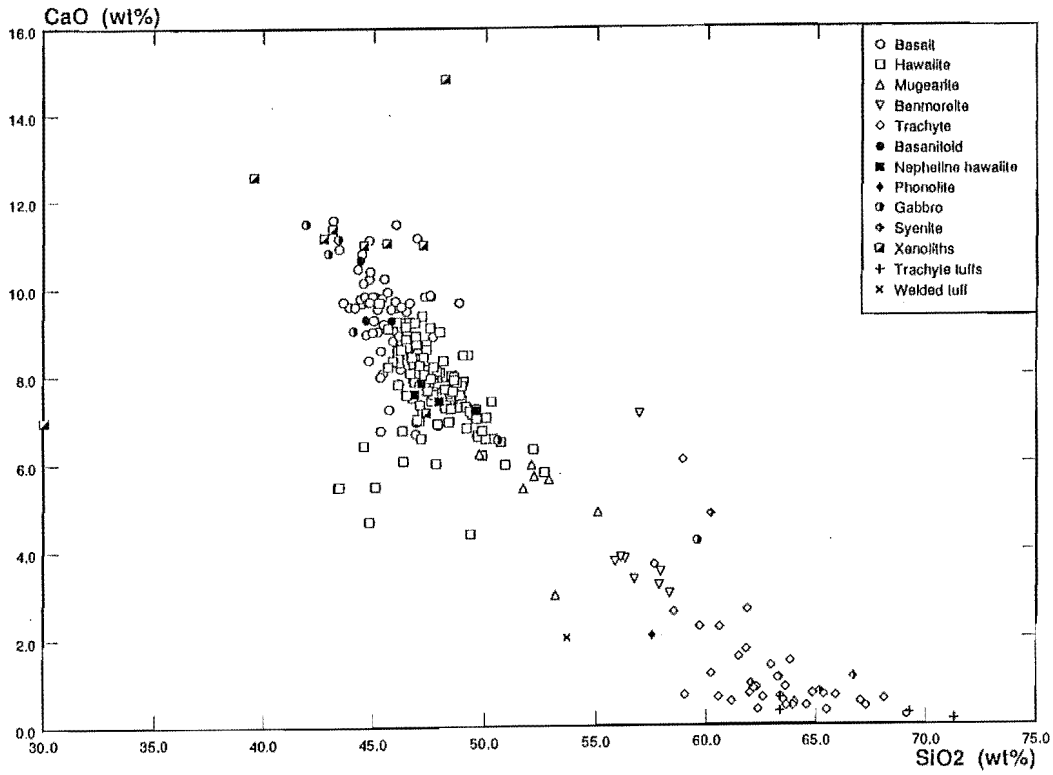

Figure 5.9: CaO (wt%) versus SiO_2 (wt%) for Akaroa Volcanic Group.

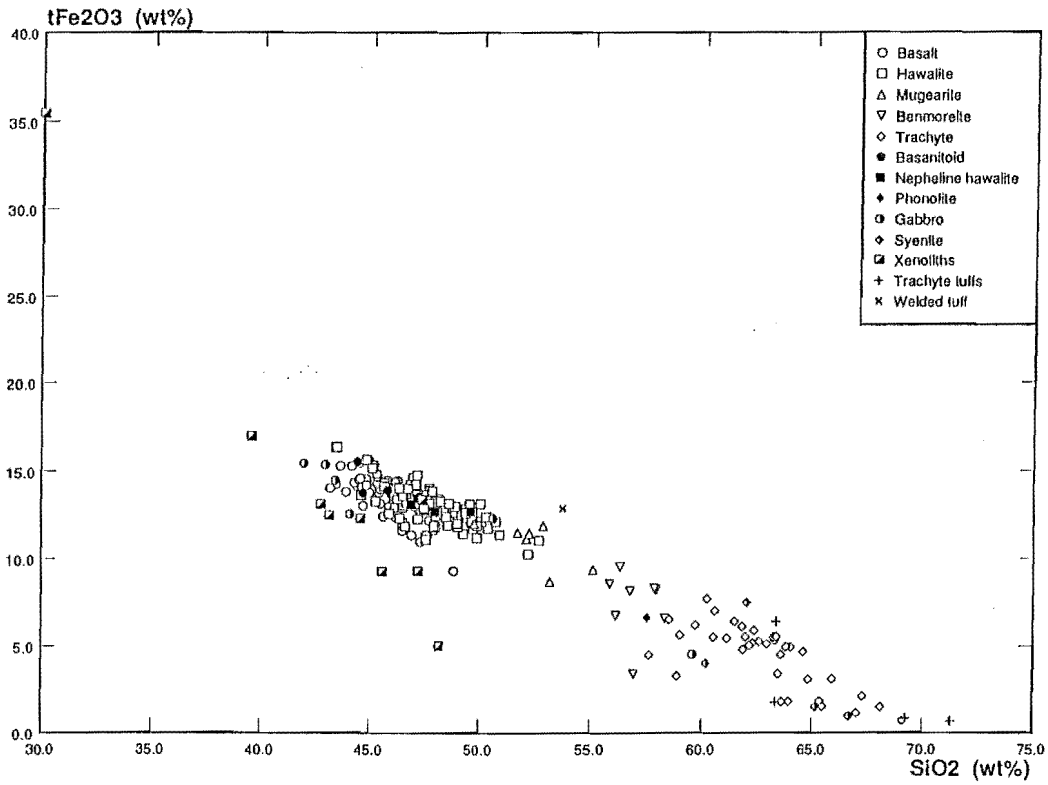

Figure 5.10: tFe_2O_3 (wt%) versus SiO_2 (wt%) for Akaroa Volcanic Group.

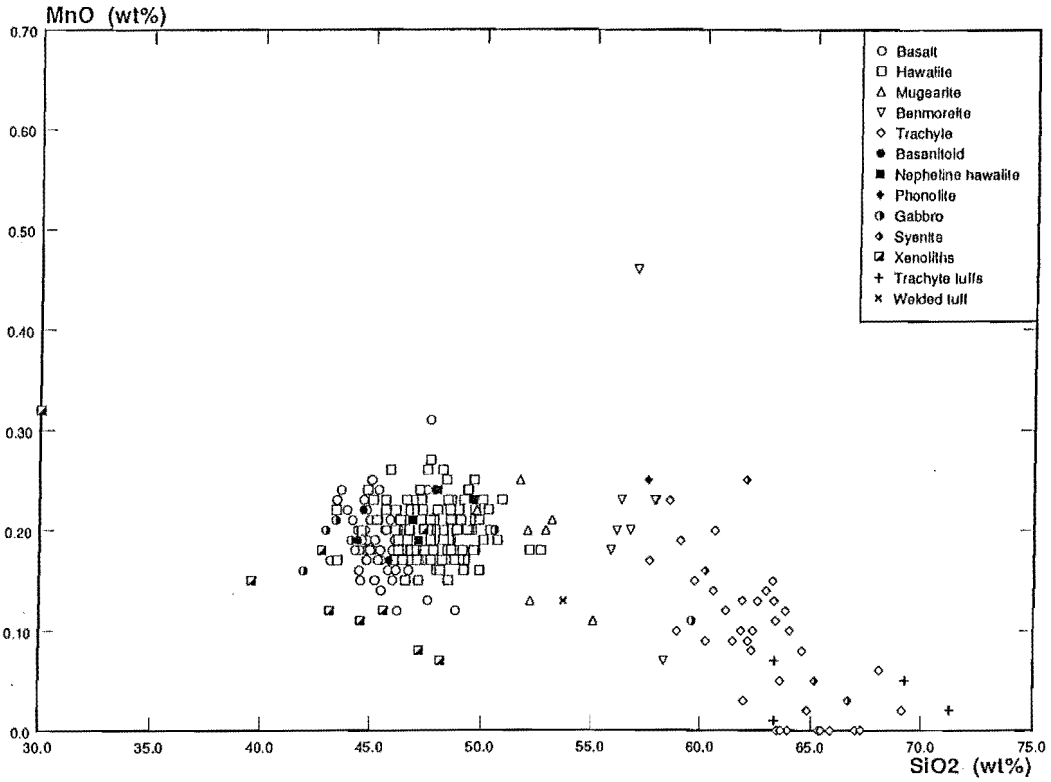

Figure 5.11: MnO (wt%) versus SiO_2 (wt%) for Akaroa Volcanic Group.

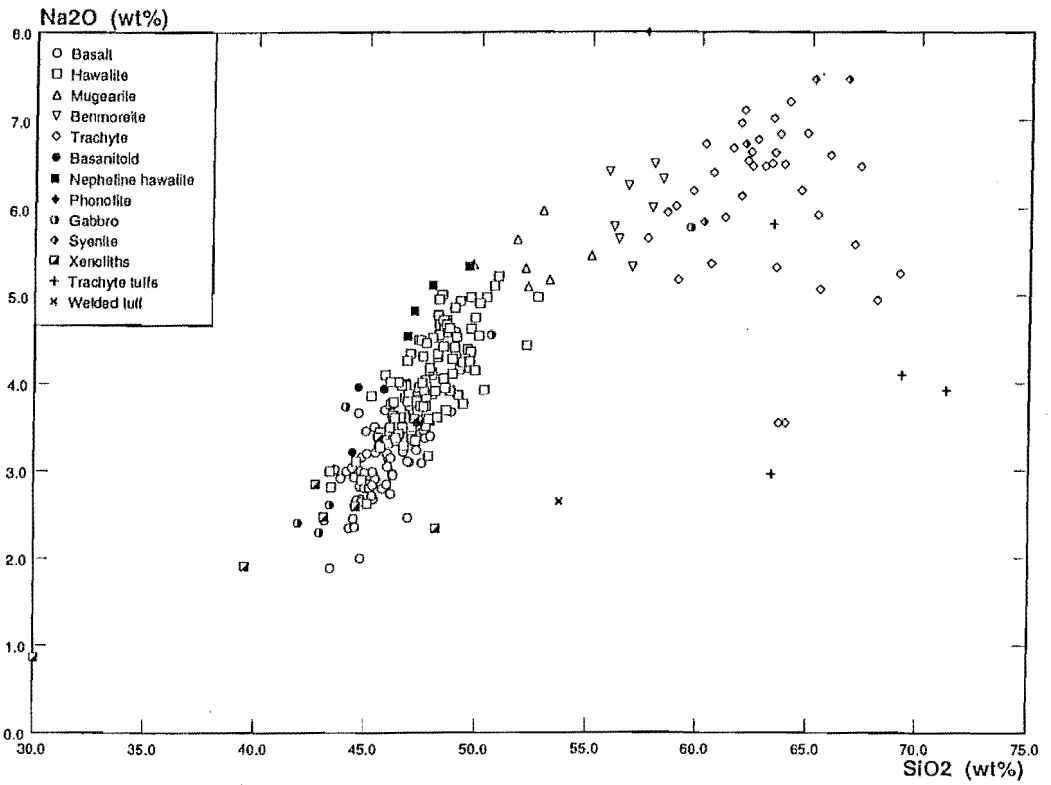

Figure 5.12: Na_2O (wt%) versus SiO_2 (wt%) for Akaroa Volcanic Group.

5.1), Ca–Na–K and *Ab–An–Or* (Fig. 5.6) diagrams.

The dispersed nature of the Na_2O and K_2O trend for more evolved rocks, especially trachytes, may reflect the susceptability of alkalis to gas/fluid transfer during the late stages of crystallisation. The K_2O contents of xenoliths from Lighthouse Reserve are very constant over a wide range of SiO_2 values, and reflect the absence of a K_2O-bearing phase and SiO_2 content controlled by the clinopyroxene:olivine:magnetite ratio.

Al_2O_3: Al_2O_3 (Fig. 5.14) remains relatively constant over a wide range of SiO_2 ($\approx$ 45–72 wt%), as a result of the simultaneous fractionation of Al_2O_3-rich (plagioclase) and Al_2O_3-poor (clinopyroxene, magnetite) phases. However, Al_2O_3 in basalts increases substantially from $\approx$ 13 wt% to 22 wt% over a narrow range of SiO_2 (43–48 wt%), reflecting the importance of olivine (and also clinopyroxene) as phenocryst phases which concentrate Al_2O_3 in the liquid. Xenoliths show a parallel trend of rapidly increasing Al_2O_3 with increasing SiO_2, due to variations in the ratio of cumulus olivine + magnetite + clinopyroxene to cumulus plagioclase.

Lavas of the basanite–phonolite series show a slow but steady increase in Al_2O_3 from 16 wt% to 18 wt%, presumably because plagioclase fractionation is less significant than in the hawaiite–trachyte sequence.

P_2O_5: P_2O_5 (Fig. 5.15) increases rapidly in basalts and hawaiites from $\approx$ 0.4 wt% to $>$ 1.3 wt%. Although apatite is a ubiquitous groundmass phase, it usually accounts for $<$ 6% of the mode and the crystallisation of olivine + clinopyroxene + magnetite + plagioclase phenocrysts will concentrate P_2O_5 in the liquid. The sudden decrease in P_2O_5 from mugearite to trachyte ($<$ 0.2 wt%) coincides with the appearance of red-brown apatite as a phenocryst phase in mugearites and its persistence in benmoreites, some trachytes, and the syenite of Onawe Peninsula.

5.2.3 Multiple Fractionation Lineages in the Akaroa Volcanic Group

The variations in the degree of silica saturation, normative mineralogy and major element geochemistry are interpreted in terms of a spectrum of sub-parallel, sodic alkaline lineages. These lineages range from a dominant, weakly undersaturated alkali olivine basalt–hawaiite–mugearite–benmoreite–trachyte lineage with *ne*-, *hy*- and *qz*-normative variants, to a moderately undersaturated basanite–nepheline hawaiite–nepheline mugearite–nepheline benmoreite–phonolite lineage. Peralkaline differentiates may occur in all lineages. Multiple fractionation lineages have been recognised in other volcanic provinces, such as the Dunedin Volcanic Group (Coombs

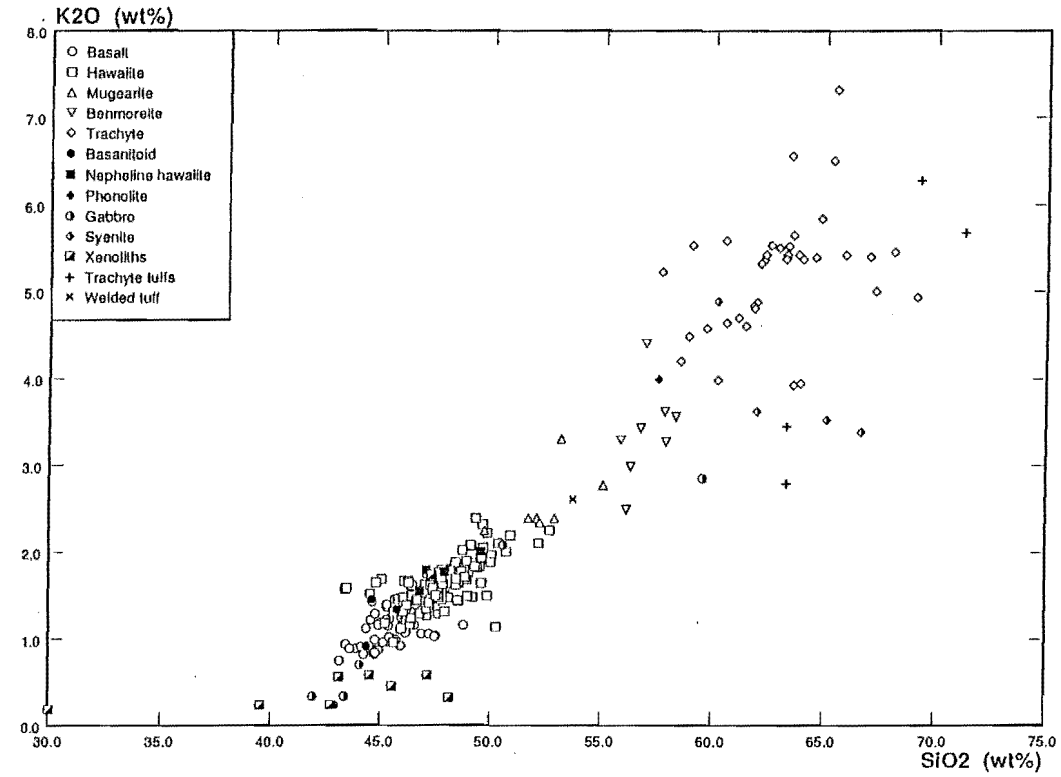

Figure 5.13: K_2O (wt%) versus SiO_2 (wt%) for Akaroa Volcanic Group.

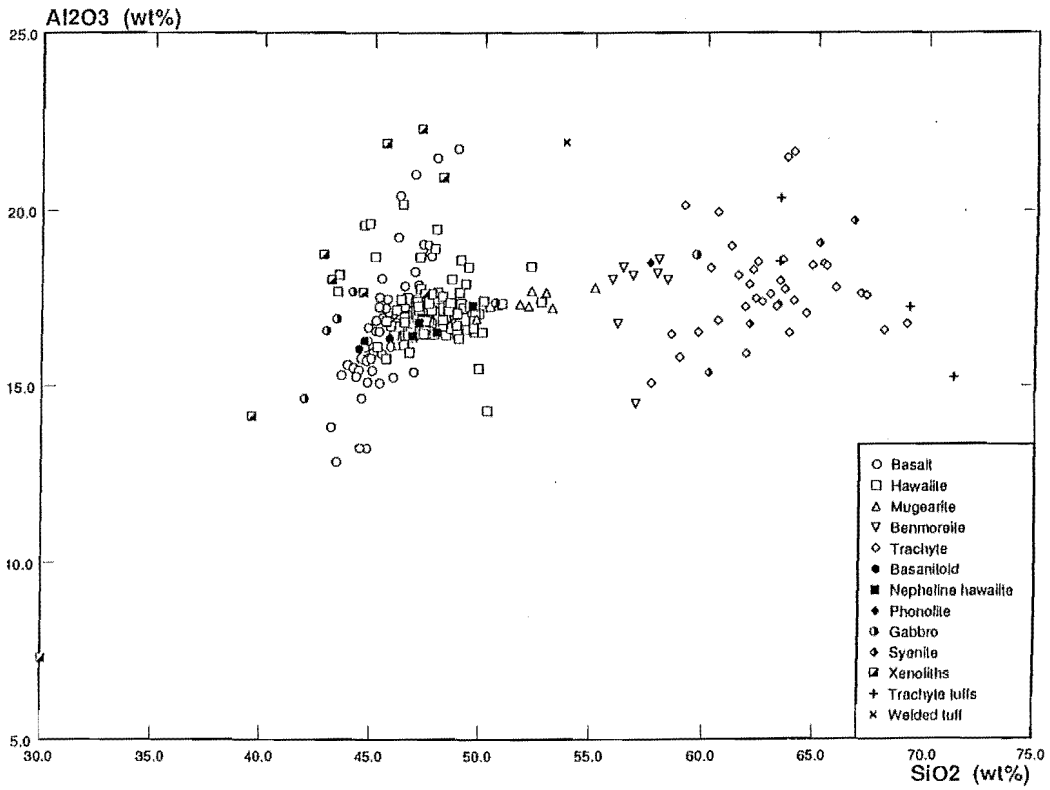

Figure 5.14: Al_2O_3 (wt%) versus SiO_2 (wt%) for Akaroa Volcanic Group.

and Wilkinson, 1969), the Lyttelton Volcanic Group (Weaver and Sewell, 1986) and the Hawaiian volcanic province (MacDonald and Katsura, 1964). Miyashiro (1978) suggested the existence of a "straddle" trend, from weakly *ne*-normative basalts through *hy*-normative to *qz*-normative and peralkaline differentiates. This trend "straddles" the low pressure thermal divide olivine–diopside–plagioclase in the basalt tetrahedron (Yoder and Tilley, 1962), and Miyashiro (1978) suggests this might result from magma generation or differentiation at very high pressures (> 10 kbars), in hydrous and/or oxidising conditions. The range of lavas present in the Akaroa Volcanic Group requires that only some magma batches were generated under such conditions. Even so, not all Akaroa Volcanic Group lava types can be accounted for. The "spectrum of fractionation lineages" model, as proposed by Coombs and Wilkinson (1969) is therefore considered a better model for Akaroa Volcanic Group lavas.

The mineralogy and geochemistry of the alkali olivine basalt–trachyte series is well defined, in particular by studies of the Hawaiian and Hebridean associations (eg. Muir and Tilley, 1961; Yoder and Tilley, 1962; MacDonald and Katsura, 1964; Tilley and Muir, 1962; Tilley *et al*, 1967), and in New Zealand by studies of the Dunedin Volcanic Group (eg. Coombs and Wilkinson, 1969; Price and Taylor, 1973; Price and Chappell, 1975; Coombs *et al*, 1986). The basanite–phonolite lineage was tentatively proposed by Coombs and Wilkinson (1969) to account for the evolution of a number of moderately undersaturated rocks from East Otago. Subsequently, examples of this lineage have been described from other volcanic provinces (eg. Goldich *et al*, 1975; Sun and Hanson, 1975; Irving and Price, 1981; Kyle, 1981; Clague and Frey, 1982; Gamble *et al*, 1986).

5.3 TRACE ELEMENT GEOCHEMISTRY

5.3.1 Variation of Trace Element Abundances with Fractionation

The trace element geochemistry of Akaroa Volcanic Group lavas is presented pictorially in Figures 5.16–5.28. All trace elements have been plotted against zirconium as an index of fractionation. Zr has been chosen as the most useful index of fractionation for Akaroa Volcanic Group lavas for the following reasons:

1. Zr has a wide range of concentrations in non-cumulate rocks, and is abundant in all Akaroa Volcanic Group lavas (50–1218 ppm). Only Ba and Sr exhibit a wider range of concentrations and these elements do not behave incompat-

ibly. Zr concentrations can be determined with high precision by the XRF procedures used in this study (refer Appendix E).

2. Zr appears to behave as an incompatible element ($K_D \leq 0.001$) and Zr-rich phases (eg. zircon) have not been found in any lavas. Consequently, Zr will increase consistently with progressive fractionation, unaffected by any fractionating phase.

3. Zr does not appear to be affected by late-stage "volatile effects" that may affect other trace elements such as La and Ce, (Weaver *et al*, 1972), nor is it sensitive to alteration and low-grade metamorphism (Tarney *et al*, 1977).

In the following discussion, trace elements have been grouped according to their behaviour, and each group is discussed separately.

Cr, Ni and V: Chromium and nickel (Figs. 5.16, 5.17) decrease exponentially with increasing Zr. Cr decreases very rapidly in basalts from > 400 ppm to < 100 ppm over a very limited range of Zr ($\approx$ 150–250 ppm). Over the same Zr range, Ni in basalts decreases from $\approx$ 240 ppm to < 50 ppm. Hawaiites have Cr contents of 20–100 ppm and Ni contents of < 10 ppm to 50 ppm, whereas more evolved lavas (mugearite–trachyte) have very low Cr and Ni contents: < 25 ppm and < 10 ppm, respectively. Lavas of the basanite–phonolite series behave similarly. Xenoliths from Lighthouse Reserve and the gabbro of Onawe Peninsula are distinctive in having noticeably lower Zr contents (50–100 ppm) than the most primitive basalt lavas, and near vertical variation in Cr and Ni (20–510 ppm and 10–270 ppm respectively) over a very restricted 50 ppm range in Zr. Conversely, Cr and Ni in the monzodiorite and monzonite schlieren in the gabbro, and the syenite from Onawe Peninsula follow the trend displayed by fine grained lavas.

Vanadium (Fig. 5.18) shows a linear decrease in basalts and hawaiites, from > 300 ppm to < 20 ppm, while V contents in mugearites–trachytes are uniformly low at < 20 ppm. Lavas of the basanite–phonolite series follow the same trend. Xenoliths from Lighthouse Reserve and the gabbro from Onawe Peninsula have much lower abundances of Zr than the most primitive basaltic lavas, and near-vertical variation in V from $\approx$ 150 ppm to 880 ppm, over a restricted 50 ppm range of Zr. V in schlieren from the gabbro, and the syenite from Onawe Peninsula follows the trend displayed by fine grained lavas.

For fine grained lavas, Cr and Ni have a similar behaviour to MgO (Fig. 5.7), and V behaves like TiO_2 (Fig. 5.8). Cr and Ni abundances are controlled by olivine fractionation, and near-vertical variations of these elements in basalt lavas indicates the bulk mineral-liquid distribution coefficients of Cr and Ni between olivine and basalt magmas were very large ($K_D \gg 1$). V abundances are probably being controlled by the fractionation of magnetite, and possibly olivine and clinopyroxene.

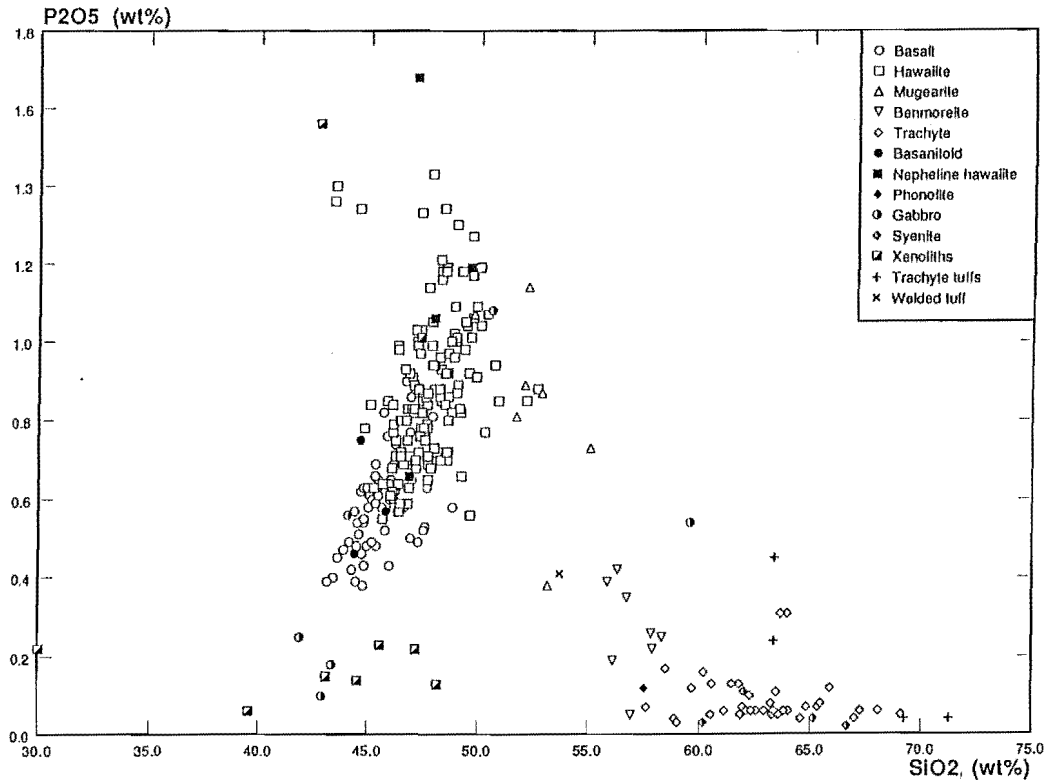

Figure 5.15: P_2O_5 (wt%) versus SiO_2 (wt%) for Akaroa Volcanic Group.

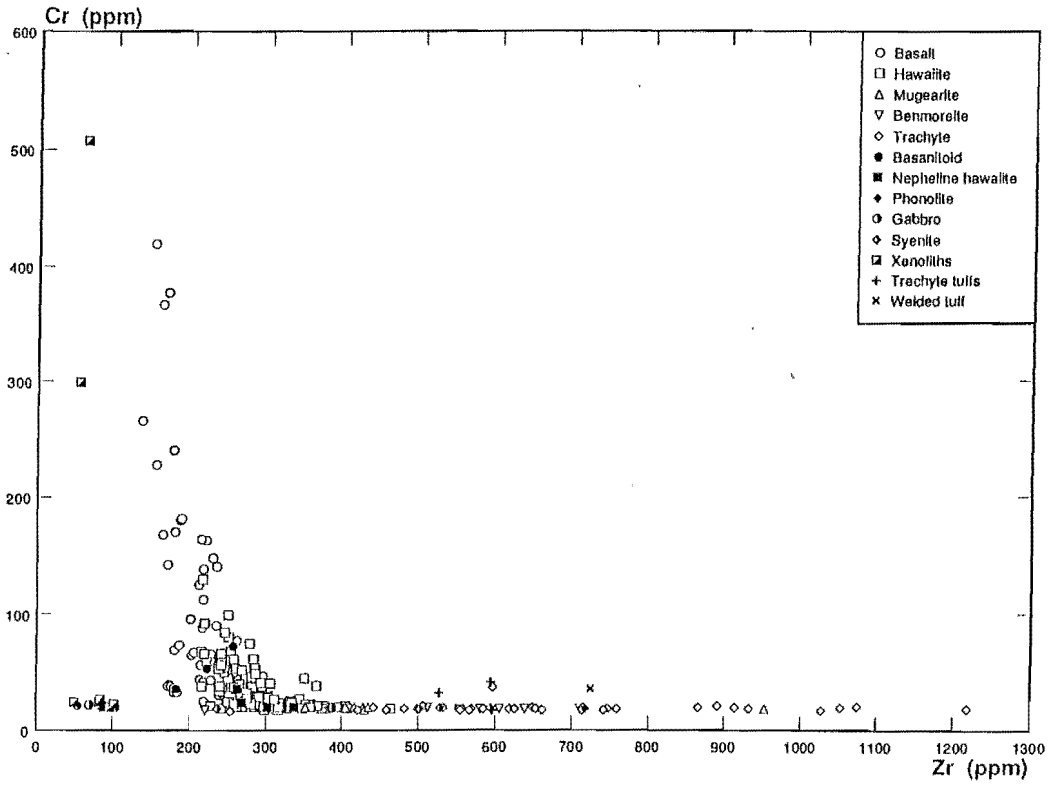

Figure 5.16: Cr (ppm) versus Zr (ppm) for Akaroa Volcanic Group.

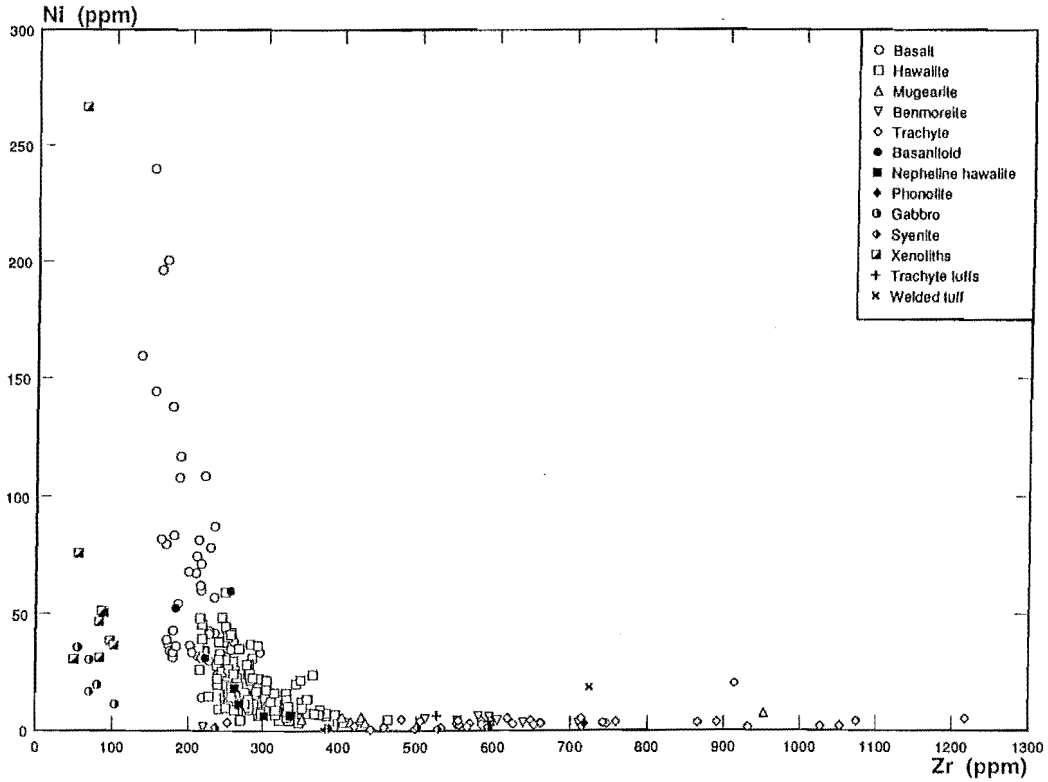

Figure 5.17: Ni (ppm) versus Zr (ppm) for Akaroa Volcanic Group.

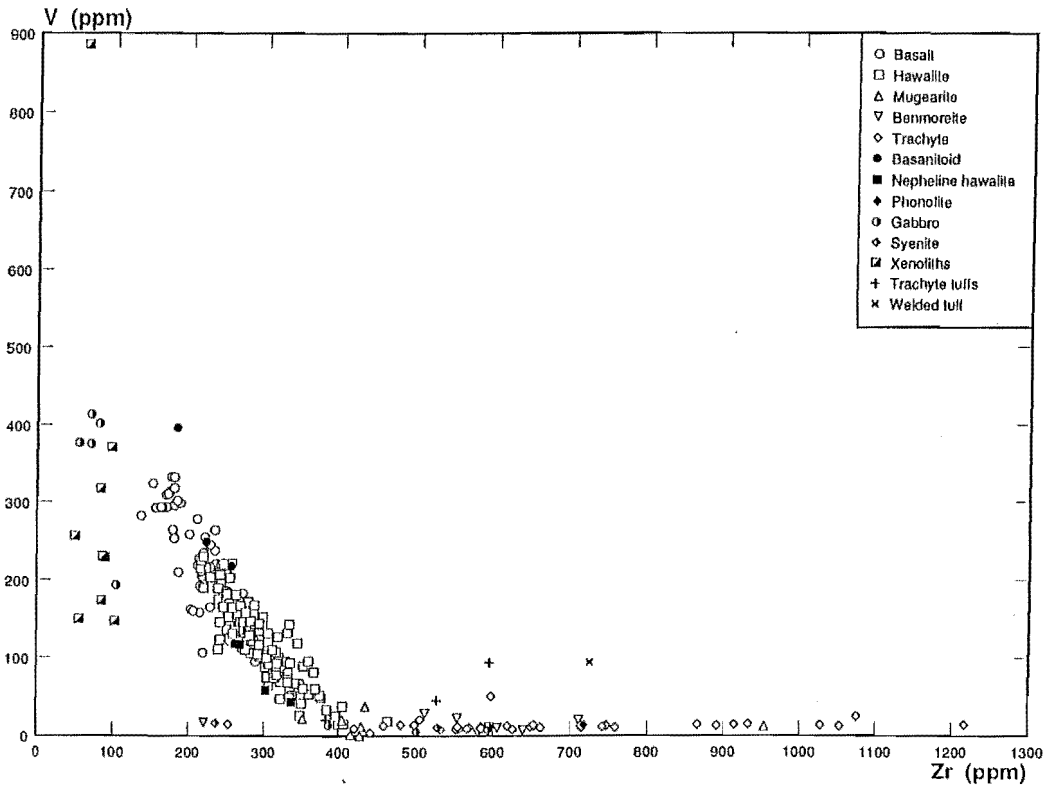

Figure 5.18: V (ppm) versus Zr (ppm) for Akaroa Volcanic Group.

Low Zr abundances in xenoliths and the gabbro reflect the cumulate nature of the rocks — Zr will concentrate preferentially in the cumulus liquid, and consequently cumulates will have lower Zr abundances than the primary basalt magma. Variations in Cr, Ni and V abundances are a consequence of variations in the ratio of modal olivine:clinopyroxene:magnetite:plagioclase.

Y, Nb, Rb, La, Ce, Nd: Yttrium, niobium, rubidium, lanthanum, cerium and neodymium abundances increase with increasing Zr abundance (Figs. 5.19–5.24).

Trends are initially linear with an increasing concave-downwards component from Nb through La, Ce and Nd to Y, at higher levels of Zr abundance. The Rb trend has a weak concave-upwards component at higher levels of Zr. On any of the graphs (Figs. 5.19–5.24), all rock types appear to belong to the same trend or liquid line-of-descent. In particular, xenoliths and the gabbro and syenite of Onawe Peninsula project on the same trend as lavas of the basalt–trachyte and basanite–phonolite lineages. In comparison, xenoliths and the gabbro from Onawe Peninsula clearly project off the main trend on plots of Cr, Ni, V, Sr and Zn.

For basalts, hawaiites, basanitoids and nepheline hawaiites (and generally speaking, xenoliths and the gabbro from Onawe Peninsula), there is a very high correlation between the trace element concerned (Y, Nb, Rb, La, Ce, Nd) and Zr, as shown by the tight clustering of points about the trend line. In comparison, mugearites–trachytes, the syenite from Onawe Peninsula and the phonolite show a rapid decrease in the degree of correlation; trachytes, in particular, show considerable scatter. The high correlation for basic lavas indicates that Y, Nb, Rb, La, Ce and Nd behaved incompatibly in the magma(s) from which these lavas were derived. The scatter in projections for more evolved rocks may reflect some combination of one or more of:

- Large variations in the bulk mineral-liquid distribution coefficient, related to changes in magma composition, temperature, or crystallising phases
- "Volatile effects" in which incompatibles are transferred to/from the crystallising lava by liquid or volatile phases. Hydrated peralkaline glasses, for example, are known to loose alkalis and alkaline earth elements (Noble, 1968)
- Variable contamination by crustal material during ascent and/or prolonged low-P fractionation in a high level, crustal magma reservoir.

For all of the graphs (Figs. 5.19–5.24) the trend of the trace elements against Zr may be extrapolated back through, or close to, the origin. In terms of how close the extrapolated trends approach the origin, the trace elements have the order Nb

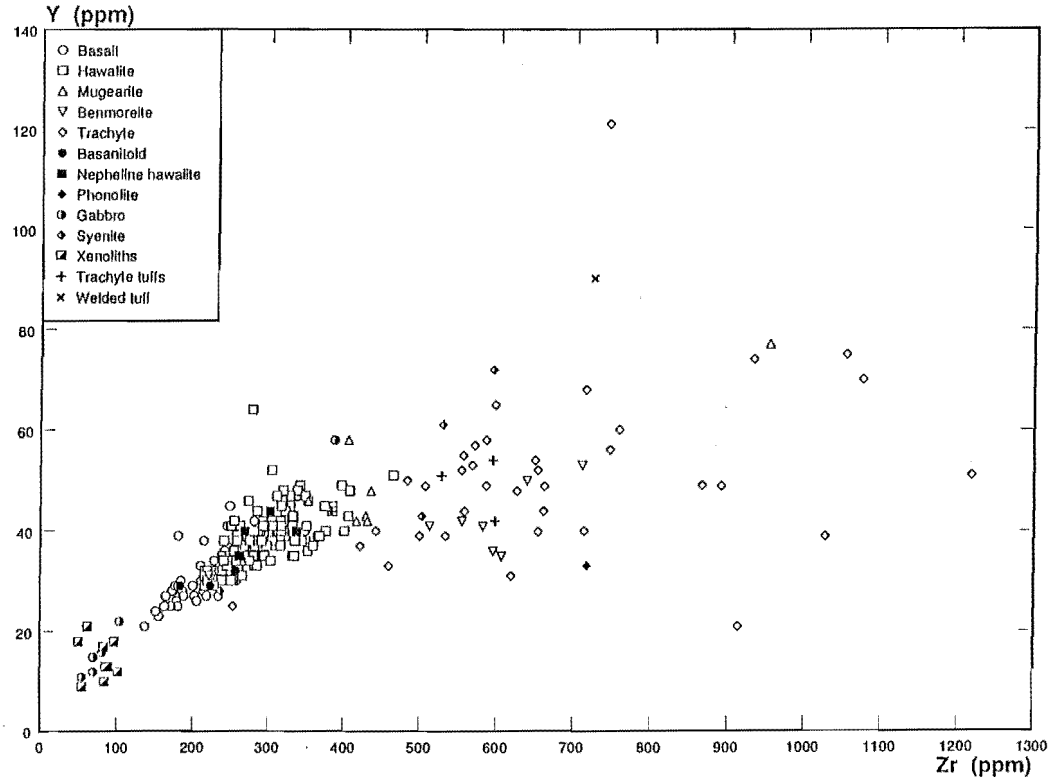

Figure 5.19: Y (ppm) versus Zr (ppm) for Akaroa Volcanic Group.

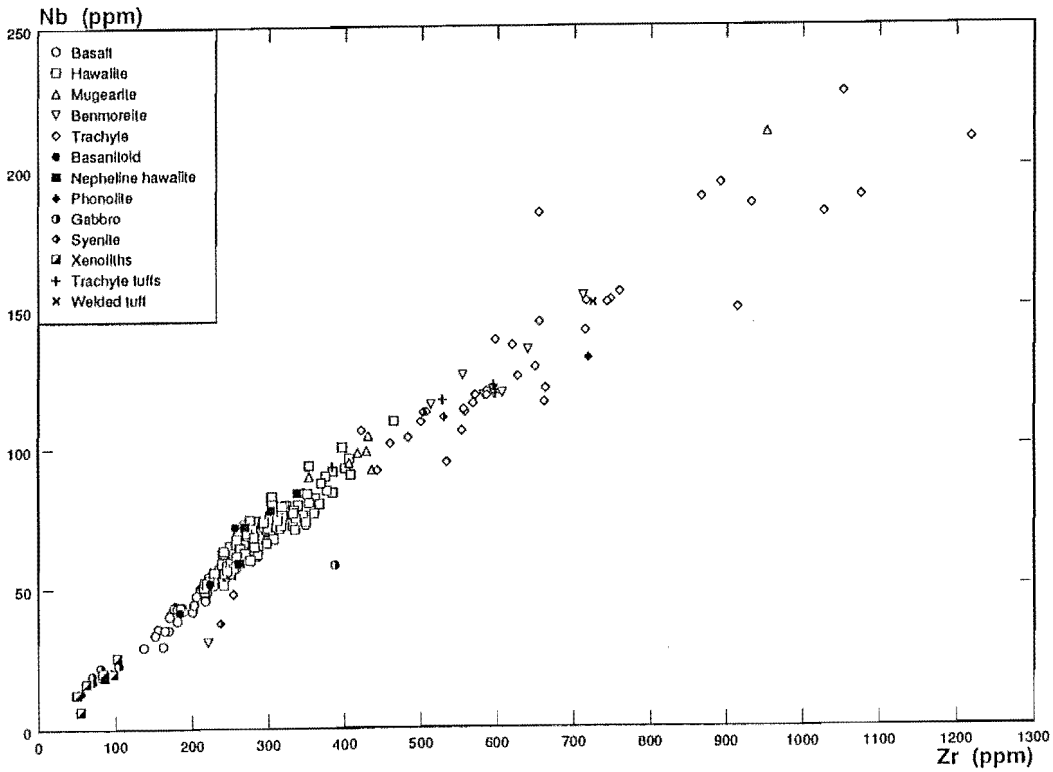

Figure 5.20: Nb (ppm) versus Zr (ppm) for Akaroa Volcanic Group.

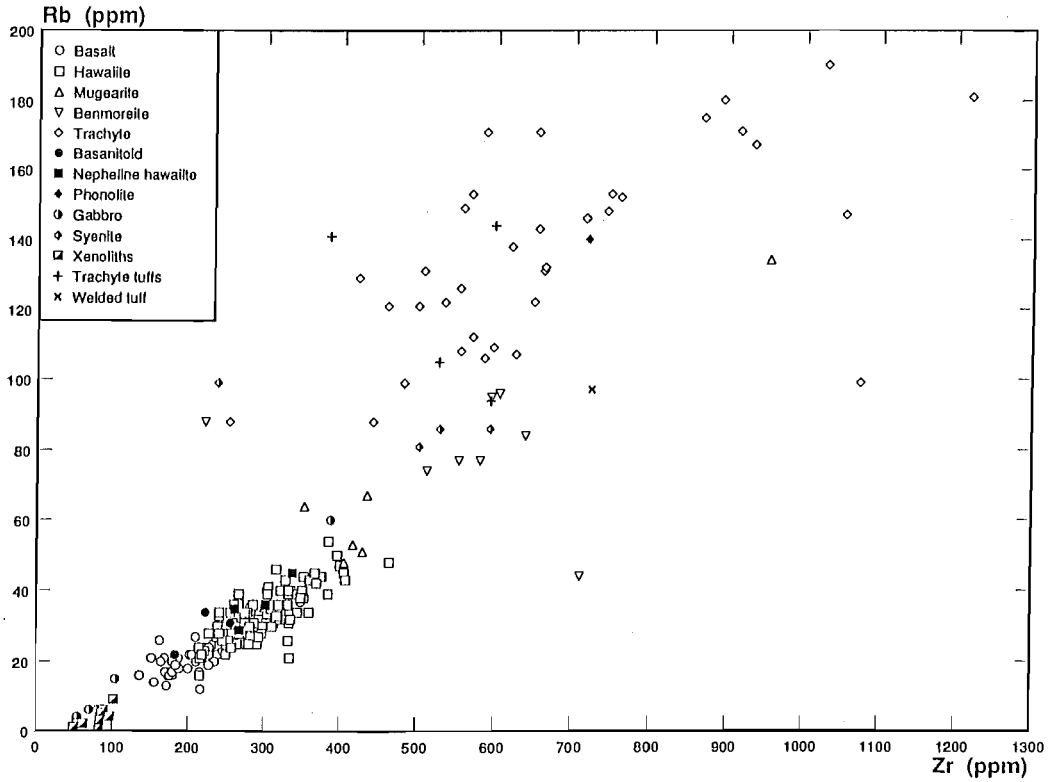

Figure 5.21: Rb (ppm) versus Zr (ppm) for Akaroa Volcanic Group.

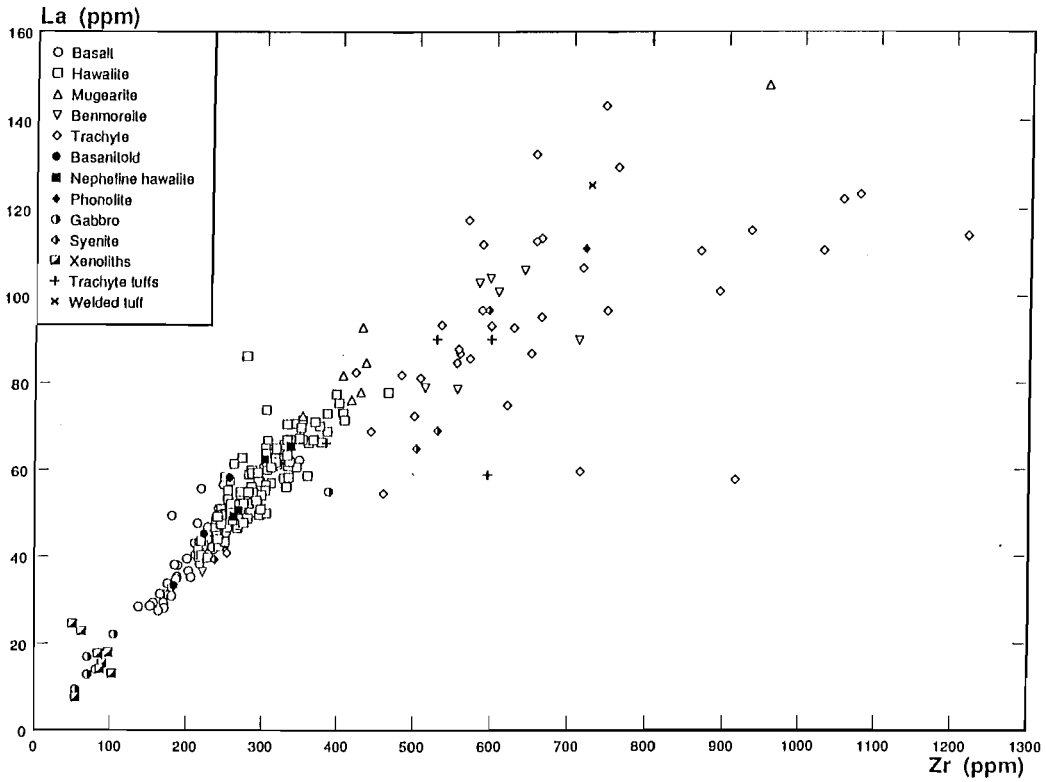

Figure 5.22: La (ppm) versus Zr (ppm) for Akaroa Volcanic Group.

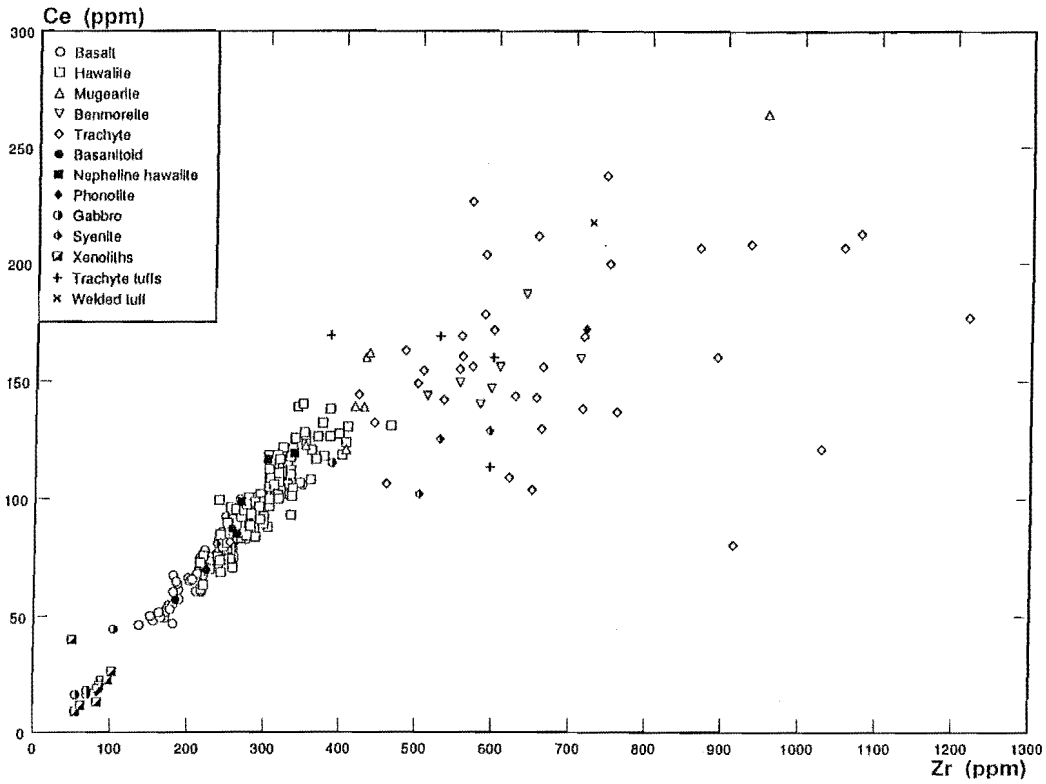

Figure 5.23: Ce (ppm) versus Zr (ppm) for Akaroa Volcanic Group.

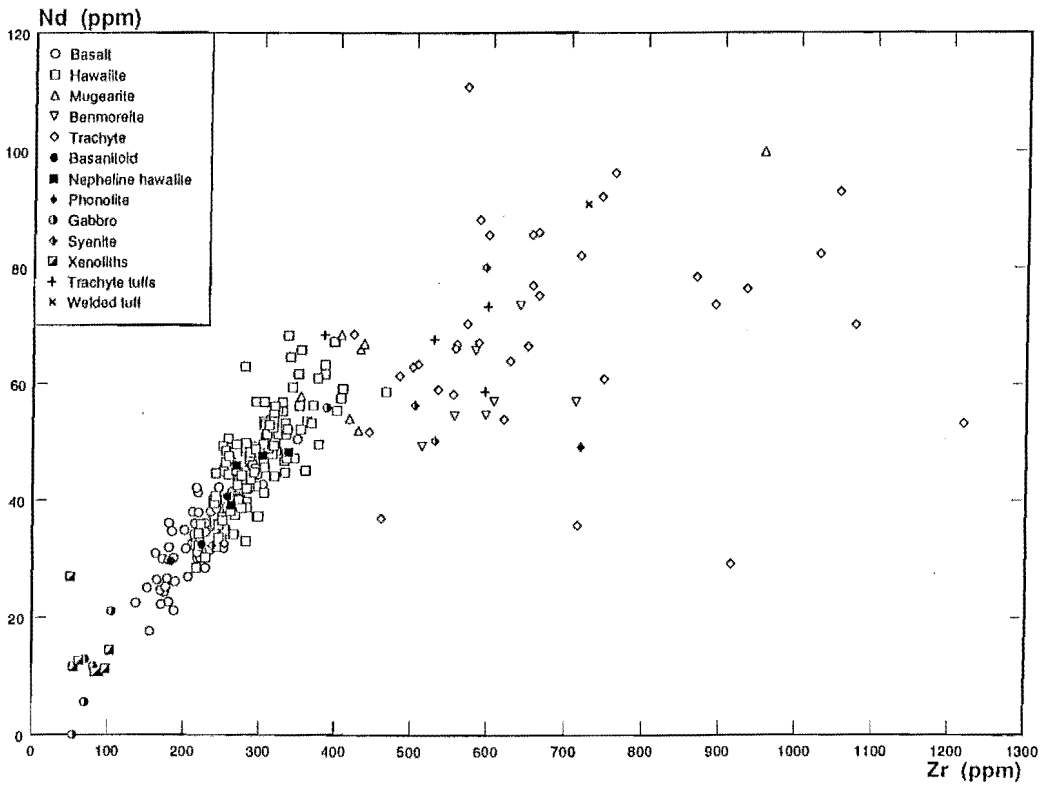

Figure 5.24: Nd (ppm) versus Zr (ppm) for Akaroa Volcanic Group.

> La > Nd > Ce > Y > Rb, where ">" means "intersects an axis closer to the origin than".

In any solid/liquid system, the relative abundance of a pair of elements (such as Nb and Zr or Ce and Zr) will be constant if the bulk distribution coefficients between the crystalline phases and the liquid for the two elements remain equal (Schilling and Winchester, 1967; Gast, 1968). Any such pair of elements, when plotted one against another, will produce a linear trend through the origin; with the slope of the line equal to the ratio of the two elements. For all the elements under consideration (with the possible exception of Rb), bulk distribution coefficients remain constant, at least over the range basalt–hawaiite, suggesting that the bulk distribution coefficients are close to zero for basic lavas (Weaver *et al*, 1972). Weak concave components in the trends, over the mugearite–trachyte compositional range, result from changes in the ratio of Nb, Y, Rb, La, Ce, or Nd to Zr, and reflect changes in bulk distribution coefficients.

On plots of Y, Rb, La and Nd (Figs. 5.19, 5.21, 5.22, 5.24), the syenite from Onawe Peninsula exhibits significant variations in abundances over a limited range of Zr. For example, for the syenite, over the range 502–594 ppm Zr (an 18% increase):

- Y ranges from 43 ppm to 72 ppm (a 67% variation)
- La ranges from 64.9 ppm to 96.8 ppm (a 49% variation)
- Nd ranges from 50.3 ppm to 80.1 ppm (a 59% variation)

Variations in the gabbro from Onawe Peninsula are similar though less spectacular. Variations in rare earth element abundances within the syenite and gabbro can also be observed (refer to section 5.4).

The trends for Nb, Y, Rb, La, Ce and Nd plotted against Zr indicate that these elements, in general, behave in an incompatible or near-incompatible fashion, and are not affected by any fractionating phase.

Sr and Ba: Strontium (Fig. 5.25) behaves as an incompatible element in basaltic and basanitoid magmas, increasing from 467 ppm to 1120 ppm over a 57 ppm range in Zr reflecting olivine and clinopyroxene rather than plagioclase as the dominant fractionating phase. However, in more evolved rocks Sr behaves compatibly, and is affected by plagioclase fractionation. Sr in hawaiites shows little consistent variation, remaining nearly constant at $\approx$ 800 ppm. However in Zr-rich hawaiites, mugearites–trachytes, phonolites and the syenite of Onawe Peninsula, Sr decreases from $\approx$ 800 ppm to $<$ 100 ppm, reflecting the removal of Sr from the magma by plagioclase fractionation. In particular, the decrease in strontium from $\approx$ 800 ppm

to > 400 ppm in Zr-rich hawaiites is correlated with the presence of extremely plagioclase-phyric hawaiites (up to 50% plagioclase phenocrysts) in the upper parts of the Saddle Hill and Lighthouse Road sections (see chapter 2).

The range of Sr abundances shown by xenoliths from Lighthouse Reserve (219–1332 ppm) and the gabbro from Onawe Peninsula (442–636 ppm) is attributed to variations in the proportion of (Sr-bearing) cumulus plagioclase between samples.

In all rock types except trachytes, barium behaves incompatibly (Fig. 5.26) increasing from 0 ppm in some xenoliths from Lighthouse Reserve to ≈ 1000 ppm in benmoreites over a range of 700 ppm Zr.

Low-Zr trachytes show extreme enrichment in Ba (up to 2061 ppm), and this is thought to be the result of either prolonged plagioclase fractionation concentrating Ba in the magma, or contamination by crustal material or fluid/volatile phases. Depletion of Ba in Zr-rich trachytes is attributed to fractionation of Alkali feldspar. Ba is known to substitute for K (and sometimes Ca and Na) in alkali feldspar (Deer *et al*, 1966).

Zn, Ga, Pb, Th: Gallium, lead and thorium all increase linearly with increasing Zr, over the entire range of rock types (Figs. 5.27, 5.28), indicating that these elements are not fractionated by any crystallising phase. Zinc shows considerable variation in xenoliths from Lighthouse Reserve, and is probably substituting for Fe^{2+} in magnetite (Deer *et al*, 1966), the modal proportion of which varies significantly between xenoliths.

5.3.2 Tectonic Environment

Tectonically, Akaroa Volcanic Group lavas are "within-plate" basalts (ocean island or continental basalts) according to their projection onto the Ti/100–Zr–Y*3 tectonic discrimination diagram (Fig. 5.29) of Pearce and Cann (1973).

5.3.3 Trace Element Ratios

Variations in trace element ratios can provide important information when evaluating multiple models for the origin and evolution of magmas. Of particular interest, in the case of the Akaroa Volcanic Group, is the relationship between the most primitive basalts and a primary melt derived from mantle material, and the influence of crustal contamination on the formation of trachytic magmas. Plots of Zr/Y and Zr/Nb versus Zr are presented in Figures 5.30 and 5.31.

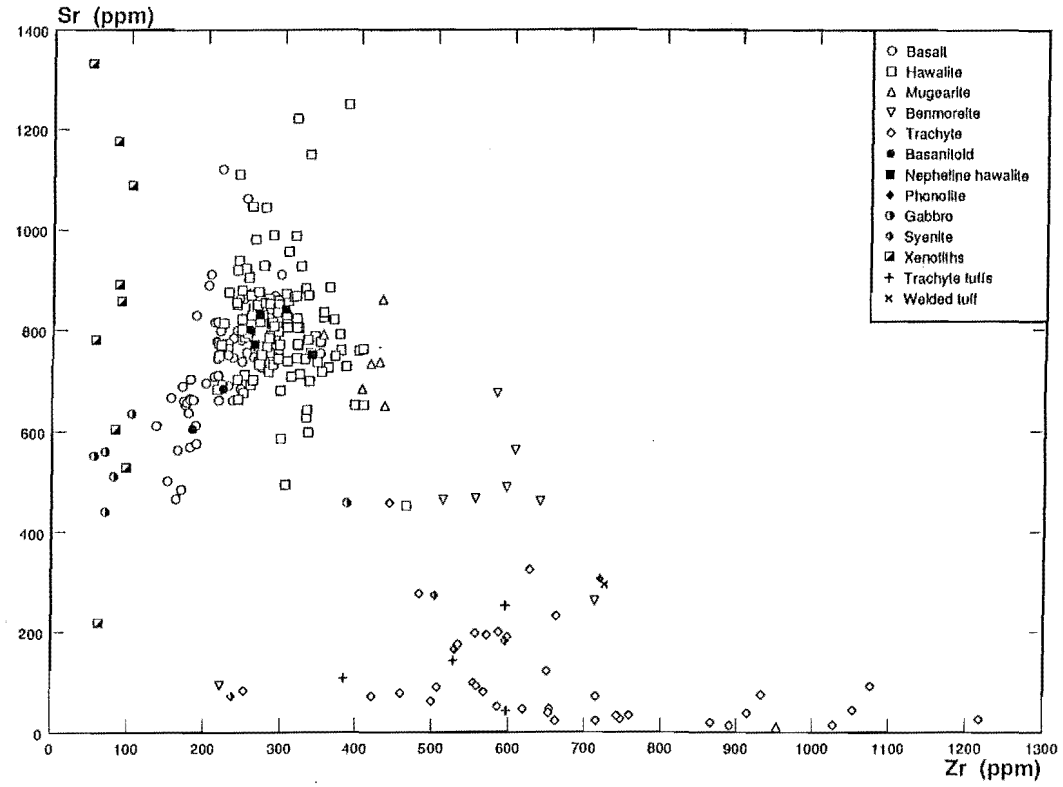

Figure 5.25: Sr (ppm) versus Zr (ppm) for Akaroa Volcanic Group.

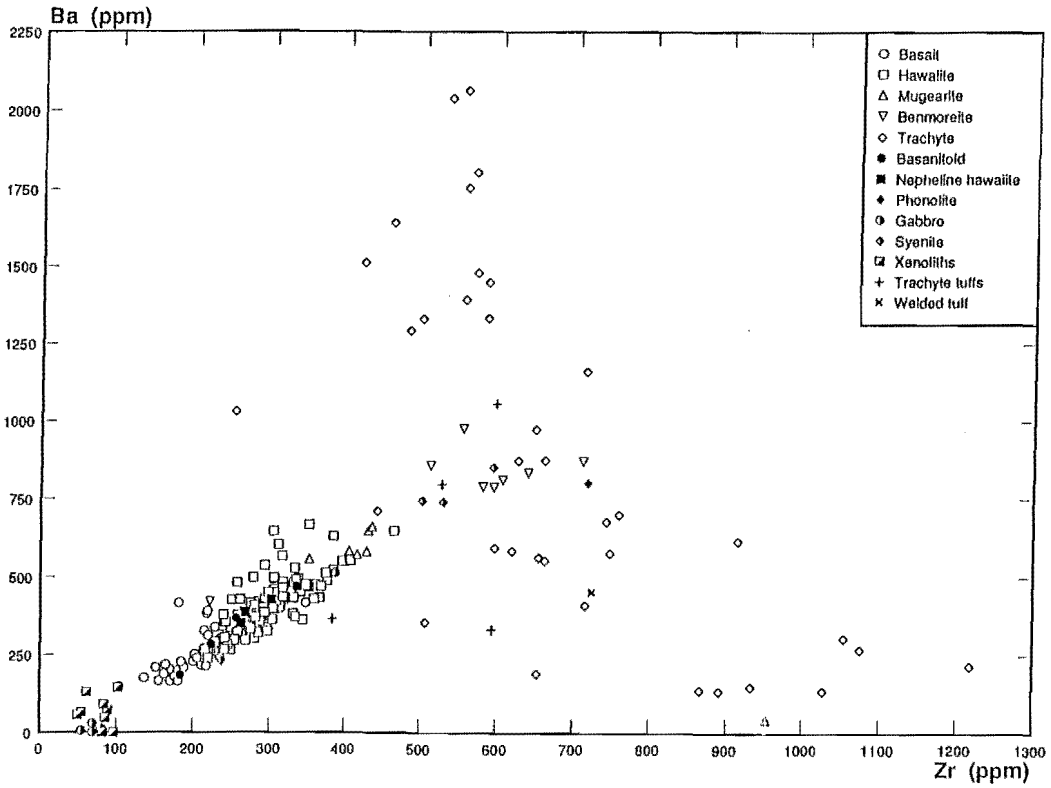

Figure 5.26: Ba (ppm) versus Zr (ppm) for Akaroa Volcanic Group.

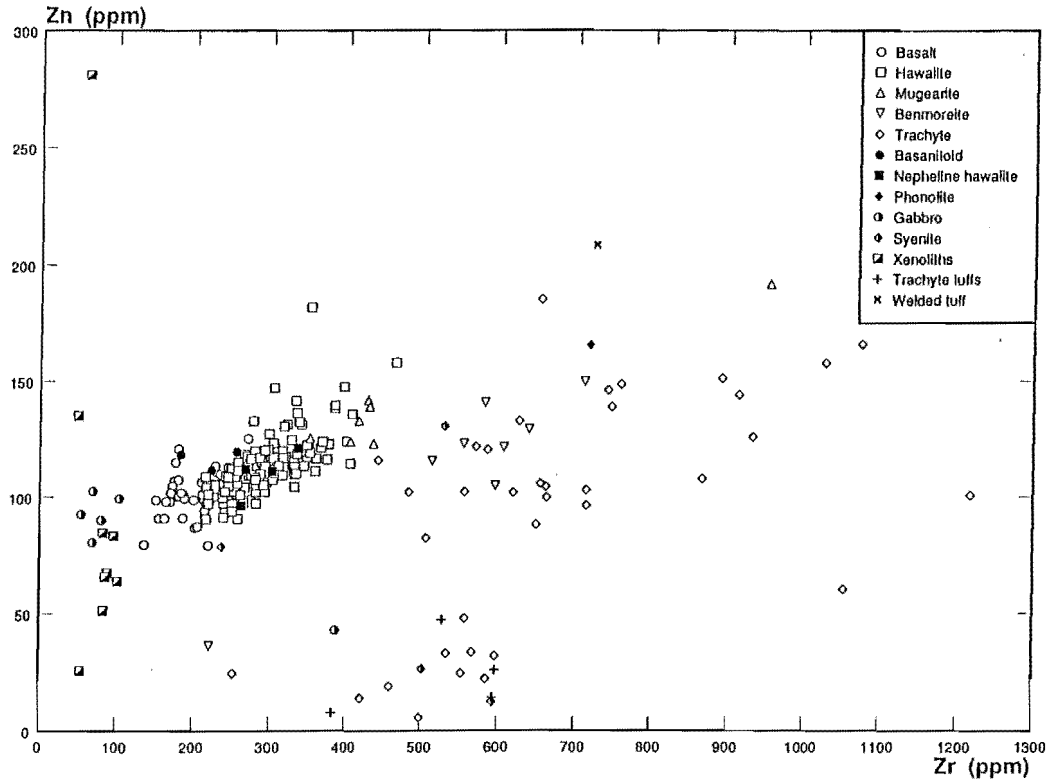

Figure 5.27: Zn (ppm) versus Zr (ppm) for Akaroa Volcanic Group.

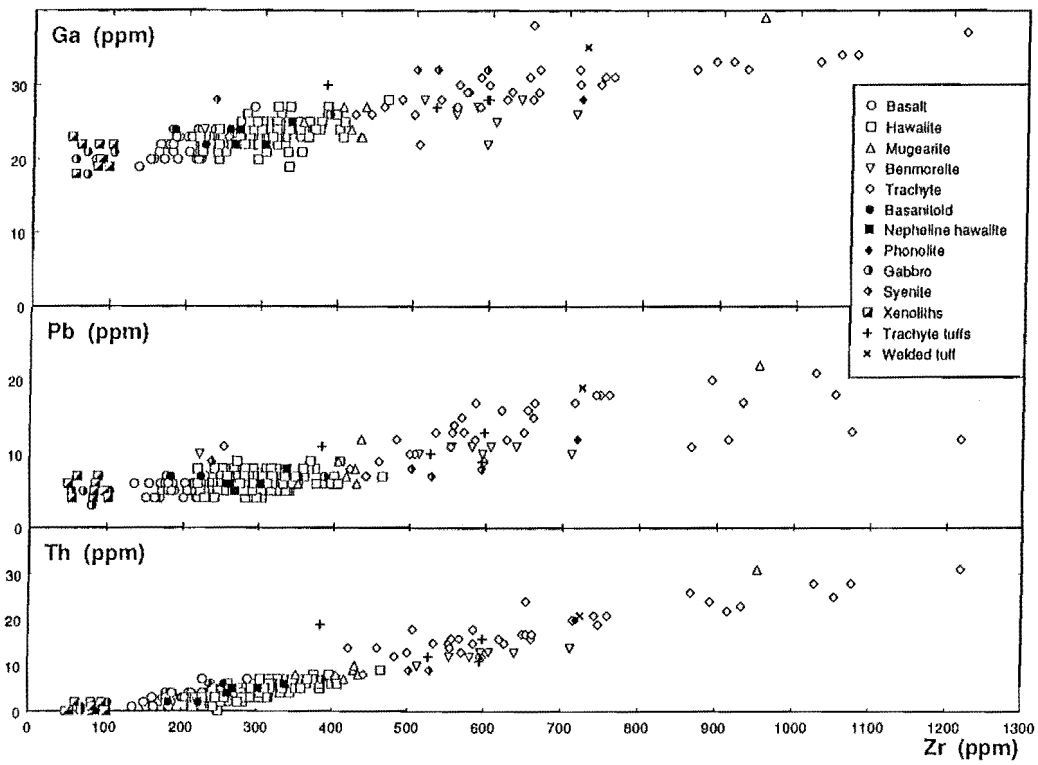

Figure 5.28: Ga, Pb and Th (ppm) versus Zr (ppm) for Akaroa Volcanic Group.

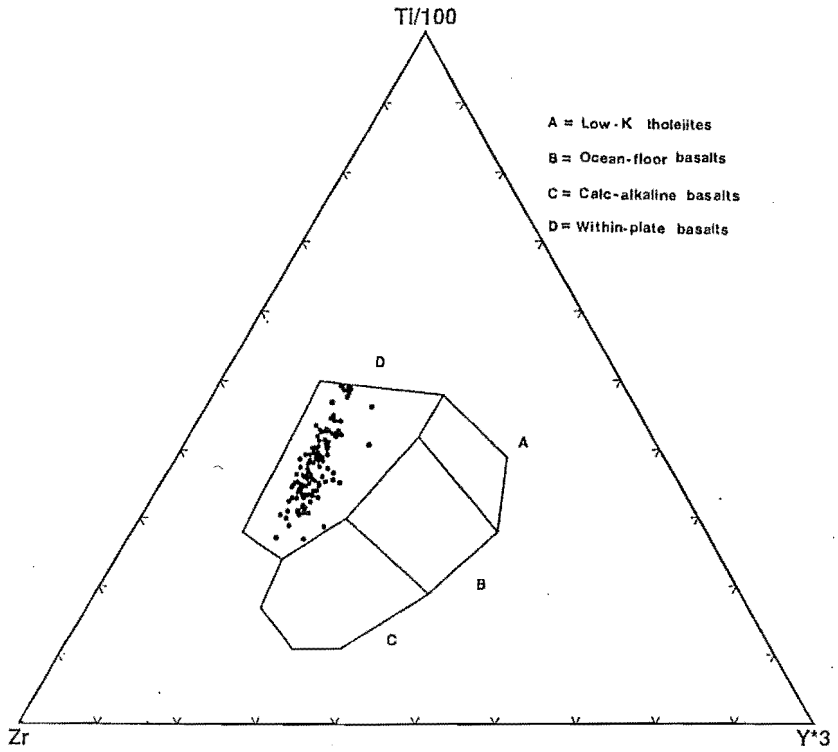

Figure 5.29: Pearce and Cann (1973) tectonic discrimination diagram for Akaroa Volcanic Group.

Basic Akaroa Volcanic Group lavas (basalts, hawaiites, basanitoids, nepheline hawaiites) project into the "within-plate basalts" field (Pearce and Norry, 1979) on a plot of Zr/Y versus Zr plot (Fig. 5.30). The component of variation in Zr/Y ratios parallel to vector **a** may result from:

1. Source heterogeneities
2. Variations in the degree of partial melting of a garnet lherzolite source
3. Progressive melting of a single source
4. Fractional crystallisation in which garnet is an important phase

Garnet has not been observed in any Akaroa Volcanic Group lavas. Undersaturated lavas are generally thought to result from lower degrees of partial melting (< 3 %, depending on degree of enrichment of the source), and under these conditions, lavas of the basanite–phonolite lineage would be expected to have Zr/Y ratios consistently different from lavas of the basalt–trachyte lineage. However, lavas of the basanite–phonolite association are well dispersed throughout the field of Akaroa Volcanic Group lavas. Variations in Zr/Y are therefore most likely to be the result of source heterogeneity, in particular, the amount of garnet in the source.

Vector **b** represents increasing Zr at constant Zr/Y, and since this is accompanied by a rapid decrease in Cr, variations with components parallel to vector **b** result from fractional crystallisation.

Basic Akaroa Volcanic Group lavas have Zr/Nb ratios (Fig. 5.31) of ≈ 4.0, typical of alkaline rocks. There is a subtle but persistent decrease in Zr/Nb ratios with increasing differentiation, attributed to slight variations in the bulk mineral-liquid distribution coefficient of Nb. The Zr/Nb ratio is insensitive to variations in the degree of partial melting (compared with Zr/Y) and variations in the Zr/Nb ratios of Akaroa Volcanic Group lavas at constant Zr are attributed to minor source heterogeneity. In comparison, intraplate Eocene–Oligocene volcanics from the Chatham Islands have Zr/Nb ratios of 3–11.5, and significant enrichment of the source region is postulated (Morris, 1985).

Nb/Th ratios may be useful in assessing whether crustal contamination has had any influence on the evolution of Akaroa Volcanic Group lavas. Nb is derived from mantle sources, whereas Th is concentrated in the crust. A significant decrease in the Nb/Th ratio may therefore reflect crustal contamination of evolving magmas. A plot of Nb versus Th for Akaroa Volcanic Group lavas is presented in Figure 5.32, and basic statistics for the Nb/Th ratio in non-cumulate rocks are presented in Table 5.4.

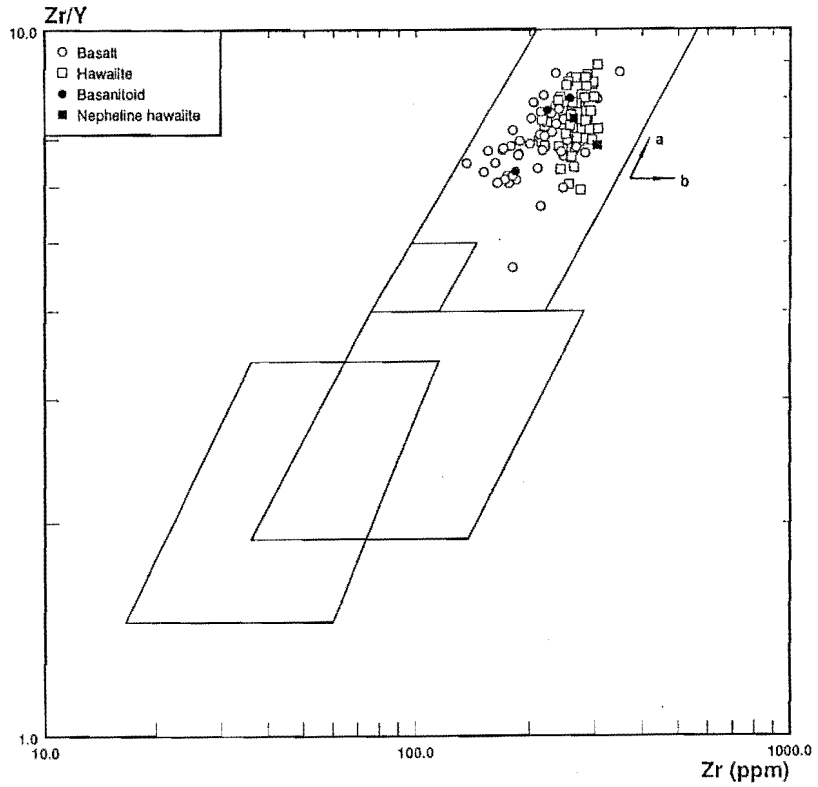

Figure 5.30: Zr/Y versus Zr (ppm) for Akaroa Volcanic Group.

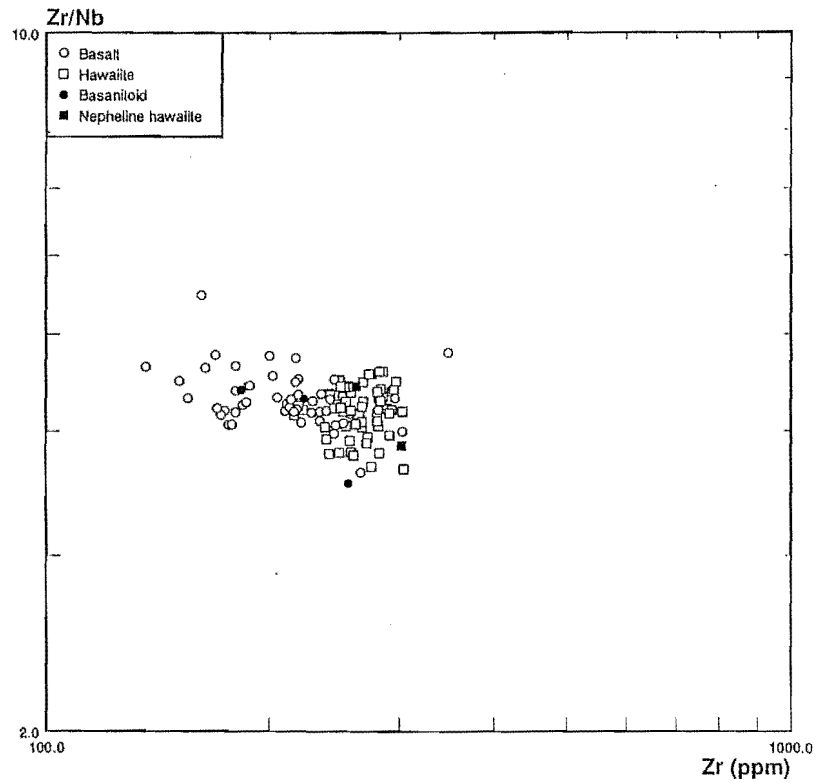

Figure 5.31: Zr/Nb versus Zr (ppm) for Akaroa Volcanic Group.

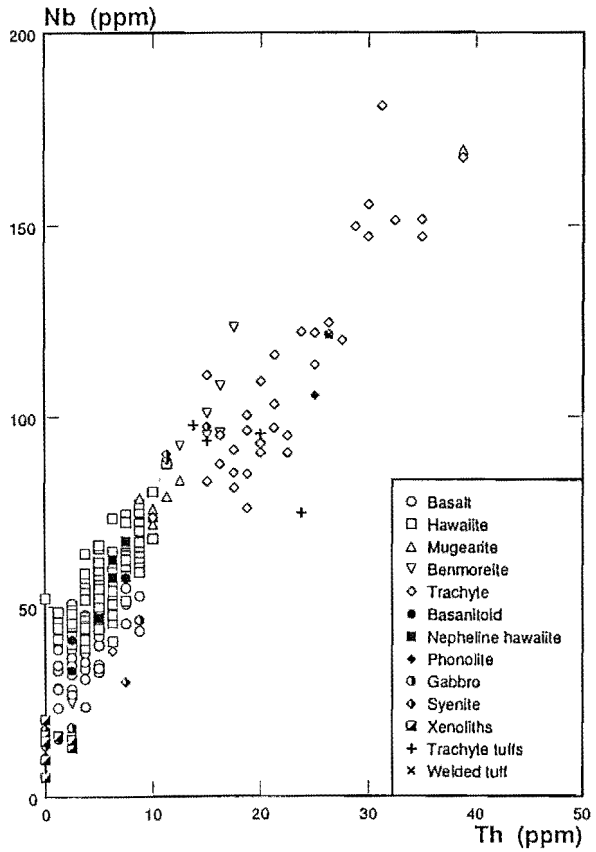

Figure 5.32: Nb (ppm) versus Th (ppm) for Akaroa Volcanic Group.

Table 5.4: Nb/Th ratios in different non-cumulate rock types of the Akaroa Volcanic Group.

Rock type	n	$\bar{x}$	s
basalt	60	19.13	9.23
hawaiite	139	17.18	8.07
mugearite	7	10.96	2.16
benmoreite	9	10.60	2.05
trachyte	43	8.08	1.66

Mean Nb/Th ratios suggest that there is a significant decrease in Nb/Th ratios from basalt/hawaiite to mugearite/benmoreite and again from mugearite/benmoreite to trachyte, indicating increasing influence of crustal contamination in formation of evolved rocks. However, the calculated ratios of each rock type mask variations within a rock type.

Figure 5.32 is interpreted in the light of two trends:

1. A basalt–trachyte trend with high Nb/Th ratios, that has resulted essentially from fractional crystallisation with no crustal contamination.
2. A sub-parallel trend of trachytes and minor mugearites/benmoreites with lower Nb/Th ratios, which represent evolved magmas that have suffered some crustal contamination.

5.4 Rare Earth Element Geochemistry

Rare earth element (REE) analyses presented in appendix I were determined for 12 samples from Akaroa Volcanic Group, (see appendix E for a description of the analytical method); 6 samples are from this study, and six samples are from Falloon (1982). Major element analyses, CIPW norms and trace element analyses for the six samples from Falloon (1982) are presented in Table 5.5. The major and trace element analyses were determined in the same laboratory and following the same methods as analyses presented in this thesis. Furthermore, there is no observable difference between the chemistry of these samples and samples from the same area collected during this study. Accordingly, the REE patterns determined for samples from Falloon (1982) are considered in all respects comparable with Akaroa Volcanic Group chemistry presented in this thesis.

REE patterns for Akaroa Volcanic Group lavas from this study and Price and Taylor (1980), and REE patterns from other volcanic provinces for comparison, are presented in Figures 5.33 to 5.37. All REE analyses, including those cited from the literature, have been normalised to chondrite composition using the same set of normalising factors (see Table I1, Appendix I for a list of values). Overall, Akaroa Volcanic Group lavas have REE abundances characterised by

1. An approximately linear, light rare earth element (LREE) enriched REE pattern typical of alkaline associations. Ce_N/Yb_N ratios increase slowly from basalt to trachyte.

Table 5.5: Major and trace element analyses and CIPW norms for samples from Falloon (1982) for which rare earth element analyses are presented. Major element analyses in wt%; trace element analyses in ppm.

Sample Id	N36C1392	N36C1305	N36C1303	N36C1340	N36C1369	N36C1376
SiO_2	45.72	44.11	46.23	48.37	52.71	57.82
TiO_2	3.15	2.80	3.35	2.74	1.67	0.76
Al_2O_3	15.60	13.06	16.40	16.65	16.99	17.14
Fe_2O_3	3.16	3.27	3.06	2.82	2.38	2.20
FeO	10.53	10.92	10.20	9.40	7.93	5.51
MnO	0.18	0.19	0.20	0.23	0.20	0.22
MgO	5.87	10.83	4.75	4.00	2.51	0.96
CaO	9.40	10.90	8.25	7.48	5.46	2.95
Na_2O	2.91	2.51	3.86	4.22	5.63	5.90
K_2O	0.92	0.88	1.48	1.86	2.52	3.93
P_2O_5	0.42	0.38	0.72	0.82	0.70	0.24
LOI	2.95	0.32	1.44	1.44	1.99	2.64
Total	100.84	100.17	99.88	100.03	100.69	100.27
or	5.44	5.20	8.75	10.99	14.89	23.22
ab	24.62	12.57	27.94	32.88	41.87	49.92
an	26.79	21.77	23.05	20.99	13.64	8.68
ne	–	4.70	2.56	1.53	3.13	–
wo-di	7.14	12.45	5.50	4.49	3.70	1.83
en-di	3.82	7.86	2.78	2.12	1.43	0.47
fs-di	3.09	3.81	2.59	2.31	2.33	1.46
en-hy	2.24	–	–	–	–	0.87
fs-hy	1.82	–	–	–	–	2.71
fo	6.00	13.39	6.34	5.49	3.38	0.74
fa	5.36	7.16	6.52	6.58	6.08	2.53
mt	4.58	4.74	4.44	4.09	3.45	3.19
il	5.98	5.32	6.36	5.20	3.17	1.44
ap	0.97	0.88	1.67	1.90	1.62	0.56
Total	97.86	99.85	98.50	98.59	98.70	97.63
Rb	19.7	19.1	30.0	37.0	59.5	92.2
Sr	530.7	489.4	700.9	929.7	654.5	331.8
Y	29.4	22.6	36.5	39.6	46.1	51.9
Zr	162.0	148.5	254.7	273.6	383.7	119.2
Nb	40.9	37.9	70.5	85.5	105.1	587.8

N36C1392 *hy*-basalt dike, grid reference N36C/039161
N36C1305 *ne*-basalt flow, grid reference N36C/022116
N36C1303 *ne*-hawaiite flow, grid reference N36C/026113
N36C1340 *ne*-hawaiite flow, grid reference N36C/003154
N36C1369 *ne*-mugearite flow, grid reference N36C/991158
N36C1376 *hy*-mugearite flow, grid reference N36C/994144

2. A steady increase in absolute REE abundances with differentiation.

3. Development of negative Eu anomalies and depleted middle rare earth element (MREE) patterns in more evolved lavas.

Basalts and hawaiites (Fig. 5.33) have linear, LREE-enriched REE patterns, with Ce_N/Yb_N ratios of 7.33 to 8.98. There is a progressive increase in abundance of all REEs through the sequence basalt–hawaiite. For example, Ce_N increases from 55 to 111.3 and Yb_N increases from 7.5 to 12.4, from sample N36C1305 to sample N36C1340.

Mugearites, trachytes and phonolites (Fig. 5.34), have similar LREE-enriched patterns, with Ce_N/Yb_N ratios of 8.33 to 9.19. There is, however, a progressive depletion in MREE abundances relative to LREE and HREE abundances, resulting in increasing Ce_N/Sm_N and decreasing Tb_N/Yb_N ratios. For example, Ce_N/Sm_N increases from 2.4 (sample N36C1369) to 4.7 (sample N36D3619). The relative depletion in MREE abundances is accompanied by the progressive development of negative Eu anomalies in *hy*-normative mugearites and trachytes.

REE patterns for the syenite from Onawe Peninsula (Fig. 5.35) have similar REE abundances and Eu anomalies to mugearites and trachytes. However, there is a significant enrichment of HREEs relative to LREEs and MREEs, which is reflected in significantly lower Ce_N/Yb_N ratios of 4.98 to 5.32, compared to basalt–trachyte lavas. The gabbro from Onawe Peninsula is depleted in REE abundances compared to basalt lavas, and has a distinct positive Eu anomaly. Distinct variations in overall REE abundances exist between REE patterns determined in this study and patterns presented by Price and Taylor (1980). There is no evidence that these variations reflect sampling or analytical errors. Furthermore, variations in Y, Rb, La and Nd abundances in the syenite and gabbro have already been noted (see section 5.3). Accordingly, variations in REE abundances between samples, for the syenite and gabbro, are considered to represent real variations in trace element abundances, and provide evidence of chemical heterogeneity within the syenite and gabbro bodies.

The distinctive depletion of MREEs in the phonolite (and to a lesser extent in mugearites and trachytes) is not uncommon in alkaline volcanic provinces similar to Akaroa Volcano. REE patterns for six phonolites from other volcanic provinces are presented in Fig. 5.36, and are compared with the Akaroa Volcanic Group phonolite and trachytes from Akaroa Volcanic Group and Dunedin Volcano Group in Fig. 5.37.

REE patterns for the most primitive basalts are consistent with them having been derived from small degrees ($< 5\%$) of partial melting of a REE-enriched (relative to chondrite) garnet lherzolite source (Hanson, 1980). Enrichment in abundances of

Figure 5.33: Chondrite-normalised REE patterns for Akaroa Volcanic Group basanitoids, basalts and hawaiites.

Figure 5.34: Chondrite-normalised REE patterns for Akaroa Volcanic Group mugearites, trachytes and the phonolite. Sample P&T #123 is from Price and Taylor (1980). The grayscale region is the area of projection of REE patterns for basic lavas from Figure 5.33.

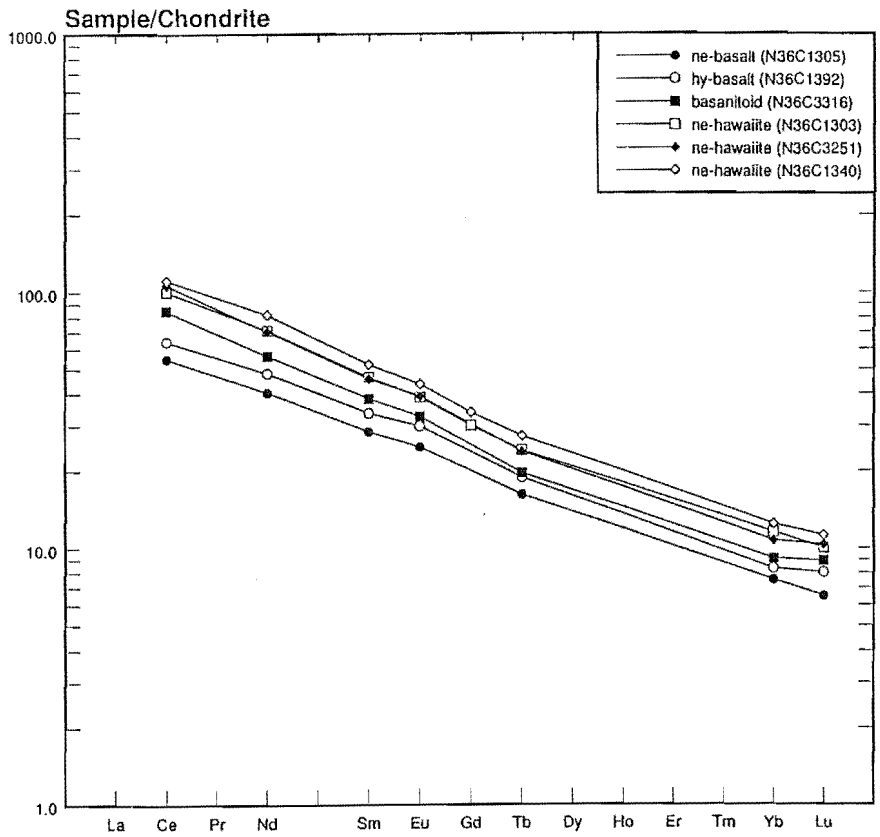
Sample/Chondrite
1000.0
100.0
10.0
1.0
La
Ce
Pr
Nd
Sm
Eu
Gd
Tb
Dy
Ho
Er
Tm
Yb
Lu
ne-basalt (N36C1305)
hy-basalt (N36C1392)
basanitoid (N36C3316)
ne-hawaiite (N36C1303)
ne-hawaiite (N36C3251)
ne-hawaiite (N36C1340)

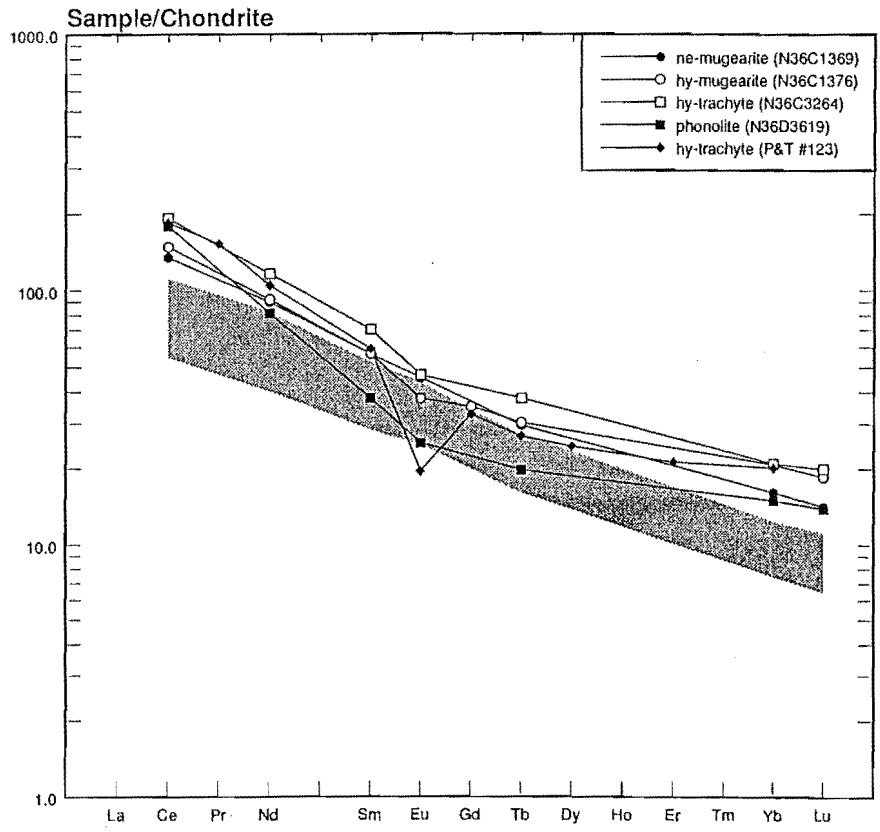
Sample/Chondrite
1000.0
100.0
10.0
1.0
La
Ce
Pr
Nd
Sm
Eu
Gd
Tb
Dy
Ho
Er
Tm
Yb
Lu
ne-mugearite (N36C1369)
hy-mugearite (N36C1376)
hy-trachyte (N36C3264)
phonolite (N36D3619)
hy-trachyte (P&T #123)

Figure 5.35: Chondrite-normalised REE patterns for the Akaroa Volcanic Group syenite and gabbro from Onawe Peninsula. Samples P&T #85 and P&T #86 are from Price and Taylor (1980). The grayscale region is the area of projection of REE patterns for lavas from Figures 5.33 and 5.34.

Figure 5.36: Chondrite-normalised REE patterns for selected phonolites from other volcanic provinces. Antarctica 25793: Antarctica (Kyle, 1981); Bokkos 743: Bokkos, Nigeria (Irving and Price, 1981); McBride X-32: McBride Province, Australia (Irving and Price, 1981); Heldburg 1007: Heldburg, E. Germany (Irving and Price, 1981); Fernando de N. FN14-3: Fernando de Noronha (Kay and Gast, 1973); Dunedin 7: Dunedin Volcanic Group (Price and Taylor, 1973).

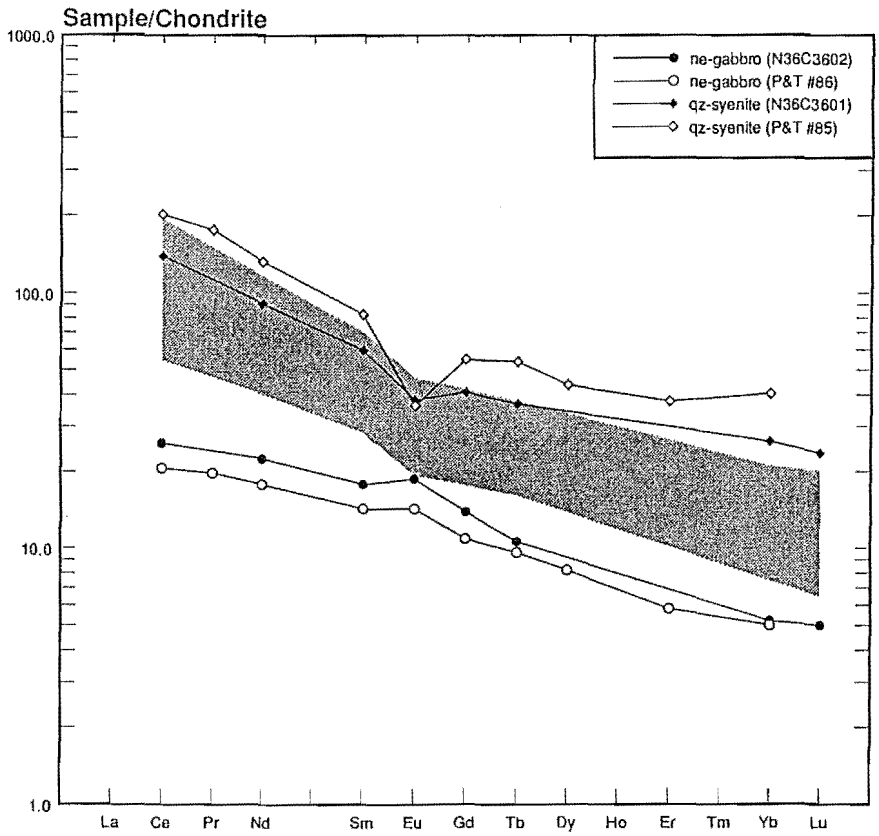
Sample/Chondrite
1000.0
100.0
10.0
1.0
ne-gabbro (N36C3602)
ne-gabbro (P&T #86)
qz-syenite (N36C3601)
qz-syenite (P&T #85)
La
Ce
Pr
Nd
Sm
Eu
Gd
Tb
Dy
Ho
Er
Tm
Yb
Lu

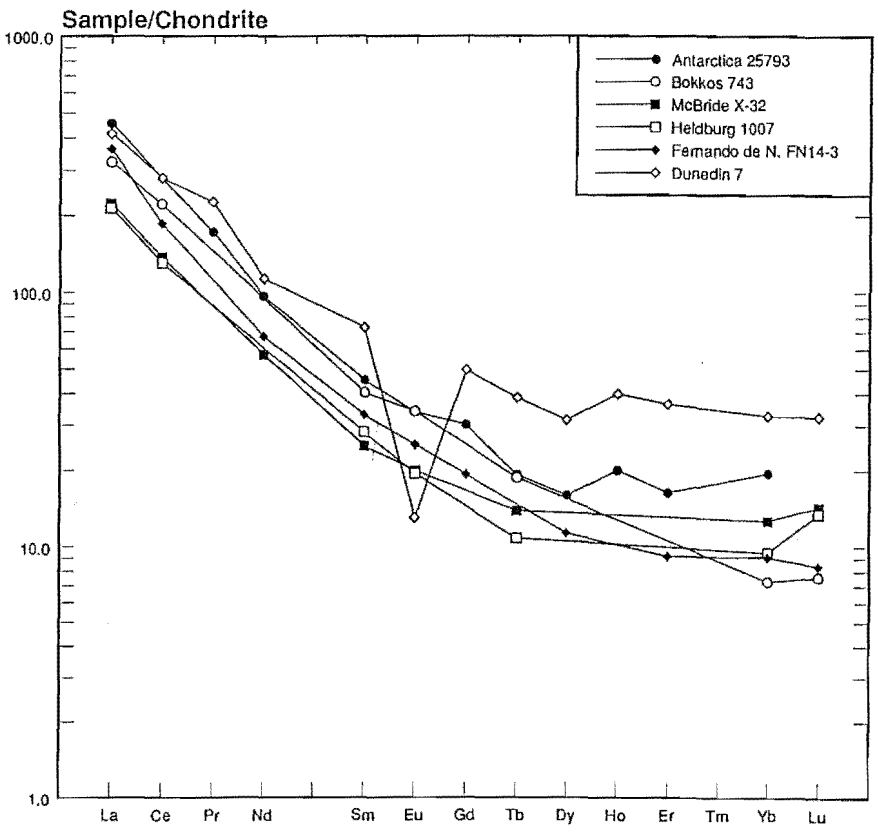
Sample/Chondrite
1000.0
100.0
10.0
1.0
Antarctica 25793
Bokkos 743
McBride X-32
Heldburg 1007
Fernando de N. FN14-3
Dunedin 7
La
Ce
Pr
Nd
Sm
Eu
Gd
Tb
Dy
Ho
Er
Tm
Yb
Lu

all REEs from basalt through hawaiite composition is consistent with fractionation of olivine + clinopyroxene + plagioclase + magnetite. Olivine has very low K_d's for all REEs and its fractionation will result in an overall increase in REE abundances without changing the shape of the REE pattern. Clinopyroxenes have lower K_d's for the LREE and Eu, while plagioclase has a high K_d for Eu. Fractionation of both clinopyroxene and plagioclase will negate any Eu effects, while increasing overall REE abundances and enriching LREEs relative to HREEs. Fractionation of olivine + clinopyroxene + plagioclase + magnetite is consistent with petrographic and other geochemical data.

The depletion of MREEs, and the development of negative Eu anomalies, in mugearites, trachytes and phonolites may be attributed to the fractionation of amphibole, apatite, plagioclase and alkali feldspar. Fractionation of amphibole will deplete MREEs and to some extent HREEs, and produce a positive Eu anomaly in the residual liquid. Apatite fractionation will enrich LREEs and HREEs relative to MREE and produce a positive Eu anomaly in the residual liquid. Fractionation of plagioclase, anorthoclase or K-feldspar will strongly deplete the residual liquid in Eu, more than enough to mask the influence of apatite and amphibole on Eu.

The HREE enrichment in the syenite may result from fractionation of K-feldspar, apatite and amphibole, while HREE enrichment, and the positive Eu anomaly in the gabbro results from cumulate plagioclase and biotite.

5.5 Spidergrams

Normalised trace element diagrams ("spidergrams") for mafic Akaroa Volcanic Group lavas (Fig. 5.38) show the typical enriched and humped patterns of within-plate magmas and are characterised by increasing enrichment (relative to mantle) from Ba to Nb–La and decreasing enrichment (relative to mantle) from Nb–La to Yb, reflecting the control of REE abundances by refractory garnet in the mantle source. Subtle variations are, however, apparent. A positive Th–K–Nb slope associated with a weak positive Ti anomaly is a common feature. A *ne*-basalt (N36C3652) and a *qz*-basalt (N37A3353) have negative K anomalies. Weaver *et al* (1989) reports that marked negative K anomalies are common among both alkaline and subalkaline rocks from the South Island of New Zealand and the Sub-Antarctic Islands, and may be a regional source characteristic. The basanitoid (N36C3316) and a *ne*-basalt (N36C1305) have weak negative Zr and Hf anomalies. Similar Zr and Hf anomalies have been reported for alkaline and subalkaline rocks from Dunedin, Banks Peninsula, Canterbury and South Westland, which Weaver *et al* (1989) suggested might be a regional source characteristic or possibly a reflection of the refractory behaviour of a Zr-Hf mineral in the source. However, care should be taken not too read to

Figure 5.37: Chondrite-normalised REE patterns for the Akaroa Volcanic Group phonolite and a trachyte, compared with phonolites from other volcanic provines. Sample P&T #123 is from Price and Taylor (1980). Sample P&T #7 is from Price and Taylor (1973). The grayscale region is the area of projection of REE patterns for phonolite lavas from Figure 5.36, excluding sample Dunedin 7.

Figure 5.38: Normalised trace element diagrams for mafic Akaroa Volcanic Group lavas. Normalising factors are those of Thompson *et al* (1983) for chondrites, except Rb, K and P.

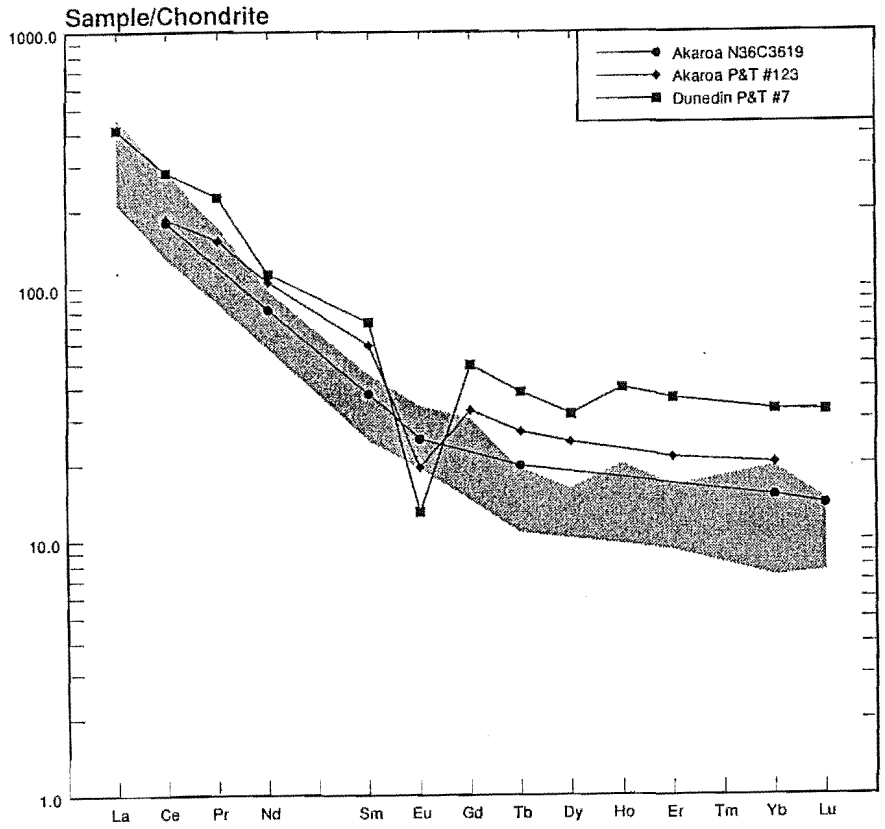
Sample/Chondrite
1000.0
100.0
10.0
1.0
Akaroa N36C3619
Akaroa P&T #123
Dunedin P&T #7
La
Ce
Pr
Nd
Sm
Eu
Gd
Tb
Dy
Ho
Er
Tm
Yb
Lu

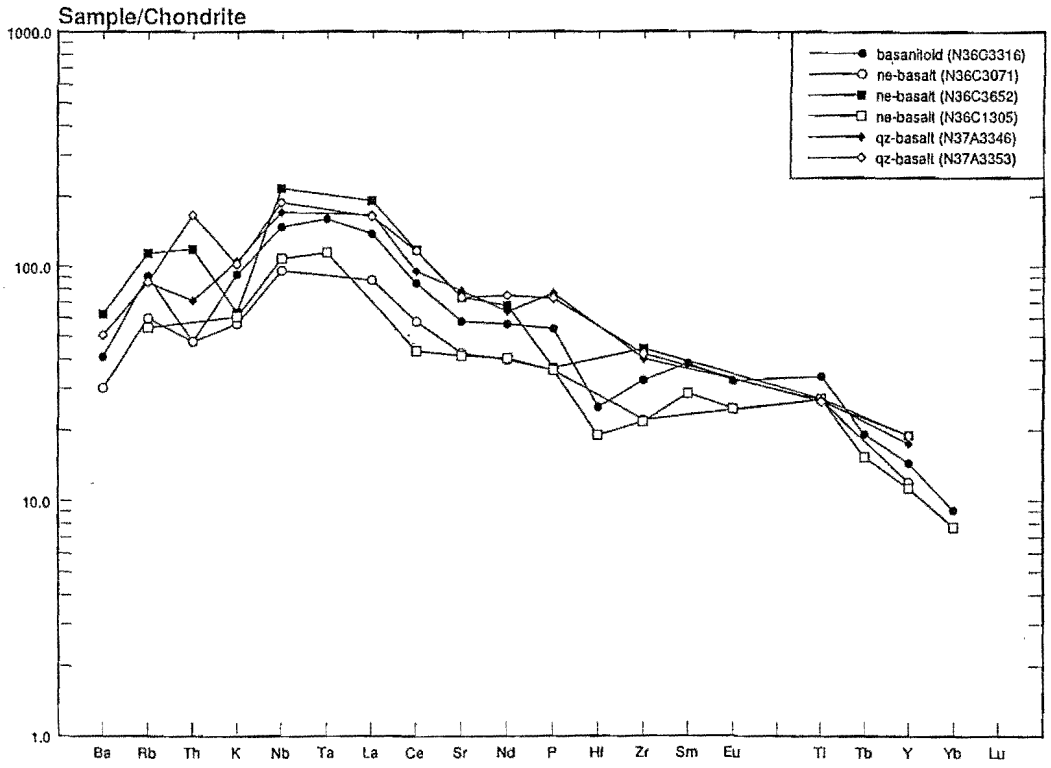
Sample/Chondrite
1000.0
100.0
10.0
1.0
basanitoid (N36C3316)
ne-basalt (N36C3071)
ne-basalt (N36C3652)
ne-basalt (N36C1305)
qz-basalt (N37A3346)
qz-basalt (N37A3353)
Ba
Rb
Th
K
Nb
Ta
La
Ce
Sr
Nd
P
Hf
Zr
Sm
Eu
Ti
Tb
Y
Yb
Lu

much into these small anomalies, as some may fall within the range of analytical error and others may be an artifact of the order in which the elements are plotted. The strong positive Th anomaly in sample N37A3353 (a *qz*-basalt) is indicative of crustal contamination. The absence of paired negative K and P anomalies indicates that K_2O- and P_2O_5-bearing accessory phases are not significant refractory mantle phases during partial melting, and could be used to constrain the lower limit of estimates of the degree of partial melting.

In general, normalised trace element patterns for mafic Akaroa Volcanic Group lavas are typical of oceanic and continental alkaline lavas (Fig. 5.39), and especially other alkalic intraplate volcanic associations of the South Island of New Zealand (Fig. 5.40).

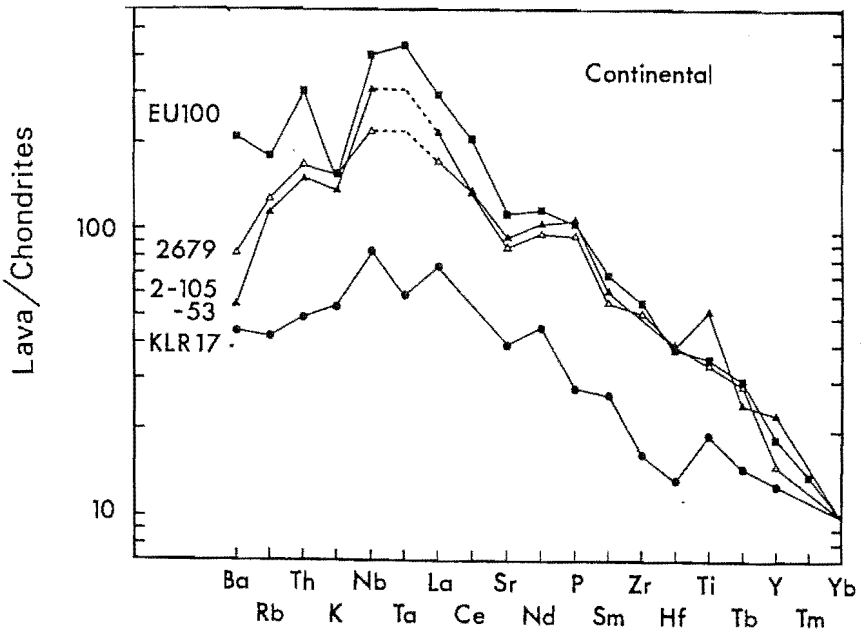

Figure 5.39: Normalised trace element diagrams of representative oceanic and continental alkalic and strongly-alkalic lavas. Key: EU100, melilitite, Hegau, Germany (unpublished data); 2679, basanite, Mt Shadwell, Australia (Frey *et al*, 1978); 2-105-53, basanite, Dry Valley, Antarctica (Kyle, 1981); KLR 17, alkali olivine basalt, Gregory Rift, East Africa (Baker *et al*, 1977). Normalising factors are those of Thompson *et al* (1983) for chondrites, except Rb, K and P. After Thompson *et al* (1983).

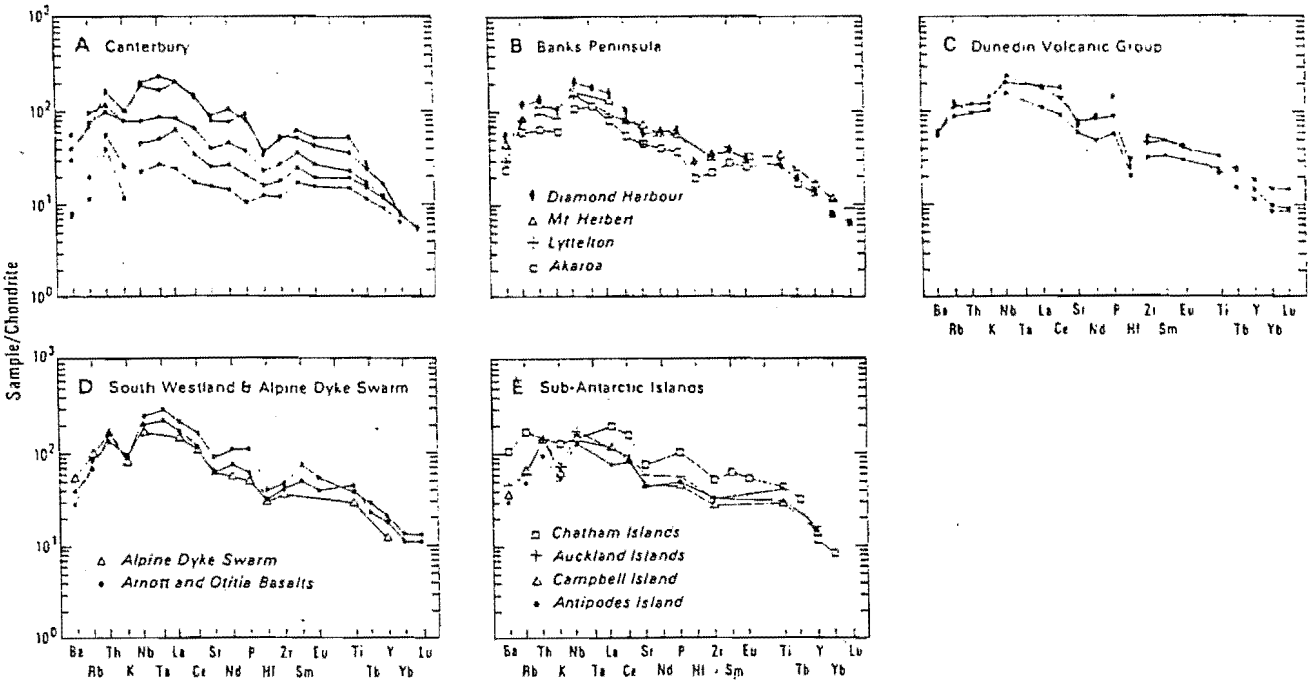

Figure 5.40: Normalised trace element diagrams for selected mafic rocks from South Island and the Sub-Antarctic and Chatham Islands. Normalising factors are those of Thompson *et al* (1983) for chondrites, except Rb, K and P. After Weaver *et al* (1989).

Chapter 6

ISOTOPE GEOCHEMISTRY

6.1 Introduction

$^{87}Sr/^{86}Sr$ isotope ratios have been determined for 22 samples from the Akaroa Volcanic Group covering a wide range of rock types including end-members of the basalt–trachyte and basanite–phonolite lineages, and the syenite and gabbro of Onawe Peninsula. $^{143}Nd/^{144}Nd$ isotope ratios have also been determined for three of these samples. Sr and Nd isotope data are presented in Appendix J and detailed descriptions of the analytical methods are presented in Appendix E.

6.2 $^{87}Sr/^{86}Sr$ Isotope Ratios

Initial $^{87}Sr/^{86}Sr$ isotope ratios are summarised as histograms for mafic (gabbro, basanitoid, basalt and hawaiite), intermediate (mugearite) and felsic (phonolite, trachyte) lavas (Fig. 6.1).

Mafic lavas have low initial $^{87}Sr/^{86}Sr$ isotope ratios (0.70293–0.70314) which cluster about a mean of 0.70302 ± 2. Two mugearites have initial $^{87}Sr/^{86}Sr$ isotope ratios of 0.70307–0.70322 and overlap substantially with the mafic population at the ± 2 s.d. level. These ratios are typical of oceanic and continental alkali basalt provinces, such as Hawaii (O'Nions *et al*, 1977), Kenya (Norry *et al*, 1980), Iceland and Sao Miguel (White and Hofmann, 1982), and are comparable with mafic lavas from other intraplate volcanics of the South Island of New Zealand. Akaroa Volcanic Group mafic lavas have similar initial $^{87}Sr/^{86}Sr$ isotope ratios to mafic lavas of the Lyttelton Volcanic Group (0.7029–0.7032) and the Cookson Volcanics of northern Canterbury

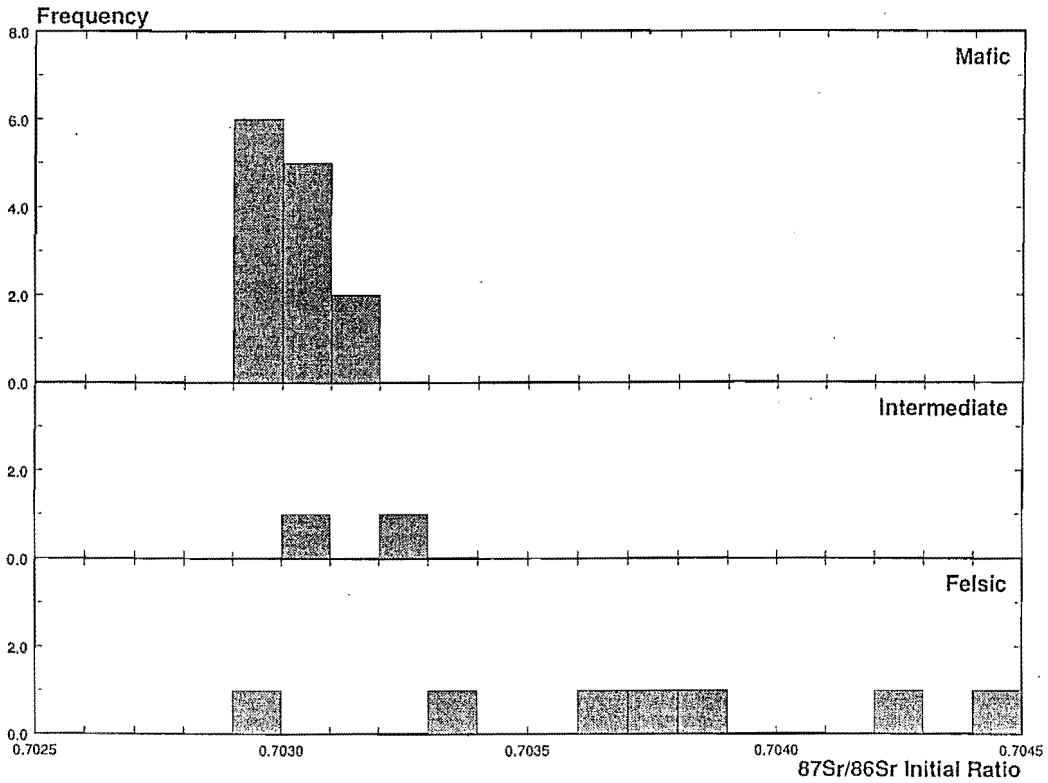

Figure 6.1: Histograms of initial $^{87}Sr/^{86}Sr$ for mafic, intermediate and felsic lavas of the Akaroa Volcanic Group.

(0.7029–0.7033), and overlap with lower ratios of the Diamond Harbour and Mt Herbert Volcanic Groups (0.7029–0.7038) of Banks Peninsula (Fig. 6.2, Weaver *et al*, 1989). Mafic rocks of the Dunedin Volcanic Group have lower initial $^{87}Sr/^{86}Sr$ isotope ratios ($\approx$ 0.7027–0.7029).

In contrast to mafic and intermediate lavas, felsic lavas exhibit a wide range of $^{87}Sr/^{86}Sr$ isotope ratios, from 0.70295 to 0.70447. If the phonolite and the syenite from Onawe Peninsula are excluded, then it is apparent that Akaroa Volcanic Group trachytes have significantly higher initial $^{87}Sr/^{86}Sr$ isotope ratios (0.70365–0.70447) than mafic and intermediate lavas, and that there is a positive correlation between initial $^{87}Sr/^{86}Sr$ isotope ratio and silica saturation. Such ratios would indicate either that the trachytes were derived from a mantle source enriched in LREEs and Rb relative to the source of mafic lavas, or that crustal contamination was a significant factor in their differentiation. On all major element, trace element and REE graphs, trachytes appear to be comagmatic with other Akaroa Volcanic Group lavas, and this would indicate that higher initial $^{87}Sr/^{86}Sr$ isotope ratios in the trachytes reflect progressive contamination of a fractionating magma by more radiogenic crustal material. This conclusion is supported by the dominance of silica-saturated, *hy-* and *qz*-trachytes over undersaturated *ne*-trachytes, compared with the predominance of undersaturated *ne*-normative lavas in the basalt–benmoreite compositional range.

The broad range of initial $^{87}Sr/^{86}Sr$ isotope ratios for felsic lavas encompasses the range of felsic lavas from the Dunedin Volcanic Group (0.7035–0.7043) and substantially overlaps with those of the Lyttelton Volcanic Group (0.7033–0.7052, see Fig. 6.2).

The isotopic composition of the phonolite compared to trachyte lavas is notable. The phonolite (N36C3619) has an initial $^{87}Sr/^{86}Sr$ isotope ratio of 0.70295 which is almost identical to the lowest $^{87}Sr/^{86}Sr$ isotope ratio for a mafic lava (0.70293 for *ne*-hawaiite N36C3069) and the basanitoid (N36C3316, $^{87}Sr/^{86}Sr$ = 0.70297). It is significant that the end-members of the basanite–phonolite lineage of Akaroa Volcanic Group have almost identical low initial $^{87}Sr/^{86}Sr$ isotope ratios, as this would appear to preclude crustal contamination or mantle enrichment processes as factors in the differentiation of the basanite–phonolite lineage. Rather, a model in which the Akaroa Volcanic Group phonolite is derived from a basanitic magma purely by fractional crystallisation is indicated.

6.3 $^{143}Nd/^{144}Nd$ Isotope Ratios

$^{143}Nd/^{144}Nd$ isotope ratios were determined for a *ne*-basalt, *ne*-hawaiite and a *ne*-trachyte. The mafic lavas have similar high initial $^{143}Nd/^{144}Nd$ isotope ra-

tios (0.512949–0.512952), whereas the *ne*-trachyte has a distinctly lower initial $^{143}Nd/^{144}Nd$ isotope ratio of 0.512867.

6.4 Isotopic constraints on the source of Akaroa Volcanic Group lavas

Three Akaroa Volcanic Group lavas, for which both $^{87}Sr/^{86}Sr$ and $^{143}Nd/^{144}Nd$ isotope ratios are available, are shown on a ϵ_{Nd}–$^{87}Sr/^{86}Sr$ diagram (Fig. 6.3), along with all other Banks Peninsula isotope data (Weaver, *pers. comm.*) and fields for other oceanic and continental alkali basalt provinces shown for comparison. Akaroa Volcanic Group lavas plot within the field for magmas derived from a time-integrated, LREE-depleted mantle source, reflecting the high $^{143}Nd/^{144}Nd$–low $^{87}Sr/^{86}Sr$ character of Akaroa Volcanic Group lavas. The implication is that Akaroa Volcanic Group magmas were generated by partial melting of a depleted mantle source region — a mantle source which was impoverished in large ion lithophile (LIL) elements and LREEs (especially Rb and Nd) with respect to Sr and Sm for a long period of geological time. These data are, however, inconsistent with other geochemical data (eg. REE data — see section 5.5) which clearly show that Akaroa Volcanic Group lavas are enriched in LIL elements and LREEs. Furthermore, in contrast to the high Sm/Nd–low Rb/Sr source indicated by isotopic ratios, Akaroa Volcanic Group lavas have low Sm/Nd and high Rb/Sr ratios (Fig. 6.4) consistent with derivation from an enriched mantle source. If the observed low Sm/Nd–high Rb/Sr (compared to "bulk earth") character of Akaroa Volcanic Group magmas was a (geologically) long-lived feature of the mantle source region, then normal isotopic decay would result in low $^{143}Nd/^{144}Nd$ and high $^{87}Sr/^{86}Sr$ isotope ratios. The fact that the opposite is true (ie. Akaroa Volcanic Group lavas have high $^{143}Nd/^{144}Nd$ and low $^{87}Sr/^{86}Sr$ isotope ratios) indicates that isotopic and incompatible trace element ratios have become "decoupled". This decoupling of isotopic and incompatible trace element ratios is a characteristic feature of oceanic and continental alkali basalt magmas, and a number of processes have been proposed to account for it.

Although extreme fractionation could alter the Sm/Nd and Rb/Sr ratios, alkali basalts such as those of the Akaroa Volcanic Group could not have undergone such degrees of fractional crystallisation and maintained their basaltic composition. Since the mantle source region appears to be depleted, and the most primitive magmas derived from the partial melting of this source are enriched, it might be suggested that the partial melting event itself altered the Sm/Nd and Rb/Sr ratios. This model would require extremely small degrees of partial melting ($< 1\%$), and even so, with the limited data available on distribution coefficients for incompatible elements between mantle minerals and melts, it seems unlikely that even very small degrees of partial melting would have sufficient effect. Furthermore, there is some debate

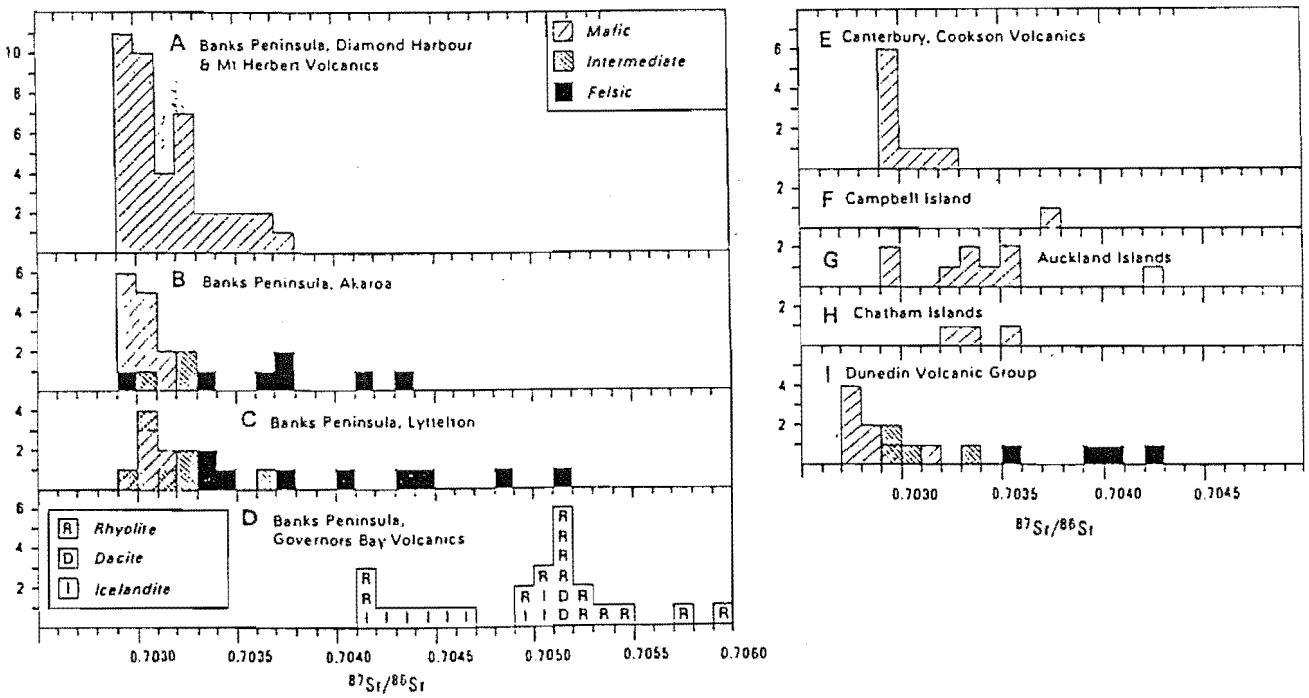

Figure 6.2: Histograms of initial $^{87}Sr/^{86}Sr$ isotope ratios for South Island and the Sub-Antarctic and Chatham Islands provinces (after Weaver *et al*, 1989).

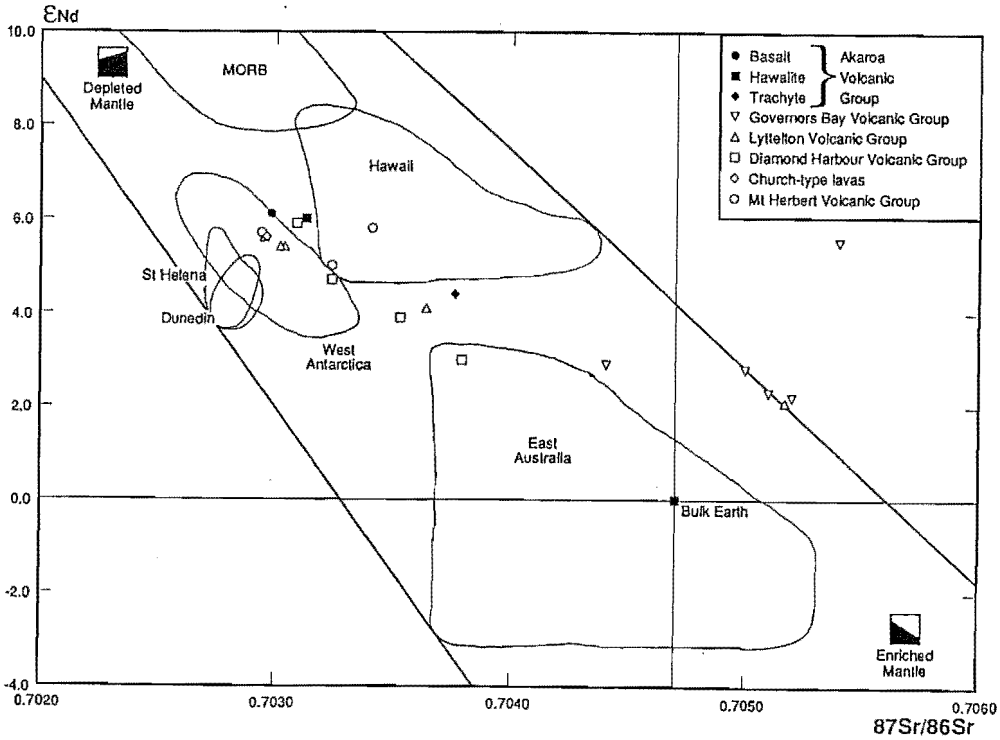

Figure 6.3: ϵ_{Nd} versus $^{87}Sr/^{86}Sr$ for Akaroa Volcanic Group lavas, with lavas from other Banks Peninsula volcanic groups and fields from other volcanic provinces.

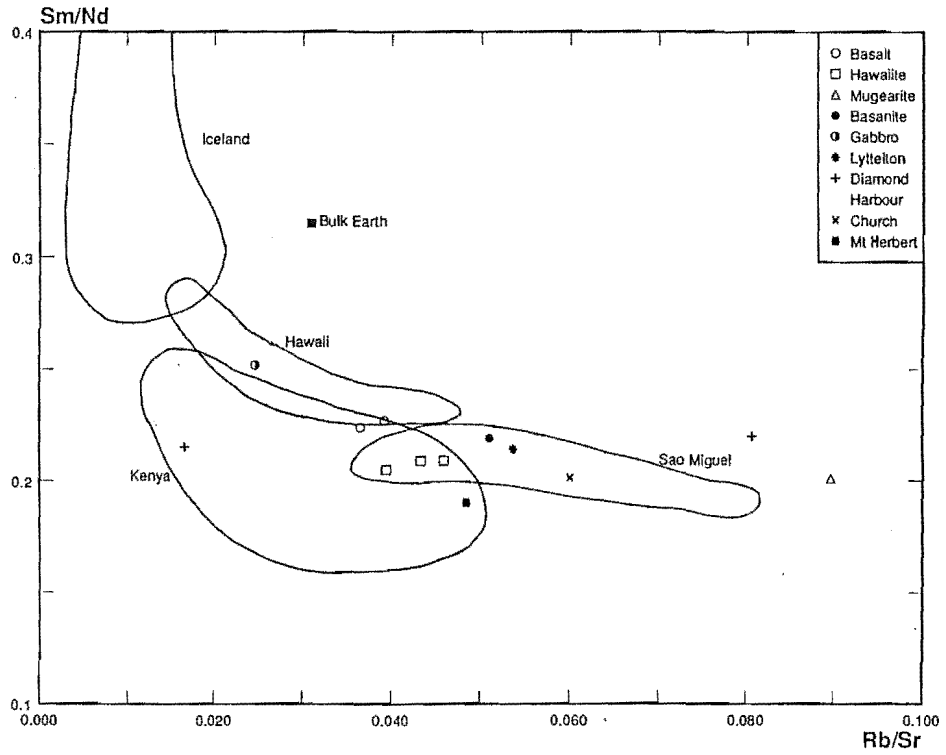

Figure 6.4: Sm/Nd versus Rb/Sr for Akaroa Volcanic Group lavas, with lavas from other Banks Peninsula volcanic groups and fields for other volcanic provinces.

as to whether a melt formed by < 1% partial melting could physically be separated from the residual mantle source. Consequently, processes resulting in trace element enrichment of the mantle source region or melt, prior to, during, or immediately after the partial melting event have been postulated by numerous authors (eg. O'Nions *et al*, 1977; Carter *et al*, 1978; Hawkesworth *et al*,1979; Menzies and Murthy, 1980a; Norry *et al*, 1980).

Trace element enrichment processes are complex, multi-stage events (Irving, 1980; Menzies and Murthy, 1980b). In terms of timing, trace element enrichment processes may be an early event unrelated to magma genesis (possibly very small < 1% partial melts), the trigger that initiates partial melting (Lloyd and Bailey, 1975; Boettcher *et al*, 1979; Boettcher and O'Neil, 1980), or may themselves be triggered by the partial melting event. A variety of fluids may be involved, ranging from very small volume partial melts to larger volumes of H_2O- or CO_2-rich fluids (Menzies and Wass, 1983). Multiple processes may be active, including anatexis and fluid migration. Zone refining may be an important process in mantle metasomatism (Harris, 1957). A 10% partial melt percolating through 10× the volume of mantle from which it was derived will adopt the trace element pattern equivalent to a 1% partial melt (Norry and Fitton, 1983). There is some evidence of different hydrous phases in the same mantle xenolith (eg. amphibole and mica) having different Sr and Nd isotope abundances, indicating that multiple enrichment events may be involved (Menzies and Murthy, 1980b).

The origins of metasomatised mantle xenoliths have been studied by numerous workers in order to elucidate mantle processes, but most mantle xenoliths in which modal metasomatism has been recognised are thought to be derived from within the lithosphere (Harte, 1983; Menzies, 1983, Hawkesworth *et al*, 1983), rather than the asthenosphere where alkali basalt magmas are thought to originate, making evaluation of the role of metasomatism in alkali basalt genesis difficult to assess (Norry and Fitton, 1983). In this context, note that Akaroa Volcanic Group lavas have isotopic ratios that overlap the field of the Hawaiian oceanic intraplate suite (Fig. 6.3), suggesting the involvement of asthenospheric rather than lithospheric mantle as a source for both regions. Studies of peridotitic and lherzolitic mantle xenoliths suggest the presence of exotic minerals or intergranular components enriched in large ion lithophile (LIL) elements (Frey and Green, 1974; Dasch and Green, 1975; Menzies, 1976; Basu and Murthy, 1977; Menzies and Murthy, 1978a,b), consistent with derivation from < 5% partial melts of a garnet peridotite source. Menzies (1976) reports a LREE-enriched component in a spinel lherzolite, and "fertile harzburgite" has been described (Frey and Green, 1974; Hervig *et al*, 1977). Xenoliths depleted in LIL elements have also been described (Menzies and Murthy, 1978a; Jackson and Wright, 1970).

It is very difficult to assess the role of mantle metasomatism in the genesis of Akaroa Volcanic Group lavas, especially with the limited isotope data available

and the absence of mantle-derived xenoliths. However, with the limited data currently available, mantle metasomatism appears to provide the best explanation of the decoupling of isotopic ratios and trace element ratios.

6.5 Evidence for contamination of Akaroa Volcanic Group lavas

The mafic lavas of the Akaroa Volcanic Group (and of South Island alkaline volcanic provinces in general) have generally low initial $^{87}Sr/^{86}Sr$ isotope ratios, indicating that most mantle derived magmas have not been contaminated by continental crust. Conversely, felsic lavas have significantly higher initial $^{87}Sr/^{86}Sr$ isotope ratios, reflecting the susceptability of these low-Sr magmas to crustal contamination. On a ϵ_{Nd}–$^{87}Sr/^{86}Sr$ diagram (Fig. 6.3), felsic lavas of the Akaroa, Lyttelton and Governors Bay Volcanic Groups trend away from the mantle array in a direction consistent with crustal contamination. In comparison, the trend of lavas from the Diamond Harbour and Mt Herbert Volcanic Groups is subparallel to the mantle array, and the variation evident within the Diamond Harbour Group is attributed to a limited degree of mantle source isotopic heterogeneity (Sewell, 1985).

Hawkesworth *et al* (1979) reported $^{87}Sr/^{86}Sr$ isotope ratios of 0.7032–0.7052 and $^{143}Nd/^{144}Nd$ isotope ratios of 0.51300–0.51276 for alkali basalts from Sao Miguel in the Azores, and noted that the negative correlation between Sr and Nd isotopes had a shallower slope than that of the mantle array. They concluded that this was not the result of high level contamination by seawater or oceanic sediments, but indicative of recent mixing processes. However, contamination models were eliminated as much because of the lack of a suitable source for the contaminant as that the actual Sr-Nd isotope trend did not match with calculated trends for the contamination model.

In the case of Akaroa Volcanic Group trachytes, the smooth transition in trace element and major element abundances from basalt to trachyte lavas, and the strong evidence for fractional crystallisation being the dominant differentiation process (at least over the basalt–benmoreite compositional range), suggests that fractional crystallisation is occuring concurrently with the mixing or contamination process. A process involving the mixing of two magmas would seem less likely because of the difficulty of locating a suitable, silica-rich magma. Akaroa Volcanic Group trachytes are unlikely to be the result of metasomatic processes in the mantle, because such processes would not alter the $^{87}Sr/^{86}Sr$ and $^{143}Nd/^{144}Nd$ isotope ratios in the short period that Akaroa Volcano has been active. $^{87}Sr/^{86}Sr$ isotope ratios of 0.705–0.710 may be generated in 150 Ma (Hawkesworth *et al*, 1979). High initial $^{87}Sr/^{86}Sr$

isotope ratios correlate with high SiO_2, low Nb/Th and low Nd ratios, indicating crustal contamination.

High-level contamination of evolving magmas by seawater or crustal material would therefore seem a more suitable model. In the case of Akaroa Volcanic Group lavas, seawater can be eliminated as a contaminant for the same reasons expounded by Hawkesworth *et al* (1979). All samples were collected from subaerial flows, so any interaction with seawater must therefore have taken place in the magma reservoir, with resulting characteristic pyroclastic activity expected. Mixing a basalt with an isotopic composition of $^{87}Sr/^{86}Sr = 0.703$ and $^{143}Nd/^{144}Nd = 0.5130$ with seawater will not alter the $^{143}Nd/^{144}Nd$ isotope ratio of the basalt significantly, and the resulting mixing trend is nearly horizontal (Hawkesworth *et al*, 1979).

There is, however, little problem in locating a suitable source of radiogenic crustal contaminant. The volcanics of Banks Peninsula were erupted onto a basement high of Triassic Torlesse terrane and Lower Tertiary sediments. These sediments are exposed above sea level near the centre of the eroded Lyttelton crater (Weaver and Sewell, 1986) and xenoliths of petrogaphically similar sediments have been recognised in the welded tuff from Onawe Peninsula (see chapter 2), indicating that the sedimentary basement extends beneath Akaroa Volcano. Weaver and Sewell (1986) report $^{87}Sr/^{86}Sr$ isotope ratios of 0.7088–0.7333 and $^{143}Nd/^{144}Nd$ isotope ratios of 0.5122–0.5124 for Torlesse lithologies and Charteris Bay Sandstone. Contamination of Akaroa Volcanic Group magmas by these sediments could potentially have a significant effect on the isotopic characteristics of erupted lavas. Modelling of combined assimilation/fractional crystallisation (AFC) processes by Weaver *et al* (1989) and Sewell and Weaver (1989) indicate that such process may help to explain the evolution of subalkaline potassic andesite-dacite lavas of the Governors Bay Volcanic Group and mildly potassic early Lyttelton Volcanic Group lavas, although the exact nature of the contaminant is difficult to assess because of the likelihood of multiple sources of contamination (metasediments, metasediment-derived dacites, dacite melts and residues).

There is clear evidence, precedent and opportunity for crustal contamination of Akaroa Volcanic Group lavas, and good justification for attempting to model the evolution of (especially felsic) lavas by AFC processes.

Chapter 7

PETROGENESIS

7.1 Introduction

In this chapter, petrographical, mineralogical and geochemical data presented in previous chapters are discussed with the aim of placing constraints on the genesis of, and relationships between, Akaroa Volcanic Group magmas. A petrogenetic model is proposed to account for the evolution of Akaroa Volcanic Group lavas, and the viability of this model is tested using computer modelling based on the least-squares approximation technique.

7.2 Character of the Akaroa Volcanic Group

The character of the Akaroa Volcanic Group may be summarised as follows:

- A mildly to moderately alkaline association comprising two sub-parallel sodic alkaline lineages — a weakly undersaturated alkali olivine basalt–hawaiite–mugearite–benmoreite–trachyte lineage with *ne*-, *hy*- and *qz*-normative variants, and a moderately undersaturated basanite–nepheline hawaiite–nepheline mugearite–nepheline benmoreite–phonolite lineage. Peralkaline differentiates occur in each lineage. In the alkali olivine basalt–trachyte lineage, basic lavas are typically *ne*-normative whereas felsic lavas are typically *qz*-normative.
- Basic lavas are dominated by olivine, Ti-rich calcic clinopyroxene, titanomagnetite and plagioclase phenocrysts. Minor biotite and amphibole occur in

coarse-grained basic lavas. Groundmass phases include clinopyroxene, plagioclase, titanomagnetite, minor olivine and apatite. In more evolved lavas, plagioclase and titanomagnetite become the dominant phenocryst phases, with minor apatite, olivine, clinopyroxene, and rare kaersutite megacrysts. Groundmass phases include plagioclase, clinopyroxene, titanomagnetite and apatite. Felsic lavas contain minor plagioclase and titanomagnetite phenocrysts in a groundmass of plagioclase with minor alkali feldspar, quartz, clinopyroxene, fayalitic olivine, titanomagnetite and apatite. Arfvedsonite and aenigmatite may also be present in peralkaline lavas.

- The consistent variation in major and trace element abundances and REE patterns indicate rocks of the Akaroa Volcanic Group are comagmatic:
  - Exponential decrease in MgO, TiO_2, Cr, Ni and V.
  - Linear decrease in CaO and FeO.
  - Linear increase in Na_2O, K_2O, Y, Nb, Rb, La, Ce, Nd, Ga, Pb, Th and Ba.
  - Al_2O_3 increases rapidly in basalts, but is relatively constant in more evolved lavas.
  - P_2O_5 and Sr increase rapidly from basalts to hawaiites, then decrease rapidly from mugearites to trachytes.
  - All rocks have approximately linear, parallel, LREE-enriched REE patterns (Ce_N/Yb_N in the range 7–9.5). REE abundances increase with differentiation and there is a progressive development of Eu anomalies and MREE depletion in felsic lavas.

  These variations are consistent with evolution by fractional crystallisation of olivine, clinopyroxene, titanomagnetite, plagioclase, apatite, and possibly kaersutite. The LREE-enriched REE patterns are indicative of magma generation by small degrees of partial melting of a garnet peridotite mantle source.

- Sm/Nd and Rb/Sr trace element ratios, LIL element abundances and REE patterns clearly indicate an enriched mantle source, yet initial $^{87}Sr/^{86}Sr$ and $^{143}Nd/^{144}Nd$ isotope ratios are consistent with derivation of Akaroa Volcanic Group magmas from a time-integrated, LREE-depleted mantle source. Mantle enrichment events prior to or associated with the generation of Akaroa Volcanic Group magmas, or very small degrees of partial melting ($\leq 1\%$) are indicated. High initial $^{87}Sr/^{86}Sr$ isotopes of felsic lavas indicate high-level crustal contamination may be an important process in the evolution of these lavas.

7.3 Significance of Compositional Groups

Before attempting to model the petrogenesis of Akaroa Volcanic Group lavas, it is important to evaluate the significance of some compositional groups with a view to identifying different processes and/or eliminating some samples from the modelling calculations.

7.3.1 High Al_2O_3/ C-normative and Silica-Saturated Rocks

It was pointed out in chapter 5 that some samples from Akaroa Volcano have normative C and/or high Al_2O_3 contents. The presence of *hy*- and *qz*-normative variants is also unusual in what is otherwise a distinctly mildy alkaline association. Some 42 samples ($\approx$ 15% of those analysed) have C (0.07–12.04 wt%) in the norm. Histograms of wt% C by rock type are presented in Fig. 7.1. The trachyte tuffs and breccias from Onawe and Takamatua Peninsulas, trachyte clasts from the breccias, and the welded tuff from Onawe Peninsula show the greatest range of C and the highest value of C (12.04% in sample N36C3140 from the welded tuff). All other C-normative samples are *hy*- or *qz*-normative lavas, and the amount of normative C increases with silica saturation (compare Fig. 7.1 C and D). There is also a strong correlation between high Al_2O_3 contents, normative C and silica saturation (Fig. 7.2). Rocks with high Al_2O_3 contents and normative C ($\pm$ *hy, qz*), other than the xenoliths from Lighthouse Reserve, are interpreted as having been contaminated by crustal material. Evidence has already been presented in chapter 6 for contamination of Akaroa Volcanic Group lavas by crustal material, including the correlation of high initial $^{87}Sr/^{86}Sr$ isotope ratios with silica saturation. As noted in chapter 6, sample N36C3140 from the welded tuff on Onawe Peninsula has sedimentary xenoliths and incipient cordierite, and it has amongst the highest Al_2O_3 (21.93%), normative C (12.04%) and *qz* (16.58%) contents of any Akaroa Volcanic Group lava.

7.3.2 Scatter in Felsic Rocks

A number of chemical variation diagrams (see chapter 5) show considerable scatter among felsic lavas (mugearites, benmoreites and trachytes), which can be characterised by:

- A gain in Al_2O_3 (relative to SiO_2) and Rb (relative to Zr).

Figure 7.1: Histograms of normative C (wt%) by rock type. A–qz-trachyte intrusions, flows and dikes, qz-syenite; B–qz-trachyte clasts, trachyte and basalt tuffs; C–hy-normative basalts, hawaiites and mugearites; D–qz-normative basalts and hawaiites.

Figure 7.2: Histograms of Al_2O_3, and normative C, qz and hy for Akaroa Volcanic Group lavas. A–Absolute frequency distribution of Al_2O_3 for all 278 Akaroa Volcanic Group analyses; B–Frequency distribution of C-normative lavas as a percent of all lavas in the Al_2O_3 range; C–Frequency distribution of hy-normative lavas as a percent of all lavas in the Al_2O_3 range; D–Frequency distribution of qz-normative lavas as a percent of all lavas in the Al_2O_3 range.

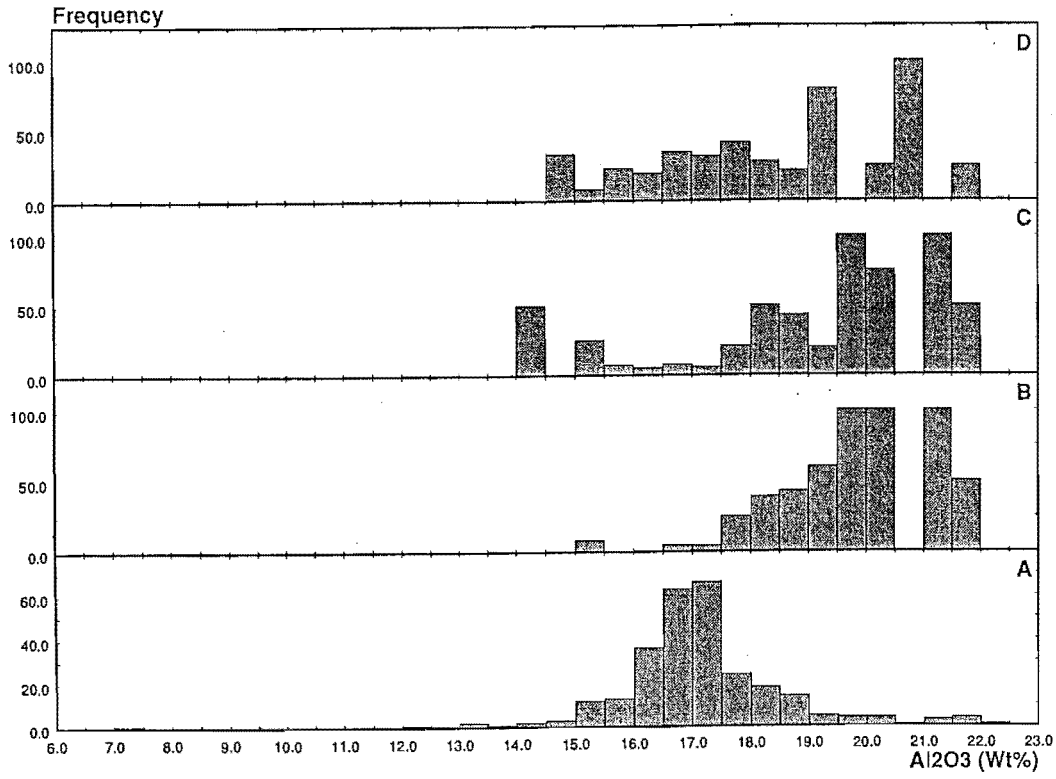
Frequency
D
C
B
A
100.0
50.0
0.0
60.0
40.0
20.0
6.0
7.0
8.0
9.0
10.0
11.0
12.0
13.0
14.0
15.0
16.0
17.0
18.0
19.0
20.0
21.0
22.0
23.0
Al2O3 (Wt%)

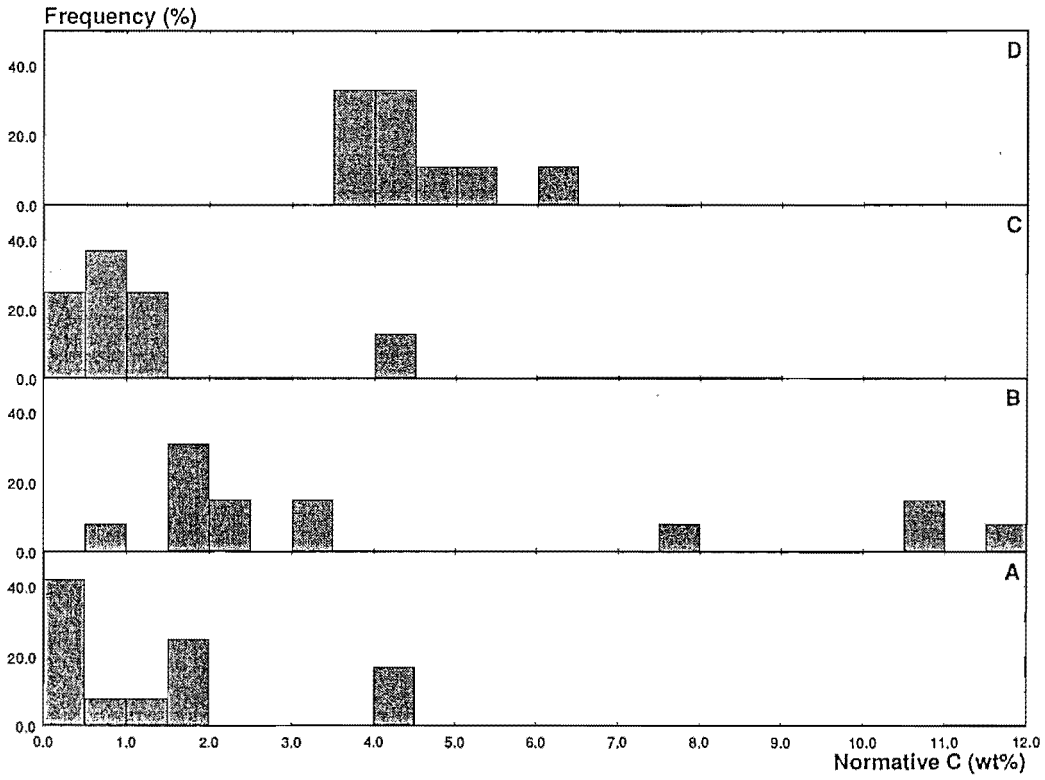
Frequency (%)
D
C
B
A
40.0
20.0
0.0
1.0
2.0
3.0
4.0
5.0
6.0
7.0
8.0
9.0
10.0
11.0
12.0
Normative C (wt%)

- A loss of Na_2O and K_2O (relative to SiO_2), and Y, La, Ce and Nd (relative to Zr).

The fact that felsic lavas are "well-behaved" on plots of MgO, TiO_2, CaO, Fe_2O_3, MnO and P_2O_5 (relative to SiO_2), and Cr, Ni, V and especially Nb (relative to Zr), suggests that the scatter is not the result of some crystal fractionation process. There is a high correlation between the extent of a lava's deviation from the main trend (the degree of "scatter") and it's Al_2O_3 and normative C, hy and qz contents, which strongly suggests that crustal contamination is a major cause of the scatter. Some rocks, especially the tuffs, may have been affected by alteration and the associated alkali loss would result in C appearing in the norm.

A significant minority, however, of the felsic lavas which show scatter on variation diagrams do not have abnormal Al_2O_3 contents or contain normative C, although some are hy- or qz-normative. These lavas show significant scatter on Y, Ce, Rb and Nd (against Zr) diagrams but limited scatter on Na_2O and K_2O (against SiO_2) diagrams. This would indicate that these lavas have been affected by late-stage or post-magmatic fluid- and/or vapour-phase transfer processes. Such processes are common among the products of extreme fractionation. Peralkaline lavas often appear to have lost Na (Noble, 1965) and gained or lost Si, K, the halogens and the alkaline earth elements (Noble *et al*, 1967; Noble, 1968) on or very shortly after crystallisation. Weaver *et al* (1972) note that some suites of trachytic and pantelleritic lavas from the East African Rift show loss of Ce and La (relative to Zr) and that rare earth elements are known to form volatile fluorides.

7.3.3 The Basanite–Phonolite Lineage

Does the basanite–nepheline hawaiite–nepheline mugearite–nepheline benmoreite–phonolite lineage proposed in chapter 5 really exist? The samples assigned to this lineage account for only 2.9% of all samples analysed from the Akaroa Volcanic Group. Examples of all members of the lineage except nepheline benmoreite have been reported here or in Falloon (1982). Comparing equivalent members of the basanite–phonolite and alkali olivine basalt–trachyte lineages, there is no statistically significant difference in mineralogy, and on most chemical variation diagrams the two lineages can not be separated.

However, there are a number of features which set members of the two lineages apart:

- Members of the basanite–phonolite lineage are moderately undersaturated with high average normative ne contents ($\overline{x} = 6.8\%$, $s = 1.83$, $n = 8$) com-

pared with the weakly undersaturated and less *ne*-normative lavas of the alkali olivine basalt–trachyte lineage ($\overline{x}$ = 2.48, s = 1.79, n = 148 for all *ne*-normative lavas).

- On an alkali–silica diagram, basanite–phonolite lavas are clearly more alkali-rich. In addition, the trend for basanite–phonolite lavas is steeper — that is, the extent of enrichment in alkalis increases with SiO_2 content. An analysis of a nepheline mugearite (N36C1315) reported by Falloon (1982) with 5.65% normative *ne* plots along this trend. The basanite–phonolite trend falls mid-way between the alkali olivine basalt–trachyte trend of the Akaroa Volcanic Group and the basanite–phonolite trend of the Dunedin Volcanic Group (Coombs and Wilkinson, 1969).

- Felsic members of the basanite–phonolite lineage become progressively more undersaturated with increasing SiO_2, whereas felsic members of the alkali olivine basalt–trachyte lineage become progressively more oversaturated (*qz*-normative).

- Basanite–phonolite lavas show less iron enrichment (Fig. 5.5), and have higher *Or* (Fig. 5.6) and Na_2O (Fig. 5.12), relative to alkali olivine basalt–trachyte lavas.

- REE patterns for mafic members of both lineages are indistinguishable, but the phonolite has a very distinctive concave-downward "dished" appearance, compared with trachytes which have a relatively straight overall pattern and a pronounced Eu anomaly. The "dished" pattern is typical of phonolites from many other volcanic provinces and is attributed to the effects of kaersutite fractionation as a significant process in their evolution. On the other hand, the pronounced Eu anomaly in trachytes points to their evolution being dominated by feldspar fractionation.

- The phonolite has a distinctly lower initial $^{87}Sr/^{86}Sr$ isotope ratio compared to the trachytes of the alkali olivine basalt–trachyte lineage, and contamination has clearly not been as important in the evolution of the phonolite (if at all) as it apparently has in the evolution of the trachytes.

The advantage of establishing two lineages is that it provides a better basis on which to compare and contrast the different processes that may operate at different stages in the evolution of Akaroa Volcanic Group lavas, such as magma generation, fractional crystallisation and combined assimilation/fractional crystallisation.

7.4 Generation of Akaroa Volcanic Group Magmas and the Nature of the Mantle Source

7.4.1 Models of Magma Genesis

Yoder and Tilley (1962), in their pioneering work on the origin of basaltic magmas and the melting relations of natural and synthetic rock systems, showed that basalts are the partial melt products of a more primitive rock (garnet peridotite), and that the region of magma generation is at depths of > 60 km. Establishment of the two major basalt types (tholeiite and alkali basalt) takes place in the region of magma generation; thus alkali basalt magmas are generated at greater depths than tholeiitic magmas and involve smaller degrees of partial melting of the mantle source.

Green and Ringwood (1967), in a detailed experimental investigation of the relations in Yoder and Tilley's "basalt tetrahedron" (Fig. 7.3) and the genesis and fractionation of natural basaltic compositions under conditions of high pressure and temperature, showed that the composition of the first liquid formed by a partial melting event is depth/pressure dependent, and sensitive to the depth segregation of the partial melt from the residual phases. Small to moderate degrees of partial melting (< 20%) of a pyrolite source composition and segregation of the melt at depths of 35–70 km will produce alkali olivine basalt magma. Experiments on olivine tholeiite fractionating at 10–20 kb showed that the olivine field of crystallisation contracts and aluminous orthopyroxene becomes the liquidus phase, followed later by subcalcic aluminous clinopyroxene. The effect is to drive residual liquids towards the plane of critical undersaturation. Fractionation of 15% pyroxene from an olivine tholeiite produces a residual liquid of olivine basalt lying on the plane of critical undersaturation. Continued fractionation of orthopyroxene (± subcalcic aluminous clinopyroxene) will drive the residual liquid across the plane of critical undersaturation into the alkali basalt field (Table 7.1). Experiments on alkali olivine basalt showed that aluminous orthopyroxene remains on the liquidus between 11–15 kb and is accompanied by subcalcic aluminous clinopyroxene. Crystallisation of these two phases drives the residual liquid deeper into the alkali olivine basalt field. At 13.5 kb, crystallisation of 2.5% aluminous orthopyroxene and 7.5% subcalcic aluminous clinopyroxene from an alkali olivine basalt generates a residual liquid with 5–6% normative nepheline and 23% normative olivine — an olivine-rich basanite. Similar results can be obtained by crystallisation of 20% subcalcic aluminous clinopyroxene at 18 kb.

The continuum of compositions from alkali olivine basalts to olivine basanites and olivine nephelinites suggests a common fractionation mechanism. The above studies show that a pathway from olivine tholeiites through alkali olivine basalts to the

Table 7.1: Fractionation of olivine basalt at 13.5 kb and 18 kb (after Green and Ringwood, 1967).

Pressure (kb)		13.5	18
Temperature (°C)		1310	1335
Nature and estimated percentage of minerals		10% Opx	5% Opx 10% Cpx
Composition of crystal extract:			
SiO_2		53.8	51.9
Al_2O_3		6.4	8.6
FeO		6.6	5.8
MgO		30.3	25.6
CaO		2.9	8.1
Composition of residual liquid:			
	Initial liquid		
SiO_2	47.1	46.4	46.3
TiO_2	2.3	2.6	2.7
Al_2O_3	14.2	15.0	15.1
Fe_2O_3	0.4	0.5	0.5
FeO	10.6	11.1	11.5
MnO	0.2	0.2	0.2
MgO	12.7	10.8	10.4
CaO	9.9	10.6	10.2
Na_2O	2.2	2.5	2.6
K_2O	0.4	0.5	0.5
CIPW norm of residual liquid:			
or	2.7	3.0	3.3
ab	18.9	16.8	17.8
ne	-	2.4	2.3
an	27.3	28.1	27.8
di	17.6	19.9	18.6
hy	1.3	-	-
ol	27.2	24.2	24.3
il	4.4	5.0	5.1
mt	0.6	0.7	0.8
$Mg/(Mg+Fe^{++})$	0.68	0.63	0.62

edge of the basanite (6% normative nepheline) field exists, but this pathway is not capable of yielding the entire range of basanites (10–15% normative nepheline) and nephelinites (15–30% normative nepheline) observed. Studies of this series of rocks (Bultitude and Green, 1968, 1971; Green and Hibberson, 1970; Green, 1969, 1970, 1973) showed that under anhydrous conditions, the dominant phases crystallising at up to 30 kb are olivine and clinopyroxene, but extraction of these phases does not lead to a substantive increase in nepheline content. Separation of orthopyroxene (± subcalcic clinopyroxene) is required to generate basanites and nephelinites by fractionation of alkali olivine basalt. Bultitude and Green (1968, 1971) showed that addition of H_2O to alkali olivine basalt melts causes an expansion of the primary field of crystallisation of orthopyroxene at high pressures. This was confirmed by experiments with an olivine basanite containing 11% normative nepheline (Green, 1973).

Similarly, Kushiro *et al* (1972), in an experimental study of the melting relationships of garnet lherzolite, showed that 10–15% melting of garnet lherzolite with 2% phlogopite would produce an alkali picrite basalt at 30 kb (approximately 100 km) under anhydrous conditions. Smaller degrees of partial melting would produce less magnesian basanitic magma under the same conditions.

These results indicate that, provided H_2O and CO_2 are present in the source regions of basaltic magmas, fractionation by crystallisation of orthopyroxene extends across the entire compositional range from olivine tholeiite through alkali olivine basalt to basanite and nephelinite. Orthopyroxene fractionation will deplete the magma of SiO_2 and enrich it in CaO and alkalis. A higher pressure (20–35 kb) is required for the alkali olivine basalt–basanite transition than for the olivine tholeiite–alkali olivine basalt transition (10–20 kb).

Note that these experiments emphasize the role of fractional crystallisation, primarily because of experimental constraints. Chemical equilibrium is independent of relative proportions of liquid and crystalline phases — thus the chemical equilibrium between 5% crystals and 95% liquid would not change if proportions were reversed to 5% liquid and 95% crystalline phases. Thus fractional crystallisation of primary melts at high pressure, and partial melting of a mantle source can generate the same basalt compositions, and the residual refractory phases after partial melting are given by the compositions of phases on the liquidus of the basalt.

Taking anhydrous pyrolite as the mantle source composition, at 35–70 km depth, whether olivine tholeiite or alkali olivine basalt is formed depends on the degree of partial melting. 5–10% partial melting leaves residual olivine, abundant aluminous orthopyroxene ± aluminous clinopyroxene and the liquid is an olivine-rich alkali basalt. At 25% partial melting, much of the clinopyroxene and orthopyroxene enter the liquid, which becomes an olivine tholeiite. At high pressures ($\approx$ 27 kb, 1250°C) an olivine basanite (10% normative *ne*, 26% olivine) could be formed by a par-

tial melt of 3–6% of pyrolite with 2–4% water present, leaving a garnet peridotite residuum.

Schwarzer and Rogers (1974) could find no systematic differences in major element composition between alkali olivine basalts from continental, oceanic and island arc environments. This was interpreted as evidence that alkali olivine basalt is a primary magma generated at sufficient depth in the mantle that major element chemistry is unaffected by chemical and thermal differences between mantle regions underlying continental, oceanic and island arc environments. For example, note the overlap of the Akaroa Volcanic Group with the Hawaiian field on a ϵ_{Nd}–$^{87}Sr/^{86}Sr$ plot (Fig. 6.3), interpreted as evidence that the mantle source for both provinces was in the asthenosphere. Furthermore, Schwarzer and Rogers (1974) noted that late differentiates of trachyte lava can be classified into four kinds of residual liquid (peralkaline oversaturated, peraluminous oversaturated, peralkaline undersaturated and peraluminous undersaturated) and that the liquid composition produced by differentiation of trachytic magma is not dependent on prolonged fractionation or fractionation of any particular phase or combination of phases, but is a function of the degree of (under-)saturation of the parental basaltic magma.

Frey *et al* (1978) showed that a single pyrolite source composition could yield a range of magma types, depending on the degree of partial melting and the degree of trace element enrichment of the source prior to melting. A source enriched in Ba, Sr, Th and LREE at 6–9 × chondrite abundances and in Ti, Zr, Hf, Y and HREE at 2–3 × chondrite abundances could yield olivine melilite (4–6% melt), olivine nephelinite and basanite (5–7% melt), alkali olivine basalt (11–15% melt) or olivine basalt and olivine tholeiite (20–25% melt) magma. If the source rock has chondritic relative REE abundances at 2–5 × chondritic levels, smaller degrees of partial melting are required to generate olivine melilite (0–4% melt) and basanite (1% melt) magmas. However, under these conditions it is not possible to generate olivine tholeiite magmas.

These studies suggest a model for the generation of Akaroa Volcanic Group magmas involving small to moderate degrees ($< 20\%$) of partial melting of a garnet peridotite mantle source at depths of 60–100 km. Moderate degrees of partial melting generated melts that fractionated to produce members of the alkali olivine basalt–trachyte lineage. Basanitic magmas that fractionated to produce members of the basanite–phonolite lineage may have been generated either by smaller degrees of partial melting leaving residual orthopyroxene, or by high-pressure fractionation of orthopyroxene from an alkali olivine basalt melt.

7.4.2 Identification of Primary Akaroa Volcanic Group Melts

One purpose of petrogenetic studies is the use of major and trace element constraints to elucidate processes of magma genesis and evolution. It is necessary to first identify those magmas that are primary melts, as the nature of the primary melt produced by the partial melting event has a major controlling influence on the evolutionary path and the nature of late-stage differentiates.

O'Hara (1965) argues that nearly all observed basaltic magmas have suffered extensive fractionation during their journeys to the surface and do not represent primary liquids. Evidence for this comes from the fact that many basaltic liquids are close to an olivine-plagioclase-pyroxene cotectic when erupted. In comparison, experimental studies show liquids formed at depth in the mantle and in equilibrium with olivine ($\pm$ orthopyroxene) depart significantly from the low pressure cotectics. This view may be correct in many instances (especially continental tholeiites). MacDonald and Katsura (1964) demonstrated that high-level olivine fractionation was important in modifying the composition of Hawaiian tholeiites.

On the other hand, many occurrences of alkali basalts, basanites and nephelinites have since been described which erupted very quickly and with sufficient velocity to bring large mantle xenoliths and high pressure xenocrysts to the surface. Under these conditions, it is unlikely that olivine crystals would have been efficiently removed from the melt.

Three criteria have been suggested by various authors (eg. McBirney, 1984; Sun and Hanson, 1975; Wilkinson, 1982) for identifying primary parental melt compositions: (i) the presence of mantle-derived xenoliths and megacrysts, (ii) Mg number (100 $Mg/(Mg + Fe^{2+})$) of lavas, and (iii) concentrations of compatible trace elements such as Cr and Ni.

Xenoliths of Mantle Origin in Alkali Basalt Suites

Occurrences of peridotitic and pyroxenitic xenoliths in alkali basalt, basanite and nephelinite lavas have been recorded from many localities (see Menzies (1983) for an extensive list). In most localities, spinel lherzolite is the dominant xenolith rock type, and the constituent orthopyroxenes characteristically contain substantial amounts of Al_2O_3 — typically 3–7%. The complex thermal history and equilibration textures commonly exhibited by these xenoliths has lead most workers to the conclusion that such xenoliths are of accidental origin rather than cognate origin relative to their host magma, and represent samples of (i) parental upper mantle, (ii) mantle residua, (iii) ancient cumulates, (iv) conduit precipitates, or (v) any of

these modified by the passage of basaltic magmas.

The significance of the presence of these mantle-derived xenoliths in alkaline basaltic magmas, in terms of identifying primary melts, is that they imply rapid ascent of the host magma from the zone of partial melting without substantive fractional crystallisation or reaction with wallrock material. If xenoliths can not be effectively removed from the ascending magma, then it would seem unlikely that crystals of olivine, pyroxene and plagioclase could effectively be removed. The presence of mantle-derived xenoliths in alkaline basaltic magmas erupted at the earth's surface is one line of evidence that the host magma has not been substantially modified from the original partial melt, and can therefore be used as an estimate of the composition of the melt that formed in equilibrium with the mantle source.

In the case of Akaroa Volcanic Group lavas, mantle-derived xenoliths have not been observed. However, their absence does not necessarily imply that all Akaroa Volcanic Group magmas have undergone substantial modification during ascent.

Mg Numbers of Liquids in Equilibrium with Mantle Peridotites

The term Mg number is used in this thesis to refer to the atomic ratio 100 Mg/(Mg + Fe^{2+}). Frey *et al* (1978) use the term "Mg-value" for the same ratio, while Wilkinson (1982) uses the terms "M-value" and "mg"[1].

The calculated Mg number of an aphyric basalt, or of the source peridotite with which a basaltic liquid (for which the Mg number is known) is assumed to have been in equilibrium, is a function of the equilibrium distribution coefficient K_D for Fe and Mg between olivine and liquid:

$$K_{D_{ol/liq}}^{Fe/Mg} = \frac{(X_{FeO}^{ol})}{(X_{FeO}^{liq})} \frac{(X_{MgO}^{liq})}{(X_{MgO}^{ol})}$$

where X_a^b is the mole fraction of chemical species a in phase b. Roedder and Emslie (1970) determined that $K_{D_{ol/liq}}^{Fe/Mg} \approx 0.3$ and is independent of temperature and oxygen fugacity over a wide range of T–f_{O_2} conditions (1150–1300°C, $f_{O_2} = 10^{-0.68}$–10^{-12} atm). Based on experimental studies, Irving (1971) showed that $K_{D_{ol/liq}}^{Fe/Mg}$ was independent of pressure for basaltic compositions up to 30 kb. McBirney (1984) quotes

[1] M = 100 Mg/(Mg+Fe^{2+}) if Fe^{2+} and Fe^{3+} are known. When Fe^{3+} is unknown or is relatively small, the parameter mg = 100 Mg/(Mg+$\sum$Fe) is used, where $\sum$Fe is total iron calculated as Fe^{2+}.

$K_{D_{ol/liq}}^{Fe/Mg} = 0.3 \pm 0.03$ and Wilkinson (1982) adopts a value of 0.33. Data from refractory ultramafic inclusions in alkali basalts and kimberlites indicate that the compositional variation of residual mantle olivine ranges from Fo_{88} to Fo_{92} (Green, 1970). Thus, primary basalt magma in equilibrium with mantle olivine should have Mg numbers of 68–77 (Green, 1971) for $K_{D_{ol/liq}}^{Fe/Mg} = 0.3$. Frey *et al* (1978) suggests the least refractory upper mantle peridotite compositions have Mg numbers of $\approx$ 88–89, for which basalt magmas derived from such a source must have Mg numbers of $\approx$ 68–75.

Wilkinson (1982) notes that histograms of Mg numbers for ocean floor basalt glasses from many localities (Fig. 7.4) are characterised by (i) a wide range of Mg numbers (35–70), (ii) maxima in the range 55–65, and (iii) a small percentage (<1–5%) of compositions in which the Mg number approaches 70. Similar histograms of Mg numbers have been reported for large populations of crystalline basalts (Bence *et al*, 1979; Papike and Bence, 1978; Walker *et al*, 1979; Stolper and Walker, 1980). Significantly, the histogram of Mg numbers of the average compositions of alkali olivine basalts from 64 alkali volcanic provinces (Fig. 7.4) shows a similar distribution (Schwarzer and Rogers, 1974), as does a histogram of 3000 oceanic-island basalts (Stolper and Walker, 1980). These distributions are not as expected of a conventional fractional crystallisation model in which the highest frequencies are for parental liquids. Perhaps mantle sources are more heterogeneous and Fe-rich than previously thought. Based on this apparent natural limit to Mg numbers, and data relating to mantle olivine compositions already cited, an Mg number of 70±2 has been widely adopted as one parameter defining primary unfractionated basaltic melt compositions and many studies assume basalts with lower Mg numbers have undergone ferromagnesian fractionation.

Direct, accurate assessment of the primary magma composition of Akaroa Volcanic Group is difficult because of the overall evolved nature of Akaroa Volcanic Group lavas. The dominant lava type is hawaiite, rather than basalt. Few Akaroa Volcanic Group lavas have Mg numbers > 60 and the maxima for basaltic lavas is in the range 42–52 (Fig. 7.5), indicating that even the most primitive Akaroa Volcanic Group basalts have undergone fractionation of ferromagnesian minerals, probably during their ascent from the mantle source region to a high-level crustal reservoir. As noted in chapter 5, the mineralogy of Akaroa Volcanic Group basalts and basanitoids is consistent with olivine and clinopyroxene fractionation. It is possible to estimate both the amount of olivine (± clinopyroxene) fractionation and the composition of the primary magma by assuming:

1. The primary magma of the Akaroa Volcanic Group was in equilibrium with residual mantle olivine of composition Fo_{88}–Fo_{92} and had an Mg number in the range 68–77.

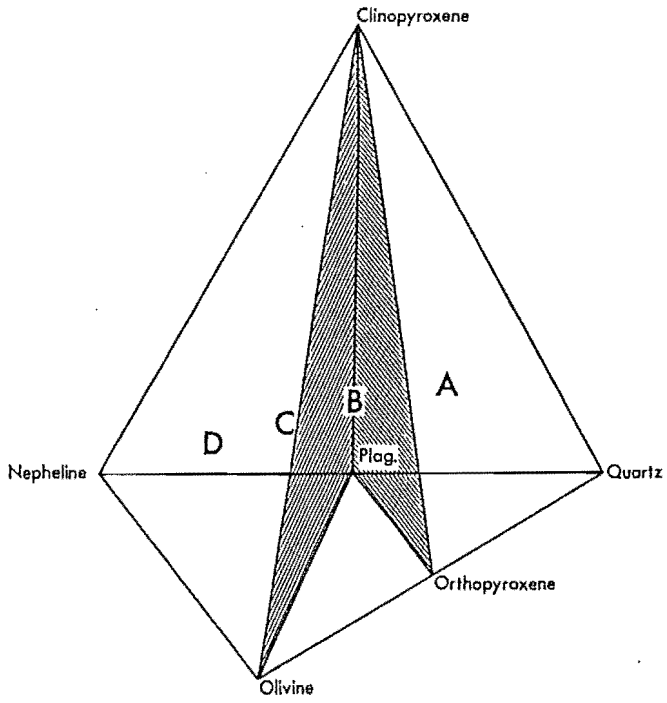

Figure 7.3: Representation of the major mineralogy of basalts using Yoder and Tilley's "basalt tetrahedron". The plane olivine-clinopyroxene-plagioclase is referred to as the plane of critical undersaturation. A–field of quartz tholeiites; B–field of olivine tholeiites; C–field of alkali olivine basalts; D–field of olivine basanites.

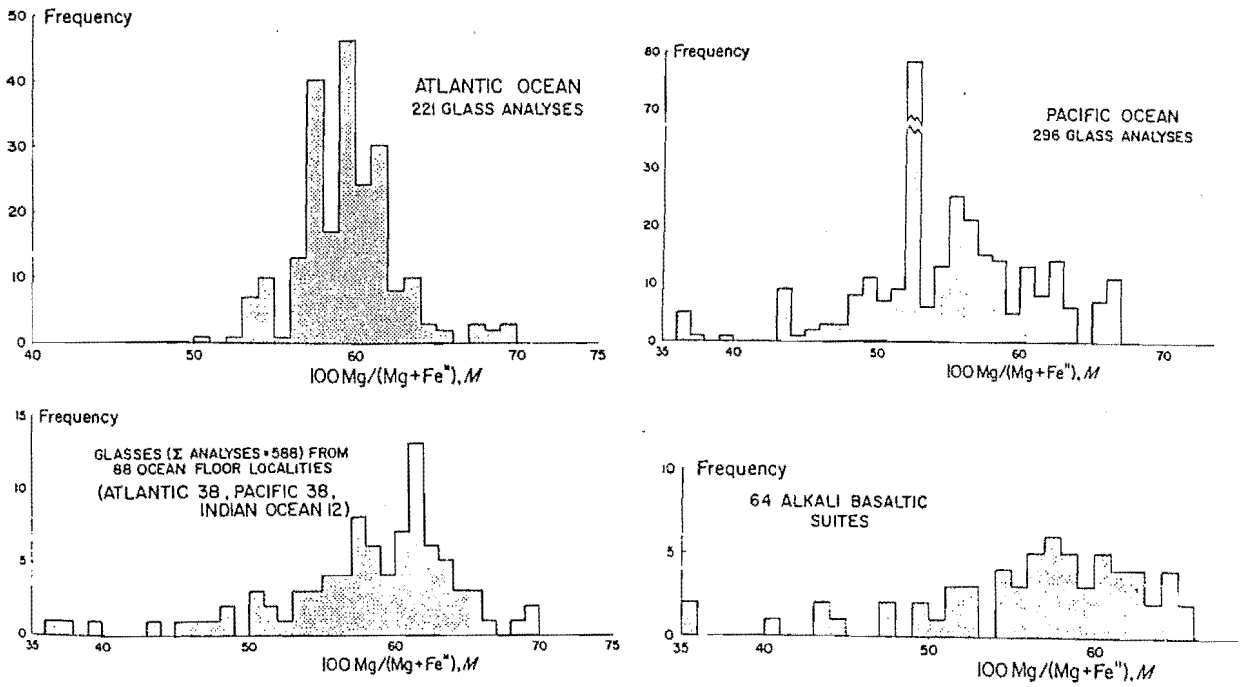

Figure 7.4: Frequency histograms of Mg numbers for ocean floor basalts and alkali basaltic suites (after Wilkinson, 1982).

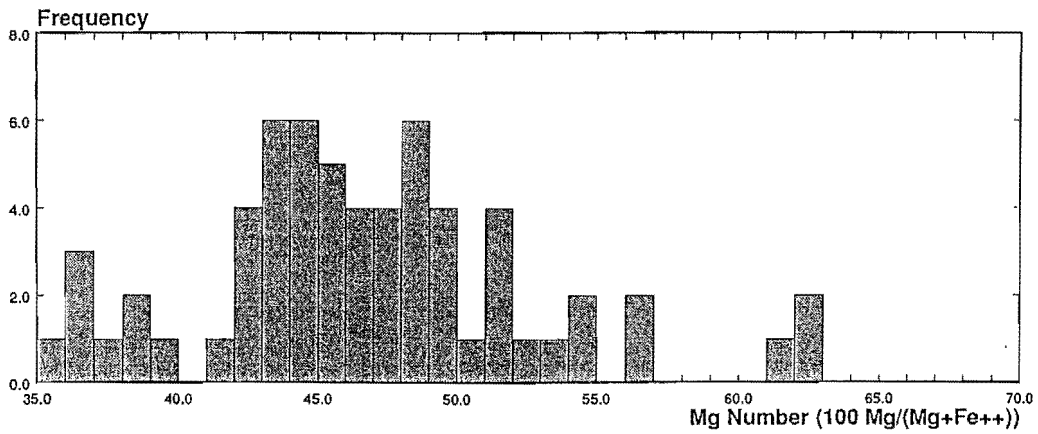

Figure 7.5: Absolute frequency histogram of Mg numbers for Akaroa Volcanic Group basalts and basanitoids.

2. The most primitive Akaroa Volcanic Group basalts were derived from this primary magma solely by fractionation of olivine.

and adding olivine of an appropriate composition to the most primitive basalt composition until the resulting magma composition has an Mg number > 68. Five samples from Akaroa Volcanic Group were selected for this calculation. Samples N36C3037, N36C3071 and N36C3652 are the most primitive lavas (all *ne*-basalts) collected during this study and have Mg numbers in the range 61.55–62.50. Sample N36C3316 is a basanitoid collected during this study (Mg number = 45.97) and sample N36C1305 is a *ne*-basalt (Mg number = 63.87) from Falloon (1982). The last two samples were selected because they are the most primitive alkali olivine basalt and basanitoid for which REE data are also available. Calculations were performed for pure olivine fractionation, and the calculated primary magma compositions and % olivine added are presented in Table 7.2. Using these results, estimates of the degree of partial melting can be made. Taking average mantle pyrolite (Ringwood, 1975) as a model source composition, and assuming that K_2O and P_2O_5 are completely partitioned into the melt, then the K_2O and P_2O_5 contents of pyrolite and the liquid (the primary magma calculated above) define the degree of partial melting. The assumption that K_2O and P_2O_5 are completely partitioned into the melt is based on the extremely low K_2O and P_2O_5 contents of the liquidus phases of basaltic magmas and the absence of phlogopite on the liquidus of basaltic magmas at high pressures unless K_2O contents are very high (Green and Ringwood, 1967). These calculations may be invalidated if mantle apatite, phlogopite or amphibole are involved in the genesis of these magmas, or if K_2O contents have been affected by crustal contamination or wall rock interaction during the magma's ascent through the continental crust. Results are presented in Table 7.2.

A number of points should be noted:

1. Overall, the estimates of small degrees of partial melting are generally consistent with models of basalt genesis discussed previously. If anything, the values are a little on the low side.

2. The estimate of the percent partial melting for the basanitic magma is noticeably lower than estimates of the percent partial melting for alkali olivine basalts, as expected.

3. Results are internally consistent for K_2O, and for P_2O_5. For example, the values of percent partial melting for basalts calculated using P_2O_5 have a mean of 6.2 and a standard deviation of 0.26. However, estimates of the degree of partial melting based on P_2O_5 are about twice those based on K_2O. Perhaps the pyrolite composition used is not representative of the mantle source for Akaroa Volcanic Group magmas. For example, using another pyrolite model

Table 7.2: Simple models of "primary basalt magma" derived by addition of olivine to primitive Akaroa Volcanic Group lavas, and estimates of the degree of partial melting required to generate the model magmas from a pyrolite source composition.

Sample	N36C3037		N36C3071		N36C3652		N36C1305		N36C3316		Pyrolite
Rock type	*ne*-basalt		*ne*-basalt		*ne*-basalt		*ne*-basalt		basanitoid		
% olivine added		16		15		15		18		27	
SiO_2	43.41	42.73	44.77	43.93	44.44	43.65	44.11	43.22	45.78	43.99	45.1
TiO_2	2.86	2.40	2.79	2.37	2.83	2.41	2.80	2.30	3.52	2.57	0.2
Al_2O_3	12.85	10.79	13.23	11.25	13.24	11.25	13.06	10.71	16.34	11.93	4.6
Fe_2O_3	–	–	–	–	–	–	–	–	–	–	0.3
FeO	12.83	13.14	12.81	13.10	13.07	13.32	13.86	14.02	12.51	13.12	7.6
MnO	0.23	0.22	0.17	0.17	0.16	0.16	0.19	0.19	0.17	0.18	0.1
MgO	10.31	15.76	10.72	15.77	10.88	15.90	10.83	16.87	5.11	15.71	38.1
CaO	10.91	9.20	11.11	9.48	10.80	9.22	10.90	8.98	9.28	6.84	3.1
Na_2O	1.89	1.59	2.00	1.70	2.46	2.09	2.51	2.06	3.94	2.88	0.4
K_2O	0.94	0.79	0.82	0.70	0.92	0.78	0.88	0.72	1.34	0.98	0.02
P_2O_5	0.40	0.34	0.38	0.32	0.39	0.33	0.38	0.31	0.57	0.42	0.02
Mg number	61.55	68.13	62.50	68.20	62.34	68.03	63.87	68.19	45.97	68.10	
% melting based on:											
K_2O		2.5		2.9		2.6		2.8		2.0	
P_2O_5		5.9		6.3		6.1		6.5		4.8	

1. For each sample, the left hand column is the original sample analysis used for the calculation, and the right hand column is the model calculated from the original analysis by addition of olivine. The rock type (eg. *ne*-basalt) is the classification of the original sample.
2. Fe_2O_3 and FeO in the original sample major element analyses were recalculated to FeO using the formula $FeO = FeO + 0.899812 \times Fe_2O_3$ because all iron is expressed as FeO in olivine analyses.
3. A microprobe analysis from an olivine phenocryst core (point #5.1, sample N36C3071, Appendix F) was used as the composition of olivine added. This composition is the most Mg-rich olivine (Fo_{84}) recorded from Akaroa Volcanic Group basalts.
4. The pyrolite composition used as a model mantle source composition is from Ringwood (1975).

composition (K_2O = 0.13%, P_2O_5 = 0.06%; from Ringwood, 1966) which Ringwood (1975) thought was "probably too high in ... K, Na, and P, owing to choice of the particular basalt component", the estimates based on K_2O and P_2O_5 are in much better agreement with one-another, but are much higher than expected — 17–23% for alkali olivine basalt magmas and 14–18% for basanitic magmas. A residual K_2O-bearing phase (phlogopite?) would seem unlikely, even at these levels of partial melting, as would enrichment of the source in a P_2O_5-bearing phase such as apatite. The fact that K_2O estimates are lower argues against contamination of the magma during ascent as a possible explanation for the variations, since contamination would preferentially affect K_2O contents.

It must be stressed that these calculations are very tenuous and rely on assumptions many of which can not be validated from observations of natural or synthetic systems. In particular, the assumption of olivine fractionation takes no account of the possible influences of the fractionation of chromite, spinel or orthopyroxene at high pressure. However, there is no information available (eg. xenoliths containing chromite, spinel or orthopyroxene) from Akaroa Volcano to indicate that these mineral phases were involved in the genesis of Akaroa Volcano Group magmas. While tenuous, the calculations presented here do provide at least an initial working hypothesis for the evolution of Akaroa Volcano Group magmas, which can be tested as more data become available.

Concentrations of Compatible Trace Elements

Compatible trace elements (eg. Cr and Ni) have mineral/liquid distribution coefficients > 1 for one or more major upper mantle phases (eg. olivine, pyroxene, garnet) and are therefore very sensitive to fractional crystallisation. Some workers (Batiza *et al*, 1977; Bence *et al*, 1975; Frey *et al*, 1974b; Kay *et al*, 1970) have used apparent natural limits of MgO and Ni as indicators of relatively undifferentiated basalts. Sun and Hanson (1975) suggest 300–400 ppm Ni is a reasonable concentration for an alkali basalt magma in equilibrium with mantle peridotite containing 2000 ppm Ni. Frey *et al* (1978) noted that all mafic lavas in their study (including olivine melilite, olivine nephelinite, basanite and alkali olivine basalt) that were identified as primary melts on the basis of the presence of spinel lherzolite xenoliths and/or Mg numbers in the range 68–75, had 280–460 ppm Ni and 310–520 ppm Cr.

The most primitive Akaroa Volcanic Group lavas (based on Mg number) have Ni concentrations of 15.6–239.9 ppm and Cr concentrations of 20.1–419.3 ppm. The Cr concentrations are comparable with those reported by Frey *et al* (1978), whereas the Ni concentrations are distinctly lower and are more comparable with Ni concentrations in Ross Island basanitoids (170–290 ppm) which Sun and Hanson (1975)

considered had undergone $\approx$ 10% fractionation of olivine and clinopyroxene. The depletion of Ni as opposed to Cr is consistent with the model of olivine fractionation presented in Table 7.2, since $K^{Ni}_{D_{ol/liq}} \gg K^{Cr}_{D_{ol/liq}}$. The Ni concentrations can therefore be used to estimate the amount of olivine fractionation $(1 - F)$ using the Rayleigh fractionation law (Rayleigh, 1896) as applied by Neumann *et al* (1954):

$$C_L/C_O = F^{(D-1)}$$

Results for four of the samples from Table 7.2 are presented in Table 7.3. Calculations

Table 7.3: Extent of olivine fractionation $(1 - F)$ calculated from Ni concentrations for primitive Akaroa Volcanic Group lavas.

Sample	Cr (ppm)	Ni (ppm)	Mg Number	$(1 - F) \times 100.0$
N36C3037	419.3	239.9	62.50	7.39–8.81
N36C3071	376.8	200.5	61.55	5.52–6.98
N36C3652	366.5	196.5	42.27	30.26–31.34
N36C3316	20.1	15.6	62.34	24.66–25.82

were performed using $K^{Ni}_{D_{ol/liq}} = 10.0$ (Vicenzi *et al, in press*), $C_O = 400$ ppm and 460 ppm (hence the range in F values). Only the result for N36C3316 agrees closely with the results in Table 7.2. The other samples give results of 0.5–2.0 $\times$ the % olivine fractionation calculated in Table 7.2. Considering, however, the uncertainty in the data and assumptions, the agreement is quite good. Wilkinson (1982) cautions that limiting Ni contents should be applied with care, since the use of a constant $K^{Ni}_{D_{ol/liq}}$ does not take account of pressure effects and the role of NiS. Furthermore, there is no *a priori* reason why magmas should not have equilibrated with more Fe-rich mantle peridotites than currently assumed, and this would also be an alternative explanation for the paucity of magmas with Mg numbers approaching 70. In the case of some of the Akaroa Volcanic Group lavas used in the calculation, some have up to 35% (cumulate?) olivine ($\pm$ clinopyroxene) phenocrysts which may be distorting the results.

Despite these problems, both Mg numbers and Ni concentrations indicate that even the most primitive Akaroa Volcanic Group lavas have undergone some olivine fractionation.

7.4.3 Petrogenetic Models Based on REE

The percentages of olivine fractionation calculated in Table 7.2 can also be used to estimate the REE abundances in the primary magmas in the same way that the

major element compositions were determined. During fractional crystallisation, the concentration of a given element in the melt, C_L, relative to the concentration in the parent melt, C_O, is defined by the Rayleigh fractionation law:

$$C_L/C_O = F^{(D-1)}$$

where F is the fraction of melt remaining and D is the bulk distribution coefficient for the minerals crystallising from the melt. If the values of F, D and C_L are known or estimated, then C_O can be calculated by rearranging the equation as follows:

$$C_O = C_L/F^{(D-1)}$$

Mineral-liquid distribution coefficients (K_D's) for olivine were selected from Kyle (1981), and are presented in Table 7.4. Values of F can be calculated from the % olivine fractionation in Table 7.2. Using the measured REE abundances for samples N36C1305 and N36C3316 as C_L, the REE abundances in the primary magma (C_O) can be calculated (Table 7.5).

Olivine/melt distribution coefficients are relatively constant across the REE series (≈ 0.01), so the shape of the REE pattern is not altered significantly, but REE abundances increase relative to chondrite values. Even assuming large amounts of olivine fractionation ($> 40\%$), the REE patterns retain their approximately linear, LREE-enriched character, with LREE 35–60 $\times$ chondrite relative abundances and HREE are 5–7 $\times$ chondrite relative abundances. In particular, the Ce_N/Yb_N ratios of the calculated primary magmas are virtually identical to those of samples N36C1305 and N36C3316.

If the calculated REE patterns are reasonable estimates of the actual REE patterns of primary Akaroa Volcanic Group magmas, then the LREE-enriched character of Akaroa Volcanic Group lavas is a function of the composition of the mantle source and/or the effects of the partial melting process.

There are two end-member models for melting: *batch melting* and *fractional melting*. In batch melting, the trace elements in the melt and the solid residuum are in equilibrium as melting proceeds until enough melt accumulates so that it can migrate away from the zone of melting, and melting ceases. The composition of a trace element in a partial melt derived by batch melting is defined by (Schilling, 1966):

$$C_L/C_O = 1/(D(1-F)+F)$$

where C_L is the concentration of the trace element in the melt, C_O is the initial concentration of the trace element in the system, D is the bulk solid/melt distribution coefficient at the time of removal of the melt, and F is the fraction of melt. Fractional melting involves the continuous and complete removal of small melt fractions as melting proceeds, and the composition of a trace element in the melt is defined

Table 7.4: Mineral/liquid distribution coefficients for rare earth elements, used in fractional crystallisation modelling, after Kyle (1981). Values in brackets determined by interpolation and extrapolation.

	Olivine	Clinopyroxene		Kaersutite	Plagioclase		Anorthoclase	Sanidine	Apatite
La	(0.009)*	0.02	0.10	0.31	(0.023)	(0.280)	0.219	(0.225)	(15.2)
Ce	0.009	0.04	0.18	0.49	0.023	0.215	0.173	0.223	16.6
Pr	(0.010)	(0.07)	(0.28)	(0.67)	(0.023)	(0.193)	(0.162)	(0.222)	(18.0)
Nd	0.010	0.09	0.38	0.85	0.023	0.170	0.152	0.219	21.0
Sm	0.011	0.14	0.56	1.07	0.024	0.135	0.139	0.221	20.7
Eu	0.010	0.16	0.58	1.09	0.232	1.10	1.72	2.35	14.5
Gd	0.012	(0.18)	0.70	1.16	(0.017)	0.127	0.131	(0.221)	21.7
Tb	(0.013)	0.19	(0.73)	(1.12)	(0.018)	(0.111)	(0.130)	(0.220)	(19.8)
Dy	0.014	(0.19)	0.76	1.08	0.018	0.094	0.130	0.220	16.9
Ho	(0.016)	0.195	(0.74)	(1.02)	(0.019)	(0.086)	(0.129)	(0.220)	(15.5)
Er	0.017	(0.20)	0.71	0.96	0.020	0.078	0.128	0.219	14.1
Yb	0.023	0.20	0.61	0.78	0.030	0.062	0.116	0.227	9.4
Sr	0.009	0.119	1.51	0.58	1.36	4.62	5.57	3.08	0.83
Ba	0.009	0.031	0.321	0.62	0.15	1.47	5.04	3.20	0.014
Source	1,2	1,4	3,4	3,4	1,2	4	4	3,4	5,6

1. Schnetzler and Philpotts (1970).
2. Philpotts and Schnetzler (1970).
3. Nagasawa (1973).
4. Sun and Hanson (1976).
5. Nagasawa and Schnetzler (1971).
6. Mason (1972).

for modal melting:

$$C_L/C_O = (1/D)(1-F)^{[(1/D)-1]}$$

and non-modal melting (Shaw, 1970):

$$C_L/C_O = (1/D_O)(1-PF/D_O)^{[(1/P)-1]}$$

where D_O is the value of D for the first melt increment and P accounts for the proportion of minerals which go into the melt for non-modal melting. *Continuous* melting is an intermediate process in which fractions of melt are continuously but not completely removed from the mantle residuum as melting proceeds. The concentration of a trace element is defined by the batch melting equation, using new D values and calculating a new C_O after each increment:

$$C_O = [(1-F)C_S + (F-YF)C_L]/(1-YF)$$

where F is the extent of melting for each increment, Y is the proportion of F that escapes, and C_S and C_L are the concentrations from the previous increment of melting. Using these equations, published K_D's, and assuming a mantle source mineralogy, residual mineralogy and an initial mantle source REE pattern, REE patterns for melts derived from different degrees of partial melting can be calculated (Hanson, 1980). To model the REE patterns of primary magmas, the following assumptions were made:

1. The mantle source was a garnet lherzolite consisting originally of 55% olivine, 25% orthopyroxene, 15% clinopyroxene and 5% garnet. At 5% melting, the source residuum has the composition 58% olivine, 26% orthopyroxene, 14% clinopyroxene, 2% garnet. At 15% melting there is no garnet in the residuum.

2. The mantle has a chondritic REE pattern, but REE abundances relative to chondrite may be > 1 (Hanson, 1980).

3. K_D's for melting of mantle material are taken from Hanson (1980) and are presented in Table 7.6.

Melts derived by 0–5% batch melting of this mantle source have REE patterns and Ce_N/Yb_N ratios that encompass those of samples N36C1305 (*ne*-basalt) and N36C3316 (basanitoid) from Akaroa Volcano (Fig. 7.6; Hanson, 1980). For 0% and 5% melting, the Ce_N/Yb_N ratios are $\approx$ 15 and 3, compared with 7.12 and 9.34 for samples N36C1305 and N36C3316. On the basis of this model, Akaroa Volcanic Group magmas could have been generated by $< 5\%$ partial melting of a garnet lherzolite source. This model indicates that the mode of melting has little effect on the REE pattern of the melt at small degrees of partial melting. For example, at 5% partial melting the REE patterns of melts generated by batch and continuous melting are almost identical (Fig. 7.6).

Table 7.5: Calculated chondrite-normalised REE abundances for "primary basalt magma" models, calculated from measured chondrite-normalised REE patterns assuming the olivine fractionation models presented in Table 7.2.

Sample	N36C1305		N36C3316	
	Measured	Calculated	Measured	Calculated
% olivine		23		31
Ce	55.03	45.21	84.86	62.12
Nd	40.48	33.26	56.51	41.38
Sm	28.57	23.48	38.42	28.14
Eu	24.68	20.28	32.47	23.78
Tb	15.38	12.64	19.23	14.10
Yb	7.73	6.37	9.09	6.68
Ce_N/Yb_N	7.12	7.10	9.34	9.30

Table 7.6: Mineral-silicate melt distribution coefficients used in mantle melting models (after Hanson, 1980).

	Clinopyroxene	Orthopyroxene	Olivine	Garnet
Ce	0.098	0.0030	0.0005	0.021
Nd	0.21	0.0068	0.0010	0.087
Sm	0.26	0.010	0.0013	0.217
Eu	0.31	0.013	0.0016	0.320
Gd	0.30	0.016	0.0015	0.498
Dy	0.33	0.022	0.0017	1.06
Eu	0.30	0.030	0.0015	2.00
Yb	0.28	0.049	0.0015	4.03

Models involving very small degrees of partial melting of a chondritic source with REE abundances 2–5 × chondritic abundance became popular in the 1970's (eg. Kay and Gast, 1973). However, the perceived difficulty of physically extracting very small melt fractions from the mantle residuum lead some authors to suggest that LREE-enrichment of a time-integrated LREE-depleted mantle source immediately prior to melting would allow LREE-enriched melts to be generated at larger (5–15%) degrees of partial melting. In a study of basanitoids from Ross Island, Antarctica, Sun and Hanson (1975) suggested the mantle source (a garnet peridotite) had a non-chondritic REE pattern (Fig. 7.7) with abundances of 3 × (HREE), 4 × (Sm), 6.4 × (Nd), 10.5 × (Ce) and 13.7 × (La) chondrite abundances. Using this mantle composition, nephelinites can be produced by 3–7% partial melting and alkali basalts can be produced by 7–15% partial melting. Such an enriched source model would be consistent with isotopic and trace element ratios for Akaroa Volcanic Group lavas which suggest that the source underwent metasomatic enrichment just prior to the melting process (see chapter 6).

Campbell and Gorton (1980) have suggested an alternative to simple equilibrium mantle melting models — *disequilibrium melting* — to explain the strong LREE enrichment of rocks of the alkali basalt–kimberlite suite. Attempts to model the REE patterns of alkali basalts using the fractional or batch melting equations of Shaw (1970) show that changing the degree of partial melting for magmas generated from a mantle of a given composition has a much greater effect on LREE than HREE, resulting in a "fanning" of the REE patterns and different La/Sm ratios for different degrees of LREE enrichment and partial melting (Fig. 7.8). This is in marked contrast to the subparallel patterns observed in natural assemblages (Fig. 7.9, see also Fig. 5.33 for an example from Akaroa Volcano). Campbell and Gorton (1980) propose an alternative melting model based on disequilibrium melting of a LREE-enriched accessory phase in the mantle source. Accessory phases such as apatite crystallise in the final stages of solidification of a basaltic liquid, and can therefore be expected to be among the first to melt. For equilibrium melting, the REE concentration in the liquid is governed by the equilibrium between the liquid and the residual phases (Shaw, 1970), so if the accessory phases are the first to melt and are absent from the residuum while the melt is still in equilibrium with the residuum they will have no effect on the REE concentration in the melt (Kay and Gast, 1973).

The disequilibrium melting model requires that:

- Each mantle phase (major and accessory) melts to a liquid of it's own REE and trace element composition — a process referred to as *flash melting*.
- At small degrees of partial melting, the LREE-enriched accessory phase melts to form a liquid of it's own LREE-enriched composition. Although the melt

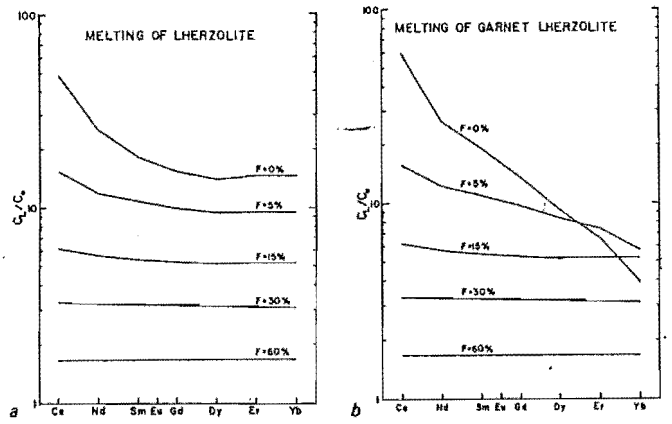

Figure 7.6: Calculated REE patterns for melts derived from different degrees of partial melting of garnet lherzolite consisting of originally of 55% olivine, 25% orthopyroxene, 15% clinopyroxene and 5% garnet. The data are normalised to the REE composition of the original garnet lherzolite. **Left:** Batch melting. **Right:** Continuous melting. After Hanson (1980).

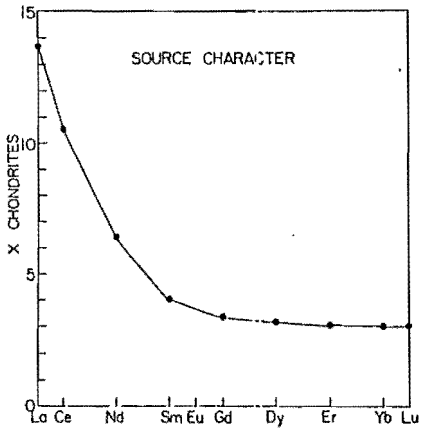

Figure 7.7: Proposed REE pattern for a LREE-enriched mantle source, after Sun and Hanson (1975).

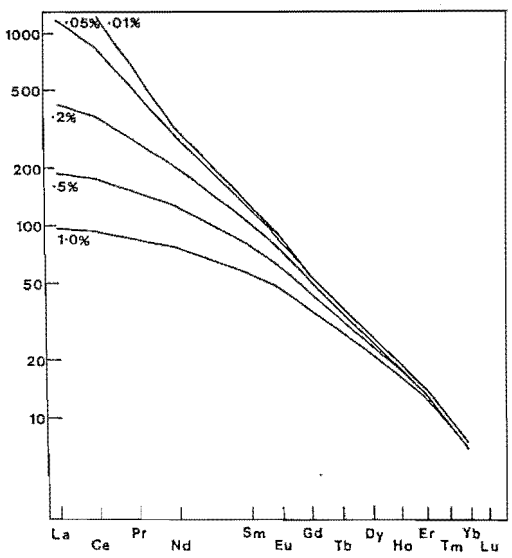

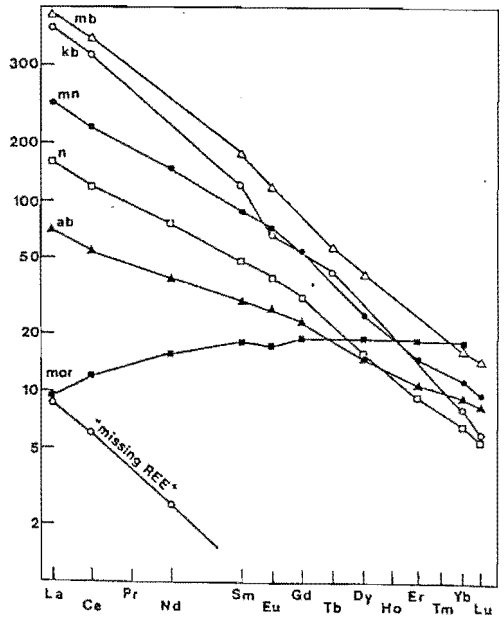

Figure 7.8: (**LEFT**) REE patterns for various degrees of partial melting of garnet peridotite containing 3.5% garnet (after Campbell and Gorton, 1980). Note the "fanning" effect caused by the strong enrichment in LREE compared to HREE, and the marked change in the La/Sm ratio with different degrees of partial melting.
Figure 7.9: (**RIGHT**) Examples of subparallel REE patterns with varying degrees of LREE enrichment, as found in natural assemblages (after Campbell and Gorton, 1980). *mb* = mafic breccia; *kb* = kimberlite; *mn* = melilite nephelinite; *n* = nephelinite; *ab* = alkali basalt; *mor* = average Atlantic MORB.

will later be diluted by mixing with the melting products of the major phases, the strongly LREE-enriched trace element pattern will remain.

- After flash melting, each melt must be removed from the source before any re-equilibration can occur between the melt and the residuum.

  In this respect, the disequilibrium melting model would appear to suffer from the same problems that beset models of alkali basalt magma genesis based on very small degrees of partial melting — the problem of physically removing such small melt fractions from the mantle residuum. However, recent studies by McKenzie (1985) of the fluid dynamic processes involved in the expulsion of melt from a matrix by compaction, suggest that the melt fraction present in the mantle melting zone at any one is likely to be very small — perhaps $<$ 1% for picritic melts — because of the forceful expulsion of the melt during compaction.

  The model does, however, allow for partial re-equilibration, based on a modification of the Shaw (1970) batch melting equation:

$$C_L = \frac{(C_{LF} \times [1 - E]) + (C_{SF} \times E)}{1 + E(D - 1)}$$

  where C_L is the final concentration of the element in the liquid, C_{LF} is the concentration of the element in the liquid after flash melting, C_{SF} is the concentration of the element in the solid residuum after flash melting, D is the equilibrium distribution coefficient for the element, and $E = S/(S + L)$ where S is the fraction of solid residuum in equilibrium with the liquid and L is the fraction of liquid. E is a measure of re-equilibration.

The disequilibrium melting model can stand moderate degrees of re-equilibration with an olivine-clinopyroxene-orthopyroxene residuum, but not re-equilibration with a garnet-bearing residuum. Changing the degree of partial melting will cause a change in the degree of LREE enrichment without significantly altering the slope of the REE pattern.

7.5 Modelling of Fractional Crystallisation

The fractional crystallisation models presented in chapter 5 for the alkali olivine basalt–hawaiite–mugearite–benmoreite–trachyte and basanite–nepheline hawaiite–nepheline mugearite–nepheline benmoreite–phonolite lineages were evaluated quantitatively using mass balance calculations based on the least-squares approximation technique of Bryan *et al* (1969).

Consider a system of n oxides and k components, for which x_{ij} is the observed amount of the ith oxide in the jth component (where $i = 1, n$ and $j = 1, k$); y_i is the observed amount of the ith oxide in the composition to be approximated; $\hat{b}_j$ is the estimated amount of the jth component required; and $\hat{y}_i$ is the estimated amount of the ith oxide required. The system can be defined by a set of linear equations represented by the matrix notation

$$XB = Y$$

where

$$X = \begin{bmatrix} x_{11} & x_{12} & x_{13} & \dots & x_{1k} \\ x_{21} & x_{22} & x_{23} & \dots & x_{2k} \\ x_{31} & x_{32} & x_{33} & \dots & x_{3k} \\ \vdots & \vdots & \vdots & & \vdots \\ x_{n1} & x_{n2} & x_{n3} & \dots & x_{nk} \end{bmatrix}$$

$$B' = [b_1, b_2, b_3, \dots b_k]$$

$$Y' = [y_1, y_2, y_3, \dots y_n]$$

B' and Y' are the transposes of the column vectors B and Y. $\hat{B}$, the estimator of B, is calculated from

$$\hat{B} = [X'X]^{-1}X'Y$$

and substituted into the left hand side of the matrix equation to obtain $\hat{Y}$, the estimator of Y. The elements of $\hat{Y}$ minimise the quantity

$$S = \sum_{i=1}^{n}(y_i - \hat{y}_i)^2$$

which is referred to as the sum of squares of residuals or $\sum r^2$.

All models were developed using major element analyses and tested by Rayleigh fractionation modelling of selected trace elements using the proportions of phases calculated from the major element models. All data were normalised to 100% volatile-free, and iron was recalculated as total FeO. Mineral/melt distribution coefficients (K_Ds) for use with the Rayleigh fractionation modelling were selected from the literature to closely approximate the range of compositions of fractionating phases, and are presented in Table 7.7.

Strongly compatible trace elements (eg. Ni, Cr and V) were omitted because the selection of K_Ds can strongly influence the acceptability of models, making the models more a test of the selection of K_Ds than a test of the least-squares solution.

Models were considered acceptable if $\sum r^2$ was low ($\sum r^2 \leq 1.0$ is reasonable; $\sum r^2 \leq 0.3$ is good; $\sum r^2 \leq 0.1$ is excellent) and the calculated trace element abundances

Table 7.7: Mineral/liquid distribution coefficients for selected trace elements used in least-squares mass balance calculations.

	Olivine	Clinopyroxene	Plagioclase†	Plagioclase‡	Titanomagnetite	Apatite	Kaersutite	Anorthoclase
Rb	0.008	0.015	0.029	0.138	0.01	0.01	0.3	0.01
Sr	0.02	0.16	1.36	4.62	0.16	0.83	0.58	5.57
Y	0.12	0.7	0.2	0.2	0.17	16.9	0.43	0.2
Zr	0.01	0.22	0.01	0.01	0.25	0.01	0.01	0.01
Nd	0.01	0.09	0.01	0.01	2.19	2.19	1.0	0.01
Source	1,6	1,6	1,6	1,6	3,6	1,6	2,3,4,5,6,7	2,7

† An_{65}

† An_{40}

1. Morris (1985b)
2. Kyle (1981)
3. Baker *et al* (1977)
4. Gunn (1972)
5. Kesson and Price (1972)
6. Roex and Erlank (1982)
7. Estimates, this study.

Table 7.8: Results of Least-squares and Rayleigh fractionation modelling for the basalt–trachyte lineage.

Model	A		B		C		D		E		F		G	
Least-squares approximations														
% Liquid	62.8		78.4		74.5		79.9		88.7		82.0		58.1	
Olivine	12.2		4.2		3.2		2.2		1.6		2.4		6.1	
Clinopyroxene	17.2		9.4		5.5		8.0		0.6		5.1		–	
Plagioclase	5.8		6.8		12.6		6.4		7.8		7.0		30.5	
Titanomagnetite	2.0		1.2		3.9		3.6		1.2		2.6		4.2	
Apatite	–		–		0.2		–		–		0.8		1.2	
Sum (residuals)^2	0.167		0.381		0.053		0.122		0.078		0.071		0.503	
Rayleigh modelling														
	Obs	*Est*	*Obs*	*Est*	*Obs*	*Est*	*Obs*	*Est*	*Obs*	*Est*	*Obs*	*Est*	*Obs*	*Est*
Rb	23	30	30	29	37	40	47	46	60	53	74	72	175	120
Sr	691	676	701	778	930	756	760	1034	655	763	465	703	20	127
Y	32	30	37	37	40	43	40	46	46	44	41	45	49	50
Zr	229	223	255	284	274	332	400	332	384	448	512	458	866	863
Nb	53	56	71	65	86	85	93	97	105	102	116	120	189	175

A: Parent is N36C1305 (*ne*-basalt), daughter is N36D3016 (*ne*-basalt).
B: Parent is N36D3016 (*ne*-basalt), daughter is N36C1303 (*ne*-hawaiite).
C: Parent is N36C1303 (*ne*-hawaiite), daughter is N36C1340 (*ne*-hawaiite).
D: Parent is N36C1340 (*ne*-hawaiite), daughter is N36C3678 (*ne*-hawaiite).
E: Parent is N36C3678 (*ne*-hawaiite), daughter is N36C1369 (*ne*-mugearite).
F: Parent is N36C1369 (*ne*-mugearite), daughter is N36A3565 (*ne*-benmoreite).
G: Parent is N36A3565 (*ne*-benmoreite), daughter is N36C3506 (*ne*-trachyte).

were within ± 20% of the observed abundances. Results are presented in Table 7.8 and Table 7.9.

For the basalt–trachyte lineage, the models illustrate the importance of olivine and clinopyroxene fractionation in mafic lavas, giving way to plagioclase in intermediate and felsic lavas. Apatite is significant in felsic lavas and titanomagnetite is ubiquitous. For the basanite–phonolite lineage, clinopyroxene and plagioclase (± minor olivine) are the dominant fractionating phases in mafic lavas. In intermediate and felsic lavas, clinopyroxene becomes less important, and apatite, kaersutite and ultimately anorthoclase become important fractionating phases. As with the basalt–trachyte lineage, titanomagnetite is ubiquitous. The discrepancies for Sr in hawaiites can best be explained by the particular $D^{Sr/liq}$ values used. If values higher than those commonly found in the literature for plagioclase compositions of An $\geq$ 50 had been used (eg. $D^{Sr/liq} = 2.5 - -5.0$), the results would have been better. Resorting to other fractionation models, such as *in situ* crystallisation (Langmuir, 1989) would not improve the results.

It is important to note that these models are only approximations and are not unique solutions. A good model simply says "this daughter magma *could* have evolved from this parent magma by fractionation of these mineral phases in these proportions". A single parent–daughter magma pair can be (and are) explained by more than one solution. The models do, however, provide quantitative proof that the fractionation models proposed on the basis of petrography, mineralogy and geochemistry, are plausible and reasonable.

7.6 Modelling of Combined Assimilation and Fractional Crystallisation

The basic tenet of the combined assimilation/fractional crystallisation model (AFC) is that the latent heat of crystallisation of the magma provides the heat required for the assimilation of wallrock. Equations describing trace element and isotopic evolution in a magma chamber affected by simultaneous assimilation and fractional crystallisation have been developed by De Paolo (1981). For a magma body (Fig. 7.10) of mass M_m which is assimilating wallrock at a rate $\dot{M}_a$[2] and crystallising phases at a rate $\dot{M}_c$, the instantaneous rate of change of the concentration of an element in the magma is given by the differential equation

$$\frac{\mathrm{d}C_m}{\mathrm{d}t} = \frac{\dot{M}_a}{M_m}(C_a - C_m) - \frac{\dot{M}_c}{M_m}(D-1)C_m$$

[2]The dot notation $\dot{X}_y$ is a short form of $\mathrm{d}X_y/\mathrm{d}t$.

Table 7.9: Results of Least-squares and Rayleigh fractionation modelling for the basanite–phonolite lineage.

Model	H		I		J		K	
Least-squares approximations								
% Liquid	71.7		66.3		69.2		53.2	
Olivine	1.6		2.9		–		7.3	
Clinopyroxene	11.1		11.3		0.8		3.9	
Plagioclase	11.1		14.9		7.9		19.5	
Titanomagnetite	4.6		4.6		1.7		3.1	
Apatite	–		–		1.1		1.5	
Kaersutite	–		–		19.4		10.0	
Anorthoclase	–		–		–		1.6	
Sum (residuals)^2	0.040		0.230		0.046		0.394	
Rayleigh modelling								
	Obs	*Est*	*Obs*	*Est*	*Obs*	*Est*	*Obs*	*Est*
Rb	34	31	36	51	53	48	140	94
Sr	685	687	841	782	735	677	306	784
Y	29	36	44	38	43	45	33	49
Zr	223	244	302	321	359	432	718	658
Nb	52	51	78	68	103	85	132	154

H: Parent is N36C3036 (basanitoid), daughter is N36C3316 (basanitoid).

I: Parent is N36C3316 (basanitoid), daughter is N37A3449 (nepheline hawaiite).

J: Parent is N37A3449 (nepheline hawaiite), daughter is N36C1315 (nepheline mugearite).

K: Parent is N36C1315 (nepheline mugearite), daughter is N36D3619 (phonolite).

where C_m is the concentration of the element in the magma, C_a is the concentration of the element in the assimilant, and D is the bulk solid/liquid distribution coefficient for the element between the magma and the fractionating phases. When $\dot{M}_a = \dot{M}_c$, the situation is analogous to zone refining. When $\dot{M}_c = 0$ (no crystal fractionation), the equation reduces to the simple binary mixing model. The significance of this is that for simple binary mixing, the concentration of the element in the magma will change in the direction of the concentration of the element in the assimilant. However, for AFC, even if $C_a < C_m$, C_m can still increase if $D < C_a/C_m$. For the general case of $M_a \neq M_c$ and constant $r = \dot{M}_a/\dot{M}_c$, the differential equation can be rewritten using

$$z = \frac{r + D - 1}{r - 1}, \text{ and } F = M_m/M_m^o$$

(where M_m^o is the initial mass of magma), transformed to change the variable from t to F, and integrated to give

$$C_m/C_m^o = F^{-z} + \left(\frac{r}{r-1}\right)\frac{C_a}{zC_m^o}(1 - F^{-z})$$

which describes the change in concentration of a trace element in a magma affected by AFC as a function of r, D and F.

For an isotopic ratio ϵ, the differential equation is

$$\frac{\mathrm{d}\epsilon_m}{\mathrm{d}t} = r\frac{\dot{M}_c}{M_m}\frac{C_a}{C_m}(\epsilon_a - \epsilon_m) = \frac{\dot{M}_a}{M_m}\frac{C_a}{C_m}(\epsilon_a - \epsilon_m)$$

where ϵ_m is the isotopic ratio in the magma and ϵ_a is the isotopic ratio in the assimilant. For arbitrary but constant $r \neq 1$, this can be rewritten and integrated as above to give

$$\epsilon_m = \frac{\frac{r}{r-1}\frac{C_a}{z}(1 - F^{-z})\epsilon_a + C_m^o F^{-z}\epsilon_m^o}{\frac{r}{r-1}\frac{C_a}{z}(1 - F^{-z}) + C_m^o F^{-z}}$$

which describes the change in the isotopic ratio of a magma affected by AFC as a function of r, D and F.

Hawaiites near the top of the succession on Lighthouse Road and High Bare Peak are very plagioclase-phyric, and may contain up to 50% phenocrysts. Such a rate of crystallisation would produce sufficient heat to assimilate wallrock material. AFC calculations were performed to test the hypothesis that *hy*- or *qz*-trachytes could be derived from a *ne*-hawaiite by combined fractional crystallisation and assimilation. A *ne*-hawaiite (sample N36C3443) with an initial $^{87}Sr/^{86}Sr$ isotope ratio of 0.70302 and 791 ppm Sr was used as the composition of the magma. The assimilant was a greywacke with an initial $^{87}Sr/^{86}Sr$ isotope ratio of 0.71039 and 247 ppm Sr (Table A1, Graham and Hackett, 1987). Curves of C_m^{Sr} versus $\epsilon_m^{^{87}Sr/^{86}Sr}$ for a range of F values were calculated for fixed D^{Sr} and r.

Results are presented in Figure 7.11, and show that a *hy*- or *qz*-normative trachyte could be derived from a *ne*-normative hawaiite by combined assimilation of greywacke and fractionation of feldspar, which is consistent with the observation that many Akaroa Volcanic Group hawaiites (especially in the upper parts of the Lighthouse Road and High Bare Peak sections) are moderately to extremely plagioclase-phyric. D^{Sr} values of 2.0–2.4 are quite reasonable given that level of plagioclase fractionation. However, it should be pointed out that each curve was calculated assuming a constant D^{Sr} and r value, and this may be an over-simplification. De Paulo (1981) has shown that the curve depicting the evolution of a magma (in terms of $^{87}Sr/^{86}Sr$ versus Sr ppm) changes significantly if the effects of decreasing r and increasing D^{Sr} are taken into account. In addition, the same (contaminated) magma composition can be modelled using different combinations of D^{Sr} and r. As an example, for the magma and assimilant compositions used in Fig. 7.11, curves calculated using $D^{Sr} = 2.0$ and r values of 0.025 and 0.035 are nearly identical to curves depicted on Fig. 7.11 that were calculated using $D^{Sr} = 2.4$ and r values of 0.035 and 0.05 respectively. Taylor (1980) has calculated that assimilation of 1 g of wallrock initially at 150°C into a magma at 1150°C could be thermally balanced by crystallisation of 3.25 g of crystals, giving an upper limit to r of ≈ 0.3. However, if the country rock was initially at 1000°C (due to the high heat flow of adjacent volcanism), the same calculation produces un upper limit to r of ≈ 1, and if increasing viscosity prevented the effective separation of crystals from the magma, then the upper limit to r would be larger still because the latent heat of crystallisation would still be available but fractional crystallisation would be suppressed (De Paulo, 1981). The values of r determined here (0.025–0.1) are well within these limits, and for a magma crystallising up to 50% phenocrysts, this represents the assimilation of $\approx$ 1.25–5.0% of crustal material.

Weaver and Sewell (1989, *pers. comm.*) have modelled the evolution of the Governors Bay and Lyttelton Volcanic Groups using AFC with a greywacke-derived dacite (initial $^{87}Sr/^{86}Sr = 0.715$, Sr = 200 ppm) rather than simply greywacke, as this produced a better result (Weaver, *pers. comm.*). Akaroa Volcanic Group lavas have been modelled using the same dacite composition (Fig. 7.12). The results are very similar to those obtained for the greywacke assimilant, with $D^{Sr} = 2.0$–2.5 and $r = 0.025$–0.1, and indicate that contamination of *ne*-normative hawaiites by either greywacke or a greywacke-derived dacite could produce *hy*- or *qz*-normative trachytes. Although the AFC model is not able to distinguish which crustal material was the assimilant, it does identify a range of possible assimilants that are consistent with the regional geology.

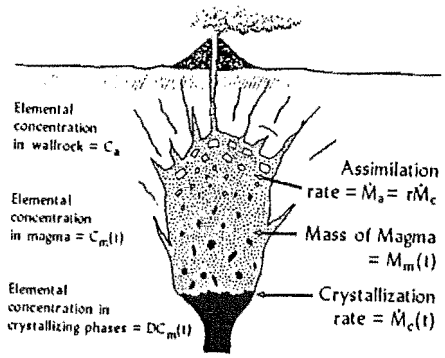

Figure 7.10: Model for assimilation and fractional crystallisation in a magma chamber (after De Paulo, 1981).

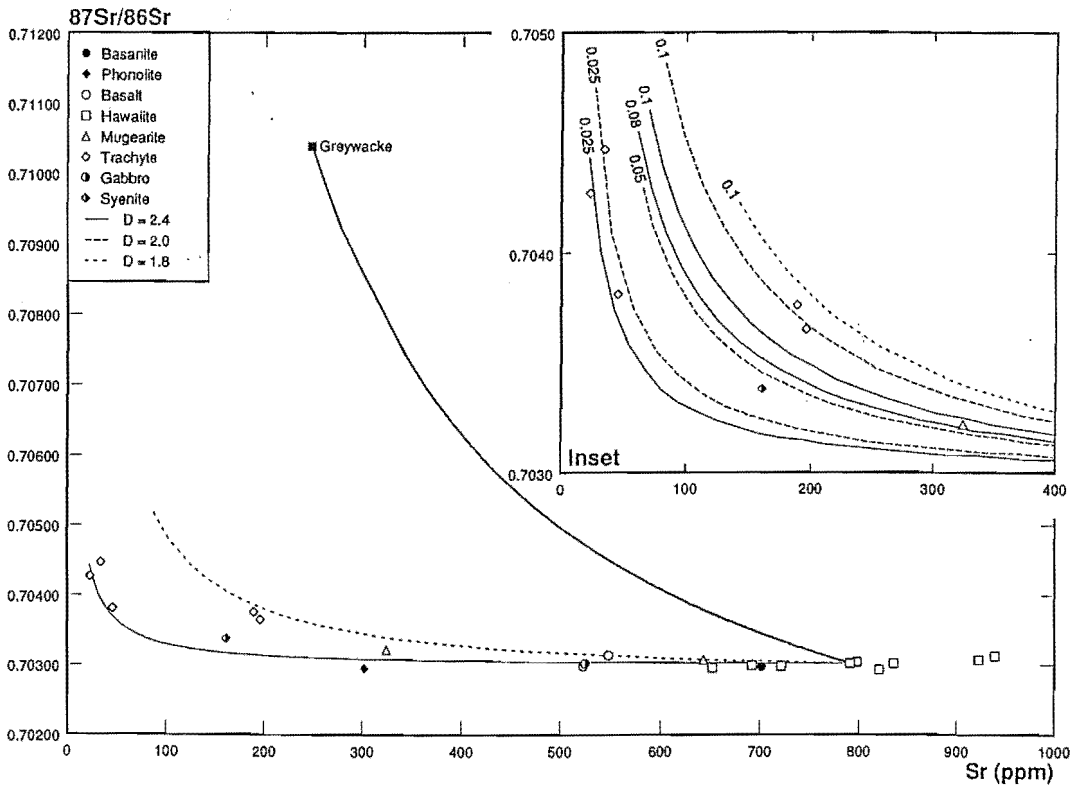

Figure 7.11: Modelling of the evolution of *hy*- and *qz*-normative Akaroa Volcanic Group trachytes from *ne*-normative hawaiite by combined assimilation of greywacke and fractional crystallisation. The greywacke assimilant is from Graham and Hackett (1980, Table A1). The heavy line connecting the greywacke and hawaiite sample N37A3443 is an approximation of the simple binary mixing curve for $D^{Sr} = 1$ and $r = 0.2$. Curves are drawn for constant values of D^{Sr} and r. Labels on the curves give the value of r. The inset gives a more detailed view of the area of interest. On the main graph only two curves are drawn (defining the upper and lower limits of all curves calculated), for clarity.

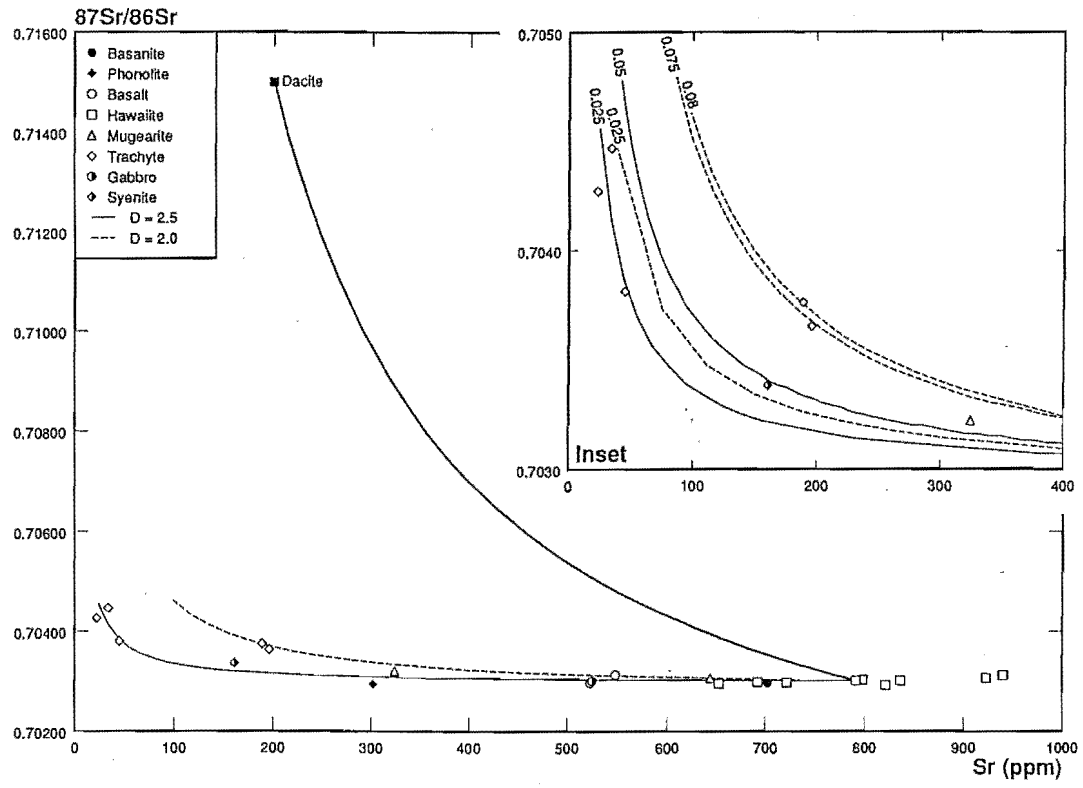

Figure 7.12: Modelling of the evolution of *hy*- and *qz*-normative Akaroa Volcanic Group trachytes from *ne*-normative hawaiite by combined assimilation of greywacke-derived dacite and fractional crystallisation. The dacite assimilant is from Sewell and Weaver (1989, *pers. comm.*). The heavy line connecting the dacite and hawaiite sample N37A3443 is an approximation of the simple binary mixing curve for $D^{Sr} = 1$ and $r = 0.2$. Curves are drawn for constant values of D^{Sr} and r. Labels on the curves give the value of r. The inset gives a more detailed view of the area of interest. On the main graph only two curves are drawn (defining the upper and lower limits of all curves calculated), for clarity.

Chapter 8

GEOLOGICAL HISTORY AND CONCLUSIONS

8.1 Geological History

Banks Peninsula, a 1200 km^2 promontory on the east coast of the South Island, New Zealand, is the largest accumulation of Miocene volcanics in the Canterbury province. The peninsula is dominated by two large, dissected, Miocene stratovolcanoes — Lyttelton and Akaroa — which were constructed on continental crust at the western end of the Chatham Rise — a bathymetric structural high extending 900 km to the east of Banks Peninsula.

Cainozoic volcanic activity began with the eruption of icelandites, dacites and peraluminous rhyolites of the Governors Bay Volcanics (11 Ma), on an irregular topography comprising Torlesse Terrane (Triassic) and Miocene sediments. Products of the activity of Lyttelton Volcano have been assigned to the Lyttelton Volcanic Group (Sewell, 1988) and comprise a mildly alkaline to transitional association of basalt–trachyte lava flows, pyroclastics and intrusives erupted 11–10 Ma. Activity was hawaiian to mildly strombolian in style. A well developed radial dike swarm, dominated by trachyte compositions, was emplaced throughout the history of the volcano. Analysis of dike orientations and the attitudes of lava flows around the crater indicates that eruptions occurred at two major centres within the volcano (Shelley, 1987). As Lyttelton activity waned, major breaches formed in the north-eastern, south-western and south-eastern sectors of the volcano.

Mt Herbert Volcanic Group (9.7–8.0 Ma) comprises a volcanic complex of mildly alkaline basalt lavas, plugs and intercalated pyroclastic deposits erupted in the

eroded crater and on the outer south-eastern flanks of Lyttelton Volcano (Sewell, 1988), and infilling a major breach in the south-east sector of Lyttelton Volcano. Mt Herbert Volcanic Group represents an intermediate stage in the migration of the focus of volcanic activity from Lyttelton to Akaroa.

The "Church-type" lavas (Sewell, 1988) comprise basanite–basalt lava flows, dikes and plugs erupted from vents in the crater and on the flanks of the dissected Lyttelton Volcano.

The Diamond Harbour Volcanic Group (7.0–5.8 Ma) comprises olivine basalt to hawaiite lava flows, dikes, plugs, minor basanites and conglomerates (Sewell, 1988).

Akaroa Volcano occupies the south-eastern two-thirds of Banks Peninsula, and has a present diameter of 30 km and a maximum elevation of 840 m. The volcano has, however, suffered extensive erosion, and the base of the volcano is submerged below sea level. At its greatest extent, Akaroa Volcano probably reached a height of 1500 m above present sea level, with a diameter of 50 km. Volumetrically, Akaroa Volcano is the major constructional element of Banks Peninsula, accounting for $\approx$ 72% (1200 km^3) of the estimated 1675 km^3 of volcanic products that form Banks Peninsula. In comparison, the estimated volumes of the other volcanic groups comprising Banks Peninsula are 350 km^3 (Lyttelton), 100 km^3 (Mt Herbert), 20 km^3 (Diamond Harbour) and 5 km^3 (Church).

Akaroa Volcano is constructed predominantly of lava flows and minor intercalated pyroclastic and epiclastic deposits, intruded by a well developed radial dike swarm and numerous domes and sills. Eruptive activity was hawaiian to mildly strombolian in character. The products of Akaroa Volcano activity belong to one of two major eruptive phases — the Early Phase (I, II and III) and the Main Phase.

The basement to Akaroa Volcano is not exposed, as it is for Lyttelton Volcano, but is presumed to be pre-Miocene continental crust similar to that exposed in the eroded centre of Lyttelton Volcano (Weaver, 1980). The oldest exposed rocks of Akaroa Volcano are basaltic lava flows of Early Phase I exposed on Onawe Peninsula. These flows are overlain unconformably by thick deposits of Early Phase II tuffs, breccias, agglomerates, lava flows, sills and a dome, almost entirely trachytic in composition. Sedimentary rock fragments, some showing signs of assimilation and recrystallisation, and associated incipient cordierite in a welded tuff from Onawe Peninsula provide evidence of the sedimentary basement that underlies Akaroa Volcano. The large volume of trachyte material is thought to represent a major episode of eruption of trachytic lava marking the end of the construction of a proto-cone.

These trachytic rocks are unconformably overlain by weathered basaltic lava flows, tuffs, lahars, scoria cones and breccias of the Early Phase III. A wide range of clast

lithologies in a pyroclastic breccia on Onawe Peninsula indicates that significant activity pre-dated the oldest exposed rocks, and a large portion of Akaroa Volcano is submerged beneath sea level. The contact between Early Phases II and III shows considerable relief indicating a period of erosion prior to eruption of Early Phase III volcanics. These rocks are interpreted as the products of a failed attempt to initiate construction of the main cone of Akaroa Volcano. The very weathered nature of Early Phase III lava flows compared to lavas of the Main Phase indicates that a period of extensive weathering and erosion pre-dated construction of the main cone of Akaroa Volcano. Few radiometric dates are available for lavas of the Early Phase, but a sample from the Tikao trachyte dome returned an age of 11.63 ± 0.46 Ma, and considering the geology of the Early Phase, these rocks are thought to be considerably older than those of the main Akaroa cone — perhaps contemporary with late stages of Lyttelton Volcano.

Syenite and gabbro exposed at the southern end of Onawe Peninsula are the only plutonic rocks known from Banks Peninsula, and probably represent the partially unroofed upper levels of a high-level magma reservoir injected into the lower stratigraphic levels of the volcano.

The bulk of exposed products of Akaroa Volcano are lava flows and minor intercalated pyroclastics of the Main Phase which forms the main cone of Akaroa Volcano. The dominant flow lithology is hawaiite, with subordinate basalt and rare basanitoid, mugearite, benmoreite and trachyte lava flows. Pyroclastic activity was dominated by eruption of basaltic ashes which formed generally thin (< 1 m), red-brown, very fine grained to fine grained, sometimes reverse or normally graded tuffs which drape underlying topography. Flank eruptions were common, producing numerous prominent basaltic scoria cones (eg. Purple Peak, Scenery Nook). Larger vents such as Scenery Nook developed a complex, active environment, as evidenced by the range of lithologies — crystal and lithic tuffs, strombolian scoria cones, base surge deposits, epiclastic and fluvially reworked pyroclastic deposits. Rare exposures of laharic deposits probably under-state the importance of lahars in construction of the cone. K-Ar dating (Stipp and McDougall, 1968; Evans, 1970; this study) indicates that the main cone was constructed over a period of approximately 1 million years (9–8 Ma), giving a rate of eruption of the order of 1–2 × $10^6 m^3 yr^{-1}$ for construction of the main cone. This is of the same order of magnitude as recent rates of eruption calculated for other shield volcanoes (Kilauea, $10^8 m^3 yr^{-1}$; Mauna Loa, 2 × $10^7 m^3 yr^{-1}$; Stearns 1966). Lava flows at the base of the Main Phase may, however, be somewhat older than 9.0 Ma — a single K-Ar age of 10.18 ± 0.33 Ma was obtained from a flow sample (N36C3305) on Takamatua Peninsula.

Throughout the eruptive history of Akaroa Volcano, the volcanic pile was intruded by dikes of the Akaroa radial dike swarm. In contrast to lava flows which are dominantly hawaiite in composition, dikes are typically trachytic in composition. Analysis of the radial distribution indicates that dikes were intruded laterally from

a central conduit under driving pressure generated in the central conduit. The central conduit was located within a broadly defined zone south to south-east of Onawe Peninsula, and coincides with the maxima of Bouguer and isostatic gravity anomalies. Gravity anomalies define a cone-shaped surface which reflects a dense sub-surface intrusive complex involving > 615 km^3 of intrusive material.

Five large trachytoid domes — Panama Rock, Devil's Gap, Pulpit Rock, View Hill, and Ellangowan — now exposed on the flanks and in the eroded crater of Akaroa Volcano, were intruded into the lava pile during its history. Panama Rock can be seen to have been fed by a large dike of the radial dike swarm, and the other domes were also probably supplied with lava from radial dikes.

As the Akaroa cone developed, the north-western flanks abutted against the south-eastern flanks of the dissected Lyttelton Volcano and outpourings of Mt Herbert Volcanic Group lavas from numerous vents in the crater and on the south-eastern and eastern flanks of Lyttelton Volcano. Akaroa Volcanic Group lavas may have reached central Banks Peninsula as early as 8.5 Ma, and can now be observed interfingered with Mt Herbert Volcanic Group lava flows at $\approx$ 600 m asl near Mt Herbert.

As eruptive activity waned, erosion became the dominant landscaping force. A radial drainage pattern, which existed during the construction of the cone, dissected the outer flanks and crater. Akaroa Harbour is thought to be the result of the extreme development of a single radial channel and the progressive development of an enlarged amphitheatre-like catchment basin by excessive headward erosion and tributary capture. Diversion of radial streams on the flanks of the volcano into the eroding crater would accelerate the process. A subsequent sea-level rise drowned the river valley, resulting in the formation of a harbour. Pigeon Bay probably represents an immature to sub-mature development of this evolutionary sequence. No evidence has been found that supports the hypothesis of cataclysmic eruption or sector collapse initiating or contributing to the development of Akaroa Harbour.

In the last 2.0 Ma, extensive glaciation of the Southern Alps supplied enormous volumes of debris to major braided river systems which deposited the debris along the east coast of the South Island. Progradation of the east coast eventually eliminated the shallow seaway between Banks Peninsula (which until that time was an island) and the mainland about 20 000 years ago.

Loess, which covers much of Banks Peninsula and around Akaroa Volcano is locally in excess of 10 m thick, was derived from the Southern Alps and Canterbury Plains to the east and the continental shelf to the west of Banks Peninsula during the last glaciation.

With the retreating of the glaciers about 6000 years ago, the sea level rose, drowning a major river valley and forming Akaroa Harbour. Coastal landforms such as sea cliffs, stacks and wave-cut platforms date back to this time.

8.2 Comparison With Other New Zealand Intraplate Volcanism

Cenozoic intraplate volcanism of alkaline to subalkaline composition is widespread in the South Island of New Zealand and the area extending south and east to the Sub-Antarctic and Chatham Islands (Fig. 8.1). Major centres include Banks Peninsula (Lyttelton and Akaroa Volcanoes, and numerous other small vents), Dunedin Volcano, and the Chatham, Antipodes, Campbell and Auckland Islands. Although widespread and diverse in detail, these centres have many features in common with each other, Akaroa Volcano and intraplate volcanism in general.

All New Zealand Cainozoic intraplate volcanic provinces (including Akaroa Volcano and the Akaroa Volcanic Group) show a predominance of mafic volcanic rocks. Significantly, hawaiites rather than basalts are volumetrically the most abundant, and this is generally attributed to fractionation of more primitive magmas during their ascent through the continental crust. The fact that mantle-derived xenoliths are absent from the central-volcano provinces, but are common in small monogenetic vents of strongly alkaline composition, supports this view.

New Zealand Cainozoic alkaline intermediate and felsic lavas commonly have major and trace element patterns and elevated initial $^{87}Sr/^{86}Sr$ isotope ratios indicative of crustal contamination. Combined assimilation and fractional crystallisation (AFC) models have been applied successfully (this study; Sewell and Weaver, 1989) to such lavas, and AFC processes are likely in all mafic–felsic suites.

Differences in isotopic composition, and incompatible trace element characteristics (eg. negative K anomalies in normalised trace element diagrams) suggest limited mantle source heterogeneity beneath the New Zealand region.

Four central-volcano alkaline volcanic provinces — the Chatham and Auckland Islands, Dunedin, and Banks Peninsula (Lyttelton) — have many features in common with Akaroa Volcano. The following paragraphs highlight these features, for comparison with the data presented in this study.

Intraplate alkaline volcanics on the Chatham Islands comprise a basalt–trachyte suite dominated by mafic lavas (Morris, 1985b). Trachytic rocks are mainly pyro-

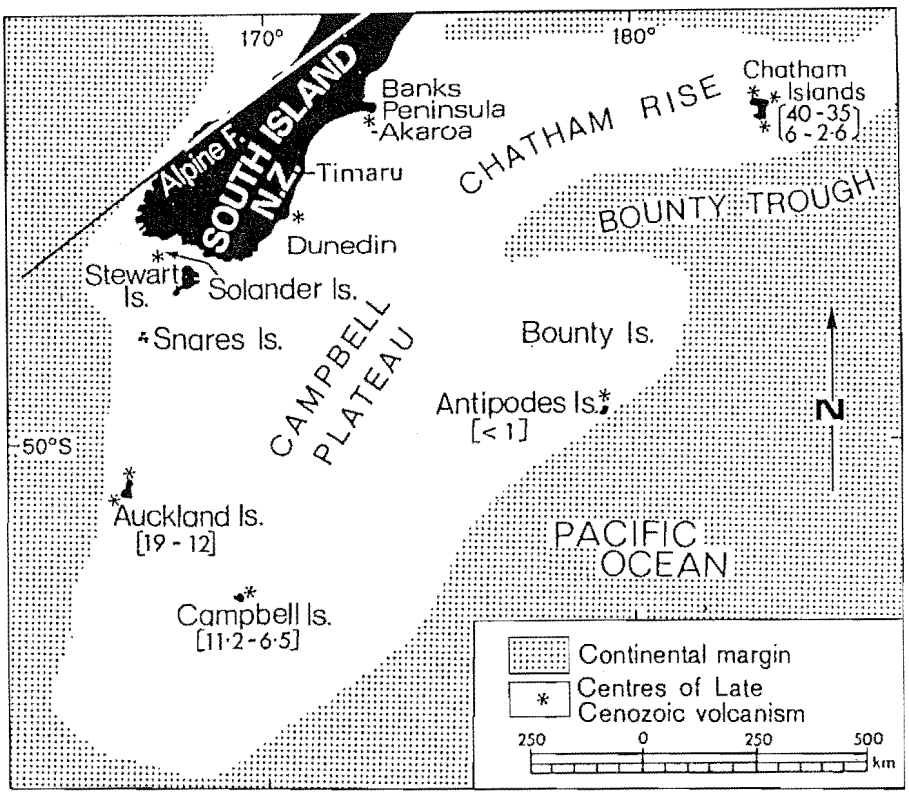

Figure 8.1: Cenozoic volcanic centres of the Campbell Plateau and Chatham Rise and adjacent Cenozoic centres on the New Zealand Mainland. Ranges of available K/Ar ranges are shown for each centre. After Gamble *et al* (1986).

clastic — trachyte flows are rare. Basic lavas have phenocrysts of olivine (Fo_{70}–Fo_{82}), titansalite, plagioclase (An_{40}–An_{65}) and titanomagnetite. Intermediate lavas have phenocrysts of feldspar, ferrosalite or aegirine (in trachytes). Quartz and arfvedsonite are also found in trachytes. Variations in modal mineralogy, and mineral and whole rock chemistry is explained by low-pressure fractionation, supported by least-squares modelling and Rayleigh fractionation modelling which shows the dominance of clinopyroxene and then plagioclase in the fractionation scheme. Magmas were probably generated by 6-15% partial melting of a source recently enriched in LREE. A few lavas have Mg numbers > 60 and high Cr and Ni values indicating that they have only fractionated olivine ± Cr-spinel. REE patterns are straight with La_N/Yb_N ratios of 9–13. Unfractionated rocks show variable incompatible element ratios suggesting limited mantle source heterogeneity, but low and approximately constant initial $^{87}Sr/^{86}Sr$ isotope ratios (0.7029–0.7030) indicate an isotopically homogeneous source. High initial $^{87}Sr/^{86}Sr$ isotope ratios in one trachyte can not be modelled by crustal contamination.

On the Auckland Islands, intrusive and extrusive Tertiary volcanic rocks form two coalesced, eroded volcanic shields — Carnley and Ross Volcanoes. Tertiary sediments and overlying volcaniclastic and volcanic rocks rest unconformably on a basement of Cretaceous granite in Carnley Harbour. Early in the succession, the nature and composition of volcanic products is diverse, including trachyte and rhyolite flows intercalated with basalt flows. The main succession is, however, dominated by basic lavas. Dikes, sills and a gabbroic intrusive complex are concentrated in the core of Carnley Harbour. Basic lavas have phenocrysts of clinopyroxene and olivine, with minor plagioclase and Fe-Ti oxides. Intermediate lavas show an increase in plagioclase and Fe-Ti oxides and a corresponding decrease in clinopyroxene and olivine. In felsic lavas, sodic plagioclase dominates, with rare alkali feldspar, quartz and Fe-Ti oxides. Megacrysts and phenocrysts of kaersutite occur in more strongly undersaturated rocks.

The Dunedin Volcanic Group (Coombs *et al*, 1986) includes all late Tertiary volcanics and shallow intrusive rocks of east and central Otago. The Major centre is Dunedin Volcano — some 25 km in diameter and a maximum elevation of 700m. Tuffs in shallow-water marine beds of the Waipuna Bay Formation indicate that initial activity commenced before the sea had completely regressed from the area, but for most of it's history, Dunedin Volcano was subaerial. Activity ranged from explosive to effusive and lasted some 3 million years (13–10 Ma). Coombs and Wilkinson (1969) proposed a spectrum of lineages from weakly *hy*- to strongly *ne*-normative, with sodic and potassic variants for both types. Lavas of the alkali olivine basalt–hawaiite–mugearite–benmoreite–trachyte lineage are generally *ne*-normative, but lavas of the basanite–nepheline hawaiite–nepheline mugearite–nepheline benmoreite–phonolite lineage are strongly *ne*-normative. Lavas have a simple mineralogy of olivine, titaniferous augite, titanomagnetite and plagioclase. Kaersutite or rhönite occurs in some members of the sodic series but is more common

in the potassic series. Most lavas exhibit straight, LREE-enriched REE patterns. Strong negative Eu anomalies are common in the phonolites. Price and Chappell (1975) postulate a model for the evolution of basalt–mugearite lavas based on low-pressure fractionation of olivine, clinopyroxene and titanomagnetite, with apatite becoming important in the mugearite–benmoreite series. Kaersutite is important in the basanite–nepheline benmoreite series. Initial $^{87}Sr/^{86}Sr$ isotope ratios of 0.70277–0.70315 (Price and Compston, 1973) are low for continental basalts. The limited range and non-radiogenic nature of the Sr isotope ratios restricts the nature and degree of contamination from crustal rocks. Consequently, contamination of lavas by crustal material does not appear to have been nearly as important in the evolution of Dunedin Volcanic Group lavas as it apparently was for Banks Peninsula lavas. Sr and Nd isotopes are consistent with derivation of Dunedin Volcanic Group magmas from a time-integrated depleted source recently enriched in LREE and incompatible trace elements.

Lyttelton Volcano, together with Akaroa Volcano, forms the bulk of the Banks Peninsula volcanic edifice. Early Lyttelton lavas were erupted on to a basement comprising Torlesse Terrane (Triassic), Miocene sediments, and icelandites, dacites and peraluminous rhyolites of the Governors Bay Volcanics. The dominant lava composition is hawaiite, with subordinate basalt, mugearite, benmoreite, trachyte and dacite. Lavas of the basalt–trcahyte series are alkaline, but the dacites are of potassic subalkaline composition. Activity was mainly hawaiian in style, but local thick airfall pyroclastic rocks attest to the existence of some strombolian parasitic cones. Mafic lavas have phenocrsyts of olivine, clinopyroxene, plagioclase and titanomagnetite. Partially resorbed kaersutite occurs in the youngest mafic lavas. Hedenbergite and rare fayalite phenocrsyts occur in peralkaline trachytes, while aenigmatite and arfvedsonite are ubiquitous groundmass phases. Basement sediments are exposed at the centre of the volcano, and the absence of pillow lavas indicates all eruptions were probably subaerial. Strong evidence exists (Sewell and Weaver, 1989, *pers. comm.*) for Lyttelton trachytes and Governors Bay rhyolites having been contaminated by continental material.

8.3 Tectonic Setting

Cenozoic intraplate mafic rocks of the South Island of New Zealand and the Sub-Antarctic Islands are of ocean-island basalt composition and are typically associated with extensional tectonic regimes, especially in continental settings.

Middle Cretaceous to late Oligocene times were characterised by extensional tectonism associated with the opening of the Tasman Sea and the separation of New Zealand from the Gondwana supercontinent ($\approx$ 50–80 Ma). This extensional tecton-

ism, which persisted through to middle Tertiary times, gave rise to graben formation and basin development, and was associated with widespread and voluminous, strongly alkaline to subalkaline mafic volcanism in Canterbury, North Otago, Marlborough, South Westland and the Chatham Islands.

The propagation of the present-day plate boundary through southern continental New Zealand was reflected by a change from extensional to compressional tectonics during the middle Tertiary.

During the Miocene, major volcanic centres of alkaline to subalkaline composition became active, at Banks Peninsula (Lyttelton, Mt Herbert and Akaroa), Dunedin, Auckland Islands and Campbell Island. Although compressional tectonics were well established by the late Miocene, alkaline intraplate volcanism continued, especially at the Banks Peninsula complex where eruptions did not cease till about 6 Ma. There was a time lag between the development of the compressional tectonic regime and the cessation of alkaline intraplate mafic volcanism, but the change to compression tectonism could be thought of as having "turned off" alkaline intraplate volcanism in the South Island of New Zealand. Exceptions include the Pliocene volcanism of the Chatham Islands and the Quaternary activity of the Antipodes Islands, but these centres are at the eastern margin of the Campbell Plateau and were outside the zone of compression.

Suggestions that the migration of late Cenozoic intraplate volcanism across the South Island of New Zealand, the Campbell Plateau and the Chatham Rise may be related to the New Zealand continental lithosphere overriding a spreading ridge and producing "hot-spot trails" (eg. Adams, 1981) do not appear to be supported by the age distribution of all Tertiary volcanics. Although both the Dunedin and Banks Peninsula volcanic complexes do record some migration of volcanic activity (eg. on Banks Peninsula, southeast from Lyttelton (11–10 Ma) to Mount Herbert (9.7–8.0 Ma) to Akaroa (9.0–8.0 Ma), the migration is not consistent, and at Banks Peninsula the latest activity (Diamond Harbour, 7.0–5.8 Ma) represents a northwesterly migration back to the Lyttelton and Mount Herbert centres.

FUTURE RESEARCH

This study has produced a great deal of new data regarding the geology and geochemistry of Akaroa Volcano, and as such, fills a significant gap in our knowledge of the geology and evolution of Banks Peninsula. In the last six years Banks Peninsula has been the subject of a number of detailed mapping, petrological and geochemical studies (eg. Dorsey, 1981; Falloon, 1982; Thiele, 1983; Sewell, 1985, 1988; Weaver and Sewell, 1986). The New Zealand Geological Survey are in the process of producing 1:50 000 metric series geological maps of the whole of Banks Peninsula (Sewell, *pers. comm.*). It would therefore seem an appropriate time to attempt to incorporate the results of these studies into a single, coherent model for the stratigraphy, petrology and geochemistry of Banks Peninsula as a whole, and its implications for the nature of the underlying lithosphere, and the tectonic environment in which Banks Peninsula evolved. This would serve to highlight those areas of Banks Peninsula and aspects of its geology which are deserving of further research.

With respect to Akaroa Volcano and the Akaroa Volcanic Group in particular, there are a number of avenues for further research. The coastline of Akaroa Volcano is dominated by spectacular cliffs, and these may contain exposures of a wide variety of volcanological features, as highlighted by the geology of Scenery Nook. A study of the cliffs around Akaroa Volcano, from the sea, may reveal a great deal of information about volcanological processes associated with the construction of a composite volcano. More detailed K-Ar dating is required to better define the age of the Akaroa Volcanic Group, especially rocks of the Early Phase which may be significantly older than those of the Main Phase. Detailed petrofabric studies, similar to those of Lyttelton Volcano (Shelley, 1985), on the trachyte domes (and in the case of Panama Rock, its feeder dike) may provide much information on the mechanism(s) of intrusion. More microprobe data, especially for intermediate and felsic lava compositions (mugearites, benmoreites, trachytes) would help to better constrain fractional crystallisation models. Additional REE analyses, and $^{87}Sr/^{86}Sr$ and $^{143}Nd/^{144}Nd$ isotope data for mafic and intermediate lavas would help to constrain models of the mantle source and partial melting processes. Only a limited number of samples have been collected from lavas of the basanite—phonolite lineage, and no samples were obtained from nepheline mugearite and nepheline benmoreite

members. A concerted effort should be made to map and sample lavas belonging to this lineage to determine its extent and importance within the Akaroa Volcanic Group. Finally, a study of the warm, sub-sea springs in Akaroa Harbour may help to solve one problem that local residents have been debating for years — where is the best spot in Akaroa Harbour to fish for cod?

ACKNOWLEDGEMENTS

I would like to thank my supervisors, Dr S. D. Weaver and Dr D. Shelley, for invaluable assistance and encouragement throughout the course of this study.

Assistance with field expenses from the New Zealand Geological Survey is gratefully acknowledged.

Special thanks is due to the many people and organisations who provided technical assistance or research facilities, including Miss L. Leonard (draughting), Mrs S. Tye (library), Mr A. Alloway (X-ray spectrometry), Mr A. Downing (photographic), Mr D. J. Jones (departmental equipment), Dr Y. Kawachi (University of Otago, electron microprobe), Mrs P. Whitla (Institute of Nuclear Sciences, K-Ar dating), and the staff of the Division of Information Technology (computing resources) who put up with me.

Analytical work (Sr-Nd Isotopes and Rare-Earth-Elements) by Dr S. D. Weaver while on sabbatical leave in Canada and England is gratefully acknowledged.

This thesis would not have been completed without the continual encouragement and support of many people, especially my parents, ET, my supervisor Dr S. D. Weaver, and Rod "I've just made another major discovery ..." Sewell (NZGS).

Most of all, I would like to thank the staff of PhD Thesis Productions Inc, especially the typist, cartographer, proof-reader, caterer, secretary, TEXnician and goffer — thanks ET. ♡ CJ.

This thesis was typeset using the TEX typesetting system written by Donald Knuth and the LATEX macros written by Leslie Lamont, and printed on an Apple Laserwriter. Graphics were generated from PostScript code.

REFERENCES

ABBOTT, M.J. (1969) Petrology of the Nandewar Volcano, N.S.W., Australia. *Contributions to Mineralogy and Petrology 20:115–134.*

ADAMS, C.J. (1975) New Zealand Potassium-Argon age list — 2. *New Zealand Journal of Geology and Geophysics 18:443–467.*

ADAMS, C.J. (1981) Migration of late cenozoic volcanism in the South Island of New Zealand and the Campbell Plateau. *Nature 294:153–155.*

ANDERSON, E.M. (1938) The dynamics of sheet intrusion. *Proceedings of the Royal Society of Edinburgh 58:242–251.*

ANDERSON, E.M. (1951) The dynamics of faulting and dike formation with application to Britain. *2nd Ed. Oliver and Boyd, Edinburgh, 206p.*

ARMON, J.W. (1973) Late Quaternary shore lines near Lake Ellesmere, Canterbury, New Zealand. *New Zealand Journal of Geology and Geophysics 17:63–73.*

BAILEY, E.B., CLOUGH, C.T., WRIGHT, W.B., RICHEY, J.E. and WILSON, G.V. (1924) Tertiary and post-Tertiary geology of Mull, Loch Aline, and Oban. *Scottish Geological Survey Memoir, 445p.*

BAKER, B.H., GOLES, G.G., LEEMAN, W.P. and LINDSTROM, M.M. (1977) Geochemistry and petrogenesis of a basalt-benmoreite-trachyte suite from the southern part of the Gregory Rift, Kenya. *Contributions to Mineralogy and Petrology 64:303–332.*

BAKER, I.(1969) Petrology of the volcanic rocks of Saint Helena Island, South Atlantic. *Geological Society of America Bulletin 80:1283–1310.*

BASU, A.R. and MURTHY, V.R. (1977) Ancient lithospheric xenolith in alkali basalt from Baja California. *Earth and Planetary Science Letters 35:239–246.*

BATIZA, R., ROSENDAHL, B.R. and FISHER, R.L. (1977) Evolution of ocean crust, 3. Petrology and chemistry of basalts from the East Pacific Rise and the Sequeiros transform fault. *Journal of Geophysical Research 82:265–276.*

BENCE, A.E. and ALBEE, A.L. (1968) Empirical correction factors for the electron microanalysis of silicates and oxides. *Journal of Geology 76:382–403.*

BENCE, A.E., BAYLISS, C.M., BENDER, J.F. and GROVE, T.L. (1979) Controls of the major- and minor-element chemistry of mid-ocean ridge basalts and glasses. *In: S. Talwani et al. (Editors), Deep Drilling Results in the Atlantic Ocean: Ocean Crust. American Geophysical Union (Maurice Ewing Series) 2:331–341.*

BENCE, A.E., PAPIKE, J.J and AYUSO, R.A. (1975) Petrology of submarine basalts from the Central Caribbean: DSDP LEG 15. *Journal of Geophysical Research 80:4775–4804.*

BOETTCHER, A.L., ONEIL, J., WINDOM, K., STEWART, D. and WILSHIRE, H.G. (1979) Metasomatism and the genesis of kimberlites and alkali basalts. *In: Proceedings of the Second International Kimberlite Conference, Washington, D.C., American Geophysical Union.*

BOETTCHER, A.L. and ONEIL, J.R. (1980) Stable isotope, chemical, and petrographic studies of high-pressures amphiboles and micas: evidence for metasomatism in the mantle source regions of alkali basalts and kimberlites. *American Journal of Science 280A:594–621.*

BRYAN, W.B., FINGER, L.W. and CHAYES, F. (1970) Estimating proportions in petrologic mixing equations by least squares approximation. *Science 163:926–927.*

BUDDINGTON, A.F. and LINDSLEY, D.H. (1964) Iron-Titanium oxide minerals and synthetic equivalents. *Journal of Petrology 5:310–357.*

BULTITUDE, R.J. and GREEN, D.H. (1968) Experimental study at high pressures on the origin of olivine nephelinite and olivine melilite nephelinite magmas. *Earth and Planetary Science Letters 3:325-337.*

BULTITUDE, R.J. and GREEN, D.H. (1971) Experimental study of crystal-liquid relationships at high pressures in olivine nephelinite and basanite compositions. *Journal of Petrology 12:121–147.*

CAMPBELL, I.H. and GORTON, M.P. (1980) Accessory phases and the generation of LREE-enriched basalts — a test for disequilibrium melting. *Contributions to Mineralogy and Petrology 72:157–163.*

CARMICHAEL, I.S.E. (1967) The iron-titanium oxides of salic volcanic rocks and their associated ferromagnesian silicates. *Contributions to Mineralogy and Petrology 14:36–64.*

CARMICHAEL, I.S.E., TURNER, F.J. and VERHOOGEN, J. (1974) Igneous petrology. *McGraw-Hill Book Company.*

CARTER, S.R., EVENSEN, N.M., HAMILTON, R.J. and O'NIONS, R.K. (1978) Continental volcanics derived from enriched and depleted source regions: Nd- and Sr-isotope evidence. *Earth and Planetary Science Letters 37:401–408.*

CHAPMAN, G.R. (1970) "Kenya phonolites", Kenya "phonolites" and "Kenya" phonolites — a classificatory and petrogenetic problem. *Journal of the Geological Society of London Proceedings 127.*

CHAYES, F. (1954) Effect of change of origin on mean and variance of two-dimensional fabrics. *American Journal of Science 252:567–570.*

CHEN, J.H. and MOORE, J.G. (1979) Late Jurassic Independence dike swarm in eastern California. *Geology 7:129–133.*

CLAGUE, D.A. and FREY, F.A. (1982) Petrology and trace element geochemistry of the Honolulu Volcanics, Oahu: Implications for the oceanic mantle below Hawaii. *Journal of Petrology 23:447–504.*

COOMBS, D.S. and REAY, A. (1986) Excursion C2 — Cenozoic alkaline and tholeiitic volcanism, eastern South Island, New Zealand. *International Volcanological Congress 1986, University of Otago, 73 pp.*

COOMBS, D.S. and WILKINSON, J.F. (1969) Lineages and fractionation trends in undersaturated volcanic rocks from the East Otago volcanic province (New Zealand) and related rocks. *Journal of Petrology 10:440–501.*

COOMBS, Douglas S., CAS, R.A., KAWACHI, Yosuke, LANDIS, C.A., MCDONOUGH, W.F. and REAY, A. (1986) Cenozoic volcanism in North, East and Central Otago. *In: SMITH, I.E.M. (Ed.) Late Cenozoic volcanism in New Zealand. Royal Society of New Zealand Bulletin 23:278–312.*

COOTE, J.A.R. (1987) Cenozoic volcanism in the Waiau area, North Çanterbury. *Unpublished M.Sc. Thesis, University of Canterbury.*

COX, A. and DALRYMPLE, G.B. (1967) Statistical analysis of geomagnetic reversal data and the precision of potassium-argon dating. *Journal of Geophysical Research 72:2604–2614.*

COX, K.G., BELL, J.D. and PANKHURST, R.J. (1979) The interpretation of igneous rocks. *George Allen and Unwin, London.*

CROSS, W., IDDINGS, J.P., PIRSSON, L.V. and WASHINGTON, H.S. (1903) Quantitative classification of igneous rocks. *University of Chicago Press.*

CURRY, K.L. and FERGUSON, J. (1970) The mechanism of intrusion of lamprophyre dikes indicated by "offsetting" of dikes. *Tectonophysics 9:525–535.*

DASCH, E.J. and GREEN, D.H. (1975) Strontium isotope geochemistry of lherzolite inclusions and host basaltic rocks. *American Journal of Science 275:461–469.*

DE PAOLO, D.J. (1981) Trace element and isotopic effects of combined wall-rock assimilation and fractional crystallization. *Earth and Planetary Science Letters 53:189–202.*

DEER, W.A., HOWIE, R.A. and ZUSSMAN, J. (1966) An introduction to the rock forming minerals. *Longman Group Limited, London.*

DELANEY, P.T., POLLARD, D.D., ZIONY, J.I. and MCKEE, E.H. (1986) Field relations between dikes and joints: emplacement processes and paleostress analysis. *Journal of Geophysical Research 91:4920– 4938.*

DELANEY, P.T. and POLLARD, D.D. (1981) Deformation of host rocks and flow of magma during growth of minette dikes and breccia-bearing intrusions near Ship Rock, New Mexico. *United States Geological Survey Professional paper 1202, 61p.*

DELANEY, P.T. and POLLARD, D.D. (1982) Solidification of basaltic magma during flow in a dike. *American Journal of Science 282:856–885.*

DORSEY, C.J. (1981) The stratigraphy, petrography and geochemistry of the Diamond Harbour Group, Banks Peninsula. *Unpublished BSc (Hons) thesis, University of Canterbury.*

DUGGAN, M.B. and REAY, A. (1986) The Timaru basalt. *In: I.E.M. Smith (Ed.), Late Cenozoic volcanism in New Zealand. Royal Society of New Zealand Bulletin 23:264–277.*

EVANS, A. LI. (1970) Geomagnetic polarity reversals in a Late Tertiary lava sequence from the Akaroa Volcano, New Zealand. *Geophysical Journal of the Royal Astronomical Society 21:163–183.*

FALLOON, T.J. (1982) The geology of the Onawe—French Farm—Wainui area, Akaroa Volcano, Banks Peninsula. *Unpublished B.Sc (Hons) Thesis, University of Canterbury.*

FEARS, D. (1985) A corrected CIPW program for interactive use. *Computers and Geosciences 11:787–797.*

FISHER, R.V. and SCHMINKE, H.U. (1984) Pyroclastic rocks. *Springer, 528p.*

FITZGERALD, J.D. and MacKINNON, I.D.R.(1977) PETPAK — A computing package for the petrologist. *Computers and Geosciences 3:637–638*

FRAZETTA, G. and VILLARI, L. (1981) The feeding of the eruptive activity of Etna Volcano. The regional stress field as a constraint to magma uprising and eruption. *Bulletin Volcanologique 44:269–282.*

FREY, F., BRYAN, W.B. and THOMPSON, G. (1974b) Atlantic Ocean floor: geochemistry and petrology of basalts from Legs 2 and 3 of the Deep Sea Drilling Project. *Journal of Geophysical Research 79:5507–5527.*

FREY, F.A., GREEN, D.H. and ROY, S.D. (1978) Integrated models of basalt petrogenesis: a study of quartz tholeiites to olivine melilitites from South Eastern Australia utilizing geochemical and experimental petrological data. *Journal of Petrology 19:463–513.*

FREY, F.A. and GREEN, D.H. (1974) The mineralogy, geochemistry and origin of lherzolite inclusions in Victorian basanites. *Geochimica et Cosmochimica Acta 38:1023–1059.*

FROST, M.J. (1965) Centre-Finding in Systems of Lines. *Geological Magazine 102:445–450.*

GAMBLE, J.A., MORRIS, P.A. and ADAMS, C.J. (1986) The geology, petrology and geochemistry of Cenozoic volcanic rocks from the Campbell Plateau and Chatham Rise. *In: SMITH, I.E.M. (Ed.) Late Cenozoic volcanism in New Zealand. Royal Society of New Zealand Bulletin 23:344–365.*

GAST, P.W. (1968) Trace element fractionation and the origin of tholeiitic and alkaline magma types. *Geochimica et Cosmochimica Acta 32:1057–1086.*

GEIST, D.J., BAKER, B.H. and MCBIRNEY, A.R. (1985) GPP — A program package for creating and using geochemical data files. *Unpublished Manual.*

GIBSON, I.L. and JAGAM, P. (1980) Instrumental Neutron Activation Analysis of rocks and minerals. *Mineralogical Association of Canada, Short Course in Neutron Activation Analysis in the Geosciences (Ed. G.K. Muecke) p109–131.*

GILLULY, J. (1929) Geology and oil and gas prospects of part of the San Rafael Swell, Utah. *US Geological Survey Bulletin 806-C, 130p.*

GOLDICH, S.S., TREVES, S.B., SUHR, H.H. and STUCKLESS, J.S. (1975) Geochemistry of the Cenozoic volcanic rocks of Ross Island and vicinity, Antarctica. *Journal of Geology 83:415–435.*

GRAHAM, I.J. and HACKETT, W.R. (1987) Petrology of calc-alkaline lavas from Ruapehu Volcano and related vents, Taupo Volcanic Zone, New Zealand. *Journal of Petrology 28:531-567.*

GREEN, D.H. (1969) The origin of basaltic and nephelinitic magmas in the earth's mantle. *Tectonophysics 7:409-422.*

GREEN, D.H. (1970) The origin of basaltic and nephelinitic magmas. *Transactions of the Leicester Literary and Philosophical Society 64:28–54.*

GREEN, D.H. (1971) Compositions of basaltic magmas as indicators of conditions of origin: application to oceanic volcanism. *Philosophical Transactions of the Royal Society of London 268:707–725.*

GREEN, D.H. (1973) Conditions of melting of basanite magma from garnet peridotite. *Earth and Planetary Science Letters 17:456–465.*

GREEN, D.H. and HIBBERSON, W. (1970) Experimental duplication of conditions of precipitation of high pressure phenocrysts in a basaltic magma. *Phys. Earth Planet. Interiors 3:247–254.*

GREEN, D.H. and RINGWOOD, A.E. (1967) The stability fields of aluminous pyroxene peridotite and garnet peridotite and their relevance in upper mantle structure. *Earth and Planetary Science Letters 3:151–160.*

GREGORY, H.E. (1917) Geology of the Navajo country. *United States Geological Survey Professional Paper 93, 161p.*

GUDMUNDSSON, A. (1984) Formation of dykes, feeder-dykes, and the intrusion of dykes from magma chambers. *Bulletin Volcanologique 47:537–550.*

GUNN, B.M. (1972) The fractionation effect of kaersutite in basaltic magmas. *Canadian Mineralogist 11:840–850.*

von HAAST, J. (1860) Report of a geological survey of Mt Pleasant. *Provincial Council of Canterbury Session XVII, December 19.*

von HAAST, J. (1864) Report on the building stones of the province of Canterbury. *Christchurch Newspapers.*

von HAAST, J. (1879) The geology of the provinces of Canterbury and Westland. *Lyttelton Times, 486p.*

HANSON, Gilbert N. (1980) Rare earth elements in petrogenetic studies of igneous systems. *Annual Review of Earth and Planetary Sciences 8:371–406.*

HARRIS, P.G. (1957) Zone refining and the origin of potassic basalts. *Geochimica et Cosmochimica Acta 12:195–208.*

HARTE, B. (1983) Mantle peridotites and processes — the kimberlite sample. *In: HAWKESWORTH, C.J. and NORRY, M.J. (Ed.) Continent basalts and mantle xenoliths. Shiva Publishing Ltd, Cheshire, UK.*

HASKIN, L.A., HASKIN, M.A. and FREY, F.A. (1968) Relative and absolute terrestrial abundances of the rare earths. *In: AHRENS, L.H. (Ed.) Origin and Distribution of the Elements, p889–912. Oxford, Pergamon.*

HAWKESWORTH, C.J., ERLANK, A.J., MARSH, J.S., MENZIES, M.A. and VAN CALSTEREN, P. (1983) Evolution of the continental lithosphere: evidence from volcanics and xenoliths in southern Africa. *In: HAWKESWORTH, C.J. and NORRY, M.J. (Ed.) Continental basalts and mantle xenoliths. Shiva Publishing Ltd, Cheshire, UK.*

HAWKESWORTH, C.J., NORRY, M.J., RODDICK, J.C. and VOLLMER, R. (1979) 143Nd/144Nd and 87Sr/86Sr ratios from the Azores and their significance in LIL-element enriched mantle. *Nature 280:28–31.*

HERVIG, R.L., SMITH, J.V. and DAWSON, J.B. (1977) Minor element content of olivine and orthopyroxene in upper-mantle xenoliths. *International Kimberlite Conference, Santa Fe, Extended Abstracts.*

HOLMES, A. (1930) Petrographic methods and calculations. *London: Thomas Murby.*

HUTTON, F.W. (1885) Sketch of the geology of New Zealand. *Quarterly Journal of the Geological Society 41:215–217.*

INGLIS, J. (1882) Notes on some of the diatomaceous deposits of New Zealand. *Transactions and Proceedings of the New Zealand Institute 15:340–346.*

IRVINE, T.N. and BARAGAR, W.R.A. (1971) A guide to the chemical classification of the common igneous rocks. *Canadian Journal of Earth Sciences 8:523–548.*

IRVING, A.J. (1980) Petrology and geochemistry of composite ultramafic xenoliths in alkalic basalts and implications for magmatic processes within the mantle. *American Journal of Science 280-A:389–426.*

IRVING, A.J. and PRICE, R.C. (1981) Geochemistry and evolution of lherzolite-bearing phonolitic lavas from Nigeria, Australia, East Germany and New Zealand. *Geochimica et Cosmochimica Acta 45:1309–1320.*

JACKSON, E.D. and WRIGHT, T.L. (1970) Xenoliths in the Honolulu Volcanic Series, Hawaii. *Journal of Petrology 11:405–430.*

JIZBA, Z.V. (1953) Mean and standard deviation of certain geologic data — a discussion. *American Journal of Science 251:899–906.*

JOHANNSEN, A. (1931) A descriptive petrography of the igneous rocks. *Chicago Press, p.89–93.*

JOHNSON, R.B. (1961) Patterns and origin of radial dike swarms associated with West Spanish Peak and Dike Mountain, south-central Colorado. *Geological Society of America Bulletin 72:579–589.*

KAY, R., HUBBERD, N.J. and GAST, P.W. (1970) Chemical characteristics and origin of ocean ridge volcanic rocks. *Journal of Geophysical Research 75:1585–1613.*

KAY, R.W. and GAST, P.W. (1973) The rare earth content and origin of alkali-rich basalts. *Journal of Geology 81:653–682.*

KELSEY, C.H. (1965) Calculation of the CIPW norm. *Mineralogical Magazine 34:276–282.*

KESSON, S. and PRICE, R.C. (1972) The major and trace element geochemistry of kaersutite and its bearing on the petrogenesis of alkaline rocks. *Contributions to Mineralogy and Petrology 35:119–124.*

KNUTSON, J. and GREEN, T.H. (1975) Experimental duplication of a high pressure megacryst/cumulate assemblage in a near-saturated hawaiite. *Contributions to Mineralogy and Petrology 52:121–132.*

KOIDE, H. and BHATTACHARJI, S. (1975) Formation of fractures around magmatic intrusions and their role in ore localization. *Economic Geology 70:781–799.*

KUDO, A.M. and WEILL, D.F. (1970) An igneous plagioclase thermometer. *Contributions to Mineralogy and Petrology 25:52–65.*

KUSHIRO, I., SHIMIZU, N., NAKAMURA, Y. and AKIMOTO, S. (1972) Compositions of coexisting liquid and solid phases formed upon melting of natural garnet and spinel lherzolites at high pressures: a preliminary report. *Earth and Planetary Science Letters 14:19–25.*

KYLE, P.R. (1981) Mineralogy and petrology of a basanite to phonolite sequence at Hut Point Peninsula, Antarctica, based on core from Dry Valley Drilling Project Drillholes 1,2 and 3. *Journal of Petrology 22:451–500.*

LANGMUIR, C.H. (1989) Geochemical consequences of *in situ* crystallisation. *Nature 340:199-205.*

LE MAITRE, R.W. (1962) Petrology of volcanic rocks, Gough Island, South Atlantic. *Geological Society of America Bulletin 73:1309–1340.*

LE MAITRE, R.W. (1976) The chemical variability of some common igneous rocks. *Journal of Petrology 17:589–637.*

LEAKE, B.E. (1978) Nomenclature of amphiboles. *Canadian Mineralogist 16:501–520.*

LIGGETT, K.A. and GREGG, D.R. (1965) Geology of Banks Peninsula. *Department of Scientific and Industrial Research Information Series 51.*

LIVINGSTON, D.E., DAMON, P.E., MAUGER, R.L., BENNETT, R. and LAUGHLIN, A.W. (1967) Argon 40 in cogenetic feldspar-mica mineral assemblages. *Journal of Geophysical Research 72:1361–75.*

LLOYD, F.E. and BAILEY, D.K. (1975) Light element metasomatism of the continental mantle: the evidence and the consequences. *In: AHRENS, L.H., DAWSON, J.B., DUCAN, A.R. and ERLANK, A.J. (Ed.) Physics and Chemistry of the Earth, Pergamon 9:389–416.*

MACDONALD, G.A. and ABBOTT, A.T. (1970) Volcanoes in the sea. *Honolulu, University of Hawaii Press, 441p.*

MACDONALD, G.A. and KATSURA, T. (1964) Chemical composition of Hawaiian lavas. *Journal of Petrology 5:82–133.*

MARSHALL, P. (1894) On a tridymite trachyte of Lyttelton. *Transactions of the New Zealand Institute 26:368–387.*

MASON, B. (1972) Minor and trace element distribution in minerals of the Muzzle River gabbro. *New Zealand Journal of Geology and Geophysics 15:465–475.*

MATHEZ, E.A. (1973) Refinement of the Kudo-Weill plagioclase thermometer and its application to basaltic rocks. *Contributions to Mineralogy and Petrology 41:61–72.*

MCBIRNEY, A.R. (1984) Igneous petrology. *Freeman, Cooper and Company, San Francisco. 504p.*

MCBIRNEY, A.R. and AOKI, K. (1968) Petrology of the island of Tahiti. *Memoire of the Geological Society of America 116:523–556.*

MCKENZIE, D. (1984) The generation and compaction of partially molten rock. *Journal of Petrology 25:713–765.*

MCKENZIE, D. (1985) The extraction of magma from the crust and mantle. *Earth and Planetary Science Letters 74:81–91.*

MENZIES, M. (1983) Mantle ultramafic xenoliths in alkaline magmas: evidence for mantle heterogeneity modified by magmatic activity. *In: HAWKESWORTH, C.J. and NORRY, M.J. (Ed.) Continental basalts and mantle xenoliths. Shiva Publishing Ltd, Cheshire, UK.*

MENZIES, M.A. (1976) Rare earth geochemistry of fused ophiolitic and alpine lherzolites — I. Othris, Lanzo and Troodos. *Geochimica et Cosmochimica Acta 40:645–656.*

MENZIES, M.A. and MURTHY, V.R. (1978a) Strontium isotope geochemistry of alpine tectonite lherzolites: data compatible with a mantle origin. *Earth Planetary Science Letters 38:346–354.*

MENZIES, M.A. and MURTHY, V.R. (1978b) Strontium isotope geochemistry of hydrous lithosphere in sub-oceanic and sub-continental regions. *In: Proceedings 4th International Conference Geochronology, Cosmochronology, and Isotope Geology: US Geological Survey Open File Report 78-701:292–295.*

MENZIES, M. and MURTHY, V.R. (1980a) Nd and Sr isotope geochemistry of hydrous mantle nodules and their host alkali basalts: implications for local heterogeneities in metasomatically veined mantle. *Earth and Planetary Science Letters 46:323–334.*

MENZIES, M. and MURTHY, V.R. (1980b) Mantle metasomatism as a precursor to the genesis of alkaline magmas — isotopic evidence. *American Journal of Science 280-A:622–638.*

MENZIES, Martin A. and WASS, Suzanne Y. (1983) CO2- and LREE-rich mantle below eastern Australia: A REE and isotopic study of alkaline magmas and apatite-rich mantle xenoliths from the Southern Highlands Province, Australia. *Earth and Planetary Science Letters 65:287–302.*

MIYASHIRO, A. (1978) Nature of alkalic volcanic rock series. *Contributions to Mineralogy and Petrology 66:91–104.*

MORRIS, P.A. (1984) Petrology of the Campbell Island Volcanics, southwest Pacific Ocean. *Journal of Volcanological and Geothermal Research 21:119–148.*

MORRIS, P.A. (1985) The geochemistry of Eocene-Oligocene volcanics on the Chatham Islands, New Zealand. *New Zealand Journal of Geology and Geophysics, 28:459–469.*

MORRIS, P.A. (1985b) Petrology of late Cretaceous alkaline volcanic rocks from the Chatham Islands, New Zealand. *New Zealand Journal of Geology and Geophysics, 28:253–266.*

MUIR, I.D. and TILLEY, C.E. (1961) Mugearites and their place in alkali igneous rock series. *Journal of Geology 69:186–203.*

NAGASAWA, H. (1973) Rare-earth distribution in alkali rocks from Oki-Dogo Island, Japan. *Contributions to Mineralogy and Petrology 39:301–308.*

NAGASAWA, H. and SCHNETZLER, C.C. (1971) Partitioning of rare-earth, alkali and alkaline earth elements between phenocryst and acidic igneous magma. *Geochimica et Cosmochimica Acta 35:953–968.*

NAKAMURA, K. (1977) Volcanoes as possible indicators of tectonic stress orientation — principle and proposal. *Journal of Volcanology and Geothermal Research 2:1–16.*

NASH, W.P., CARMICHAEL, I.E.S. and JOHNSON, R.W. (1969) The mineralogy and petrology of Mount Suswa, Kenya. *Journal of Petrology 10:409–439.*

NEUMANN, H., MEAD, J. and VITALIANO, C.J. (1954) Trace element variations during fractional crystallization as calculated from the distribution law. *Geochimica et Cosmochimica Acta 6:90–99.*

NOBLE, D.C. (1965) Gold Flat Member of the Thirsty Canyon Tuff — a pantellerite ash-flow sheet in southern Nevada. *United States Geological Survey Professional Paper 525-B:85–90.*

NOBLE, D.C. (1968) Systematic variation of major elements in comendite and pantellerite glasses. *Earth and Planetary Science Letters 4:167–172.*

NOBLE, D.C., SMITH, V.C. and PECK, L.C. (1967) Loss of halogens from crystallized and glassy silicic volcanic rocks. *Geochimica et Cosmochimica Acta 31:215–223.*

NORRISH, K. and HUTTON, J.T. (1969) An accurate x-ray spectrographic method for analysis of a wide range of geologic samples. *Geochimica et Cosmochimica Acta 33:431–453.*

NORRY, M.J., TRUCKLE, P.H., LIPPARD, S.J., HAWKESWORTH, C.J., WEAVER, S.D. and MARRINER, G.F. (1980) Isotopic and trace element evidence from lavas, bearing on mantle heterogeneity beneath Kenya. *Philosophical Transactions of the Royal Society of London, A297:259–271.*

NORRY, M.J. and FITTON, J.G. (1983) Compositional differences between oceanic and continental basic lavas and their significance. *In: HAWKESWORTH, C.J. and NORRY, M.J. (Ed.) Continental basalts and mantle xenoliths. Shiva Publishing Ltd, Cheshire, UK.*

O'HARA (1965) Primary magmas and the origin of basalts. *Scottish Journal of Geology 1:19–40.*

O'NIONS, R.K., HAMILTON, P.J. and EVENSON, N.M. (1977) Variations in 143Nd/144Nd and 87Sr/86Sr ratios in oceanic basalts. *Earth and Planetary Science Letters 34:13–22.*

OBORN, L.E. and SUGGATE, R.P. (1959) Sheet 21 — Christchurch Geological Map of New Zealand 1:250,000. *New Zealand Department of Scientific and Industrial Research, Wellington.*

ODE, H. (1957) Mechanical analysis of the dike pattern of the Spanish Peaks area, Colorado. *Geological Society of America Bulletin 68:567–576.*

ORVILLE, P.M. (1972) Plagioclase cation exchange equilibria with aqueous chloride solution: results at 700 degrees C and 2000 bars in the presence of quartz. *American Journal of Science 272:234–272.*

PAPIKE, J.J. and BENCE, A.E. (1978) Lunar mare versus terrestrial mid- ocean ridge basalts: planetary constraints on basaltic volcanism. *Geophysical Research Letters 5:803–806*

PAPIKE, J.J. CAMERON, K.L. and BALDWIN, K. (1974) Amphiboles and pyroxenes: characterization of other than quadrilateral components and estimates of ferric iron from microprobe data. *Geological Society of America, Abstracts with Programs 7:1053–1055.*

PEARCE, J.A. and CANN, J.R. (1973) Tectonic setting of basic volcanic rocks determined using trace element analysis. *Earth and Planetary Science Letters 19:290–300.*

PEARCE, J.A. and NORRY, M.J. (1979) Petrogenetic implications of Ti, Zr, Y and Nb variations in volcanic rocks. *Contributions to Mineralogy and Petrology 69:33–47.*

PEARCE, T.H. (1984) The analysis of zoning in magmatic crystals with emphasis on olivine. *Contributions to Mineralogy and Petrology 86:149–154.*

PHILPOTTS, J.A. and SCHNETZLER, C.C.(1970) Phenocryst-matrix partition coefficients for K, Rb, Sr and Ba with applications to anorthosite and basalt genesis. *Geochimica et Cosmochimica Acta 34:307–322.*

PRICE, R.C. and CHAPPELL, B.W. (1975) Fractional crystallisation and the petrology of Dunedin Volcano. *Contributions to Mineralogy and Petrology 53:157–182.*

PRICE, R.C. and COMPSTON, W. (1973) The geochemistry of the Dunedin Volcano: Strontium isotope chemistry. *Contributions to Mineralogy and Petrology 42:55–61.*

PRICE, R.C. and COOMBS, D.S. (1975) Phonolitic lava domes and other features of the Dunedin Volcano, Otago. *Journal of the Royal Society of New Zealand 5:132–152.*

PRICE, R.C. and TAYLOR, S.R. (1973) The geochemistry of the Dunedin Volcano, East Otago, New Zealand: Rare earth elements. *Contributions to Mineralogy and Petrology 40:195–205.*

PRICE, R.C. and TAYLOR, S.R. (1980) Petrology and Geochemistry of the Banks Peninsula Volcanoes, South Island, N.Z. *Contributions to Mineralogy and Petrology 72:1–18.*

RAESIDE, J.D. (1964) Loess deposits of the South Island, New Zealand, and soils formed on them. *New Zealand Journal of Geology and Geophysics 7:811–838.*

RAO, J.S. and SENGUPTA, S. (1972) Mathematical techniques for paleocurrent analysis: treatment of directional data. *Mathematical Geology 4:235–248.*

RAYLEIGH, J.W.S. (1896) Theoretical considerations respecting the separation of gases by diffusion and similar processes. *Philosophical Magazine 42:77–107.*

REICHE, P. (1938) An analysis of cross-lamination, the Cocnino Sandstone. *Journal of Geology 46:905–932.*

REILLY, W.I. (1966) Gravity map of New Zealand 1:250 000 Bouguer Anomalies, Isostatic anomalies. Sheet 21, Christchurch. *New Zealand Department of Scientific and Industrial Research.*

REILLY, W.I. (1969) Gravity map of New Zealand 1:250 000 Bouguer Anomalies, Isostatic anomalies. Sheet 25, Dunedin. *New Zealand Department of Scientific and Industrial Research.*

REILLY, W.I. (1972) Gravitational expression of the Dunedin Volcano. *New Zealand Journal of Geology and Geophysics 15:16–21.*

RICHEY, J.E. (1939) The dikes of Scotland. *Edinburgh Geological Society Transactions 13:393–435.*

RIDLEY, W.I. (1970) Petrology of the Las Canadas Volcanoes, Tenerife, Canary Islands. *Contributions to Mineralogy and Petrology 26:124–160.*

RINGWOOD, A.E. (1975) Composition and petrology of the earth's mantle. *McGraw-Hill Book Co., New York.*

ROEDDER, P.L. and EMSLIE, R.F. (1970) Olivine–liquid equilibrium. *Contributions to Mineralogy and Petrology 29:275–289.*

ROEX, A.P. and ERLANK, A.J. (1982) Quantitative evaluation of fractional crystallisation in Bouvet Island lavas. *Journal of Volcanology and Geothermal Research 13:309–338.*

ROMANO, R. (1982) Succession of volcanic activity in the Etnean area. *In: ROMANO, R. (Ed.) Mt Etna Volcano: A review of recent earth science studies. Memorie Della Societa Geologica Italiana 23:27–48.*

ROUITTI, J.T. and PRUSSIN, S.G. (1969) Photopeak method for the computer analysis of gamma-ray spectra from semiconductor detectors. *Nuclear Instrumental Methods 72:125–142.*

RUBIN, A.M. and POLLARD, D.D. (1987) Origins of blade-like dikes in volcanic rift zones. *In: DECKER, R.W., WRIGHT, T.H. and STAUFFER, P.H. (Ed.) Volcanism in Hawaii, United States Geological Survey Professional Paper 1350, 1:1449–1470.*

SCHILLING, J.G. (1966) Rare earth fractionation in Hawaiian volcanic rocks. *PhD thesis, Massachusetts Institute of Technology, Cambridge, Massachusetts.*

SCHILLING, J.G. and WINCHESTER, J.W. (1967) Rare-earth fractionation and magmatic processes. *In: RUNCORN, S.K. (Ed.) Mantles of the Earth and terrestrial planets. London: Interscience.*

SCHILLING, J.G. and WINCHESTER, J.W. (1969) Rare earth contribution to the origin of Hawaiian lavas. *Contributions to Mineralogy and Petrology 23:27–37.*

SCHMID, R. (1981) Descriptive nomenclature and classification of pyroclastic deposits and fragments: Recommendations of the IUGS subcommission on the systematics of igneous rocks. *Geology 9:41–43.*

SCHNETZLER, C.C. and PHILPOTTS, J.A. (1970) Partition coefficients of rare-earth elements between igneous matrix material and rock-forming mineral phenocrysts — II. *Geochimica et Cosmochimica Acta 34:331–340.*

SCHWARZER, R.R. and ROGERS, J.J.W. (1974) A worldwide comparison of alkali olivine basalts and their differentiation trends. *Earth and Planetary Science Letters 23:286–296.*

SEWELL, R.J. (1985) A new volcanic stratigraphy for the Miocene rocks of central Banks Peninsula. *In: Geological Society of New Zealand 1985 Conference Programme and Abstracts.*

SEWELL, R.J. (1985) The volcanic geology and geochemistry of Central Banks Peninsula and relationships to Lyttelton and Akaroa Volcanoes. *Unpublished PhD thesis, University of Canterbury, New Zealand.*

SEWELL, R.J. (1988) Late Miocene volcanic stratigraphy of central Banks Peninsula, Canterbury, New Zealand. *New Zealand Journal of Geology and Geophysics 31:41–64.*

SEWELL, R.J. and WEAVER, S.D. (1989) Petrological evolution of Miocene continental intraplate volcanics of Banks Peninsula, New Zealand. *Abstract in "Continental Magmatism" — IAVECI General Assembly, Sante Fe, New Mexico. New Mexico Bureau of Mines and Mineral Resource Bulletin 131:238.*

SHAW, D.M. (1970) Trace element fractionation during anatexis. *Geochimica et Cosmochimica Acta 34:237–243.*

SHELLEY, D. (1975) Manual of optical mineralogy. *Elsevier, Netherlands.*

SHELLEY, D. (1985) Determining paleo-flow directions from groundmass fabrics in the Lyttelton radial dykes, New Zealand. *Journal of Volcanology and Geothermal Research 25:69–79.*

SHELLEY, DAVID (1987) Lyttelton I & II, the two centres of the Lyttelton Volcano. *New Zealand Journal of Geology and Geophysics 30:159–168.*

SIMKIN, T. and SMITH, J.V. (1970) Minor-element distribution in olivine. *Journal of Geology 78:304–325.*

SMITH, Eugene I. and STUPAK, William A.(1977) A Fortran IV program for the classification of volcanic rocks using the Irvine and Baragar classification scheme. *Computers and Geosciences 4:89–99*

SMITH, L. (1970) Petrology and geological history of the lower part of Akaroa Volcano. *Unpublished B.Sc (Hons) thesis, University of Canterbury.*

SNEDECOR, G.W. and COCHRAN, W.G. (1980) Statistical methods. *7th Ed., The Iowa State University Press, Ames, Iowa, USA, 507p.*

SPEIGHT, R. (1908) On a soda amphibole trachyte from Cass' Peak. *Transactions of the New Zealand Institute 40:176–184.*

SPEIGHT, R. (1917) The geology of Banks Peninsula. *Transactions of the Royal Society of New Zealand 49:365–392.*

SPEIGHT, R. (1923) The intrusive rocks of Banks Peninsula. *Records of the Canterbury Museum 2:121–150.*

SPEIGHT, R. (1924) The basic volcanic rocks of Banks Peninsula. *Records of the Canterbury Museum 2:239–267.*

SPEIGHT, R. (1933) The source of the Mount Herbert lavas. *Records of the Canterbury Museum 4:41–51.*

SPEIGHT, R. (1938) The dykes of the Summit Road, Lyttelton. *Transactions of the Royal Society of New Zealand 68:82–99.*

SPEIGHT, R. (1940) The basal beds of the Akaroa Volcano. *Transactions of the Royal Society of New Zealand 70:60–76.*

SPEIGHT, R. (1943) The geology of Banks Peninsula — A revision. Part I — Physiography. *Transactions of the Royal Society of New Zealand 73:13–26.*

SPEIGHT, R. (1944) The geology of Banks Peninsula — A revision. Part II — The Akaroa Volcano. *Transactions of the Royal Society of New Zealand 74:232–254.*

SPENCE, D.A. and TURCOTTE, D.L. (1985) Magma-driven propagation of cracks. *Journal of Geophysical Research 90:575–580.*

SPIEGEL, M.R. (1972) Theory and problems of Statistics. *SI (metric) Edition. Schaums outline series, McGraw-Hill International Book Co., New York, 359p.*

STEARNS, H.T. (1966) Geology of the State of Hawaii. *Pacific Books, Palo Alto, California.*

STEIGER, R.H. and JAEGER, E. (1977) Subcommission on geochronology: Convention on the use of decay constants in geo- and cosmochronology. *Earth and Planetary Science Letters 36:359–362.*

STIPP, J.J. and McDOUGALL, I. (1968) Geochronology of the Banks Peninsula Volcanoes, New Zealand. *New Zealand Journal of Geology and Geophysics 11:1239–1260.*

STOLPER, E. and WALKER, D. (1980) Melt density and the average composition of basalt. *Contributions to Mineralogy and Petrology 74:7–12.*

SUN, S.S. and HANSON, G.N. (1975) Origin of Ross Island basanitoids and limitations upon the heterogeneity of mantle sources for alkali basalts and nephelinites. *Contributions to Mineralogy and Petrology 52:77–106.*

SUN, S.S. and HANSON, G.N. (1976) Rare earth element evidence for differentiation of McMurdo Volcanics, Ross Island Antarctica. *Contributions to Mineralogy and Petrology 54:139–155.*

TARNEY, J., SAUNDERS, A.D. and WEAVER, S.D. (1977) Geochemistry of volcanic rocks from the island arcs and marginal basins of the Scotia sea region. *In: Vol. 1 Maurice Ewing Series p.367–378 "Island Arcs, Deep Sea Trenches and BackArc Basins" Washington, American Geophysical Union.*

TAYLOR, Jr., H.P. (1980) The effects of assimilation of country rocks by magmas on $^{18}O/^{16}O$ and $^{87}Sr/^{86}Sr$ systematics in igneous rocks. *Earth and Planetary Science Letters 47:243.*

TERRY, R.D. and CHILINGAR, G.V. (1955) Comparison charts for visual estimation of percentage composition. *Journal of Sedimentary Petrology 25:229–234.*

THIELE, B. (1983) Basement geology of the Lyttelton Volcano, Banks Peninsula. *Unpublished MSc thesis, University of Canterbury, NZ.*

THOMPSON, R.N., DICKEN, A.P., GIBSON, I.L. and MORRISON, M.A. (1982) Elemental fingerprints of isotopic contamination of Hebridean Palaeocene mantle-derived magmas by Archaean sial. *Contributions to Mineralogy and Petrology 79:159–168.*

THOMPSON, R.N., ESSON, J. and DUNHAM, A.C. (1972) Major element chemical variation in the Eocene lavas of the Isle of Skye, Scotland. *Journal of Petrology 13:219–253.*

THOMPSON, R.N., MORRISON, M.A., DICKIN, A.P. and HENDRY, G.L. (1983) Continental flood basalts ... Arachnids rule OK? *In: HAWKESWORTH, C.J. and NORRY, M.J. (Ed.) Continental basalts and mantle xenoliths. Shiva Publishing Ltd, Cheshire, UK.*

TILL, R. (1977) The HARDROCK package, a series of Fortran IV computer programs for performing and plotting geochemical calculations. *Computers and Geosciences 3:185–243.*

TILLEY, C.E., YODER, H.S. and SCHAIRER, J.F. (1967) Melting relations of volcanic rock series. *Yearbook of the Carnegie Institute of Washington 65:260–269.*

TILLEY, C.E. and MUIR, I.D. (1962) The Hebridean Plateau magma type. *Transactions of the Edinburgh Geological Society 19:208–215.*

TUFTE, E.R. (1983) The visual display of quantitative information. *Graphics Press, Cheshire, Connecticut, 197p.*

VICENZI, E.P., MCBIRNEY, A.R., WHITE, W.M. and HAMILTON, M. (in press) The geology and geochemistry of Isla Marchena, Galapagos Archipelago: An ocean island adjacent to a mid-ocean ridge.

WALKER, G.P.L. (1958) Geology of the Reydarfjordur area, eastern Iceland. *Quarterly Journal of the Geological Society of London 114:367–390.*

WALKER, D., SHIBATA, T. and DE LONG, S.E. (1979) Abyssal tholeiites from the Oceanographer Fracture Zone. 2. Phase equilibria and mixing. *Contributions to Mineralogy and Petrology 70:111–125.*

WASHINGTON, H.S. (1917) Chemical analysis of igneous rocks. *United States Geological Survey Professional Paper 99, p1162–1165.*

WEAVER, S., SEWELL, R. and DORSEY, C. (1985) Extinct volcanoes: A guide to the geology of Banks Peninsula. *Geological Society of New Zealand Guidebook #7.*

WEAVER, S.D. (1980) An introduction to the geology of Lyttelton Volcano. *In: Weaver, S.D. and Lewis, D.W., Geological Society of New Zealand 1980 Conference Field Excursions Guide Book.*

WEAVER, S.D., BARLEY, M.E., DE LAETER, J.R. and COOTE, A. (1986) Fits with isochrons: Ages and origins of Canterbury rhyolites. *In: Geological Society of New Zealand 1986 Conference Programme and Abstracts. Geological Survey of NZ Misc Publication 35A.*

WEAVER, S.D., SCEAL, J.S.C. and GIBSON, I.L. (1972) Trace element data relevant to the origin of trachytic and pantelleritic lavas in the East African Rift system. *Contributions to Mineralogy and Petrology 36:181–194.*

WEAVER, S.D. and SEWELL, R.J. (1986) Cenozoic volcanology of Banks Peninsula. *In: Houghton, B.F. and Weaver, S.D. (Ed.) South Island igneous rocks: Tour guides A3, C2 and C7. New Zealand Geological Survey 13:39–63.*

WEAVER, S.D., SMITH, I.E.M, SEWELL, R.J., GAMBLE, J.A., MORRIS,P.A., DUGGAN, M.B., GIBSON, I.L. and PANKHURST, R.J. (1989) New Zealand Intraplate Volcanism. *In: JOHNSON, R.W., KNUTSON, J. and TAYLOR, S.R. (Eds) Intraplate Volcanism in Eastern Australia and New Zealand. Australian Academy of Science and Cambridge University Press, p157–188.*

WHITE, W.M. and HOFMANN, A.W. (1982) Sr and Nd isotope geochemistry of oceanic basalts and mantle evolution. *Nature 296:821–825.*

WILKINSON, J.F.G. (1982) The genesis of mid-ocean ridge basalt. *Earth-Science Reviews 18:1–57.*

WILLETT, R.W. (1943) Diatomaceous earth, Wainui, Akaroa. *New Zealand Journal of Science and Technology 25:90.*

WILLIAMS, H. (1936) Pliocene volcanics of the Navajo–Hopi country. *Geological Society of America Bulletin 47:111–171.*

YODER, H.S. and TILLEY, C.E. (1962) Origin of basaltic magmas: An experimental study of natural and synthetic systems. *Journal of Petrology 3:342–532.*

YOSHI, M. and HIRANO, H. (1977) Test data for the normative calculation programs. *Bulletin of the Geological Society of Japan 28:401–412.*

ZIONY, J.I. (1966) Analysis of systematic jointing in part of the Monument Upwarp, Southeastern Utah. *Los Angeles, University of California, Ph.D. thesis, 152p.*